Chiral Pyridyl Phosphinite Catalysts and the Development of Structure Selectivity Relationships in the Asymmetric Hydrogenation of Trisubstituted Alkenes

Inauguraldissertation

zur
Erlangung der Würde eines Doktors der Philosophie
vorgelegt der
Philosophisch-Naturwissenschaftlichen Fakultät
der Universität Basel
von

David Harrison Woodmansee
aus
San Diego, USA
Basel 2010

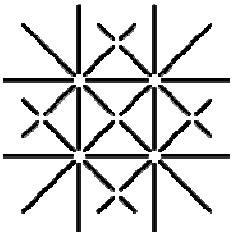

creative commons

Attribution-Noncommercial-No Derivative Works 2.5 Switzerland

---

You are free:

to Share — to copy, distribute and transmit the work

Under the following conditions:

Attribution. You must attribute the work in the manner specified by the author or licensor (but not in any way that suggests that they endorse you or your use of the work).

Noncommercial. You may not use this work for commercial purposes.

No Derivative Works. You may not alter, transform, or build upon this work.

- For any reuse or distribution, you must make clear to others the license terms of this work. The best way to do this is with a link to this web page.
- Any of the above conditions can be waived if you get permission from the copyright holder.
- Nothing in this license impairs or restricts the author's moral rights.

Your fair dealing and other rights are in no way affected by the above.

This is a human-readable summary of the Legal Code (the full license) available in German:
http://creativecommons.org/licenses/by-nc-nd/2.5/ch/legalcode.de

Disclaimer:
The Commons Deed is not a license. It is simply a handy reference for understanding the Legal Code (the full license) — it is a human-readable expression of some of its key terms. Think of it as the user-friendly interface to the Legal Code beneath. This Deed itself has no legal value, and its contents do not appear in the actual license. Creative Commons is not a law firm and does not provide legal services. Distributing of, displaying of, or linking to this Commons Deed does not create an attorney-client relationship.

Quelle: http://creativecommons.org/licenses/by-nc-nd/2.5/ch/deed.en Datum: 3.4.2009

Genehmigt von der Philosophisch-Naturwissenschaftlichen Fakultät auf Antrag von:

Prof. Dr. Andreas Pfaltz

Prof. Dr. Thomas Ward

Basel, den 25.5.2010

Prof. Dr. Eberhard Parlow

Dekan

This thesis was supervised by Prof. Dr. Andreas Pfaltz from February 2006 to May 2010 at the University of Basel, Department of Chemistry.

Acknowledgements

I would like to thank my supervisor Professor Dr. Andreas Pfaltz for the opportunity to work in his research group, for his support and the freedom in developing my project.

I would like to thank Professor Dr. Thomas R. Ward for co-examination of this thesis and Prof. Dr. Helma Wennemers for chairing the defense.

I am very grateful to Marc-André Müller, Denise Rageot, and Felix Voss for their hard work in their masters' research and the continuous support for my own endeavors.

I thank Dr. Axel Franzke, Dr. Stephen Kaiser, and Dr. Rui Fraga for the many insightful and stimulating discussions.

I am grateful to Markus Neuburger for collecting X-ray data and his hard work in solving problematic structures.

I thank Dr. Daniel Häussinger for supporting my own NMR-measurments.

I thank Jaroslav Padevet for solving numerous computer and NMR problems.

I am grateful to Lars Tröndlin and Dominik Frank for their help with instruments and chemicals.

I thank Marina Mambelli-Johnson for her constant support and her willingness to go beyond what was required.

I thank Dr. Heinz Nadig measured the EI and FAB mass spectra and Werner Kirsch determined all elemental analyses.

I thank the members of the workshop for technical support, especially Mr. Koller for his support with the glove box.

I thank all the past and present members of the Pfaltz group who made my time in Basel enjoyable. The colleagues in lab 208 are especially acknowledged for the good working atmosphere.

I am grateful to Dr. Hong Liu and Dr. Yu Ge, my industrial mentors for their support and sound advice, without which I would not have pursued a Ph.D. in a foreign country.

I am very grateful to my parents for their support throughout my education.

I am very grateful to meinen Schwiegereltern Barbara und Hendrik, for their support and occasional medical attention.

I am deeply grateful and indebted to my wife Constanze Treugut for her advice, support and sacrifice.

Summary

The current trend in developing asymmetric catalysts is towards creating specialized molecules with tailored functions for increased selectivity in classes of substrates rather than general catalysts capable of broad application. In addition, the capacity to generate groups of catalysts with incremental changes to overall structure allows for a more detailed analysis of contributions to the structure selectivity relationships for a variety of substrates. This information can then be used to identify ideal catalysts or improve selectivity and activity of for a particular system.

Asymmetric hydrogenation of substituted alkenes with chiral iridium N,P complexes that were developed from the achiral Crabtree Complex have proven to be extraordinary selective and active catalysts. Screening a series of trisubstituted alkenes on 1st and 2nd generation catalysts indicated a strong enantioselectivity dependence on the phosphorus and pyridine substituents. In particular, the substituents in the *ortho* position of the pyridine ring were found to have significant control over the catalyst.

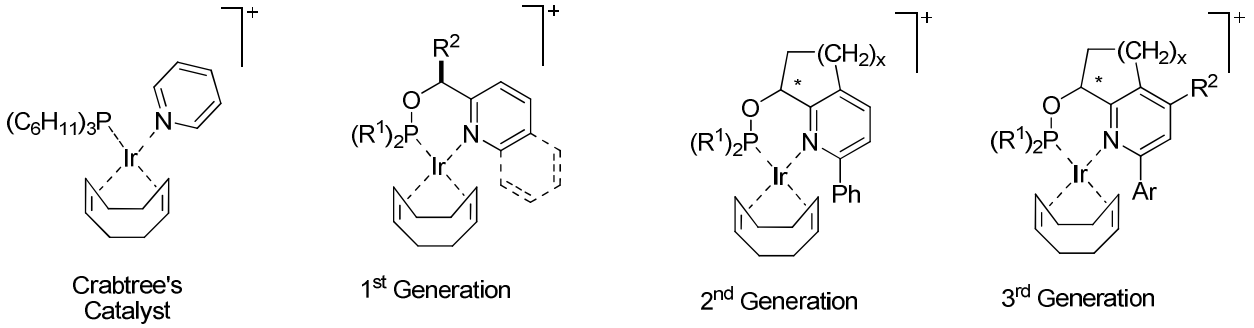

The synthesis of the 3rd generation of chiral pyridyl phosphinite catalysts takes advantage of a flexible late phase incorporation of the functional groups which govern the selectivity of the asymmetric hydrogenation to span a range of steric and electronic properties. The screening of these catalysts in the asymmetric hydrogenation of several classes of trisubstituted alkenes provided clear insight to the factors controlling enantioselectivity which were proven to vary greatly with the nature of the substrate and catalyst. Several catalysts with exceptional selectivity were identified for multiple examples of trisubstituted alkenes which had proven difficult with previous system.

Chapter 1

Iridium Catalyzed Asymmetric Hydrogenation of Alkenes with Chiral N,P and C,N Ligands

1.1 Introduction

The development of highly enantioselective rhodium-diphosphine catalysts in the early 70s marked the beginning of a new era in asymmetric synthesis. For the first time practically useful enantioselectivities could be obtained with synthetic chiral catalysts. The well-known L-Dopa process developed by Monsanto at that time[1] demonstrated that these catalysts can be applied on an industrial scale, and since then hydrogenation has played a dominant role in industrial asymmetric catalysis.[2] Today, asymmetric hydrogenation remains a corner stone of the modern organic chemists' repertoire of reliable catalytic methods for the construction of optically active compounds.[3] High enantioselectivity, low catalyst loadings, essentially quantitative yields, perfect atom economy, and mild conditions are attractive features of this transformation as evident in the ever growing list of publications using these methods.

A plethora of chiral phosphine ligands are known which induce very high enantioselectivity in rhodium- and ruthenium-catalyzed hydrogenations. However, the range of alkenes that can be hydrogenated with high enantiomeric excess is still limited. Both rhodium and ruthenium catalysts require the presence of a coordinating functional group adjacent to the C=C bond, hydrogenation of dehydro-amino acid derivatives or allylic alcohols being typical substrate classes. A caveat of this reactivity in regard to unfunctionalized alkenes is that these catalysts generally display low reactivity and unsatisfactory enantioselectivity. Thus, their application has been restricted largely to certain classes of properly functionalized substrates.

Some years ago the Pfaltz group discovered a new class of chiral iridium N,P-ligand complexes which overcame the limitations of the rhodium and ruthenium based systems.[4] Early transition metal metallocenes catalysts capable of asymmetric hydrogenation of a range of unfunctionalized alkenes in excellent enantioselectivities have been reported but under onerous conditions.[5] Moreover, iridium N,P based systems showed exceptionally high activity in the hydrogenation of unfunctionalized tri- and even tetrasubstituted alkenes. In this respect, they resembled the Crabtree catalyst, $[Ir(pyridine)(Cy_3P)(COD)]PF_6$ (Cy = cyclohexyl, COD = cyclooctadiene),[6] which provided the stimulus for this work. In addition, promising results were also obtained with certain functionalized alkenes for which no suitable catalysts were available. In this chapter, we discuss the special properties and scope of these catalysts with special emphasis on recent developments.[7]

1.2 Mechanistic Studies

1.2.1 Initial Studies: An Unexpected Anion Effect

Initial studies with iridium complexes derived from chiral phosphinooxazolines (PHOX ligands) and (*E*)-1,2-diphenyl-1-propene as substrate gave encouraging results (Scheme 1).[4a,8] With 4 mol% of catalyst (X = PF_6^-) at 10-50 bar hydrogen pressure up to 98% ee could be obtained. However, the turnover numbers were disappointingly low.

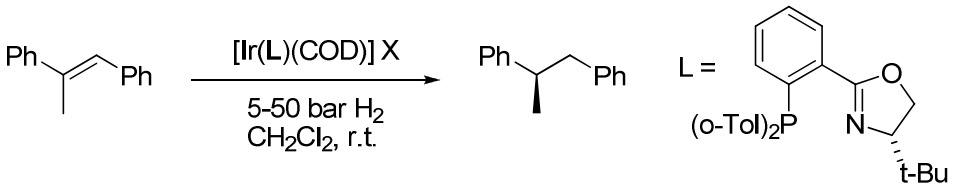

Scheme 1

Kinetic studies demonstrated that with 4 mol% of catalyst in a 0.3 M solution of alkene at 7 bar hydrogen pressure the reaction was extremely fast and reached completion within less than one minute.[9] Lower catalyst loadings resulted in decreased conversion. Although the initial rate was still high at 1 mol% catalyst loading a rapid and essentially complete deactivation of the catalyst was observed before 50% of the alkene was consumed. Deactivation is a known problem of the Crabtree catalyst, which is attributed to the formation of inactive hydride-bridged trinuclear complexes.[6] In the case of Ir(PHOX) complexes as well NMR analysis of deactivated reaction mixtures suggested the presence of such hydride-bridged species. In subsequent studies a trinuclear Ir(PHOX)-hydride complex was isolated and characterized by NMR and X-ray analysis.[10] This complex proved to be remarkably stable and all experiments to convert it back into a catalytically active species failed.

Attempts to increase conversion by variation of the solvent, hydrogen pressure, or the catalyst and substrate concentration were unsuccessful. Coordinating solvents and additives such as amines, or coordinating anions such as halides, carboxylates, and even the very weakly coordinating triflate ion were found to deactivate the catalyst. The best results were obtained in anhydrous dichloromethane or 1,2-dichloroethane using cationic Ir-PHOX complexes with hexafluorophosphate as counterion. Rigorous exclusion of moisture and oxygen resulted in increased conversion. When the reaction was set up in carefully dried dichloromethane in a glove

box, full conversion could be achieved with only 0.5 mol% of catalyst. However, reactions at such low catalyst loadings were difficult to reproduce.

After extensive experimentation a simple solution for avoiding catalyst deactivation was discovered, when testing an Ir-PHOX catalyst with tetrakis[3,5-bis(trifluoromethyl)phenyl]borate (BAr_F^-) as counterion.[4a] Iridium complexes with this bulky, apolar and extremely weakly coordinating anion[11] did not suffer from deactivation and full conversion could be routinely obtained with catalyst loadings as low as 0.02 mol%.[12] In addition, the BAr_F salts proved to be much less sensitive to moisture than the corresponding hexafluorophosphates. Tetrakis(pentafluorophenyl)borate and tetrakis(perfluoro-tert-butoxy)aluminate were equally effective with very high turnover frequency whereas catalysts with hexafluorophosphate and tetrafluoroborate gave only low conversion while reactions with triflate were completely ineffective (Figure 1).

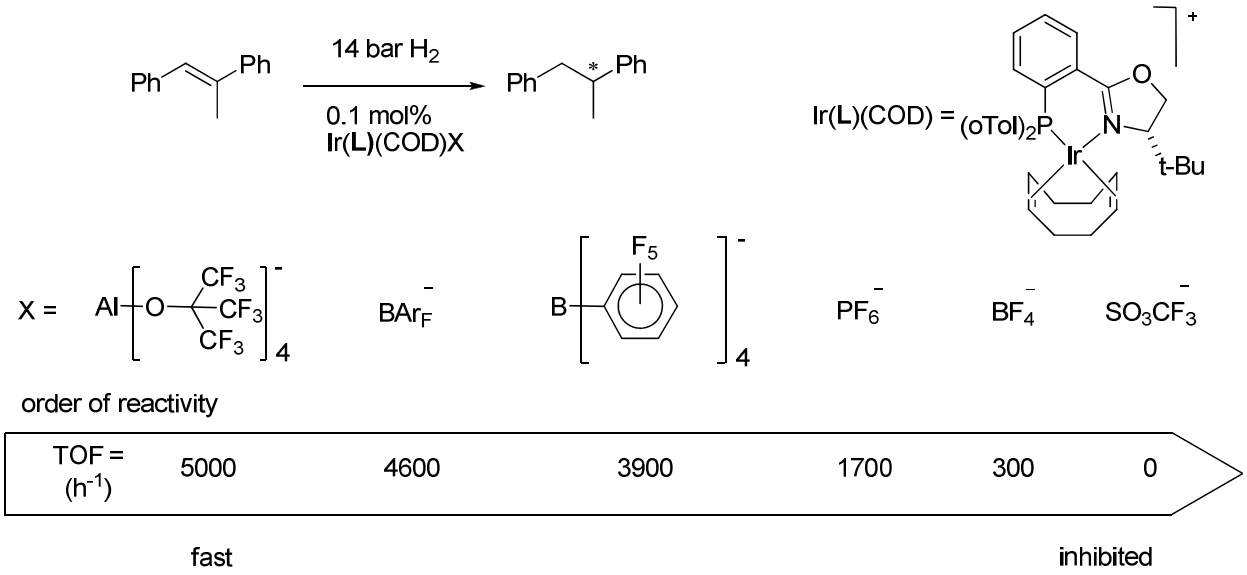

Figure 1. Order of reactivity of the complexes [Ir(PHOX)(COD)]X by TOF measured at 4°C with E-α-methylstilbene as substrate.

How can these bulky, extremely weakly coordinating anions prevent catalyst deactivation? A comparative kinetic study of catalysts with different anions provided a plausible answer.[12] With PF_6^- as counterion the rate dependence on alkene concentration was first order, whereas the rate order observed for the corresponding BAr_F^- complex was close to zero. This striking difference may be explained by the stronger coordination of PF_6^- or formation of a tight anion pair which slows down the addition of the alkene to the catalyst to such an extent that it

becomes rate-limiting. In contrast the essentially non-coordinating BAr_F^- ion does not interfere with alkene coordination and the catalyst remains saturated with alkene even at low substrate concentration. The slower reaction of the PF_6^- salt with the alkene could explain its higher tendency to undergo deactivation. If we assume that deactivation is caused by the formation of hydride bridged species leading to an inactive trinuclear complex, then the critical step in the catalytic cycle is the reaction of the Ir-hydride intermediate with the alkene. If alkene insertion is very fast, as in case of the BAr_F^- counterion, hydrogenation dominates over the deactivation pathway, whereas with the PF_6^- analogue the alkene reacts more slowly and deactivation becomes a significant competing process.

Virtually every iridium catalyst of the formula $[Ir(L^*)(COD)]^+ [X]^-$ for asymmetric alkene hydrogenation that has appeared after the initial counterion effect studies was based on BAr_F^- as the preferred anion. [7d] The anion effect is broadly applicable in iridium catalyzed reductions as experiments with a direct analogue of the Crabtree catalyst of the formula $[Ir(pyridine)(Cy_3P)(COD)]BAr_F$ indicates (Figure 2).

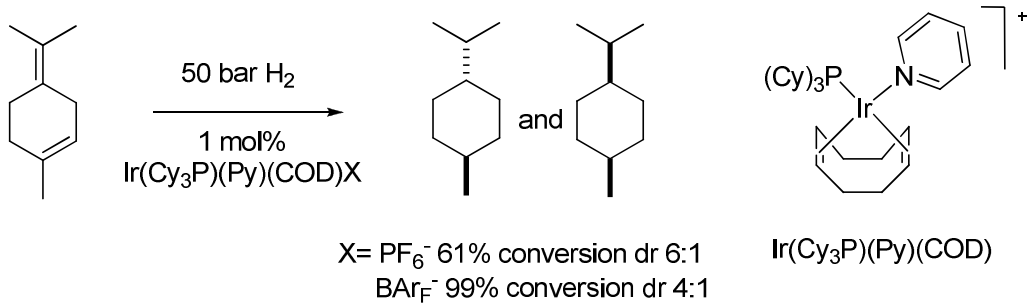

Figure 2. Comparison of Crabtree catalyst with the BAr_F analogue.

Hydrogenation of δ-terpinene (Figure 2) proceeded in higher conversion with Crabtree's catalyst with BAr_F counter ion rather than the normal PF_6. The BAr_F counter ion performed better in all instances where the more coordinating PF_6 salt failed to reach complete hydrogenation. [13]

1.2.2 NMR Investigations of Iridium PHOX Hydride Complexes

In early work of Crabtree and co-workers, alkene dihydride intermediates formed during hydrogenation of cyclooctadiene using $[Ir(pyridine)(PCy_3)(COD)]PF_6$ in dichloromethane at 0°C were detected by NMR spectroscopy.[14] In a more recent complementary study Mazet et al found that when $[Ir(PHOX)(COD)]BAr_F$ complex **1** was treated with hydrogen at -40 °C for 5

min in [D_8]-THF, alkene dihydride intermediates were formed which were characterized by NMR spectroscopy.[15a] Two new signals appeared in the hydride region that were assigned to a single dihydride complex **2c** formulated as [Ir(PHOX)$(H)_2$(COD)]BAr_F (Scheme 2).

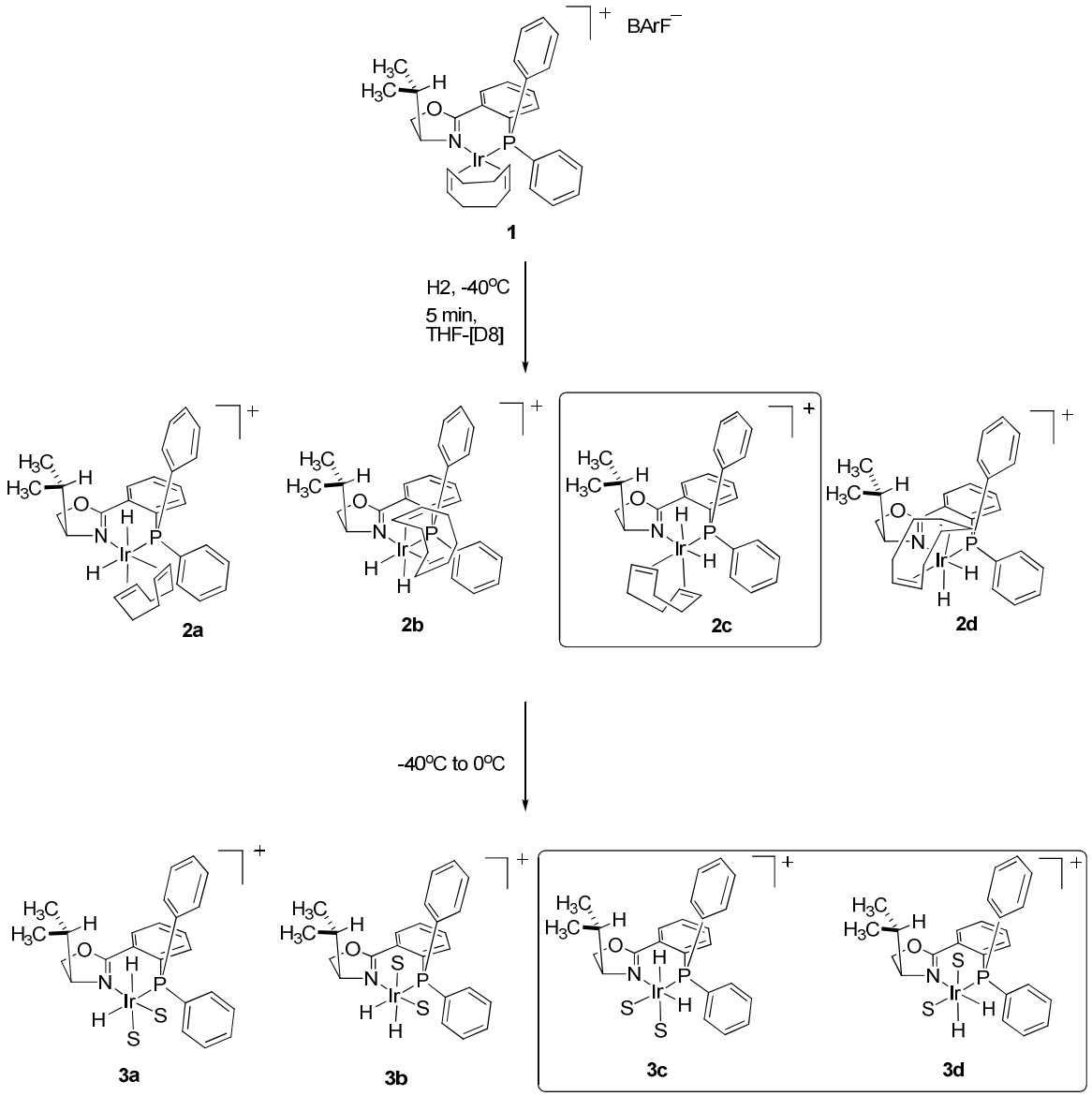

Scheme 2

The predominance of isomer **2c** over **2a** or **2b** is consistent with Crabtree's findings, who convincingly demonstrated that in the reaction of H_2 with [Ir(pyridine)(PR_3)(COD)]PF_6 the formation of an Ir-H bond trans to the N ligand is electronically favored.[17] Highly selective formation of isomer **2c** results from H_2 addition to the more sterically encumbered face of the starting complex because dihydrogen addition to the sterically more accessible face leading to

isomer **2d** would build up steric strain between the chelating COD ligand and the isopropyl group in the oxazoline ring and the pseudoaxial P-phenyl group. When the solution containing complex **2c** was warmed to 0˚C under hydrogen a gradual consumption of isomer **2c** was observed accompanied by the appearance of two new hydride complexes **3c** and **3d** with concomitant formation of cyclooctane.

1.2.3 Computational Studies and Additional Experiments

DFT (Density Functional Theory) calculations on the complete structures of complexes shown in Scheme 2 have been carried out by Mazet et al.[15] The fully minimized structures of the four possible cis-dihydrides formed by oxidative addition of H_2 to $[Ir(PHOX)(COD)]^+$ were calculated. The most stable structure corresponded to the reaction product **2c** that was shown to be formed exclusively in the NMR experiment. Isomers **2a** and **2d** were 10.6 and 4.9 kcal/mol higher in energy, whereas for isomer **2b** no stable chelate structure could be located due to severe steric interactions which prevent the formation of an Ir-N bond. The four possible $[Ir(PHOX)(H)_2(solvent)_2]^+$ complexes **3a-d** resulting from hydrogenation of the cyclooctadiene ligand were also examined and again the two most stable structures corresponded to the isomers observed in the NMR experiments. These results show that steric interactions are very important and may dominate over electronic factors. Consequently, computational studies of potential reactions pathways should be based on full catalyst and substrate structures rather than simple model systems.

Unfortunately, attempts to observe and characterize intermediates under catalytic conditions have been unsuccessful so far. When considering which intermediates may be formed during catalysis, one of the first issues which becomes apparent is what ligands are coordinated to iridium during catalysis. An alkene dihydride iridium complex which incorporates a bidentate N,P ligand has a sixth coordination site available for an additional ligand. Whereas coordination of a second molecule of alkene seems highly unlikely due to steric hindrance, dihydrogen and dichloromethane may both be effective ligands for iridium.

Thus two plausible catalytic cycles have been considered, one via an Ir dihydride complex **A** the other via an $IrH_2(\eta^2\text{-}H_2)$ complex **B** (Figure 4). The first is analogous to the well-established mechanism for rhodium diphosphine-catalyzed hydrogenation of alkenes going through Ir(I) and Ir(III) intermediates.[16]

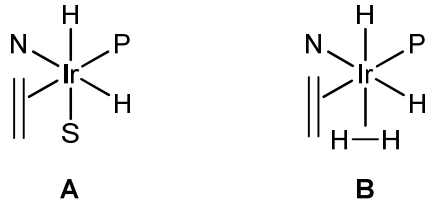

Figure 3. Possible Ir(III) and Ir(V) hydride intermediates (S = solvent).

Experimental support for an Ir(I)-Ir(III) mechanism was provided by Chen and Dietiker.[18] They reported an elegant experimental investigation of the hydrogenation of styrene with [Ir(PHOX)(COD)]BAr_F in the gas phase by means of electrospray ionization tandem mass spectrometry. By means of reversible deuterium labeling the investigators found masses corresponding only to intermediates with a mass corresponding to a dihydride complex with no presence of a trihydride species and concluded that no Ir(V) species with PHOX could be present in the catalytic reaction.

Based on DFT calculations Brandt et al proposed a catalytic cycle via Ir(III) and Ir(V) intermediates in which an additional dihydrogen molecule coordinated to an Ir-dihydride undergoes oxidative addition during migratory insertion.[19] However, since an extremely truncated model for the ligand and substrate (ethylene) was used which neglected the severe steric interactions present in the actual catalysts it seems premature to rule out an Ir(I)-Ir(III) cycle. From subsequent calculations on the full catalyst and substrate structures which were based on the postulated Ir(III)-Ir(V) cycle, a simple qualitative quadrant model was derived for rationalizing the observed enantioselectivities. Further studies by the same investigators on a complete complex with stereoelectronic contributions from both trans α- and β-methylcinnamic esters were investigated and applied to the model (Figure 4).[20] The authors concluded that in the case of the trans-β-methylcinnamic ester electronic and steric factors cooperated in their model to give high enantioselectivity. In the case of the trans-α-methylcinnamic ester steric interactions placed the migrating hydride onto the alpha carbon which would be electronically disfavored and thus lead to lower selectivities, both substrate selectivity observations being reflected by experimental results.

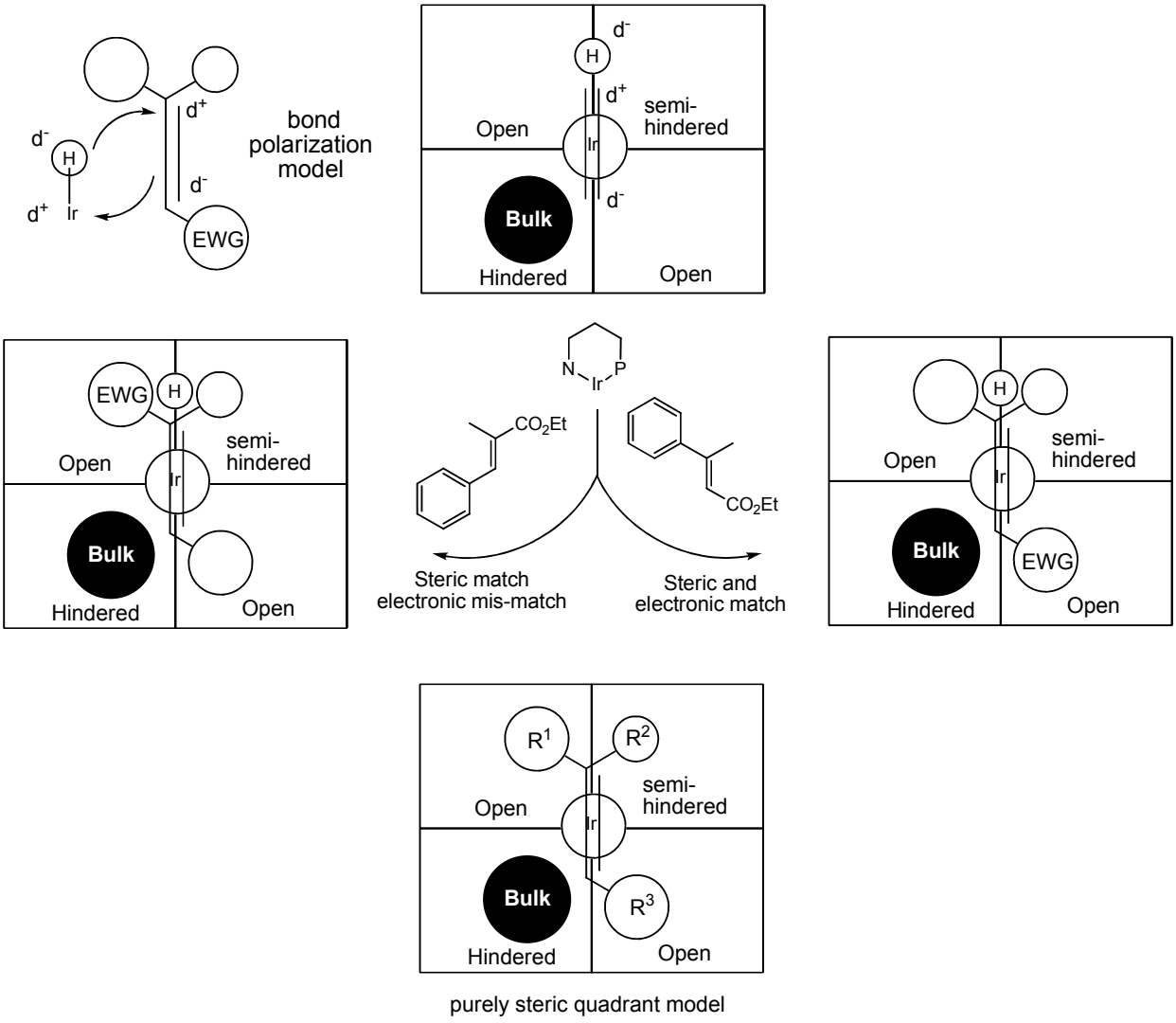

Figure 4. Anderssons quadrant model.

Fan et al also reported DFT calculations on the complete ligand and substrate structures with an iridium carbene based complex for an Ir(III)-Ir(V) catalytic cycle which reproduced the correct selectivity order for three different substrates.[21] Calculations on complete ligands and real substrates that reproduce experimentally determined enantioselectivities gives plausible credence to these authors' computational experiments.

Preliminary studies by Meuwly and Roseblade[15b-c] indicated that calculated pathways beginning from $[Ir(P\text{^}N)(H)_2(\eta^2\text{-}H_2)(\eta^2\text{-alkene})]^+$ complexes lead to predicted enantioselectivities which are opposite to the experimentally observed values. While competing pathways involving solvated Ir(I)-Ir(III) intermediates were somewhat higher in energy (by a few

kcal/mol), calculated transition states energies were in reasonable agreement with the experimentally observed enantioselectivities. Taking into account that CH_2Cl_2 as the solvent is present in much higher concentration than H_2, the Ir(I)-Ir(III) and Ir(III)-Ir(V) cycles become energetically very similar, making it difficult to distinguish between them based on calculations alone.

Thus, additional experimental and computational studies will be needed to draw definitive conclusions regarding the mechanism of Ir-catalyzed asymmetric hydrogenation. The Ir(I)-Ir(III) and Ir(III)-Ir(V) cycles seem to be similar in energy, so it may well be that depending on the catalyst, substrate and the hydrogenation conditions, one or the other pathway will be preferred, or both cycles could operate in parallel.

1.3 Asymmetric Hydrogenation of Trisubstituted Alkenes

1.3.1 Asymmetric Hydrogenation of Standard Test Substrates

Largely unfunctionalized trisubstituted alkenes are the most commonly investigated hydrogenation substrates in iridium catalyzed reductions.[7] As previously stated, strongly coordinating groups such as basic amines, alcohols, and strongly donating Lewis bases can in general slow the iridium catalysts down to a point where they are not effective. However, a number of alkenes with moderately Lewis basic functionalities such as acids, alcohols, esters, ketones, ethers, halogens and other similar groups adjacent or in proximity to the C=C bond have been successfully reduced with very high functional group tolerance and stereoselectivity. There is an increasing appearance of more coordinating functionalities such as enamines, indoles, imines and even pyridines, all of which will be touched on later sections of this chapter.

A survey of a list of typical ligands with reasonable asymmetric induction for the reduction of a commonly tested set of trisubstituted alkenes (Table 1) reveals several common features (Figure 5). Virtually all of the ligands consist of a heterocycle with a sp^2 hybridized nitrogen atom as a hard σ donor and a strong soft donor moiety such as a trisubstituted phosphorus atom or an N-heterocyclic carbene forming the second portion of the chelating ligand. Six membered metallacycles are the most investigated with the exception of the seven membered carbene ligand **9**, the seven membered spirocycles SpinPHOX **15a-c**, and the rigid spiroindanes SiPHOX **16a-d**. Stereogenic units have been incorporated with varying degrees of

success in all regions of the metallacycle backbone. Although some ligands display a wider range of acceptable enantioselectivity no single catalyst can be said to be generally applicable to all alkenes. The current trend is towards good selectivity in a given class of substrates with modifications to many of the existing scaffolds in an attempt to improve selectivity for important targets.

Many similarities to the classic PHOX ligand **5a-c** are clearly visible from the given ligand list in figure 5. As indicated by NMR and computational studies (see section 2.2 and 2.3) the coordinated alkene takes a position in a trans orientation from the soft donation moiety (i.e. phosphorus or carbene substituent) and adjacent to the nitrogen atom. In the PHOX system this places the alkene into close proximity with the stereogenic center of the ligand to create a well defined chiral environment. Ring size of the metallacycle plays an extremely important role in governing catalyst reactivity. Catalysts derived from ligands **8a-f** and **10a-d** are some of the most selective catalysts known for unfunctionalized trisubstituted alkenes.[20, 21-24] While they have proven very selective for trisubstituted alkenes they fail to produce high selectivity or reactivity with the substrate classes of tetrasubstituted alkenes, terminal alkenes, and 1,3-dienes.

The catalyst derived from ligand **9** perform well with several classes of alkenes albeit with slightly lower enantioselectivities in reduction of trisubstituted alkenes but are remarkably reactive towards 1,3-dienes.[7a, 20] Further examples of size of the iridium metallacycle controlling selectivity and reactivity comes from the substrate profile of the 5-membered iridium chelates from ligands **12a-e,** which reduce tetrasubstituted alkenes under mild conditions and high conversions but give unacceptable enantioselectivity with less substituted alkenes.[7c]

On consultation of Table 1 it becomes apparent that small changes in overall geometry about the metal center as well as the donation capabilities to the metal center can have a drastic effect on the selectivity. PHOX ligand **5b** compared with the later permutation of SimplePHOX ligand **7a** have the same 4-tert-butyl-4,5-dihydrooxazole moiety as a stereo defining group and nearly the same steric environment about the phosphorus atom yet they give drastically different enantioselectivity. ThrePHOX **6a-f** ligands are highly selective and active catalysts which incorporate effective modifications on the PHOX progenitor. In comparison to both PHOX and the later derivative SimplePHOX the stereogenic unit of ThrePHOX has been moved to the center of the backbone and transmits chirality to both sides of the chelate.[25a-c]

Other features of note are observed when the phosphinite group of SimplePHOX is replaced by a phosphine in the newer NeoPHOX ligand **14a-c**, resulting in some small improvements in enantioselectivity but with the added advantages of a phosphine over the more reactive phosphinite.[25d] The lack of overall changes to selectivity for these simple substrates may reflect that alteration in overall geometry, most importantly the bite angle, matter more to reactivity then electronic changes to the soft donor group. Ligands **20a-b** provide reasonable selectivity but actually less than the parent SimplePHOX and at a cost of a more complicated synthesis, strong indication that optimal interactions were disrupted by the excess chiral and steric encumbrance.[25e]

Other examples of adding too much bulk in the context of the general substrates comes in the form of ligand **24**.[26] While the ligand maintains many of the stereochemical features of ligand **5c** the added bulk leads to much lower enantioselectivities and conversion by disrupting interactions necessary for substrate binding. Similar effects are seen with ligands **21a-d**, which are closely related to the very active catalysts derived from **8a-c**, **10a-d**, and **11a-b** with the exception of the deleterious addition of extra ring rigidity and steric encumbrance from the carbon bridge.[27a]

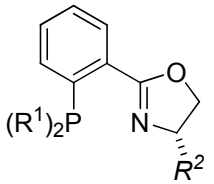

5a R^1 = Ph R^2 = *i*-Pr
5b R^1 = *o*-Tol R^2 = *t*-Bu
5c R^1 = Ph R^2 = *t*-Bu
ref [4, 5, 7-12, 35b-c, 44b, 52]

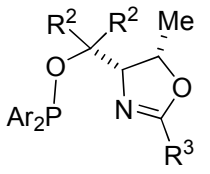

6a Ar = Ph R^2 = Bn R^3 = Ph
6b Ar = Cy R^2 = Bn R^3 = Ph
6c Ar = *o*-Tol R^2 = Bn R^3 = Ph
6d Ar = Ph R^2 = Me R^3 = Ph
6e Ar = Ph R^2 = Bn R^3 = 3,5-di-CH_3-C_6H_3
6f Ar = Ph R^2 = Bn R^3 = 3,5-di-*t*-Bu-C_6H_3
ref [25b-c, 38a, 44b, 45]

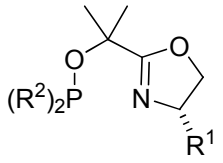

7a R^1= *t*-Bu R^2 = *o*-Tol
7b R^1= *i*-Pr R^2 = *o*-Tol
7c R^1= *i*-Pr R^2 = Ph
7d R^1= *t*-Bu R^2 = Ph
ref [25a, 29a, 52]

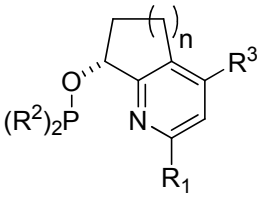

8a n = 1 R^1 = Ph R^2 = *t*-Bu R^3= H
8b n = 1 R^1 = Ph R^2 = *o*-Tol R^3= H
8c n = 2 R^1 = Ph R^2 = *o*-Tol R^3= H
8d n = 1 R^1 = Ph R^2 = *t*-Bu R^3= Me
8e n = 1 R^1 = Ph R^2 = *o*-Tol R^3= Me
8f n = 2 R^1 = Ph R^2 = *o*-Tol R^3= Me
ref [22-24, 29b, 45]

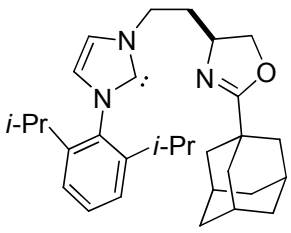

9
ref [7, 21, 32-33, 41]

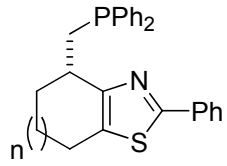

10a n= 1
10b n= 2
10c n= 3
10d n= 2 Ph = *o*-Tol
ref [7, 30a]

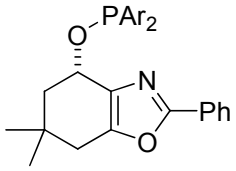

11a Ar = Ph
11b Ar = *o*-Tol
ref [7]

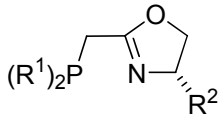

12a R^1 = Ph R^2 = *i*-Pr
12b R^1 = Cy R^2 = CH_2-*t*-Bu
12c R^1 = Cy R^2 = Ph
12d R^1 = Cy R^2 = Bn
12e R^1 = *o*-Tol R^2 = *i*-Pr
12f R^1 = Ph R^2 = CH_2-*t*-Bu
12g R^1 = Adm R^2 = Ph
12h R^1 = Adm R^2 = *t*-Bu
ref [34, 39]

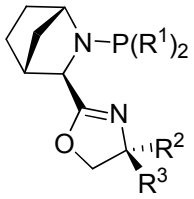

13a R^1 = Ph R^2 = H, R^3 = *i*-Pr
13b R^1 = *o-Tol* R^2 = H, R^3 = *i*-Pr
13c R^1 = Ph R^2 = Ph R^3 = Ph
13d R^1 = Ph R^2 = H, R^3 = *t*-Bu
ref [30a, 31, 42, 43, 44a, 44a-b]

Figure 5. Frequently used N,P and C,N ligands.

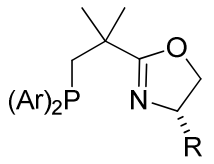

14a Ar = Ph R = *t*-Bu
14b Ar = *o*-Tol R = *t*-Bu
14c Ar = Xyl R = *t*-Bu
14d Ar = Ph R = *i*-Pr
ref [25d, 52]

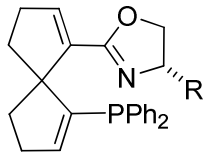

15a (R,S) R = *i*-Pr
15b (R,S) R = *i*-Bu
15c (S,S) R = *i*-Bu
ref [51b]

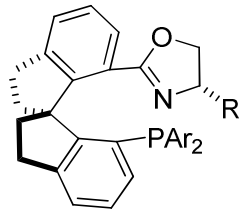

16a Ar = Xyl R = Bn
16b Ar = 3,5-di-*t*-Bu-C_6H_3 R = Bn
16c Ar = 3,5-di-*t*-Bu-C_6H_3 R = H
16d Ar = 3,5-di-*t*-Bu-C_6H_3 R = *i*-Pr
ref [36b, 51a]

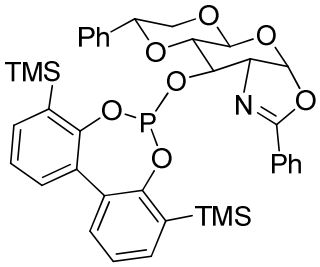

17
ref [27b]

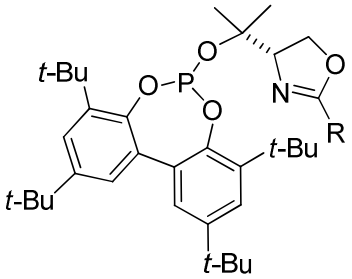

18a R = Ph
18b R = 2,6-di-CH_3-C_6H_3
ref [38b]

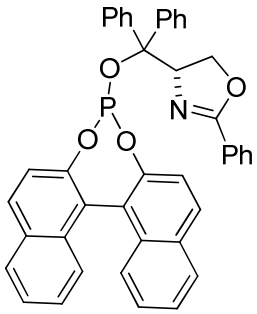

19
ref [38b]

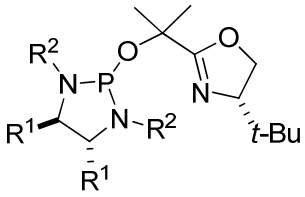

20a R^1 = Ph R^2 = 3-OMe-C_6H_5
20b R^1 = Ph R^2 = 4-OMe-C_6H_5
20c R^1 = Ph R^2 = 4-*t*-Bu-C_6H_5
20d R^1 = Ph R^2 = 4-Ph-C_6H_5
20e R^1 = Ph R^2 = 2-napthyl
20f R^1 = Ph R^2 = 1-napthyl
20g R^1 = -$(CH_2)_2$- R^2 = 4-Me-C_6H_5
ref [25e]

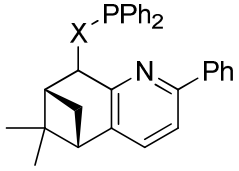

21a *trans* X = CH_2
21b *cis* X = CH_2
21c *trans* X = O
21d *cis* X = O

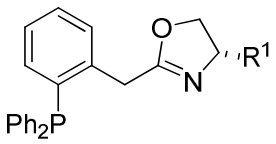

22a R^1= *i*-Pr
22b R^1 = *t*-Bu
ref [35c]

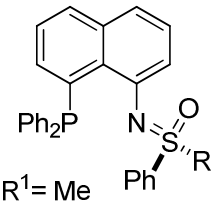

23a R^1= Me
23b R^1= Et
23c R^1= *i*-Bu
23d R^1 = $Ph(CH_2)_2$
ref [35a-b, 46b]

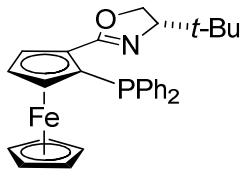

24
ref [26, 35c, 36a 46a]

Figure 5 continued.

Table 1. Asymmetric hydrogenation of standard substrates with chiral N,P and C,N iridium catalysts.

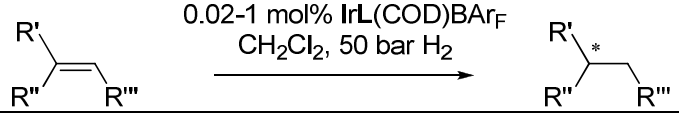

		Ligand ee %[a]						
	Substrate	**5**	**6**	**7**	**8**	**9**	**10**	**11**
25a	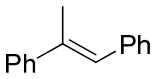	**b** 97	**a** 99	**a** 98	**a-c** 99	99	**a-d** 99	**a** 99
25b	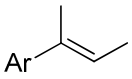	**b** 81	**a** 99	**a** 91	**a-c** 99	97	**a-d** 99	**a** 90
25c	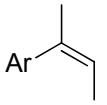	**b** 63	**e** 92	**a** 89	**a** 98	80	**-**	-
25d	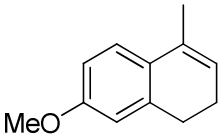	**b** 72	**f** 95	**a** 95	**a** 92	**-**	**b** 55	**b** 94
25e	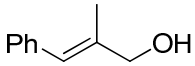	**b** 96 (95)	**a** 92	**a** 97	**a** 97	93	**b,d** 97	**b** 98 (95)
25f	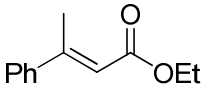	**b** 84 (96)	**f** 96	**a** 94	**a** 99	**-**	**b,d** 98	**b** 93

a) All conversions less than 99% are noted next to the enantioselectivity in brackets, Ar = 4-$MeOC_6H_4$.

Table 1 Continued.

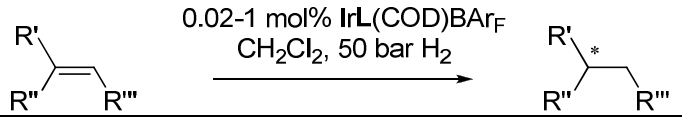

		Ligand ee %[a]						
	Substrate	**13**	**14**	**17**	**18**	**20**	**21**	**24**
25a	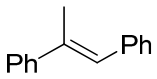	**c** 98	**a** 98	99	**a-b** 99	**b,g** 99	**a** 94 (35)	78
25b	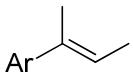	**c** 99	**a** 89	99	**b** 99	**d** 94	**a** 94	-
25c	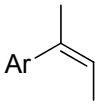	**-**	**c** 96	92	**a** 95	**f** 88	**a** 43 (18)	-
25d	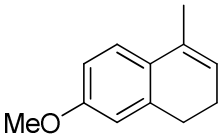	**c** 95	**b** 96	96	**-**	**e** 83	**a** 97	89 (95)
25e	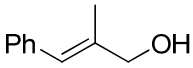	**-**	**b** 96	93	**b** 92	-	**a** 45 (5)	99
25f	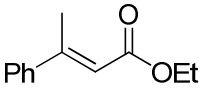	**a** 88	**a** 95	99	**b** 99 (85)	**c** 98	**a** 55 (10)	82

a) All conversions less than 99% are noted next to the enantioselectivity in brackets, Ar = 4-MeOC$_6$H$_4$.

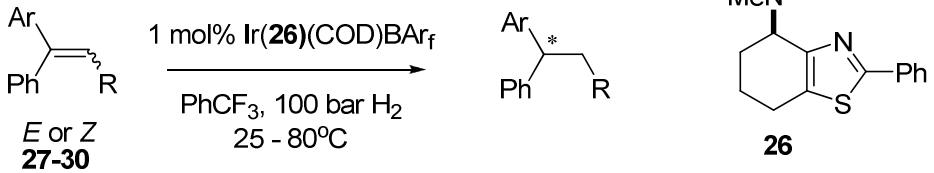

(*E*)-**27:** Ar= 4-Br-C$_6$H$_4$ R= Me: 95% ee (*S*)
(*Z*)-**27:** Ar= 4-Br-C$_6$H$_4$ R= Me: 99% ee (*R*)

(*E*)-**28:** Ar= 4-Ph-C$_6$H$_4$ R= n-pent: 99% ee (+)
(*Z*)-**28:** Ar= 4-Ph-C$_6$H$_4$ R= n-pent: 99% ee (-)

(*E*)-**29:** Ar= 2-Me-C$_6$H$_4$ R= Ph: 92% ee (+) 35% Conv L = **10b**
(*E*)-**30:** Ar= 4-CF$_3$-C$_6$H$_4$ R= Ph: 76% ee (*S*) 48% Conv

Scheme 3

While Table 1 is an important tool for many of the studies the current trend is to more elaborate and increasingly difficult substrates within a particular class of alkenes. Andersson and coworkers have published several variations of the 1,2-diaryl substrate **25a** for the fairly more difficult 1,1'diaryl class of trisubstituted alkenes (Scheme 3).[28] The authors note that the products form an important class of compounds that are pharmaceutically relevant and difficult to prepare by other available methods.

Reduction of all of the reported geminal diaryl substrates were completely under the control of the third stereo defining R-group. Particularly difficult were the sterically demanding **29** and the electron poor alkene **30**, both of which required heating to produce poor to moderate yields.

The reduction of simple trisubstituted alkenes derived from **25d** has found use in the enantioselective total synthesis of pseudopteroxazole **31c**, demethyl methoxycalamenene **32c**, and both enantiomers of mutisianthol **33c** (Scheme 4).[25d, 29]

SimplePHOX **7a** proved a useful tool to force the diastereomeric reduction of alkene **31a** to pseudopteroxazole precursor **31b** in perfect diastereoselectivity and 90% yield with only trace amounts of over reduced product. NeoPHOX catalyst from ligand **14b**, a closely related system to **7a**, furnished product **32b** in 93% ee which was then easily recrystallized to enantiopure material with 58% recovery. The *R* enantiomer of **33b** was synthesized by use of catalyst from ligand **8a** in 90% ee and 98% yield with the fully aromatized naphthalene as 2% byproduct. A higher catalyst loading of 2 mol% of catalyst from **7a** was used to produce the *S* enantiomer in 80% ee with 13% of the fully aromatized naphthalene byproduct occurring even when using 50 bar of hydrogen pressure. Lower catalysts loadings gave increased amounts of aromatization byproduct and lower enantioselectivity.

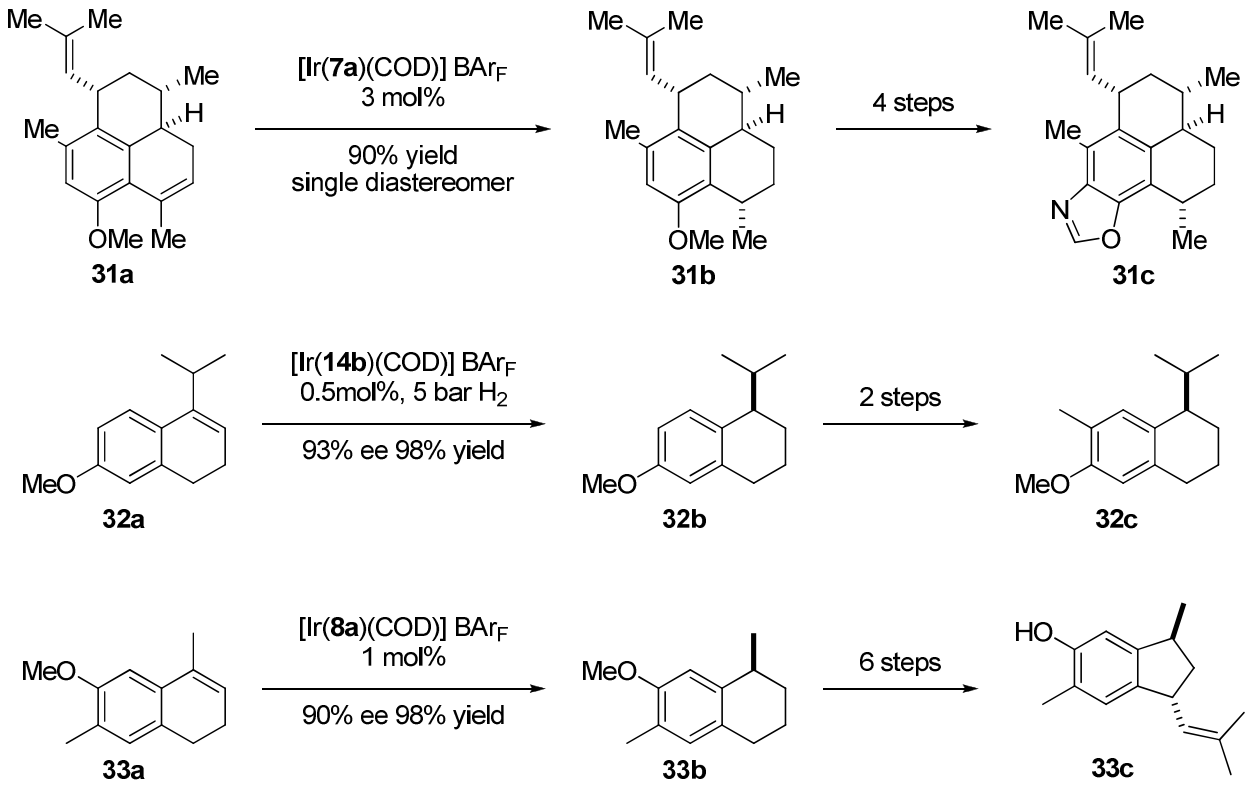

Scheme 4

Asymmetric hydrogenation of cyclic alkenes is not the sole application of this methodology in synthesis and the current trend in research is to use these catalysts in building more elaborately functionalized molecules.

1.3.2 Asymmetric Hydrogenation of Purely Alkyl Substituted Alkenes

The development of chiral homogeneous catalysts with the capacity to reduce purely alkyl substituted alkenes with high asymmetric induction and yield has been a long standing problem. Most iridium catalysts that perform well with nothing more coordinating than a phenyl group adjacent to the alkene fail to give good asymmetric induction in the absence of an aromatic substituent in close vicinity to the C=C bond.[7]

As a first step to solving this problem Bell et al started an active screening project utilizing *E* and *Z* isomers of compound **34a** as a model (Scheme 5).[23] Although **34a** contains an aromatic substituent for analytical purposes the functional group has been moved 3 bonds away from the carbon carbon double bond. If any coordination took place through this remote site the effect was expected to be weak. Out of the screening effort pyridine phosphinite ligands **8a-c**

were identified as excellent ligands giving high enantioselectivity and conversion. Both *E* and *Z* isomers gave acceptable enantioselectivity. As observed in other cases the *E* and *Z* isomers were converted to opposite enantiomers. In order to rule out any small interactions from the distal aromatic ring the completely alkyl substituted alkene **35a** was reduced under standard conditions. Fittingly ligand **8a** provided the branched chiral alkane **35b** in 92% enantioselectivity.

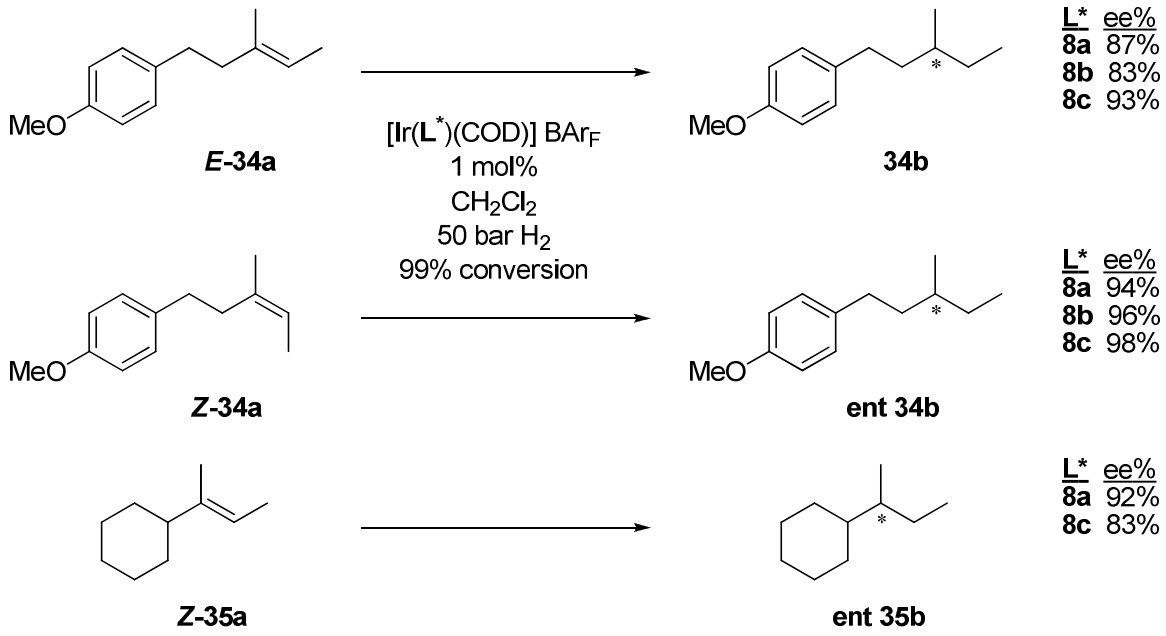

Scheme 5

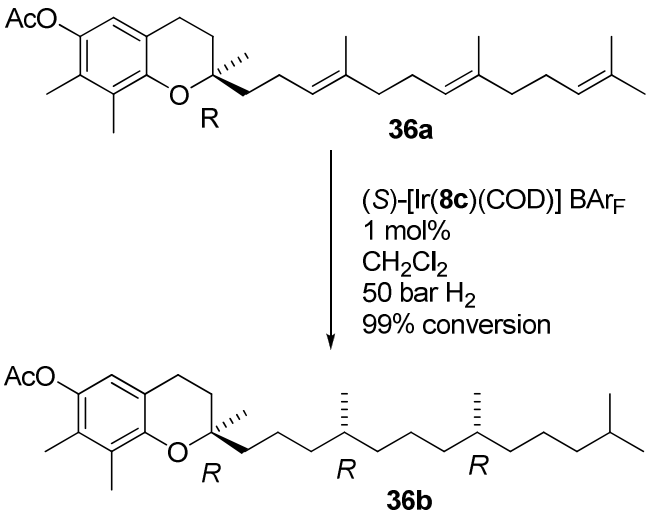

>98% *RRR* (<0.5% *RRS*; <0.5% *RSR*; <0.5% *RSS*)

Scheme 6.

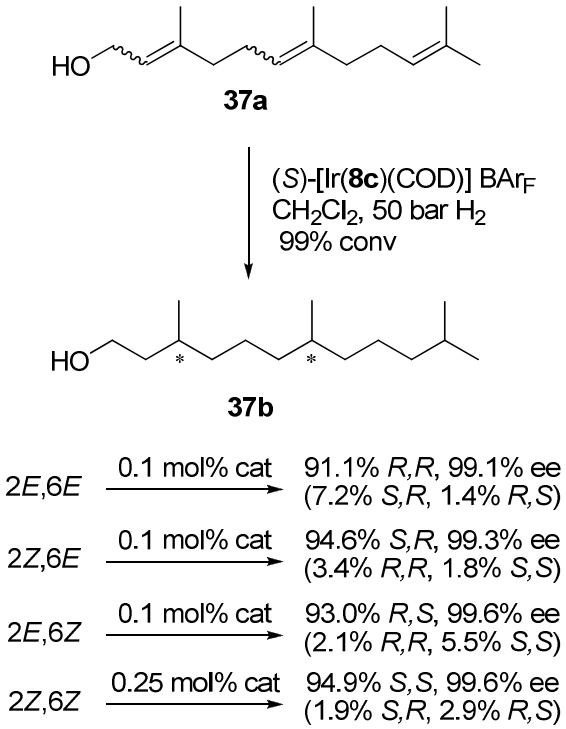

Scheme 7

Because *cis* and *trans* alkenes are converted to products of opposite configuration, it becomes possible to introduce two or more stereogenic centers with the desired relative and absolute configuration in a single step through hydrogenation of a di- or polyene by adjusting the geometry of the individual C=C bonds. This is demonstrated by the highly enantio- and diastereoselective preparation of γ-tocopherol **36b,** a component of vitamin E, from γ-tocotrienyl acetate **36a** (Scheme 6).

In a subsequent publication the fully optimized stereospecific synthesis of each individual diastereomer and its corresponding enantiomer with catalyst loadings of **8c** from 0.1 to 0.25 mol% was reported (Scheme 7).[24] Electron withdrawing protecting groups attached to the allylic alcohol slowed down the reaction rate and higher catalyst loadings were required to achieve full conversion. The authors conducted a grams scale synthesis of (*R,R*)-**37b** in comparable yield and enantioselectivity to the test reactions, illustrating the practicality of this approach.

1.3.3 Asymmetric Hydrogenation of Fluorinated Alkenes

Chiral organofluorides are increasingly in demand as the pharmaceutical and materials industries seek to take advantage of the special properties these halides impart. A lack of methods to provide chiral monofluorides and trifluoromethyl groups has given the group of Andersson impetus to create new asymmetric hydrogenation routes to these valuable halides.[30]

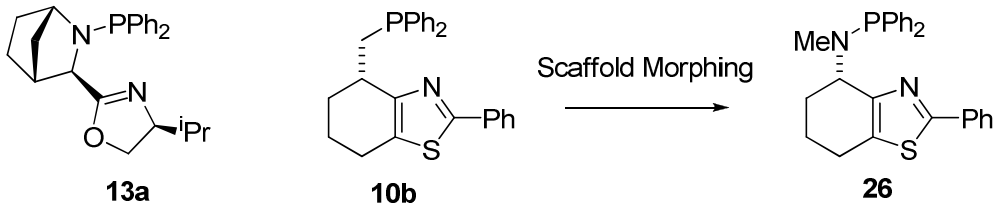

Figure 6. Scaffold morphing to improve dehalogenation profile.

A brief scope of α-fluorocinnamic acid derivatives with both trisubstituted and tetrasubstituted C=C bonds were reduced with mixed results (Scheme 8).[30a] The vinyl fluorides proved extremely difficult for catalysts that usually perform superbly on more frequently studied substrates. Elevated temperatures and pressures were required to obtain moderate to good conversions with closely related substrates. A struggle with dehalogenation occurred with the harsher conditions required for this difficult reaction. The group noticed that phosphoramide ligands **13a-c** gave lower amounts of dehalogenation and new phosphoramide **26** was developed by the group to incorporate the best of both of their original ligands (Figure 6). This catalyst gave improved enantioselectivity and less dehalogenation (Scheme 8).

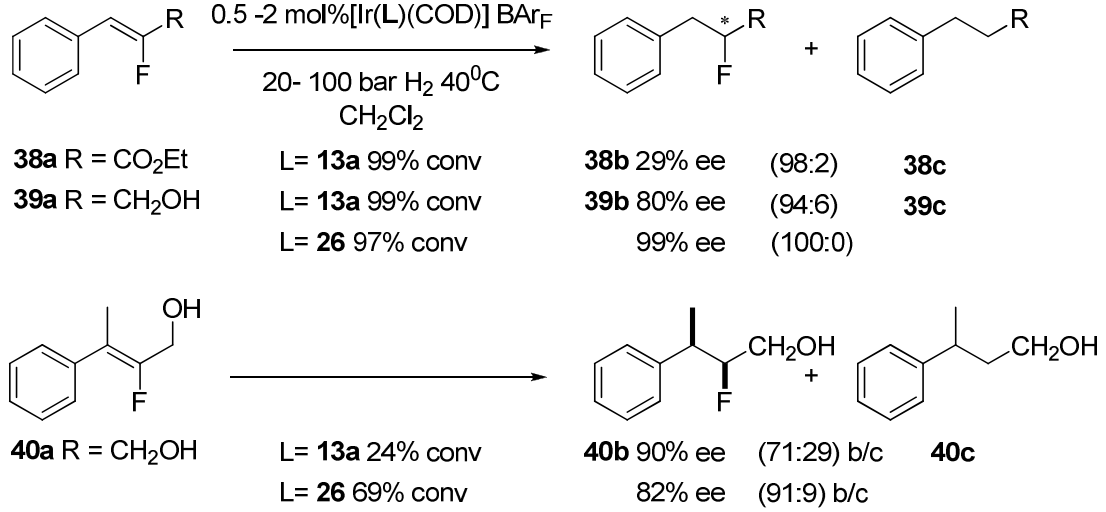

Scheme 8

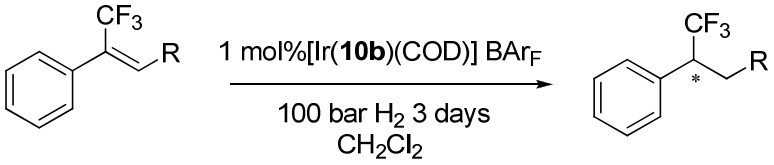

41 R = Alkyl chain 85-94% conv **42** 92-96% ee

Scheme 9

Evidently vinylfluorides represent a new challenge to iridium asymmetric hydrogenation. It is noteworthy that no examples of asymmetric reduction of vinyl fluorides without adjacent coordinating groups have been reported in the literature.[7d]

Trifluoromethyl substituted alkenes appear to also be problematic substrates for asymmetric hydrogenation as very long amounts of time and high pressures were required to achieve appreciable yields with ligand **10b** (Scheme 9).[30b] Nevertheless, useful yields and excellent enantioselectivities were obtained for most examples.

1.3.4 Asymmetric Reduction of Vinylboronates

Boronic esters have been used in a wide range of transformations. These useful reagents have been transformed into numerous functional groups and are essential reagents for several C-C bond forming reactions. Transition metal catalyzed hydroboration of alkenes often leads to mixtures of branched and linear products. Several groups have reported asymmetric reductions of vinyl boronic esters[31a-c] with chiral rhodium P,P complexes, however, the first iridium catalyzed reduction was reported by (Scheme 10).[31d]

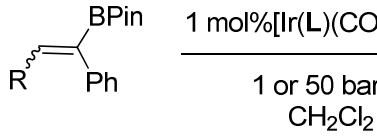

1 mol%[Ir(**L**)(COD)] BAr_F

1 or 50 bar H_2
CH_2Cl_2

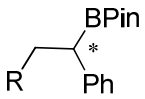

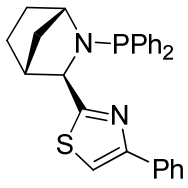

46

(*Z*)-**43a** R = Ph	L= **13b** 50 bar H_2	**43b** 98% ee 99% conv
	1 bar H_2	98% ee 64% conv
44a R = H	L= **13d** 50 bar H_2	**44b** 89% ee 99% conv
	1 bar H_2	74% ee 99% conv
(*E*)-**45a** R = BPin	L= **46** 50 bar H_2	**45b** 67% ee 99% conv
	1 bar H_2	96% ee 99% conv

Scheme 10

In contrast to normal trisubstituted aryl alkenes, a strong pressure effect was observed in this case. Interestingly, for substrate **44a** catalysts hydrogenation with Ir(**13d**) demonstrated opposite pressure dependant enantioselectivity of substrate **45a** with catalyst Ir(**46**). Poor enantioselectivity was obtained for substrates that did not contain an aromatic ring adjacent to the alkene.

1.3.5 Diastereoselective Reduction of Alkenes

Although functional group directed enantioselective hydrogenation tends to fall in the realm of rhodium and ruthenium catalysts there are many examples of diastereoselective hydrogenations with Crabtree's catalyst that are controlled by coordination of the iridium center to a Lewis basic functional group (Figure 7). When one considers that iridium catalysts do not require coordinating groups for hydrogenation activity and purely steric interactions suffice for enantioface discrimination then protection of the directing group with a large noncoordinating moiety could reverse the direction of attack by the catalyst to create the opposite diastereomer protected equivalent (Figure 7).

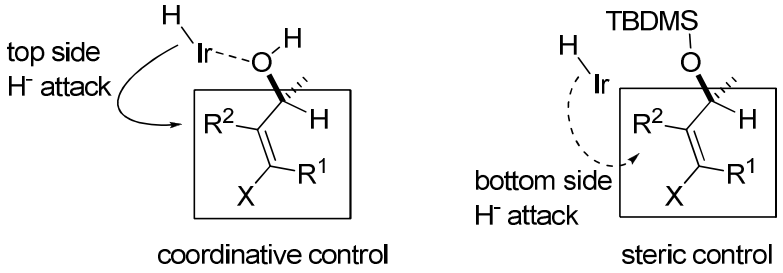

Figure 7. Diastereoselective hydrogenation based on catalyst and substrate control.

Diastereoselective hydrogenations of this type have been reported by Burgess and coworkers[32-33] using chiral protected and unprotected allylic and homo allylic alcohols as substrates with their carbene catalyst Ir(**9**). Catalyst control was found to be dominant but depending on the position and nature of the oxygen substituents moderate to strong match/ mismatch effects were observed.

This approach has been used to synthesize a variety of valuable 1,3-deoxypolyketide chirons, 1,3-hydroxymethyl chirons, vicinal dimethyl chirons, and aldol like products from

trisubstituted alkenes (Scheme 11). High diastereomeric ratios could be obtained often in greater than 90% for most cases.

A reasonably large difference in diastereomeric excess was observed between product **47b** with an adjacent methyl ester and **48b** with a primary alcohol in the equivalent position.[33a] It was noted by the authors that in cases involving a 1,3 system changing the pendant group from a primary allylic alcohol to a methyl ester caused a reversal of facial selectivity.[32a, 33b] The same effect was absent in the 1,2 systems **51b** and **52b** studied. The diastereomeric ratio in the latter case was attributed mainly to catalyst control.[33b]

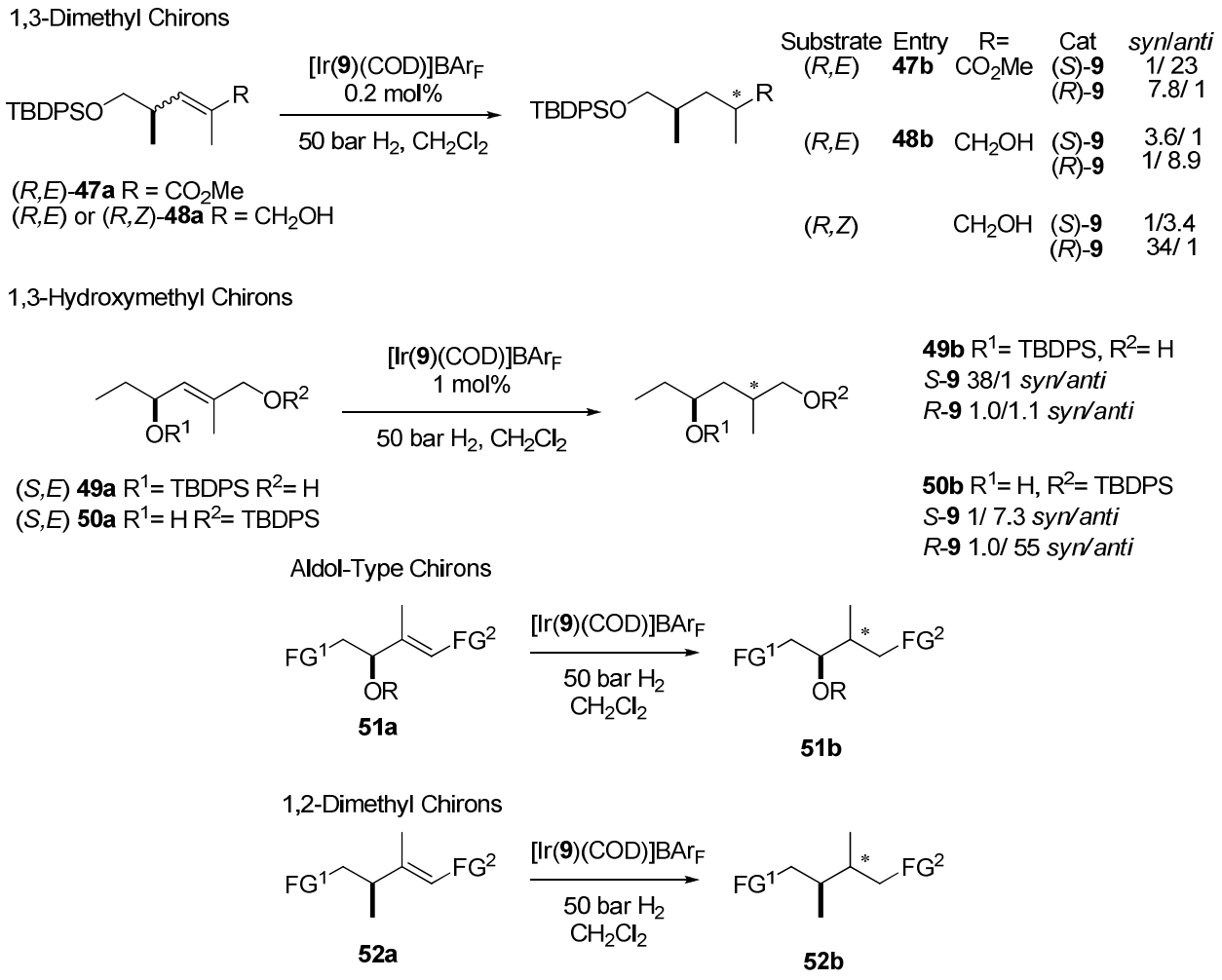

Scheme 11.

1.3.6 Redox Rearrangement of Allylic Alcohols to Chiral Aldehydes

Mazet et al have reported an efficient asymmetric isomerization reaction of allylic alcohols [34]. In a preliminary report they utilized the BAr_F analogue of Crabtree's complex to efficiently catalyze a hydride transfer from the α position of the allylic alcohol to the β position of the alkene with a concomitant formation of a formyl group. A subsequent report detailed a remarkable enantioselective variant of this process catalyzed with Ir(**12g**) and (**12h**) (Scheme 12).

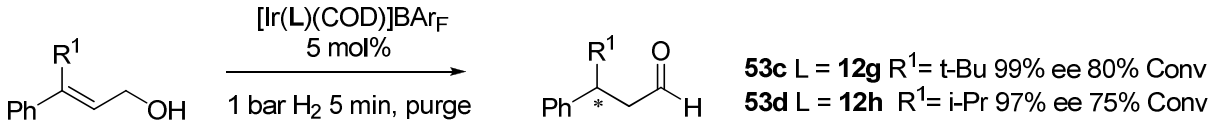

Scheme 12

The iridium catalyst was activated by briefly purging the system with atmospheric pressure of hydrogen to remove the COD ligand followed by degassing the system with vacuum and inert atmosphere to avoid over reduction. High enantioselectivities were obtained in moderate to good yields with a limited range of substrates. The system studied was very sensitive to ligand geometry, namely 5-membered metallacycles were much more efficient than 6-membered analogues and bulky substrates with aromatic substituents were required for high selectivity.

1.3.7 Conjugate Reduction

Catalytic asymmetric conjugate reductions represent one of the most venerable and investigated reaction types in catalysis. Conjugate reductions with rhodium and ruthenium diphosphine based catalysts have been heavily investigated and substituted α,β-unsaturated acids and esters are frequent substrates for these systems. Iridium N,P based reductions are more recent and far less investigated but offer chemoselectivity advantages under certain circumstances.[35a] Ester **25f** is the most regularly investigated conjugate reduction substrate and has been a general benchmark for evaluating the selectivity and reactivity of iridium N,P based catalysts for many years. It has also been described that the trans-α-methylcinnamic esters have been particularly difficult substrates for reduction and this has been rationalized by computational methods.[20] Nearly all

systems that have been investigated are based on a cinnamic acid core with different substitution patterns about the α and β carbons. Varying degrees of electrophilic groups have been incorporated to the conjugate system such as ketones, esters, acids, amides, diphenylphosphine oxides, and phosphonates.[32-33, 35-37]

Iridium catalyzed reduction of α,β-unsaturated ketones has been investigated most recently by the groups of Bolm and Hou, respectively.

Table 2. Enantioselective hydrogenations of linear α,β-unsaturated ketones.

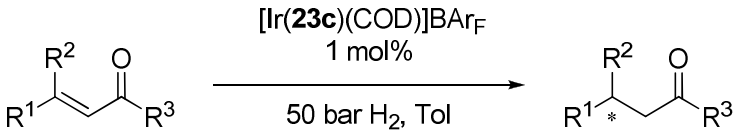

substrate	Substrate	Yield %	ee %
54a	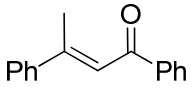	89	81
54b	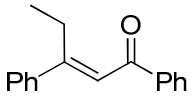	94	89
54c	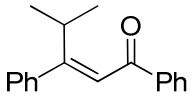	94	97
54d	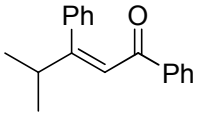	86	92
54e	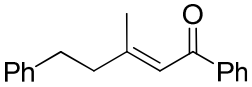	93	81
54f	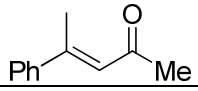	70	79

As Table 2 indicates ligand **23c** proved effective for substrates with large branched groups on the beta positions. The best selectivity was obtained for **54c** which was substituted with aromatic groups on both sides of the substrate and a large branched alkyl attached to the β position.[35a] Entries **54e** and **54f** are encouraging and may indicate that this method could be extended to more broadly useful compounds. The investigators performed a solvent study and determined the reaction to be equally selective in toluene and dichloromethane so the former was used presumably for its industrial attractiveness.

A broader range of substrates have been reduced with substitution at the α position of α,β-unsaturated ketones using ligand **5c**.[35b-c]

Table 3. Enantioselective hydrogenations of α-substituted α,β-unsaturated ketones.

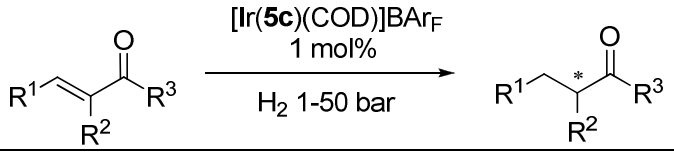

substrate	R^1	R^2	R^3	yield (conv) %	ee %
55a	Ph	Me	Me	91[a] (100[b])	98[a] (98[b])
55b	Ph	Me	Et	91[a]	98[a]
55c	Ph	Me	Ph	96[a] (100[b])	99[a] (97[b])
55d	Ph	Ph	Me	94[a]	98[a]
55e	4-$MeOC_6H_4$	Et	*n*-Pr	(100[b])	(98[b])
55f	Et	Me	Ph	89[a]	87[a]
55g	H	Bn	Ph	84[a]	86[a]
55h	2-MeC_6H_4	Me	Me	89[a]	98[a]
55i	2-$MeOC_6H_4$	Me	Me	90[a]	99[a]
55j	2-ClC_6H_4	Me	Me	89[a]	98[a]
55k	3-$MeOC_6H_4$	Me	Me	93[a]	99[a]
55l	3-ClC_6H_4	Me	Me	92[a]	98[a]
55m	3-$NO_2C_6H_4$	Me	Me	91[a]	98[a]
55n	4-$MeOC_6H_4$	Me	Me	97[a]	98[a]
55o	4-ClC_6H_4	Me	Me	92[a]	99[a]
55p	4-$NO_2C_6H_4$	Me	Me	88[a]	99[a]

a) Hydrogenations were carried out in toluene.[35b] b) Hydrogenations were carried out in dichloromethane.[35c]

Table 3 indicates that reduction of α substituted unsaturated ketones is extremely efficient with PHOX **5c**. Unfortunately, substrates lacking any aromatic ring within close proximity to the alkene were reportedly not reduced.[35c] However, a wide range of functional groups were shown to be tolerated by Bolm et al.[35b] Most impressively, nitroaromatic compounds were well tolerated under the conditions used, highlighting the extraordinary chemoselectivity that can be obtained with iridium N,P catalysts. Perhaps one of the most productive features of these studies is the ability to create a stereogenic center with high degrees of substitution and perfect acyclic stereocontrol while maintaining an unencumbered site α to the carbonyl group for further elaboration.

Substituted α,β-unsaturated amides have also been reduced with high enantioselectivity and conversion with ligand **24**.[36a] Here as well the investigations relied heavily on substrates with adjacent aromatic rings and α substitution. Catalyst loadings were moderately higher than with other systems with 2 mol% used. Table 4 indicates that ligand **24** can tolerate a wide range of substituents on the amide nitrogen but fairs best with the more sterically demanding groups such as isobutyl or benzyl. The use of more coordinating groups such methoxyethyl **56e** or the versatile Weinreb amide **56f** results in a moderate to severe erosion of enantioselectivity. Some of the more sterically demanding substrates such as **56h** were reduced with a moderate loss of enantioselectivity.

Recently developed ligand SIPHOX **16a-d** proved a valuable tool in the asymmetric reduction of α,β-unsaturated acids [36b]. In a complete break with what is typically observed with iridium based N,P ligands SiPHOX catalysts were observed to reduce the strongly coordinating carboxylic acid triethylamine salt of α methylcinnamic acid in excellent enantioselectivity and yield (Table 5). Equally surprising is the use of methanol as a solvent, which normally inhibits reductions mediated by iridium N,P catalysts.

Table 4. Asymmetric hydrogenation of α-substituted α,β-unsaturated amides with ligand **24.**

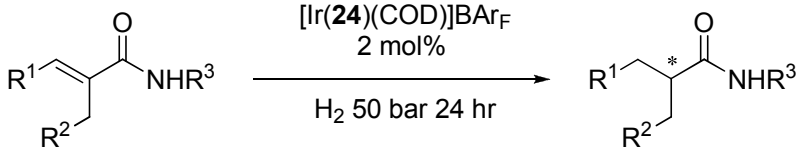

substrate	R^1	R^2	R^3	ee %
56a	Ph	Me	Ph	96
56b	Ph	Me	n-Bu	84
56c	Ph	Me	*i*-Bu	93
56d	Ph	Me	Bn	95
56e	Ph	Me	$(CH_2)_2OMe$	90
56f	Ph	*t*-Bu	*i*-Bu	96
56g	Ph	Bn	*i*-Bu	97
56h	Ph	2-Napht	*i*-Bu	87
56i	3-ClC_6H_4	Et	*i*-Bu	98
56j	4-$MeOC_6H_4$	Et	*i*-Bu	96[a]
56k	Ph	Et	*i*-Bu	97
56l	Ph	*i*-Pr	*i*-Bu	96
56m	Ph	*n*-Bu	*i*-Bu	95
56n	Ph	MeO	*i*-Bu	95
56o	*i*-Pr	H	Bn	93
56p	*n*-Pr	H	Bn	84
56q	*i*-Bu	H	Bn	87
56r	Me	H	Ph	95
56s	Ph	Me	OMe, Me	75[b]

a) 3 Mol% of catalyst was used. b) Weinreb amide.

Table 5. Asymmetric hydrogenation of cinnamic and tiglic acid derivatives.

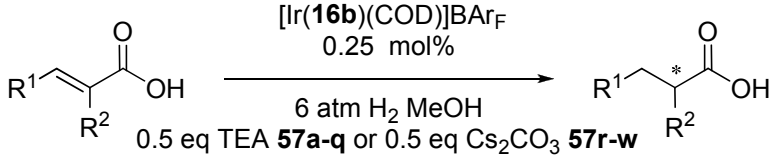

substrate	R^1	R^2	Yield %	ee %
57a	Ph	Me	99	99.2
57b	2-MeC_6H_4	Me	97	99
57c	3-MeC_6H_4	Me	98	99
57d	4-MeC_6H_4	Me	98	99
57e	2-$MeOC_6H_4$	Me	98	99
57f	3-$MeOC_6H_4$	Me	99	98
57g	4-$MeOC_6H_4$	Me	97	99
57h	2-ClC_6H_4	Me	97	96
57i	3-ClC_6H_4	Me	98	99
57j	4-ClC_6H_4	Me	97	98
57k	3-BrC_6H_4	Me	97	99
57l	4-BrC_6H_4	Me	97	98
57m	4-$CF_3C_6H_4$	Me	98	97
57n	2-naphthyl	Me	96	99
57o	furan-2-yl	Me	98	98
57p	Ph	*i*-Pr	97	99
57q	Ph	Ph	95	94
57r	Me	Me	92	99.1
57s	Et	Me	93	98
57t	*n*-Pr	Me	89	99
57u	*i*-Bu	Me	97	90
57v	*n*-Pr	Et	89	99.4
57w	Me	*n*-Pr	92	98

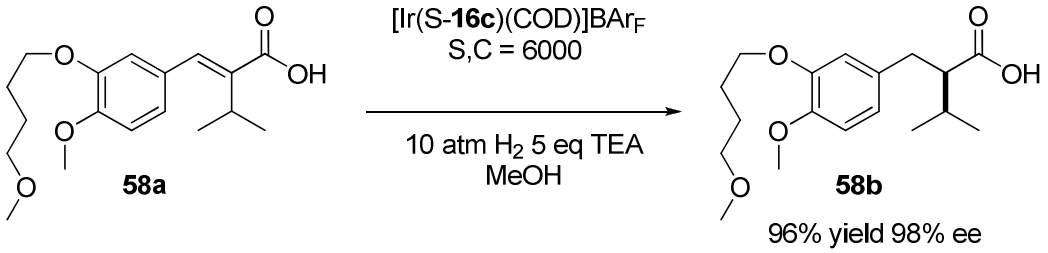

Scheme 13

Table 5 indicates an extremely efficient catalyst with very low catalyst loadings for such a highly coordinating environment. Functional group tolerance appears to be excellent with groups as reactive as arylbromides being converted in close to perfect yield.

Cesium carbonate was found to be a far more efficient additive for purely alkyl derived substrates **57r-w**. Very useful enantioselectivities were obtained for all entries with the exception of a tertiary isobutyl derived alkene **57u** which was converted with a respectable 90% ee. The yields were slightly lower for purely alkyl derived substrates but full conversions were reported by the authors.

Scheme 13 depicts an interesting application of this methodology in the synthesis of a crucial intermediate for the blood pressure lowering drug Aliskiren with the less encumbered ligand **16c**. In the presence of excess amounts of triethylamine **58b** was produced in 96% yield and 98% ee. Catalysts loadings were optimized at 0.016 mol% or S/C ratio of 6000. At S/C ratio of 10000 a slight loss of enantioselectivity and yield was noticed.

Vinyl phosphine oxides and phosphonates are highly electron deficient and can undergo conjugate reduction much like their carbonyl counter parts. The group of Andersson has reported an enantioselective reduction of both to yield chiral phosphine oxides and phosphonates (Table 6).[37]

Table 6. Asymmetric reduction of vinyl diphenylphosphine oxides and phosphonates

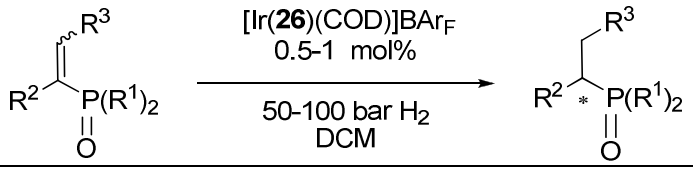

substrate	R^1	R^2	R^3	Conv %	ee %
59a	Ph	Ph	H	99	99
59b	Ph	4-$MeOC_6H_4$	H	99	99
59c	Ph	4-$CF_3C_6H_4$	H	93	99
59d	Ph	2-MeC_6H_4	H	99	99
59e	Ph	C_6H_{11}	H	99	99
59f	Ph	*t*-Bu	H	98	90
59g	Ph	CH_2CH_2OH	H	99	99
59h	OEt	Ph	*E*-CO_2Et	10	90
59i	OEt	Ph	*Z*-CO_2Et	99	99
59j	OEt	Bn	*E*-CO_2Et	99	99
59k	OEt	Ph	H	99	99
59l	OEt	CH_2CH_2OAc	*E*-CO_2Et	99	99

The authors did not report on trisubstituted diphenylphosphine oxides but apparently the results are excellent with what is usually a difficult 1,1' unsubstituted pattern about the alkene. The investigation found near perfect selectivity and yields for most of the reported compounds when using **26** as a ligand. However, a very slow reaction was noted for the *E* alkene **59h** while hydrogenation of *E* configured alkene **59j** preceded smoothly, indicating a delicate balance between structure and reactivity. Other anomalous behavior of the substrates **59h-j** is both *E* and *Z* configured alkenes produce the same enantiomer.

1.4 Asymmetric Hydrogenation of 1,1'-Disubstituted Alkenes

1,1'-Disubstituted alkenes are a challenging substrate class when compared to the more widely investigated trisubstituted alkenes. Although they react very quickly, obtaining high enantioselectivity with most ligands has been problematic. Blankenstein and Pfaltz reported the first iridium N,P based catalyst capable of reducing 1,1' disubstituted alkenes in useful selectivity with SerPHOX **60** (Scheme 14).[25a] The authors discovered a very strong dependence on hydrogen pressure with the highest selectivity obtained at atmospheric pressure of hydrogen. The later developed catalyst Ir(**6b**) was found to give higher enantioselectivities and is now commercially available as the BAr_F COD complex.[38a]

A large combined research effort of the three groups of Diéguez, Andersson, and Börner initiated a combinatorial study utilizing the SerPHOX and ThrePHOX backbones in combination with a chiral biarylphosphinite moiety, ligands **18** and **19**.[38b] A library of 96 possible phosphite oxazoline ligands was synthesized with systematic changes to the backbone and with special attention to the biaryl phosphite group.

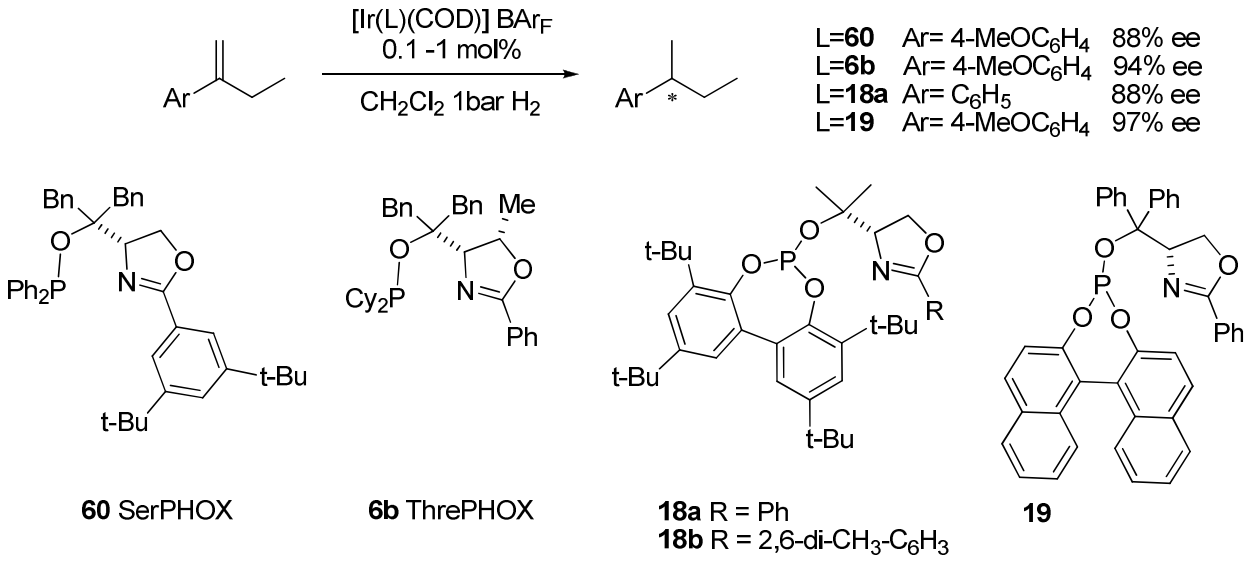

Scheme 14

Ligand **19** was found to be highly selective for the hydrogenation of 1-aryl, 1'-alkyl alkenes and ligand **18b** was found to be selective for 1-aryl, 1'-hindered aryl alkenes (Table 7).

Table 7. Asymmetric reduction of 1,1'disubstituted alkenes.

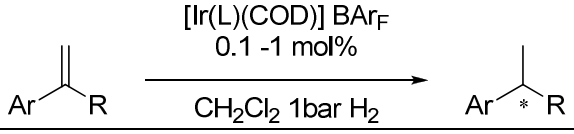

substrate	L	Ar	R	Conv%	ee%
61a	**19**	Ph	Et	100	99
61b	**19**	4-$MeOC_6H_4$	Et	100	99
61c	**19**	4-$CF_3C_6H_4$	Et	100	96
61d	**19**	Ph	*n*-Bu	100	94
61e	**19**	Ph	*i*-Bu	100	93
61f	**19**	Ph	neopentyl	100	90
61g	**19**	Ph	i-Pr	100	97
61h	**19**	Ph	cyclohexyl	100	97
61i	**19**	Ph	*t*-Bu	100	99
61j	**18a**	2-furyl	*n*-Bu	100	99
61k	**19**	2-thienyl	*n*-Bu	100	96
61l	**19**	2-pyridyl	Et	100	99
61m	**19**	2-pyridyl	*t*-Bu	100	99
61n	**18b**	Ph	2-naphthyl	100	99[a]
61o	**18b**	Ph	2-MeC_6H_4	99	99[a]
61p	**19**	4-$CF_3C_6H_4$	4-$MeOC_6H_4$	100	63[a]
61q	**19**	Ph	CH_2OH	100	95[a]
61r	**19**	Ph	CH_2OAc	100	91[a]
61s	**19**	Ph	CH_2TMS	100	96[a]
61t	**19**	4-$MeOC_6H_4$	CF_3	100	75[a]

a) Reaction was run at 50 bar hydrogen.

Ligand **19** performs excellently with the wide variety of 1,1'disubstituted alkenes reported. Substrates **61a-m** are efficiently reduced at 1 bar of hydrogen in high enantioselectivity with very little dependence on the bulk of the alkyl substituents. Strongly coordinating alkenes such as **61l** and **61m** typically perform poorly in iridium catalyzed hydrogenations but reduction with **19** clearly breaks this rule and the substrates are reduced in excellent selectivity and yield.

The more sterically demanding **61n-o** were easily reduced by Ir(**18b**), perhaps due to a more open and accommodating catalyst structure. Other changes to note are the higher pressure (50 bar) required to reduce the chelating substrates **61q-r**, the hindered **61s**, and the electron poor **61t**. The diarylmethylene substrate **61p** reveals that enantioface discrimination is also possible based on electronic rather than steric effects. Both aryl groups have very similar steric demands but distinguish themselves by their π donor and π acceptor properties. The remarkable ee of 63% may be explained by the different interaction of the iridium center with the electron poor and the electron rich aryl group and/or alignment of the catalyst dipole with the substrate dipole created by electron donor and acceptor groups.

1.5 Asymmetric Hydrogenation of Tetrasubstituted Alkene

Tetrasubstituted alkenes remain a challenging class of substrate. Buchwald and co-workers have shown that chiral zirconocene complexes can catalyze the hydrogenation of tetrasubstituted alkenes with high enantioselectivity.[5a-b] However, high catalyst loadings, long reaction times and high pressures are a disadvantage of this system.

Schrems et al identified a number of P,N ligands which have given encouraging results for this class of substrate.[39] Surprisingly the structurally simple readily accessible phosphinooxazoline **12a**, originally reported by Sprinz and Helmchen,[40] and subsequent analogues **12b-e** proved to be the most efficient ligands for several substrates (Table 8).

For a few select cases the cyclic alkene **62a-c** with simple primary alkyls as substituents were readily hydrogenated with SimplePHOX ligand **7a** and **7c**. Importantly, no epimerization at the benzylic position was observed and hydrogenation gave entirely cis product with most substrates. Aromatization of the dihydronapthelene substrates **63a-b** was a frequent side reaction, even at high pressures.

Table 8. Asymmetric reduction of tetrasubstituted alkenes.

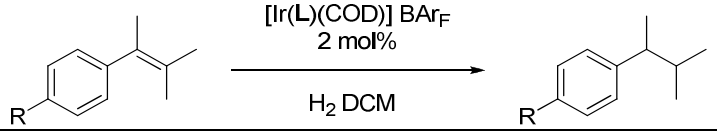

Substrate		R	L	P	t	ee%	Conv%
61a	-	MeO	**12c**	1 bar	4 h	97	99
61b	-	F	**12d**	5 bar	4 h	89	99

Substrate	R^1	R^2	L	P	t	ee%	Conv%
62a	Me	Me	**12a**	5 bar	4 h	94	99
			7c	5 bar	4 h	95	99
62b	Et	Me	**12a**	50 bar	4 h	93	99
			7a	50 bar	4 h	94	98
62c	*n*-Bu	Me	**12a**	50 bar	4 h	94	99
			7a	50 bar	4 h	95	97
62d	Ph	Me	**12a**	5 bar	4 h	95	99
62e	Me	Ph	**12a**	50 bar	4 h	88	20
62f	Et	Ph	**12a**	50 bar	4 h	93	23

For some substrates a dependence of enantioselectivity on pressure was observed with low to moderate pressures being optimal for many combinations. Ligand **12c** in combination with substrate **62a** gives an enantioselectivity of 92% at 50 bar of pressure and 97% at 1 bar, similar to the trend found in the early studies of the 1,1' disubstituted substrates.

Table 8. Continued.

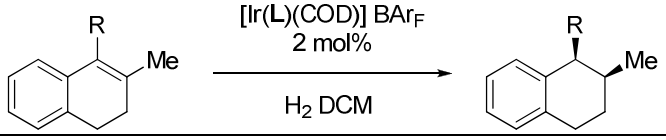

Substrate		R	L	P	t	ee%	Conv%
63a	Me	Me	**12a**	50 bar	4 h	73	99
	Me	Me	**6a**	5 bar	4 h	77	46
63a	Ph	Me	**12b**	5 bar	4 h	91	32

Substrate	L	P	mol%	ee%	Conv%
64	**5a**	50 bar	2.0	94	99
		50 bar	1.0	93	99
		50 bar	0.5	93	99
		50 bar	0.1	90	99
	12e	5 bar	2.0	96	99

Yet even more important is the observation that ligands with identical configurations gave products of opposite configuration solely on the basis of the substituent on the stereogenic center. For instance, ligand S-**12a** gives the (-) reduction product of **63a** in 65% ee at 50bar, changing the ligand to S-**12f** under identical reaction conditions gives the (+) product in 39% ee. Clearly the critical interactions with these catalysts and substrates are highly subject to the extremely crowded environment about the metal center and very small changes to either the substrate or ligand can lead to large changes in overall selectivity and yield.

Mastery of tetrasubstituted alkenes greatly expands the tools available for the synthesis of chiral carbon skeletons and tetrasubstituted alkenes have the added value of possibly creating two stereogenic centers simultaneously.

1.6 Asymmetric Hydrogenation of Trisubstituted Alkenes with Heteroatoms

Asymmetric hydrogenation of a C=C bond with a heteroatom substituent leads to highly valued chirons which can often be elaborated into more complex functionalized molecules. Most asymmetric hydrogenation routes to these chirons have relied on ruthenium or rhodium diphosphine complexes.[1-3, 7a] Iridium N,P and C,N complexes are the newest addition to catalysts capable of asymmetric hydrogenation of heteroatom substituted alkenes and in spite of the typical sensitivity of the complexes towards Lewis bases many successful hydrogenations of such alkenes have been reported in the recent literature. Indoles, enamines, enol esters, enol ethers, chromenes, furans, quinolines, and pyridines have all been successfully reduced with useful enantioselectivities using chiral iridium complexes and each shall be touched upon in the following section.

1.6.1 Enol Esters and Ethers

Zhu and Burgess have reported an asymmetric conjugate reduction of 1,3-enol ether esters (Table 9) and 1,3-enol ether alcohols (Table 10).[41] Initial reaction conditions reached full conversion of *E*-1-methoxy-1-phenylethene using ligand **9** albeit with a very low enantioselectivity of 29%.

Asymmetric hydrogenation of **65a-h** with ligand **9** indicates a difficult reaction. Enantioselectivities are moderate to good with the best selectivity for the amide **65g**. Strong steric effects were observed with increasing the size of the ester with giving an increase in ee. The steric crowding at the alkoxy bearing C atom was also observed to have a large effect on the enantioselectivity. Substituents larger than methoxy groups greatly eroded the selectivity as observed for the ethoxy ether **65e**. Secondary alkyl groups were completely deleterious to hydrogenation activity with an abysmal conversion of 15% for substrate **65f**.

Table 9. Asymmetric Hydrogenation of Vinyl Ether Esters.

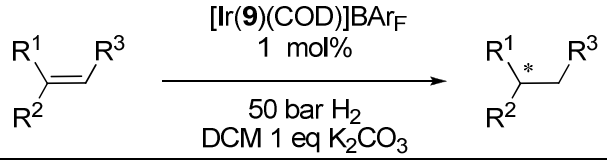

substrate	R^1	R^2	R^3	Conv%	ee%
65a	Me	OMe	CO_2H	99	63
65b	Me	OMe	CO_2Me	85	60
65c	Me	OMe	CO_2Et	99	78
65d	Me	OMe	CO_2-*t*-Bu	99	88
65e	Me	OEt	CO_2Et	99	66
65f	OMe	*i*-Pr	CO_2Me	15	nd
65g	Me	OMe	$CO_2NEtOMe$	90	90
65h	Me	OMe	COPh	5	nd

Table 10. Asymmetric Hydrogenation of Vinyl Ether Alcohols.

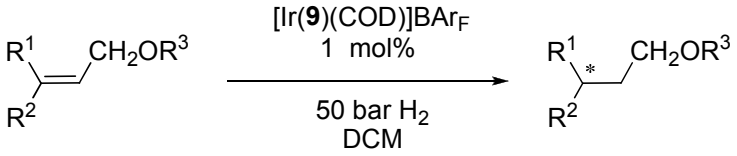

substrate	R^1	R^2	R^3	ee%
66a	Me	OMe	H	96
66b	Me	OEt	H	98
66c	*n*-Bu	OMe	H	93
66d	*i*-Pr	OMe	H	91
66e[a]	Me	OMe	TBDPS	89
66f[a]	Me	OMe	Ac	92

a) K_2CO_3 was not required for this case.

Asymmetric hydrogenation of vinyl ether alcohols proceeded in better selectivity than the ester counterparts but acid sensitivity was observed for **66a-d** and a stoichiometric equivalent of potassium carbonate relative to the substrate was required to neutralize any acidic contaminants. Larger groups on either side of the alkene eroded enantioselectivity but not to the same degree as with substrates **65a-f**.

Cheruku et al have investigated a series of enol esters.[42a] A preliminary experiment to determine the optimal protecting group with a small group of catalysts identified diphenylphosphinates as the optimal esters (Table 11).

Table 11. Ligand and Substrate Optimization Studies.

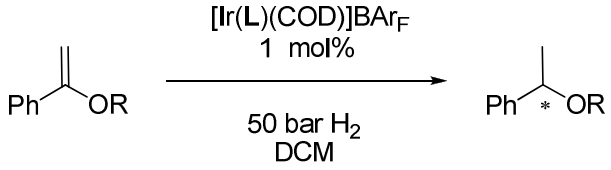

R	L 13a	L 13b	L 11a	L 10b
TMS	[a]	[a]	[a]	[a]
CH_3	[a]	[a]	[a]	[a]
Ac	[a]	full conv rac	[a]	no conv
$PO(OEt)_2$	complex mixture[b]	full conv 65% ee	[a]	no conv
$POPh_2$	30% conv 82% ee	full conv 95% ee	41% conv 63% ee	no conv

a) A complex mixture was obtained, b) Ethylbenzene was the major product.

Ligand **13b** in combination with diphenylphosphinate as the ester group gave the chiral phenylethyl diphenylphosphinate **67b** with full conversion and high enantioselectivity of 95%. Although it may seem that the diphenylphosphinate ester group is not ideal in terms of atom economy it should be noted that it is an excellent leaving group and can be readily displaced with a number of good nucleophiles. A study of both 1,1'-disubstituted vinyl phosphinates and trisubstituted vinyl phosphinates was conducted and the results are summarized in Table 12.

Table 12. Asymmetric Hydrogenation of Enol Phosphinates.

substrate	R^1	R^2	Conv%	ee%
68a	Ph	H	99	95
68b	4-MeC_6H_4	H	97	96
68c	4-*t*-BuC_6H_4	H	93	94
68d	4-MeOC_6H_4	H	48[a]	98
68e	4-BrC_6H_4	H	99	99
68f	4-$CF_3C_6H_4$	H	99	99
68g	4-$NO_2C_6H_4$	H	99	92
68h	β-naphthyl	H	99	85
68i	cyclohexyl	H	99	92
68j	t-Bu	H	99	99
68k	Ph	Me	99	96
68l	Ph	Et	90	92
68m	Ph	*i*-Pr	89	90
68n	Ph	CO_2Et	99	99
68o	4-MeC_6H_4	CO_2Et	99	99
68p	4-$CF_3C_6H_4$	CO_2Et	99	99
68q	4-BrC_6H_4	CO_2Et	99	98
68r	Me	CO_2Et	99	99
68s	Et	CO_2Et	99	99
68t	*i*-Pr	CO_2Et	99	99
68u	$ClCH_2$	CO_2Et	95[b]	93[b]
68v	*t*-Bu	CO_2Et	98	93
68w	*t*-Bu	Et	99	90
68x	*i*-Pr	Me	99	91

a) Reaction was run with 2 mol% catalyst and 10 mg poly(vinylpyridine) resin b) run at 2 mol% catalyst.

Asymmetric hydrogenation of both 1,1'-disubstituted vinyl phosphinates and the trisubstituted phosphinates with ligand **13b** were highly successful. Enantioselectivities were very high for many useful combinations including bulky alkyl groups on the stereogenic center. Substrate **68d** was very acid sensitive and an acid scavenger with increased amounts of catalyst was required to obtain reasonable results. Allylic chloride **68u** also required higher catalyst loading but was reduced efficiently and in high enantioselectivity. In many cases the enantioselectivity was higher than what can be obtained from reduction of the corresponding ketones with ruthenium based catalysts.[42a]

1.6.2 Asymmetric Hydrogenation of Furans and Chromenes

Chiral reduced heterocycles containing only oxygen are common throughout organic synthesis and are highly sought after compounds. Asymmetric hydrogenation offers an atom economical approach to these compounds in a single clean step. However, hydrogenation of prochiral furans and dehydropyrans has proven difficult, mostly attributed to the increased stability of aromatic compounds and the electron rich nature of these substrates [43a]. For a long time no suitable chiral catalysts were available until iridium N,P catalyst provided a solution for these problematic hydrogenation reactions.

ThrePHOX **6b** proved a valuable tool in the reduction of chromenes **71a-k** all of which were reduced in greater than 90% enantioselectivity. The very electron rich thiochromene **71h** required higher temperature and lower conversion was observed but the enantioselectivity remained in the useful range.

A series of furans and benzofurans were reduced in excellent enantioselectivity and conversion using iridium complexes derived from pyridine-phosphinite ligands. Tertiary butyl derived phosphinites were the preferred donor groups with ligand **8a** giving the highest enantioselectivity the most consistently. Higher temperatures and longer reaction times were required to obtain good conversion for all cases, most notably **69e** reacted very sluggishly at 40˚C.

Table 13. Asymmetric hydrogenation of substituted 4H-chromenes.

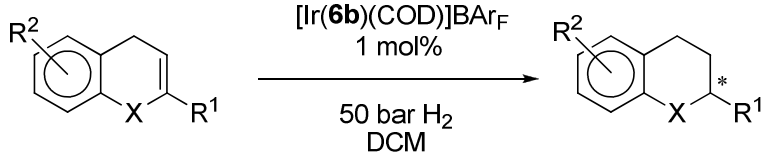

substrate	R^1	R^2	X	Conv%	ee%
71a	Me	H	O	93	95
71b	4-MeC_6H_4	H	O	99	98
71c	2-FC_6H_4	H	O	99	99
71d	4-BrC_6H_4	H	O	95	91
71e	4-ClC_6H_4	6-Cl	O	90	97
71f	Ph	7-MeO	O	99	99
71g	2-furyl	H	O	99	97
71h	Ph	H	S	73[a]	91[a]
71i	Ph	H	O	99	99
71j	cyclohexyl	H	O	99	95
71k	Ph	7-(CH=CH)$_2$-8	O	99	96

a) Reaction was conducted at 40˚C.

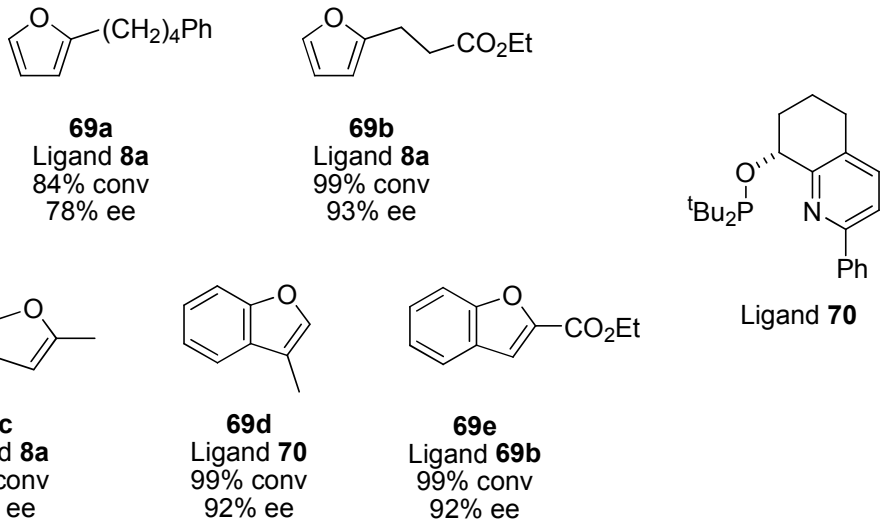

Figure 8. Asymmetric hydrogenation results for substituted furans.

These results mark the very first successful catalytic reduction of furans in high enantioselectivity and greatly expand the methods available for the synthesis of enantiopure heterocycles.

1.6.3 Asymmetric Hydrogenation of Enamines and Indoles

Much like the enol systems discussed in section 6.1 enamines are predictably difficult substrates for most iridium asymmetric hydrogenation catalysts. Both substrate and product contain basic functionalities which may act as inhibitors to the catalyst. Extended aromatic enamines such as indoles may be even more difficult substrates for asymmetric hydrogenation with an additional energetic barrier to overcome. Initial reports by Andersson indicated a very difficult reaction indeed (Table 14).[44a] Higher enantioselectivities were later reported by Baeza and Pfaltz (Table 14).[44b]

Moderate enantioselectivities were obtained with ligand **13b** at room temperature. Simply changing from a diethyl amine moiety **72a** to a pyrolidine **72g** caused a precipitous drop in enantioselectivity for both ligands **13b** and ThrePHOX **6b**. An electronic effect was observed for ligand **13b** with a drop from good selectivity with enamine **72b** with a methyl group in the para position of the aromatic ring to poor selectivity with the stronger π donating para-methoxy group with **72c**.

Steric interaction was also clearly an issue for all of the systems investigated. Most notable is the large difference in reactivity between ThrePHOX **6b** and PHOX **5c** based catalysts with respect towards the substituents bound to the nitrogen atom. ThrePHOX consistently performed best with *N*-methyl-*N*-benzyl enamines while PHOX preferred a *N*-methyl-*N*-phenyl derivative. Lowering the temperature had a favorable outcome on enantioselectivity but slowed the reaction and caused drops in conversion for **5c** and **6b**.

Table 14. Asymmetric Reduction of Enamines.

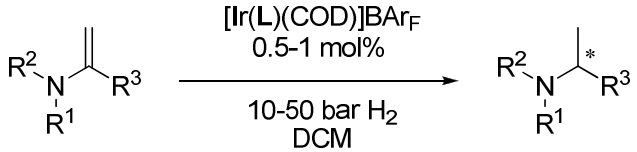

substrate	R^1	R^2	R^3	Conv%	ee%
72a	Et	Et	Ph	99[a] (99[c])	84[a] (54[c])
72b	Et	Et	4-MeC_6H_4	99[a]	87[a]
72c	Et	Et	4-MeOC_6H_4	99[a]	64[a]
72d	Et	Et	4-$CF_3C_6H_4$	99[a]	77[a]
72e	Et	Et	2-naphthyl	99[a]	64[a]
72f	Me	Ph	Ph	99[a] (98[b])	79[a] (91[b])
72g	*N,N'*-$(CH_2)_4$		Ph	66[a] (99[c])	33[a] (8[c])
72h	*N,N'*-$(CH_2$-$CH_2)_2O$		Ph	75[a]	30[a]
72i	Me	4-MeOC_6H_4	Ph	99[b]	90[b]
72j	Me	4-ClC_6H_4	Ph	99[b]	90.5[b]
72k	Me	Bn	Ph	99[cd]	92.5[cd]
72l	Me	Bn	4-MeOC_6H_4	93[c]	74[c]
72m	Me	Bn	4-ClC_6H_4	93[c]	74[c]
72n	Me	Bn	2-furan	93[ce]	74[ce]
72o	Me	Bn	t-Bu	53[b]	21[b]

a) Run with 0.5 mol% ligand **13b** at room temperature and 50 bar H_2 [44a]. b) Run with 0.5 mol% ligand **5c** at -20˚C [44b]. c) Run with 0.5 mol% ligand **6b** at -20˚C [44b]. d) MTBE was used as solvent. E) Run at 0˚C.

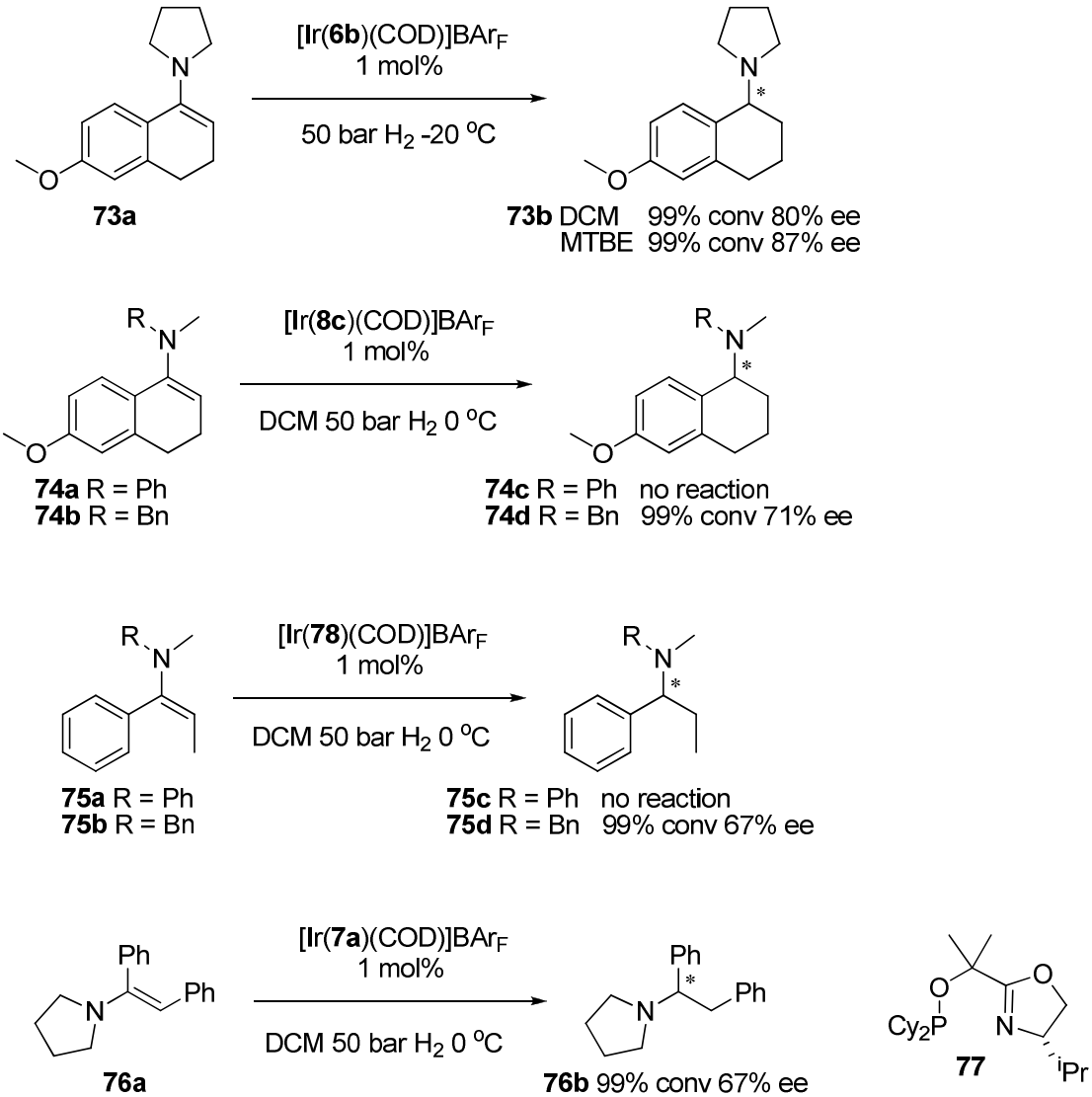

Scheme 15

A variety of ligands was used to hydrogenate **73a**, **74a-b**, **75a-b**, and **76a** with moderate results. Steric interactions were magnified and that may explain why nearly all of the substrates in Scheme 16 give less then optimal results. *N*-methyl-*N*-phenyl-amine derived enamines **74a** and **75a** were resistant to hydrogenation where the analogous *N*-methyl-*N*-benzyl-amine based enamines were completely converted with SimplePHOX ligand **77** with moderate enantioselectivity.

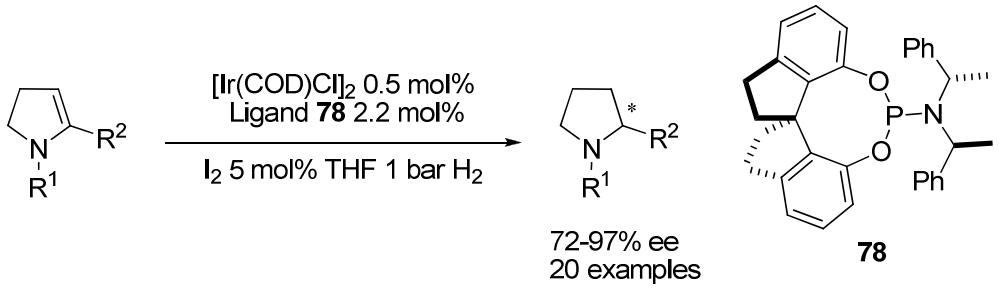

Scheme 16

It should also be mentioned that a very active and selective catalyst in the form of a monodentate phosphoramidite in combination with iridium was very successful in the reduction of cyclic enamines but the discussion of this work is beyond the scope of this chapter (Scheme 16).[44c] Enantioselectivities were reported as excellent with atmospheric pressure sufficing for full conversion in most cases.

Baeza and Pfaltz also investigated indoles which reacted very sluggish but excellent enantioselectivity could be obtained (Table 15).[45]

Hydrogenation of protected 2-indoles required higher catalyst loading and higher temperatures then used for enamines but many substrates were hydrogenated in high enantioselectivity and yield. Both electron donating groups and electron withdrawing groups interfered with catalysis but the reaction with indole **79b** could be pushed to completion by changing the solvent to chlorobenzene and increasing the temperature to 110 ˚C with very little loss in enantioselectivity. Nitroindole **79d** was completely unreactive and no hydrogenation products were observed. The boc protecting group was exchanged for acyl or tosyl groups in a few cases and with a beneficial effect to conversion for some indoles. Indole **79i** was extremely difficult to reduce but useful levels of product and enantioselectivity could be obtained with ligand **8a**. Indoles with substitution in the 3 position were very difficult to hydrogenate and reactions with esters in this position completely failed. However, simple methyl derivative **79k** was hydrogenated in excellent ee and yield.

Table 15. Asymmetric Hydrogenation of Indoles.

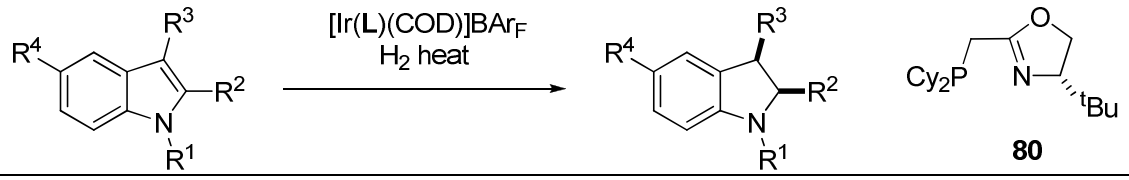

80

substrate	mol% (L)	T	R^1	R^2	R^3	R^4	Conv%[a]	ee%[a]
79a	4 (**8a**)	60 ˚C	boc	Me	H	H	89	99
79b	4 (**8a**)	60 ˚C 110 ˚C[b]	boc	Me	H	MeO	68 85[b]	99 98.5[b]
79c	4 (**8a**)	60 ˚C	boc	Me	H	F	64	98.5
79d	4 (**8a**)	60 ˚C	boc	Me	H	NO_2	0	nd
79e	1 (**6b**)	25 ˚C	boc	Ph	H	H	94[d]	88[d]
79f	1 (**6b**)	25 ˚C	boc	CO_2Et	H	H	66[d] 88[c]	92[d] 93[c]
79g	2 (**8a**)	60 ˚C	Ac	CO_2Et	H	H	97	99
79h	2 (**80**)	25 ˚C	Tosyl	Me	H	H	94	99
79i	4 (**8a**)	110 ˚C[b]	Tosyl	Ph	H	H	70[b]	98[b]
79j	4 (**8a**)	60 ˚C	Tosyl	Me	H	H	95	99
79k	2.5 (**8a**)	60 ˚C	Tosyl	H	Me	H	97	98

a) Reaction was run at 100 bar unless otherwise noted, b) chlorobenzene as solvent, 110 ˚C, c) 2 mol% of catalyst, DCM, 25 ˚C, d) reaction was run at 75 bar.

1.6.4 Asymmetric Hydrogenation of Quinolines and Pyridines

Asymmetric hydrogenation of nitrogen heterocycles is a relatively unexplored and open field. Only a handful of iridium N,P based systems have been used successfully to hydrogenate substituted quinolines and the more stable pyridines. Lu et al were the first to report a successful asymmetric hydrogenation of 2 substituted quinolines with ligand **24** (Table 16).[46a] A few reports using diphosphines and monophos variations followed until Lu and Bolm published a second iridium N,P based asymmetric hydrogenation of similar quinolines with ligand **23a** (Table 16).[46b]

Table 16. Asymmetric Hydrogenation of Quinolines.

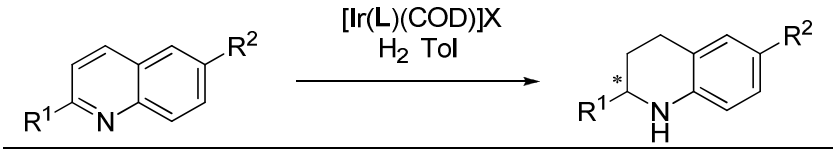

substrate	R^1	R^2	Yield%[a] Conv%[b]	ee%[a] ee%[b]
81a	Me	H	95[a] 95[b]	90[a] 87[b]
81b	Et	H	95[a] 62[b]	91[a] 77[b]
81c	*n*-Pr	H	62[b]	80[b]
81d	*i*-Bu	H	53[b]	75[b]
81e	*n*-pentyl	H	94[a] 90[b]	92[a] 65[b]
81f	Me	Me	93[a] 95[b]	92[a] 75[b]
81g	Me	F	86[a] 43[b]	89[a] 64[b]
81h	Me	MeO	95[b]	78[b]
81i	Ph	H	45[a]	3[a]
81j	$(CH_2)_2Ph$	H	92[a]	72[a]

a) Reaction was conducted at 40 bar H_2, 1 mol% [(**24**)Ir(COD)]Cl and 5 mol% I_2.[46a] b) Reaction was conducted at 60 bar H_2, 1 mol% [(**23a**)Ir(COD)]BAr_F.[46b]

Ligand **24** was surprisingly effective in the presence of 5 mol% iodine without the use of BAr_F as a counterion. Reduction of sterically demanding substrates was a problem for both systems and aromatic substitution on the 2 position of the quinoline abolished the enantioselectivity and poor conversion was obtained. Electron donating and withdrawing groups also damaged the enantioselectivity although less for Zhou's system. Nevertheless, useful enantioselectivity and yield could be obtained for simple alkyl derivatives.

A single paper from Charette and coworkers details the catalytic asymmetric hydrogenation of N-iminopyridinium ylides to substituted piperdines using PHOX ligand **82** in combination with iodine (Table 17).[46c]

Table 17. Asymmetric Hydrogenation of N-Iminopyridinium Ylides.

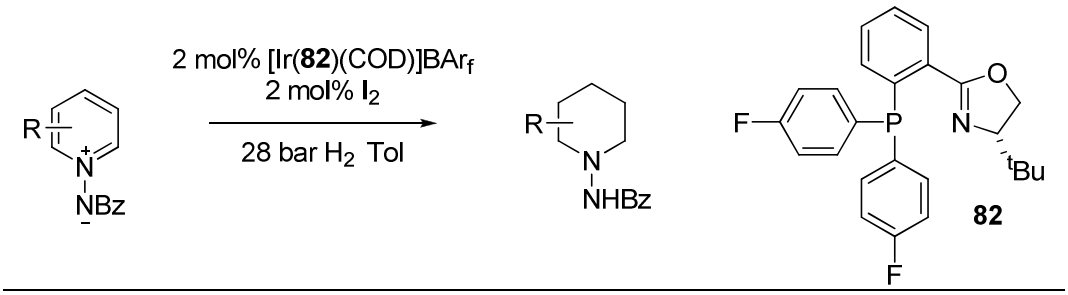

substrate	R	Yield%	ee%
83a	2-Me	90 (84[a])	90 (97[a])
83b	2-Et	96 (78[a])	83 (94[a])
83c	2-*n*Pr	98 (75[a])	84 (95[a])
83d	2-Bn	97	58
83e	2-CH_2OBn	85	76
83f	2-$(CH_2)_3OBn$	88	88
83g	2,3-dimethyl	91 (>95:5 cis:trans)	54
83h	2,5-dimethyl	92 (57:43 cis:trans)	86/84

a) Numbers in parentheses are after a single recrystallization.

Moderate to good enantioselectivities were obtained for nearly all examples but the products from **83a-c** could be recrystallized to higher enantiomeric purity. Addition of iodine was critical for catalysis as was the use of a ligand with electron-poor *para*-fluorophenyl groups on the phosphorous atom. Substitution at the 3 position of the pyridine ring was described as being difficult for both the quinolines and pyridine systems. The resulting hydrazine derivatives could be easily converted to piperdines by reduction with Raney nickel or under Birch conditions.

1.7 Asymmetric Hydrogenation of Imines

Given the importance of chiral amines to synthetic chemistry as well as other fields asymmetric hydrogenation of imines has attracted wide interest but limited success compared to C=C and C=O bond reduction. The first asymmetric hydrogenation of imines was carried out in the seventies with ruthenium and rhodium based catalysts, followed later by titanium and zirconium systems.[47] Buchwald found that Britzinger type ansa titanocenes were highly selective for the reduction of cyclic imines, albeit at long reaction times, high catalyst loading and with high pressures.[48a] Crabtree found that pyridine phosphine complexes of iridium were highly active in the reduction of imines.[6] The asymmetric synthesis of Metolachlor, an important agrochemical used in the protection of maize, is the first example of an industrially useful enantioselective reduction of imines catalyzed by an iridium complex with a Josiphos type ligand.[48b] The first use of iridium N,P complexes in the asymmetric hydrogenation of imines was reported by Pfaltz and coworkers in 1997.[48c]

Many of the systems studied required high catalyst loadings, very high pressures, elevated temperatures, and long reaction times. Several problems can be encountered with imines such as hydrolysis to starting materials, dimer and trimer formation, presence of enamine and syn/anti isomers.[47] Additionally, with the exception of N-aryl-imines the resulting amines are far more basic then the imine substrates and may cause a larger degree of product inhibition of the catalyst. Many recent advances have been made with iridium systems other than N,P ligands such as diphosphines and monodentate phosphoramidites.[49]

Initial studies with PHOX indicated a lack of an anion effect, replacement of PF_6^- by SbF_6^-, or BF_4^- as counter ion had no apparent effect on the overall reaction. However, nearly all reported catalysts within the last decade utilize BAr_F as a counterion, perhaps for the higher catalyst stability, easier handling and general reactivity towards a broader range of substrates.

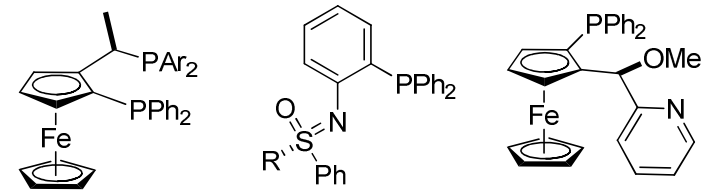

Josiphos **84** **85**

Figure 9. Ligands for asymmetric hydrogenation of imines.

Andersson reported the use of ligand **13a** in the asymmetric hydrogenation of substituted acetophenone based N-aryl imines (Table 18).[50a-b] New ligands **84** and **85** were reported by the groups of Bolm and Knochel, respectively, for asymmetric hydrogenation of imines with improved enantioselectivities and yields (Figure 9).[50c-d] Two similar chiral spirocycle based ligands SpinPHOX **15** and SiPHOX **16** proved highly effective in the asymmetric hydrogenation of these difficult substrates.[51] Baeza and Pfaltz reported three structurally similar catalysts based on PHOX in an expanded look at the earlier work and found excellent selectivity and activity at low catalyst loadings.[52]

Essentially all studies have used acetophenone based *N*-aryl ketimines as substrates or derivatives thereof. Some of the *N*-aryl groups are easily deprotected to yield branched α-aryl primary amines which can be further functionalized.

Ta**ble 18.** Asymmetric Hydrogenation of Acetophenone Based N-Aryl Ketimines.

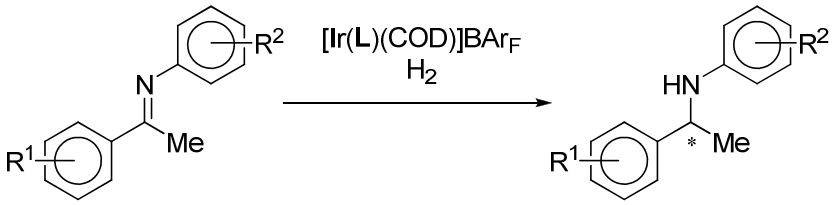

			Ligand ee%							
Imine	R^1	R^2	**5a**[a]	**13a**[b]	**14d**[c]	**15a**[d]	**16a**[e]	**77**[f]	**84**[g]	**85**[h]
86a	H	H	90	90	94	91	93	96	-	84
86b	H	4-MeO	96	89	94	90	-	95	96	85
86c	H	Ar[i]	-	-	-	-	-	-	-	94
87a	2-Me	H	-	83	-	-	-	-	-	-
87b	2-Me	4-MeO	-	-	-	-	-	-	94	-
87c	2-Me	Ar[i]	-	-	-	-	-	-	-	94
88a	3-Me	4-MeO	-	-	-	-	-	-	93	-
88b	3-Me	Ar[i]	-	-	-	-	-	-	-	93
91a	4-Me	H	-	-	-	88	94	-	-	-
91b	4-Me	4-MeO	-	-	-	-	-	-	96	-
92	4-AcO	Ar[i]	-	-	-	-	-	-	-	94
93	4-MeO	H	-	86	90	-	94	94	-	-
94a	4-MeO	4-MeO	-	86	-	-	-	-	94	-
94b	3-MeO	4-MeO	-	-	-	-	-	-	96	-
94c	2-MeO	4-MeO	-	-	-	-	-	-	90	-
95a	3-Cl	H	-	-	-	93	93	-	-	-
95b	3-Br	H	-	-	-	93	92	-	-	-
96a	4-Cl	H	96	-	95	93	90	96	-	-
96b	4-Cl	4-MeO	-	89	-	91	-	-	95	-
96c	4-Cl	Ar[i]	-	-	-	-	-	-	-	92
97a	4-Br	H	-	-	-	91	91	-	-	-
97b	3-Br	H	-	-	-	93	92	-	-	-
98a	4-CF_3	H	-	-	-	92	-	-	-	-
98b	4-CF_3	Ar[i]	-	-	-	-	-	-	-	89
99a	H	4-Cl	89	-	92	-	97	94	-	-
99b	H	4-Br	-	-	-	89	96	-	-	-
100	3,4-Xy	H	-	-	-	95	94	-	-	-

Conditions: a) 0.5 mol% cat, DCM, 5 bar H_2 0˚C, b) 0.5 mol% cat, DCM, 20 bar H_2, c) 0.5 mol% cat, DCM, 5 bar H_2 -20˚C, d) 1.0 mol% cat, DCE, 1 atm H_2 10˚C, e) 1.0 mol% cat, MTBE, 1 atm H_2, 10˚C, 4Å MS, f) 0.5 mol% cat, DCM, 5 bar H_2 -20˚C, g) 0.5 mol% cat, 2 mol% I_2, tol, 20 bar H_2, h) 1.0 mol% cat, 4:1 toluene: methanol, 10 bar H_2, i) Ar = 4-MeO-3,5-Me_2-C_6H_2.

Table 19. Asymmetric Hydrogenation of Imines.

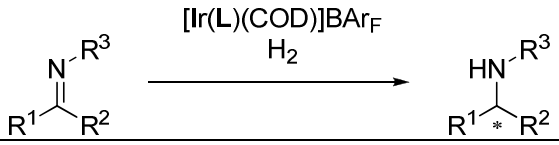

				Ligand ee%				
Imine	R^1	R^2	R^3	**13a**[a]	**14d**[b]	**15b**[c]	**84**[d]	**85**[e]
101a	Ph	Et	Ph	78	82	92	-	-
101b	Ph	Et	4-MeO-C_6H_4	-	-	-	92	-
101c	Ph	Et	Ar[f]	-	-	-	-	94
102	α-napth	Me	4-MeO-C_6H_4	-	-	-	98	-
103a	β-napth	Me	Ph	91	-	-	-	-
103b	β-napth	Me	4-MeO-C_6H_4	-	-	-	69	-
103c	β-napth	Me	Ar[f]	-	-	-	-	93
103c	β-napth	Me	Bn	-	-	93	-	-
104a	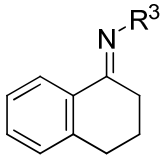		Ph	90	-	-	-	-
104b			4-MeO-C_6H_4	-	-	-	91	-
104c			Bn	-	-	96	-	-
104d			Me	-	-	98	-	-
104e			i-Bu	-	-	96	-	-

a) Conditions: 0.5 mol% cat, DCM, 20 bar H_2, b) 0.5 mol% cat, DCM, 5 bar H_2 -20˚C, c) 1.0 mol% cat, DCM, 20 atm H_2 10˚C, d) 0.5 mol% cat, 2 mol% I_2, toluene, 20 bar H_2, 20 hours, e) 1.0 mol% cat, 4:1 toluene: methanol, 10 bar H_2, 25˚C, 20 hr, f) Ar = 4-MeO-3,5-Me_2-C_6H_2.

Several authors have conducted investigations of the *N*-aryl moiety to optimize interactions for each individual catalyst. All of the catalysts in Table 18 function well at 1 mol% catalyst loading and with ambient to moderate pressures of hydrogen. Non-coordinating solvents were preferred with the exception of Knochel's ligand **85** which gave the highest enantioselectivity in a mixture of 25% methanol in toluene.

Although all of the substrates tested in Tables 18 and 19 have a very high degree of similarity some useful trends can be identified for each individual catalyst. Different conditions were used for different catalyst systems, possibly reflecting different mechanisms for each

individual system. For instance, addition of iodine was found to give inferior results with PHOX and related ligands, yet Bolm's ligand **84** requires iodine for catalysis, a result more in agreement with iridium diphosphine complexes.[47] Other interesting deviations are the optimal conditions reported by Knochel with ligand **85** which calls for 25% methanol in toluene as a solvent. This result stands in stark contrast to Zhou's ligand **16a** which is inhibited by methanol in imine hydrogenations.

PHOX **5a**, SimplePHOX **77**, and NeoPHOX **14d** are very closely related in bite angle and overall geometry, however these catalysts differ in the electronic properties on the phosphine moiety. All of these ligands gave excellent enantioselectivity in close agreement with each other reflecting the importance of geometry and bite angle over electronic properties.[52] The authors also reported a strong temperature effect on selectivity with lower temperature giving higher enantioselectivity. Catalysts loadings as low as 0.1 mol% were effective for several substrate and catalyst combinations but with an increased pressure requirement to reach useful conversions.

In comparison ligand **13a** generally gave moderate to good enantioselectivities over a limited range of substrates, larger substituents were not tolerated well with imine **87a** reaching only 52% conversion albeit at 0.5 mol% catalyst loading. This system appeared to be the most sensitive to the size of the substrate, changing a methyl group such as in imine **86a** with an ee of 90% for an ethyl group as in **101a** decreased the enantioselectivity to 78%.

Ligand **84** gave excellent enantioselectivity for most of the reported substrates but some sensitivity to steric hindrance was also clear. Changing from α-naphthyl methyl ketimine **102** with an ee of 98% for β-naphthyl derived **103b** drops the enantioselectivity to 69%.

Inferior results with *N*-benzyl compared to *N*-aryl imines have been reported for many iridium based systems.[51b] Han et al compensated for this same negative effect with SpinPHOX **15a** by replacing the pendant isopropyl group with a bulkier *tert*-butyl group in **15b**, demonstrating control of the system can be obtained by simple ligand modification. The added bulk of **15b** made it possible to reduce the very challenging *N*-alkyl substituted imines **104d-e** in excellent enantioselectivity.

Knochel took a different approach by optimizing the substrate *N*-aryl group while investigating ligand **85**. Introduction of two meta-methyl groups in the 4-methoxyphenyl substituent increased the enantioselectivity from 84% with imine **86a** to 94% with **86c**.

Electronic effects seem to have very little influence on the overall enantioselectivity with both electron donating and withdrawing groups giving very small changes to the enantioselectivity when all other variables were the same. Substrate geometry seems to play a much more influential role with this particular class of substrates.

1.8 References

[1] Knowles, W. S. *Angew. Chem. Int. Ed.* **2002**, 41, 1998.

[2] Blaser, H. U., Schmidt, E., Eds. *Asymmetric Catalysis on Industrial Scale*, Wiley-VCH; Weinheim, **2004**.

[3] (a) Brown, J. M. Hydrogenation of Functionalized Carbon-Carbon Double Bonds. In *Comprehensive Asymmetric Catalysis*; Jacobsen E. N., Pfaltz, A., Yamamoto, Y., Eds.; Springer: Berlin, 1999; Vol. I, Chapter 5.1. (b) Noyori, R. *Angew. Chem. Int. Ed.* **2002**, 41, 2008.

[4] (a) Lightfoot, A.; Schnider, P.; Pfaltz, A. *Angew. Chem. Int. Ed.* **1998**, 37, 2897. (b) Pfaltz, A.; Blankenstein, J.; Hilgraf, R.; Hörmann, E.; McIntyre, S.; Menges, F.; Schönleber, M.; Smidt, S. P.; Wüstenberg, B.; Zimmermann, N. *Adv. Synth. Catal.* **2002**, 345, 33.

[5] (a) Broene, R. D.; Buchwald, S. L. *J. Am. Chem. Soc.* **1993**, 115, 12569. (b) Troutman, M. V.; Appella, D. H.; Buchwald, S. L. *J. Am. Chem. Soc.* **1999**, 121, 4916. (c) Conticello, V. P.; Brard, L.; Giardello, M. A.; Tsuji, Y.; Sabat, M.; Stern, C. L.; Marks, T. J. *J. Am. Chem. Soc.* **1992**, 114, 2761.

[6] Crabtree, R. H. *Acc. Chem. Res.* **1979**, 12, 331.

[7] (a) Cui, X.; Burgess, K. *Chem. Rev.* **2005**, 105, 3272. (b) Källström, K.; Munslow, I.; Andersson, P. G. *Chem. Eur. J.* **2006**, 12, 3194. (c) Roseblade, S. J.; Pfaltz, A. *Acc. Chem. Res.* **2007**, 40, 1402. (d) Church, T. L.; Andersson, P. G. *Coord. Chem. Rev.* **2008**, 252, 513.

[8] Helmchen, G.; Pfaltz, A. Acc. Chem. Res. **2000**, 33, 336.

[9] Blackmond, D. G.; Lightfoot, A.; Pfaltz, A.; Rosner, T.; Schnider, P.; Zimmermann, N. *Chirality* **2000**, 12, 442.

[10] Smidt, S. P.; Pfaltz, A.; Martínez-Viviente, E.; Pregosin, P. S.; Albinati, A. *Organometallics* **2003**, 22, 1000.

[11] Krossing, I.; Raabe, I. *Angew. Chem. Int. Ed.* **2004**, 43, 2066.

[12] Smidt, S. P.; Zimmermann, N.; Studer, M.; Pfaltz, A. *Chem. Eur. J.* **2004**, 10, 4685.

[13] Wüstenberg, B.; Pfaltz, A. *Adv. Synth. Catal.* **2008**, 350, 174.

[14] Crabtree, R. H.; Demou, P. C.; Eden, D.; Mihelcic, J. M.; Parnell, C. A.; Quirk, J. M.; Morris, G. E. *J. Am. Chem. Soc.* **1982**, 104, 6994.

[15] (a) Mazet, C.; Smidt, S. P.; Meuwly, M.; Pfaltz, A. *J. Am. Chem. Soc.* **2004**, 126, 14176. (b) Meuwly, M.; Roseblade, S. J.; Pfaltz, A. Univ. of Basel, unpublished results. (c) Roseblade, S. J.; Pfaltz, A. *C. R Chimie.* **2007**, 10, 178.

[16] (a) Gridnev, I. D.; Imamoto, T. *Acc. Chem. Res.* **2004**, 37, 633. (b) Halpern, J. *Science* **1982**, 217, 401. (c) Brown, J. M.; Chaloner, P. A.; *J. Chem. Soc. Chem. Commun.* **1978**, 321. (d) Feldgus, S.; Landis, C. R. *J. Am. Chem. Soc.* **2000**, 122, 12714.

[17] Burk, M. J.; McGrath, M. P.; Wheeler, R.; Crabtree, R. H. *J. Am. Chem. Soc.* **1988**, 110, 5034.

[18] Dietiker, R.; Chen, P. *Angew. Chem. Int. Ed.* **2004**, 43, 5513.

[19] Brandt, P.; Hedberg, C.; Andersson, P. G. *Chem. Eur. J.* **2003**, 9, 339.

[20] Hedberg, C.; Källström, K.; Brandt, P.; Hansen, L. K.; Andersson, P. G. *J. Am. Chem. Soc.* **2006**, 128, 2995.

[21] Fan, Y.; Cui, X.; Burgess, K.; Hall, M. B. *J. Am. Chem. Soc.* **2004**, 126, 16688.

[22] (a) Kaiser, S.; Smidt, S. P.; Pfaltz, A. *Angew. Chem. Int. Ed.* **2006**, 45, 5194. (b) Liu, Q. B.; Yu, C. B.; Zhou, Y. G. *Tetrahedron. Lett.* **2006**, 47, 4733.

[23] Bell, S.; Wüstenberg, B.; Kaiser, S.; Menges, F.; Netscher, T.; Pfaltz, A. *Science* **2006,** 311, 642.

[24] Wang, A.; Wüstenberg, B.; Pfaltz, A. *Angew. Chem. Int. Ed.* **2008**, 47, 2298.

[25] (a) Blankenstein, J.; Pfaltz, A. *Angew. Chem. Int. Ed.* **2001**, 40, 4445. (b) Menges, F.; Pfaltz, A. *Adv. Synth. Catal.* **2002**, 344, 40. (c) Smidt, S. P.; Menges, F.; Pfaltz, A. *Org. Lett.* **2004**, 6, 2023. (d) Schrems, M. G.; Pfaltz, A. *Chem. Commun.* **2009**, 41, 6210. (e) Schönleber, M.; Hilgraf, R.; Pfaltz, A. *Adv. Synth. Catal.* **2008**, 350, 2033.

[26] Li, X.; Li, Q.; Wu, X.; Gao, Y.; Xu, D.; Kong, L. *Tetrahedron: Asymmetry* **2007**, 18, 629.

[27] (a) Verendel, J. J.; Andersson, P. G. *Dalton. Trans.* **2007**, 47, 5603. (b) Diéguez. M.; Mazuela, J.; Pàmies, O.; Verendel, J. J.; Andersson, P. G. *J. Am. Chem. Soc.* **2008**, 130, 7208.

[28] Tolstoy, P. I.; Engman, M.; Paptchikhine, A.; Bergquist, J.; Church, T. L.; Leung, A. W. M.; Andersson, P. G. *J. Am. Chem. Soc.* **2009**, 131, 8855.

[29] (a) Harmata, M.; Hong, X. *Org. Lett.* **2005**, 7, 3581. (b) Bianco, G. G.; Ferraz, H. M. C.; Costa, A. M.; Costa-Lotufo, L. V.; Pessoa, C. U.; de Moraes, M. O.; Schrems. M. G.; Pfaltz, A.; Silva, L. F. *J. Org. Chem.* **2009**, 74, 2561.

[30] (a) Engman, M.; Diesen, J. S.; Paptchikhine, A.; Andersson, P. G. *J. Am. Chem. Soc.* **2007**, 129, 4536. (b) Engman, M.; Cheruku, P.; Tolstoy, P.; Bergquist, J.; Völker, S. F.; Andersson, P. G. *Adv. Synth. Catal.* **2009**, 351, 375.

[31] (a) Ueda, M.; Saitoh, A.; Miyaura, N. *J. Organomet. Chem.* **2002**, 642, 145. (b) Morgan, J. B.; Morken, J. P. *J. Am. Chem. Soc.* **2004**, 126,15338. (c) Moran, W. J.; Morken, J. P. *Org. Lett.* **2006**, 8, 2413. (d) Paptchikhine, A.; Cheruku, P.; Engman, M.; Andersson, P. G. *Chem. Commun.* **2009**, 40, 5996.

[32] (a) Zhou, J.; Ogle, J. W.; Fan, Y.; Banphavichit, V.; Zhu, Y.; Burgess, K. *Chem. Eur. J.* **2007**, 13, 7162. (b) Zhou, J.; Burgess, K. *Angew. Chem. Int. Ed.* **2007**, 46, 1129. (c) Zhou, J.; Zhu, Y.; Burgess, K. *Org. Lett.* **2007**, 9, 1391.

[33] (a) Zhu, Y.; Burgess, K. *J. Am. Chem. Soc.* **2008**, 130, 8894. (b) Zhao, J.; Burgess, K. *Org. Lett.* **2009**, 11, 2053. (c) Zhao, J.; Burgess, K. *J. Am. Chem. Soc.* **2009**, 131, 13236.

[34] (a) Mantilli, L.; Mazet, C. *Tetrahedron Lett.* **2009**, 50, 4141. (b) Mantilli, L.; Gérard, D.; Torche, S.; Besnard, C.; Mazet, C. *Angew. Chem. Int. Ed.* **2009**, 48, 5143.

[35] (a) Lu. S. M.; Bolm, C. *Chem. Eur. J.* **2008**, 14, 7513. (b) Lu, S. M.; Bolm, C. Angew. Chem. Int. Ed. **2008**, 47, 8920. (c) Lu, W. J.; Chen, Y. W.; Hou, X. L. *Angew. Chem. Int. Ed.* **2008**, 47, 10133.

[36] (a) Lu, W. J.; Hou, X. L. *Adv. Synth. Catal.* **2009**, 351, 1224. (b) Li, S.; Zhu, S. F.; Zhang, C. M.; Song, S.; Zhou, Q. L. *J. Am. Chem. Soc.* **2008**, 130, 8584.

[37] Cheruku, P.; Paptchikhine, A.; Church, T. L.; Andersson, P. G.; *J. Am. Chem. Soc.* **2009**, 131, 8285.

[38] (a) McIntyre, S.; Hörmann, E.; Menges, F.; Smidt, S. P.; Pfaltz, A. *Adv. Synth. Catal.* **2005**, 347, 282. (b) Mazuela, J.; Verendel, J. J.; Coll, M.; Schäffner, B.; Börner, A.; Andersson, P. G.; Pàmies, O.; Diéguez, M. *J. Am. Chem. Soc.* **2009**, 131, 12344.

[39] Schrems, M. G.; Neumann, E.; Pfaltz, A. *Angew. Chem. Int. Ed.* **2007**, 46, 8274.

[40] Sprinz, J.; Helmchen, G. *Tetrahedron Lett.* **1993**, 34, 1769.

[41] Zhu, Y.; Burgess, K. *Adv. Synth. Catal.* **2008**, 350, 979.

[42] (a) Cheruku, P.; Gohil, S.; Andersson, P. G. *Org. Lett.* **2007**, 9, 1659. (b) Cheruku, P.; Diesen, J.; Andersson, P. G. *J. Am. Chem. Soc.* **2008**, 130, 5595.

[43] (a) Zhou, Y. G. *Acc. Chem. Res.* **2007**, 40, 1357. (b) Valla, C.; Baeza, A.; Menges, F.; Pfaltz, A. Synlett **2008**, 3167.

[44] (a) Cheruku, P.; Church, T. L.; Trifonova, A.; Wartmann, T.; Andersson, P. G.; *Tetrahedron Lett.* **2008**, 49, 7290. (b) Baeza, A.; Pfaltz, A. *Chem. Eur. J.* **2009**, 15, 2266. (c) Hou, G. H.; Xie, J. H.; Yan, P. C.; Zhou, Q. L. *J. Am. Chem. Soc.* **2009**, 131, 1366.

[45] Baeza, A.; Pfaltz, A. *Chem. Eur. J.* **2010,** in press.

[46] (a) Lu, S. M.; Han, X. W.; Zhou, Y. G.; *Adv. Synth. Catal.* **2004,** *346*, 909. (b) Lu, S. M.; Bolm, C. *Adv. Synth. Catal.* **2008**, 350, 1101. (c) Legault, C. Y.; Charette, A. B. *J. Am. Chem. Soc.* **2005**, 127, 8966.

[47] Blaser, H. U.; Spindler, F. Hydrogenation of imino groups. In *Comprehensive Asymmetric Catalysis*; Jacobsen, E. N., Pfaltz, A., Yamamoto, Y. Eds. Springer; Berlin: **1999**, Vol. I, Chapter 6.2.

[48] (a) Willoughby, C. A.; Buchwald, S. L. *J. Am. Chem. Soc.* **1994**, 116, 11703. (b) Blaser, H. U. *Adv. Synth. Catal.* **2002**, 344, 17. (c) Schnider, P.; Koch, G.; Pretot, R.; Wang, G.; Bohnen F, M.; Kruger, C.; Pfaltz, A. *Chem. Eur. J.* **1997**, 3, 887.

[49] (a) Xiao, D.; Zhang, X.; *Angew. Chem. Int. Ed.* **2001**, 40, 3425. (b) Mršić, N.; Minnaard, A. J.; Feringa, B. L.; Vries, J. G. *J. Am. Chem. Soc.* **2009**, 131, 8358.

[50] (a) Trifonova, A.; Diesen, J. S.; Chapman, C. J.; Andersson, P. G. *Org. Lett.* **2004**, 6, 3825. (b) Trifonova, A.; Diesen, J. S.; Andersson, P. G. *Chem. Eur. J.* **2006**, 12, 2318. (c) Moessner, C.; Bolm, C. *Angew. Chem. Int. Ed.* **2005**, 44, 7564. (d) Cheemala, M. N.; Knochel, P. *Org. Lett.* **2007**, 9, 3089.

[51] (a) Zhu, S. F.; Xie, J. B.; Zhang, Y. Z.; Li, S.; Zhou, Q. L. *J. Am. Chem. Soc.* **2006**, 128, 12886. (b) Han, Z.; Wang, Z.; Zhang, X.; Ding, K. *Angew. Chem. Int. Ed.* **2009,** 48, 5345.

[52] Baeza, A.; Pfaltz, A. *Chem. Eur. J.* **2010**, 16, 4003.

Chapter 2

Development of Chiral N,P Iridium Complexes For Asymmetric Hydrogenation, Flexible Synthesis and Scalable Methods

"I love fools' experiments, I am always making them."- Charles Darwin

2.1 Introduction

Catalytic asymmetric hydrogenation is one of the most widely used and reliable catalytic methods for the preparation of optically active compounds.[1] State of the art catalysts are capable of delivering excellent enantioselectivity with very low catalyst loadings and atom economy that approaches ideal for many substrates. For these reasons asymmetric hydrogenation is the most utilized synthetic catalytic asymmetric methodology in industry and forms the critical transformation in several commercial scale processes.[2] Logically, discovery of high performance chiral catalysts depends on the development of appropriate ligands[3] and this field is in constant development with new generations of ligands appearing every year.

Chiral rhodium- and ruthenium diphosphine based catalysts are known which induce very high enantioselectivity in asymmetric hydrogenations.[4-7] However, the range of alkenes that can be hydrogenated with rhodium and ruthenium catalysts with high enantiomeric excess is limited as they require the presence of a coordinating group next to the C=C bond. With unfunctionalized alkenes, these catalysts generally demonstrate a loss of reactivity and unsatisfactory enantioselectivity in comparison. Iridium complexes such as the Crabtree catalyst on the other hand are more active in the reduction of C=C bonds without adjacent coordinating functional groups and stronger coordinating functional groups are frequently observed as inhibitors of iridium based catalysts. However, there is an increased appearance of iridium based catalysts with good to excellent selectivity and activity with substrates as strongly coordinating as substituted pyridines and enamines (see section 1.6 and 1.7).

In an endeavor to synthesize chiral catalysts that more closely match the Crabtree catalyst, complexes **105** and **106** were synthesized and evaluated in our group.[8, 9] We were encouraged by the results to pursue catalysts with a 5-membered ring backbone **107a-b** and a 6-membered analogue **109** in hopes of reaching higher enantioselectivities with a more rigid system. Complexes **107a**, **107b**, and **109** proved to be remarkably active and selective in the enantioselective hydrogenation of purely alkyl substituted alkenes,[10, 11] furans,[12] and indoles[13] as well as playing a featured role in a handful of total syntheses.[14-16]

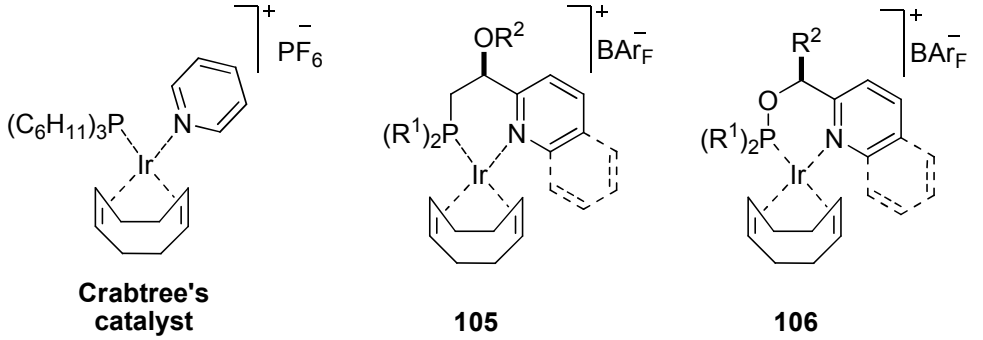

Crabtree's catalyst **105** **106**

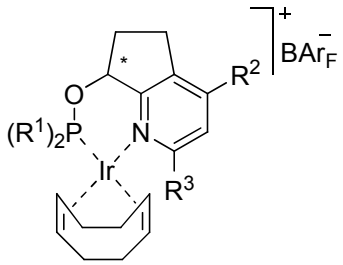

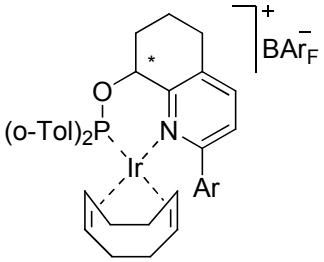

107a R^1 = *o*-Tol R^2 = H R^3 = Ph
107b R^1 = *t*-Bu R^2 = H R^3 = Ph

109 Ar = Ph

108a R^1 = Ph R^2 = Me R^3 = 2-Napth
108b R^1 = Ph R^2 = Me R^3 = 9-Anth
108c R^1 = *o*-Tol R^2 = Me R^3 = 9-Anth
108d R^1 = *o*-Tol R^2 = Me R^3 = 2,4,6-tri-Me-Ph
108e R^1 = *t*-Bu R^2 = Me R^3 = 2,4,6-tri-Me-Ph
108f R^1 = *t*-Bu R^2 = Me R^3 = 3,5-di-*t*-Bu-4-MeOPh
108g R^1 = *o*-Tol R^2 = Me R^3 = 3,5-di-*t*-Bu-4-MeOPh
108h R^1 = Ph R^2 = Me R^3 = 3,5-di-*t*-Bu-4-MeOPh

110a Ar = 9-Anth
110b Ar = 2,4,6-tri-Me-Ph
110c Ar = 3,5-di-*t*-Bu-4-MeOPh

Figure 10. Complexes **105** and **106** -1st generation chiral iridium N,P complexes modeled after Crabtree's catalysts, **107a,b** and **109** -2nd generation Crabtree mimics, catalyst **108a-h** and **110a-c** -3rd generation catalysts.

The current trend in catalyst development in this field is not towards more general catalysts capable of handling all possible substitution patterns around a C=C bond but to customize a catalyst for improvement in a given class of substrates. It would therefore be highly advantageous to have an adaptable system that could be quickly modified to improve enantioselectivity. This chapter presents a flexible synthesis of a variety of N,P complexes based on the scaffolds **107** and **109** as well as practical aspects of the synthesis of the 2nd and 3rd generation catalysts.

2.2 Practical synthesis and investigation of 2nd generation catalysts

The initial synthesis by Kaiser[12] of the 2nd generation complexes relied entirely on chiral preparative HPLC to generate enantiopure pyridyl alcohols. While HPLC resolution is relatively fast and can deliver enantiopure materials the capital investment is prohibitive and many laboratories lack the means to take advantage of this technique. Additionally, the route utilized expensive reagents and chromatography for every step. Phosphinites are especially air sensitive ligands and cannot be stored for long periods of time therefore a change to a more stable phosphine moiety was also desired. On the other hand, the iridium BAr_F complexes are stable to normal organic conditions and can be handled in air with little decomposition but these organometallic complexes require prudent storage conditions.

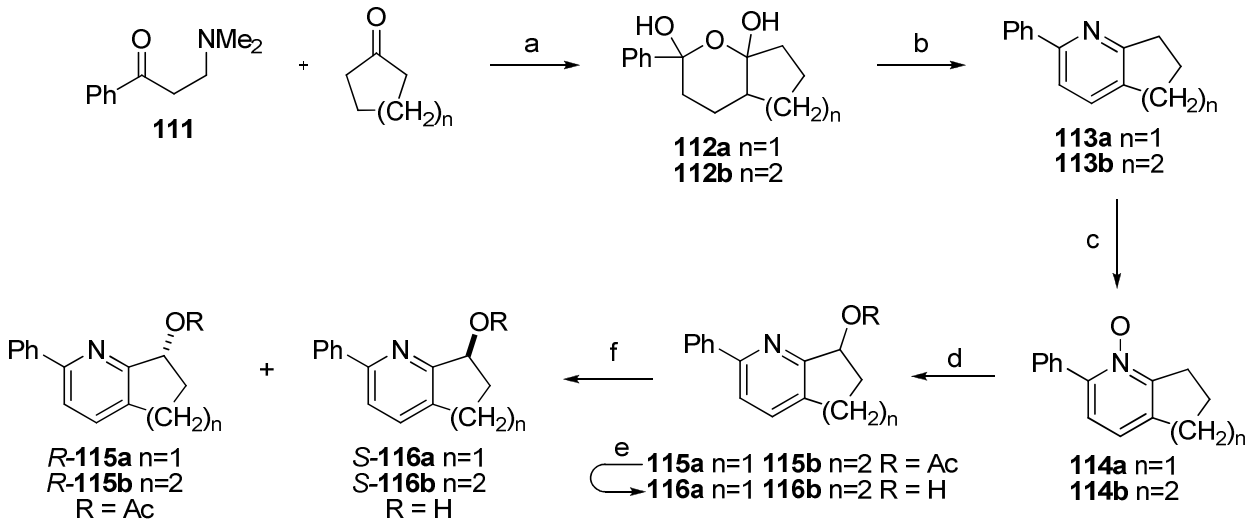

Scheme 17 Conditions: a) ketone (3 eq), 130 ˚C, 2 hours, distillation, 80-95% yield, b) NH_2OH-HCl (2 eq), ethanol, reflux 6-8 hours, distillation, 85% yield, c) H_2O_2, HOAc, quantitative, d) acetic anhydride, 25 ˚C, 1hr, 80 ˚C, 4hr, 80% yield, e) K_2CO_3, MeOH, quantitative, e) Enzymatic resolution, *Candida Antarctica* lipase B (Novozyme 435), vinyl acetate (5-20 equivalents), diisopropyl ether, 65 ˚C, 28 hours, *R*-**115a,b** >99% ee 50% yield, *S*-**116a,b** 99% ee 40-45% yield.

Synthesis of racemic alcohols **116a,b** was optimized with the expressed purpose of avoiding chromatography and maximizing yields with simple reagents (Scheme 17). Mannich base **111** was thermally reacted with either cyclohexanone or cyclopentanone to give the bridged hydrate 1,5-hemi-diketal from the 1,5 diketone on standing with ambient moisture (Scheme 18).

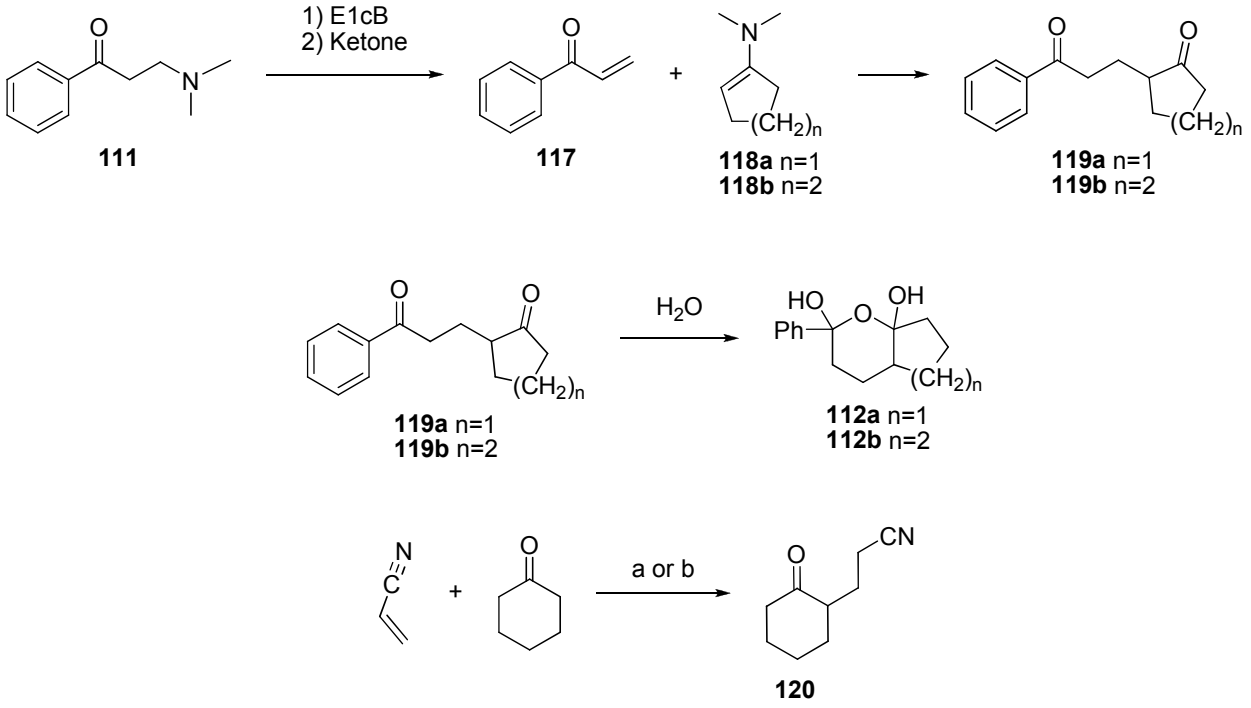

Scheme 18 Conditions: a) ketone (3eq), 130 ˚C, no reaction, b) HOAc (1 mol%), $CyNH_2$ (3.5 mol%), 86% yield.

The Mannich base **111** under goes E1cB elimination with concomitant formation of an enamine from the eliminated dimethylamine and a cycloketone. Subsequent addition of the enamine with the Michael acceptor **117** gives the 1,5-diketone **119** which under goes cyclization with an equivalent of water to give the hydrate **112**. Evidence for the enamine was given by the lack of reactivity of acrylonitrile with cyclohexanone under thermal conditions to give the 1,5-ketonitrile **120**. However, the nitrile could be easily generated in high yield by the neat reaction of a single equivalent of ketone and nitrile with catalytic amounts of cyclohexylamine and acetic acid with refluxing.

The 2-phenylpyridyl scaffolds **113a,b** were formed by ring closure with hydroxylamine hydrochloride followed by in situ oxidation of the resultant dihydropyridine in refluxing ethanol. The resulting pyridines could be purified by either distillation or precipitation of the hydrochloride salt out of acetone with concentrated acid. Oxidation of the pyridine nitrogen with a peracid such as acetic peracid or MCPBA with heat gives clean formation of the *N*-oxide. Trace impurities and color can easily be removed by recrystallization of the *N*-oxide from toluene. Boekelheide rearrangement of the *N*-oxide to the racemic pyridyl acetates **115a,b**

occasionally gives elimination byproducts, especially if greater quantities of a stronger acid are present.

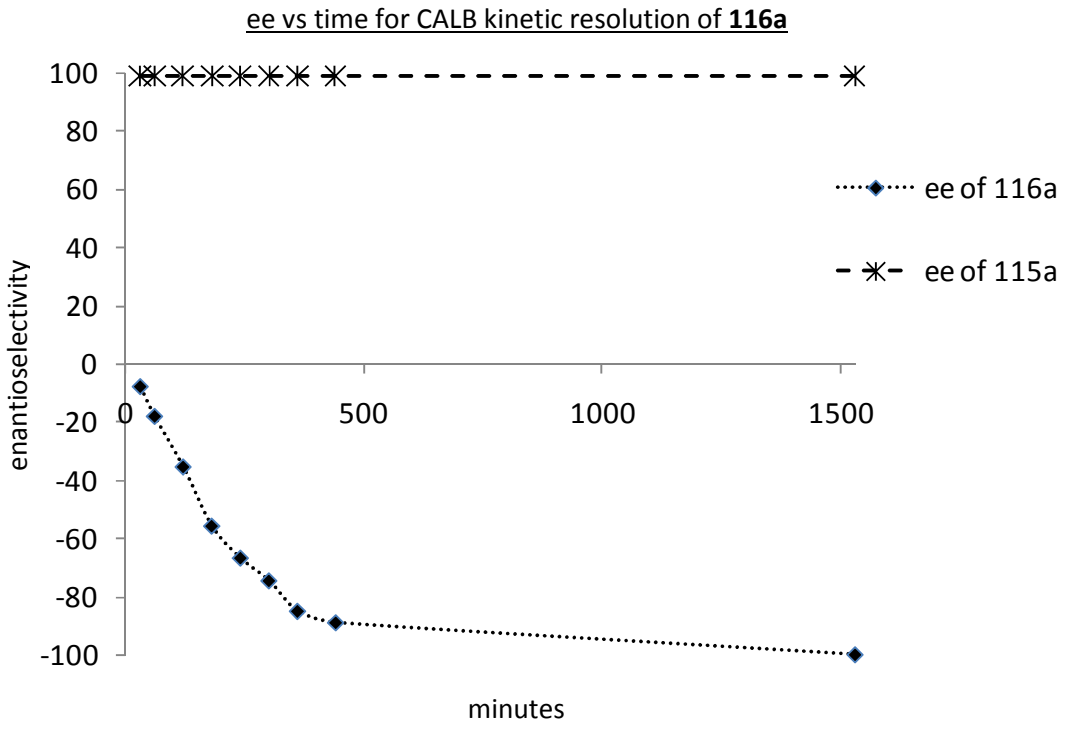

Figure 11. Plot of kinetic resolution of racemic **116a.**

Transesterfication with methanol and finely powdered potassium carbonate furnishes the racemic alcohols **116a,b**. Kinetic resolution with *Candida Antarctica* was first reported for closely related pyridyl alcohols by Uenishi.[17, 18] Optimization of the kinetic resolution followed by precipitation of *S*-**116a,b** with an equivalent of phthalic anhydride was reported recently from this laboratory.[19] The enantioselectivity of the lipase gives the *R*-acetates of **115a,b** with a constant enantioselectivity of greater than 99% (Figure 11). Maximum ee for both the acetate and alcohol is achieved with 16 hours with 10% weight to weight immobilized lipase to pyridyl alcohol. Temperature, rate of mixing and number of equivalents of acylating reagent all affect the ee of the reaction and the rate.

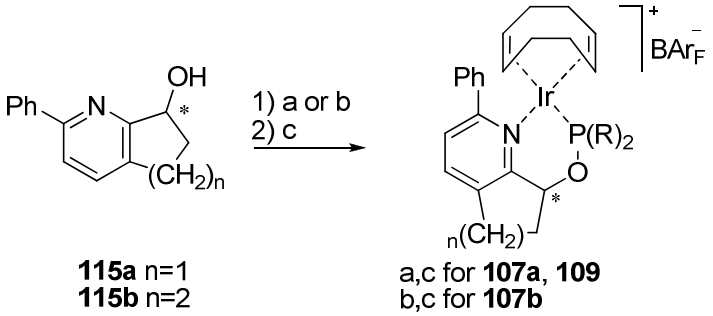

115a n=1
115b n=2

a,c for **107a**, **109**
b,c for **107b**

Scheme 19 Conditions: a) DMAP (1eq), Ar_2PCl (1eq), b) NaH (2.5 eq), (*tert*-Bu)$_2$PCl (1 eq), c), $(IrCODCl)_2$ (0.5eq), $NaBAr_F$ (1.1 eq).

The resulting enantiopure alcohols were converted to the iridium complexes by a reaction sequence outlined in Scheme 19. Diarylphosphinite complexes **107a** and **109** were synthesized with a single equivalent of DMAP and diarylphosphine chloride followed by filtration of the resulting slurry into a solution of $(IrCODCl)_2$ and $NaBAr_F$ to generate the iridium complex in 66% yield. Di-(*tert*-butyl)phosphinite complex **107b** was synthesized by deprotonation of the pyridyl alcohol in a mixture of DMF and THF in the presence of the phosphine chloride, vacuum removal of the volatiles followed by filtration into a solution of an iridium source and counterion to give 79% yield of the complex after chromatography.

Mulitgram synthesis of catalysts **107a,b** and **109** is now possible with the use of easily accessed reagents. This will greatly aid other organic chemists who wish to use these highly active and selective hydrogenation catalysts.

While the synthesis of the second generation catalysts has been improved issues exist with using this committed and linear approach to catalyst development. Some complications with phosphinite moieties are their instability for long term storage where phosphines or phosphine oxides can be stored for extended periods and can be easily prepared for use with a fresh source of metal to avoid catalyst decomposition. However, changing the soft donor phosphonite for a phosphine could affect the overall reactivity of the complex and lead to a different reactivity profile as seen in the next section.

2.3 Phosphine analogues of the second generation catalyst

Kaiser synthesized phosphine based systems **121a,b** and **122** (Table 20).[20] Verendel and Andersson[21] have reported the synthesis of a pyridyl phosphines based on a pinene skeleton **124a,b** as well with similar results. This section deals with the synthesis of **123a,b** and the postulated decomposition pathways that lead to its deactivation.

Initial signs of different reactivity of the phosphines in comparison to the phosphinite analogues were evident from the yields of complexation. Much lower yields, and in the case of **123b** virtually no yield, indicated a degradation pathway was present and active. Phosphine complexes that gave the highest yield were also the least encumbered or had wider bite angles such as **121a,b**.

Table 20. Comparison of complexation yields and initial screening results for phosphines.

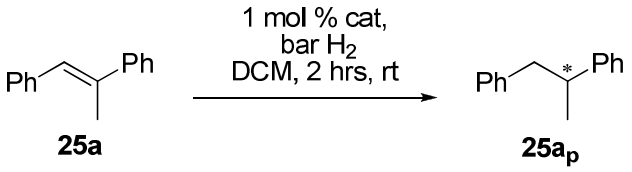

25a → **25a$_p$**

Complex	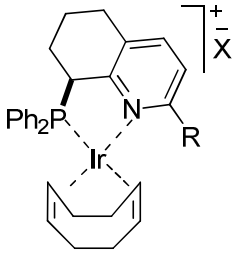 **121a** R = H **121b** R = Me X = BAr_F	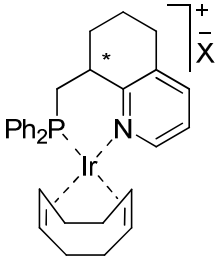 **122** X = BAr_F	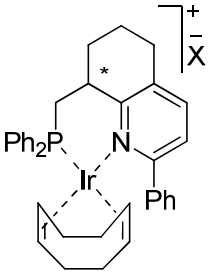 **123a** X = PF_6 **123b** X = BAr_F	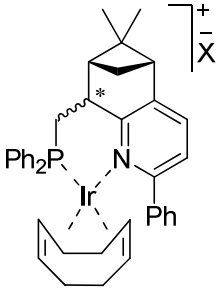 *trans* **-124a** *cis* **-124b** X = BAr_F
%yield for complexation	a- 51% yield b- 57% yield	22% yield	a- 17% yield b- not isolated	a- 20% yield b- 30% yield
Reduction results ee% (conv%)	a- 6% ee (99%) b- 53% ee (6%)	88% ee (99%)	b- 0% ee (2%)	a- 95% ee (20%) b- na ee (0%)

121a,b and **122** are reported by Kaiser,[20] **124a,b** are reported by Verendel.[21]

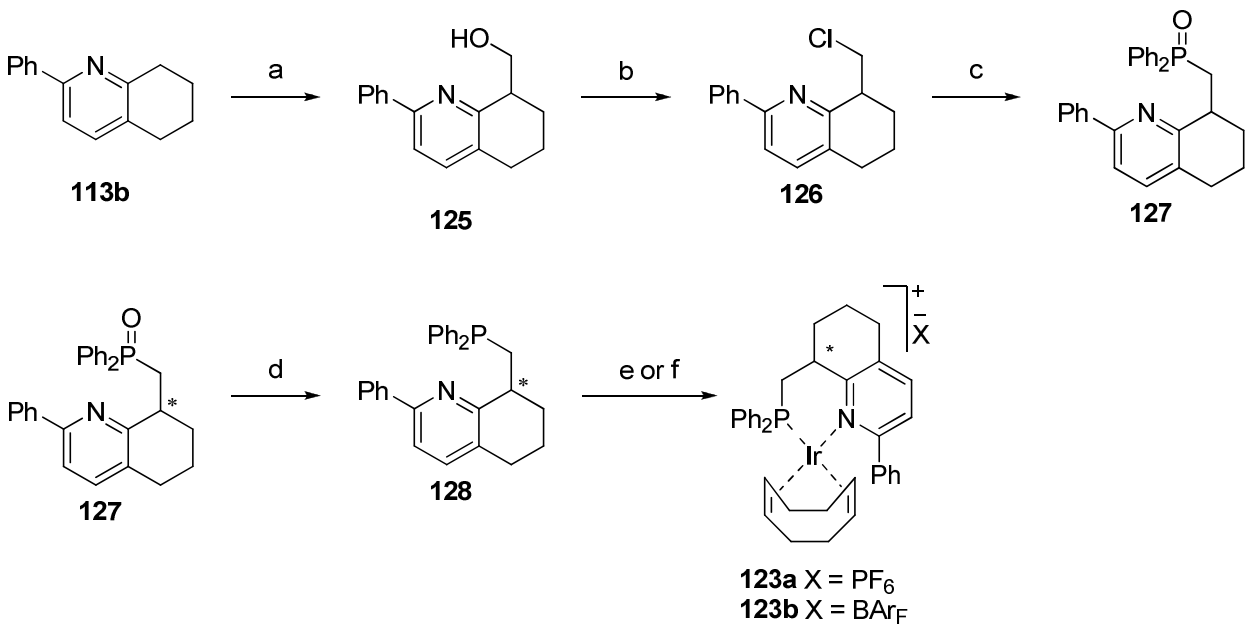

Scheme 20 Conditions: a) *n*-BuLi (1.1 eq), paraformaldehyde (1.5 eq), 61% yield, b) $SOCl_2$ (30 eq), 95% yield, c) $KPPh_2$ (1eq), H_2O_2 (excess), 68% yield, chiral AD column, d) $PhSiH_3$, e) $(IrCODCl)_2$ (0.5 eq), NH_4PF_6 (2 eq), f) $(IrCODCl)_2$ (0.5 eq), $NaBAr_F$ (1 eq).

Synthesis of the phosphines for **123a,b** was carried out as described in Scheme 20. Deprotonation of the benzylic position with a slight excess of *n*-BuLi followed by addition of solid paraformaldehyde resulted in the pyridyl alcohol **125** in 61% yield. Use of larger amounts of paraformaldehyde resulted in poly-acetals which formed intractable gel phases. Chlorination with thionyl chloride as solvent yielded the metastable chloromethyl pyridine **126** which was used immediately. Phosphinide addition with potassium diphenylphosphinide followed by quenching and oxidation with hydrogen peroxide yielded the phosphine oxide **127** in 68% yield. The phosphine oxide was easily resolved by chiral HPLC. Reduction with phenylsilane followed by filtration through alumina under Schlenk conditions yielded the phosphine **128.** Phosphorus NMR indicated a clean conversion to the desired phosphine (Figure 12).

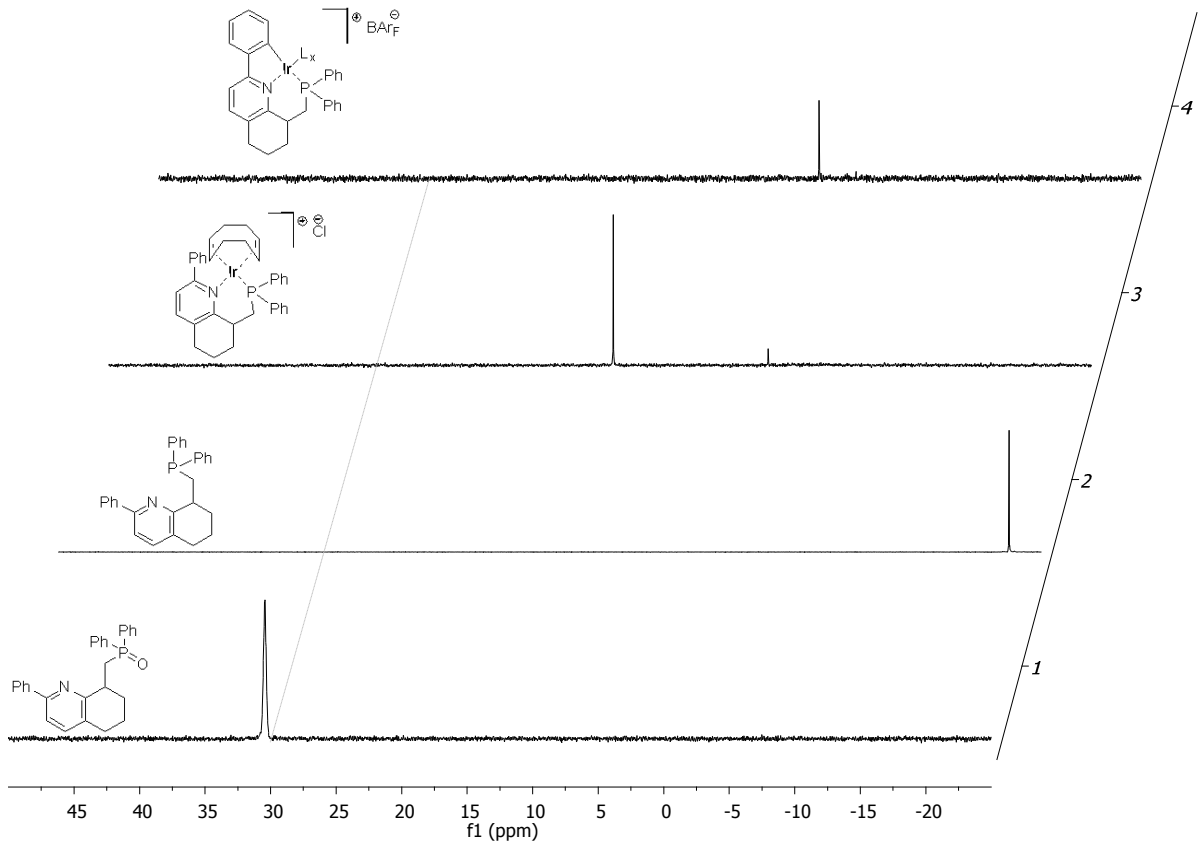

Figure 12. ^{31}P monitoring of the complexation sequence in the attempted synthesis of **123b.**

Complexation of the resulting phosphine with $(IrCODCl)_2$ resulted in the formation of two species by ^{31}P NMR with an expected signal at 12ppm for the coordinated phosphine and a new species at 0 ppm. Addition of NH_4PF_6 followed by chromatography yielded a very low quantity of the desired complex, of which x-ray quality crystals were obtained (Figure 13). The phosphine complex **123a** was virtually identical to the phosphinite systems previously studied and no obvious deviations in reactivity were apparent from the structure.

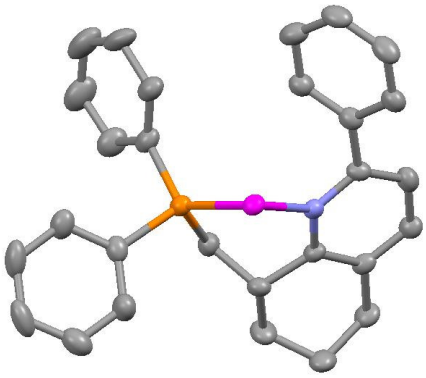

Figure 13. Ortep drawing of **123a**, COD and PF_6 are omitted for clarity.

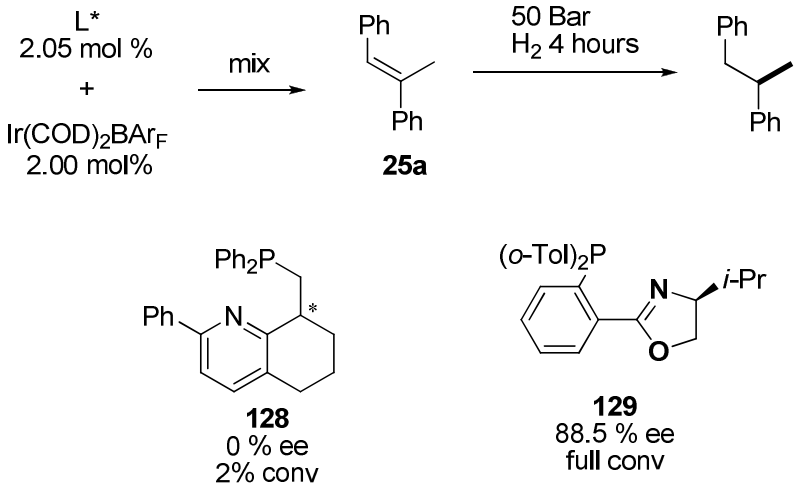

Scheme 21

Initial attempts to synthesize **123b** failed to produce complexes stable to chromatography and monitoring of the complexation sequence by ^{31}P NMR revealed the addition of the non-coordinating BAr_F counterion caused the new signal at 0 ppm to become the sole resonance. The new ^{31}P peak was right shifted where most additions of weaker counterions left shift the phosphorus signal due to increased Lewis acidity of the metal center. The ^{1}H NMR gave complex spectra from which no intelligible information could be gathered. In an attempt to ascertain whether the complexes could be used in catalytic reactions an in situ complexation/ asymmetric hydrogenation strategy was developed. In comparison with PHOX phosphine **129**

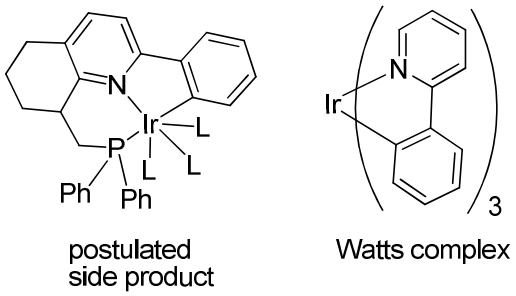

Figure 14. Side product and comparison to Watts complex.

which reduced substrate **25a** in 88% ee and full conversion pyridyl phosphine **128** completely failed to react even when prepared under rigorous exclusion of moisture and oxygen (Scheme 21). Given these data phosphine derived pyridyl N,P ligands are unstable under conditions required for hydrogenation catalysts and give poor catalysis. A possible reason for this could be cyclometalation of the 2-aryl position to make a C,N,P tridentate chelate analogous to the Watts complex (Figure 14).[22, 23] Further experiments with phosphinite based systems in the Pfaltz group led to the isolation of phosphinite analogues of the proposed side product in figure 13.[24] Oxidative addition of C-H bonds are favored by electron rich group 8 metals such as iridium and rhodium,[25] increased electron density on the metal center from a stronger σ donating phosphine ligand would promote such a reaction. From these results modification of the aromatic ring with stabilizing groups to block orthometalation is a logical step.

2.4 Development of a flexible synthesis for 3rd generation catalysts

Development of a ligand system which allows for the quick modification of the catalyst would allow for probing of how structure influences function with incremental changes to the system. It would therefore be advantageous to have an adaptable system that could be quickly modified to identify and improve enantioselectivity trends at will. This section presents a flexible synthesis of a variety of N,P complexes based on the catalysts **107a,b** and **109.** Chapter 3 details the application of these catalysts in the successful asymmetric hydrogenation of several examples of trisubstituted alkenes that gave unsatisfactory results with previous generations of catalysts.

Data from earlier work has allowed us to develop some guidelines that hav led to more selective and active catalysts in the reduction of weakly coordinating trisubstituted alkenes. Catalysts with both di-(*tert*-butyl) and di-(*ortho*-tolyl)phosphinites in combination with a 5-membered ring backbone such as **107a,b** gave superior enantioselectivity than the less bulky

phosphinite analogues. However, catalysts with a 6-membered ring based scaffold such as **109** perform best with di-(*ortho*-tolyl)phosphinites and often give better results compared to the di-(*tert*-butyl)phosphinite analogues or complexes with a less sterically demanding phosphinite. We also found the substituent in the *ortho* position of the pyridine ring to be critical to both activity and selectivity with the optimal size and shape being phenyl. Larger groups such as *tert*-butyl were not tolerated in this position while smaller groups gave lower enantioselectivity. This substitution dependence of the catalyst was seen as an opportunity to extend the reactivity and selectivity profile of the catalyst.

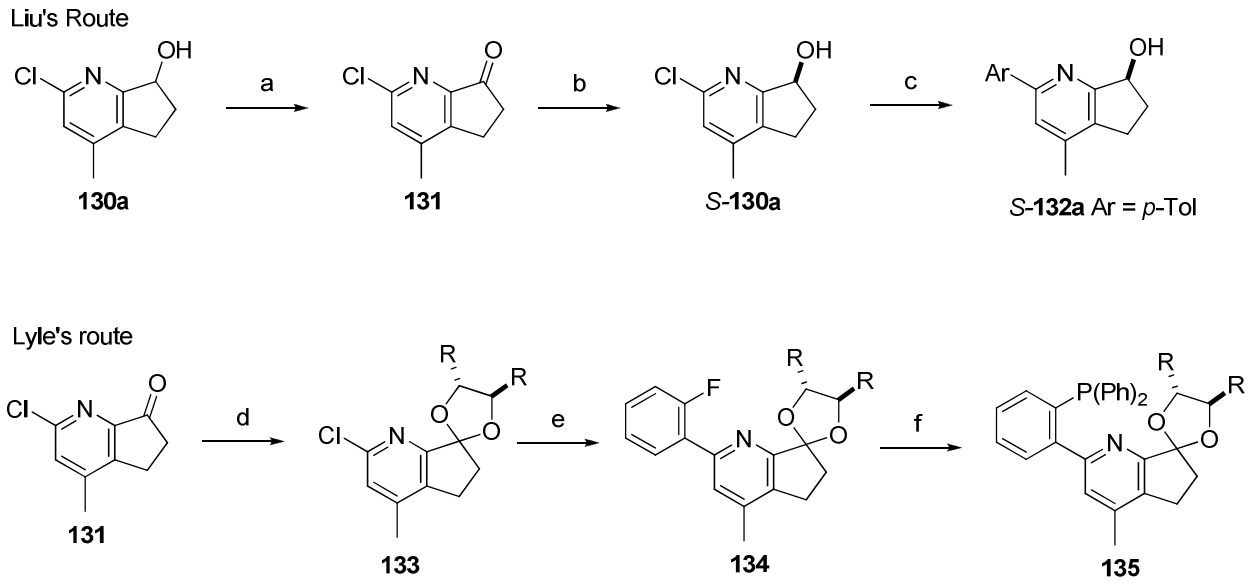

Scheme 22 Conditions: a) Swern, b) *R*-MeCBS, BH_3THF, 30 ˚C, 88% ee (99% recrystallized), c) $Pd(PPh_3)_4$ (5 mol%), $ArB(OH)_2$ (3 eq), Na_2CO_3/H_2O, EtOH,$MeOCH_2CH_2OMe$, reflux 16 h, 99% yield, d) 1,2-diols R = Me, *i*-Pr, and Ph, *p*-TsOH (cat.), benzene, reflux, 16 h, 79-85% yield, (e) *o*-F-$C_6H_4B(OH)_2$, 5 mol % of Pd_2dba_3, 10 mol % of P(*t*-Bu)$_3$, Cs_2CO_3, THF, reflux, 16 h, 81-93% yield, (f) Ph_2PH, KO*t*-Bu, 18-crown-6, THF, rt, 24 h, 72% yield.

In order to explore further structural modifications we required a flexible synthesis that would allow for the incorporation of a variety of aromatic substituents on the pyridine ring at a later phase of the route. Shortly after our initial publications Liu et al reported a route to nearly the same complexes that utilized a Suzuki coupling to install the aromatic group with a late intermediate.[26] Lyle[27-29] et al used the same strategy prior to Liu's work to build a chiral ketal based P,N ligand, albeit with different placement of the phosphorus moiety (Scheme 22).

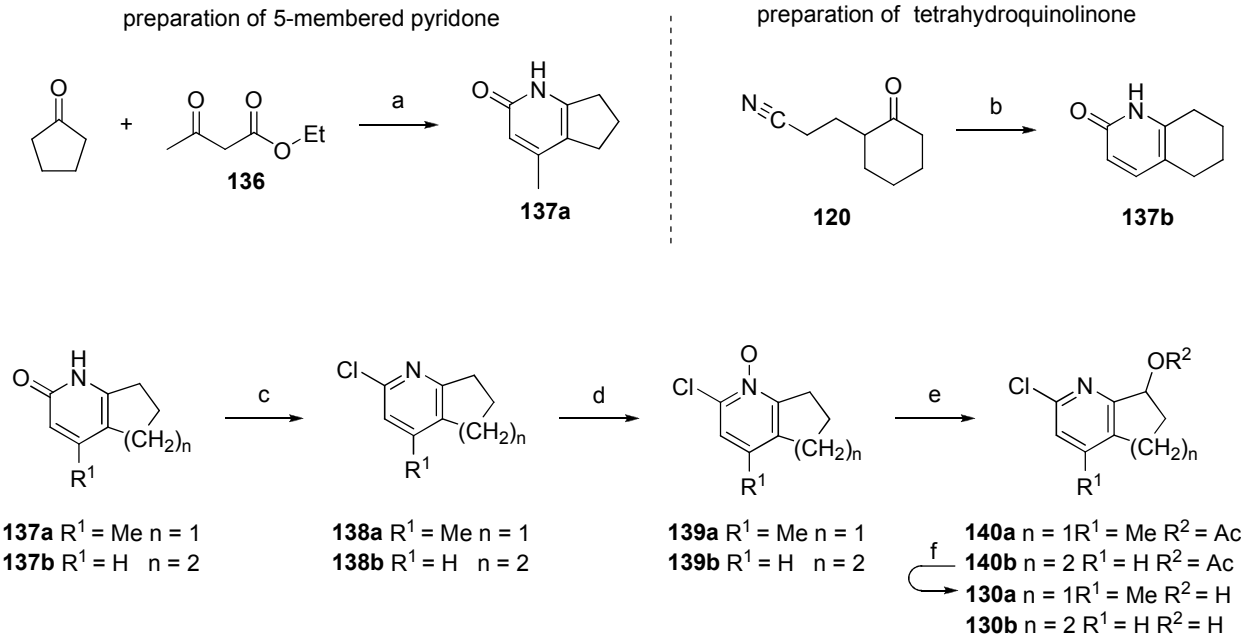

Scheme 23 Conditions: a) NH_4OAc (1eq), cyclopentanone (1 eq), ethyl acetoacetate **136** (1 eq), 135 ˚C 18 hrs, 19% yield, b) H_2SO_4, 0 to 29 ˚C, 3 hours, 43% yield, c) $PhPOCl_2$ (4 eq), 110 ˚C, 18 hrs, 80% yield, d) H_2O_2, HOAc, 100 ˚C, 93-94% yield, e) acetic anhydride, 25 ˚C, 1hr, 80 ˚C, 4hr, 77-81% yield, f) K_2CO_3, MeOH, 88-97% yield.

Racemic alcohols **130a,b** were prepared with a modified route essentially following the reports of Lyle and Liu (Scheme 23). Pyridone **137a** was prepared in a very low yield of 19% therefore an alternative preparation of **137b** from nitrile **120** was accomplished according the procedure of Meyers.[30] An improvement of 37% overall yield of **137b** was achieved but at the cost of additional time and the use of very caustic and toxic reagents. Chlorination of the pyridones proved difficult with most electrophilic reagents such as thionyl chloride or phosphoryl chloride yielding complex tar like mixtures. Use of the milder phenylphosphoryl chloride yielded the desired 2-chloropyridines in high yield. Oxidation with in situ generated peracetic acid generated the *N*-oxide in greater than 90% yield. Boekelheide rearrangement of the *N*-oxide followed by deprotection by transesterfication gave the racemic alcohols **130a,b** in over 70% yield for two steps.

Both groups reported high yields of in the cross coupling of the chlorides with simple boronic acids under optimized conditions. Unfortunately the routes relied upon the use of solvent conditions not amendable to less soluble boronic acids, large excess of reagents, and all attempts to use less reactive boronic acids or slightly different conditions failed to produce appreciable amounts of product (Scheme 24). Noting that there are very few reports of coupling hindered boronic acids with 2-pyridyl chlorides in the literature we decided to replace the

chlorine for a bromine atom but our efforts led to low yield of product and complex mixtures. This replacement is logical but Liu and Lyle's routes relied on optimization of chlorides without mention of attempts to synthesize more reactive 2-halopyridines, this may be due in part to difficulty in preparing the intermediates.

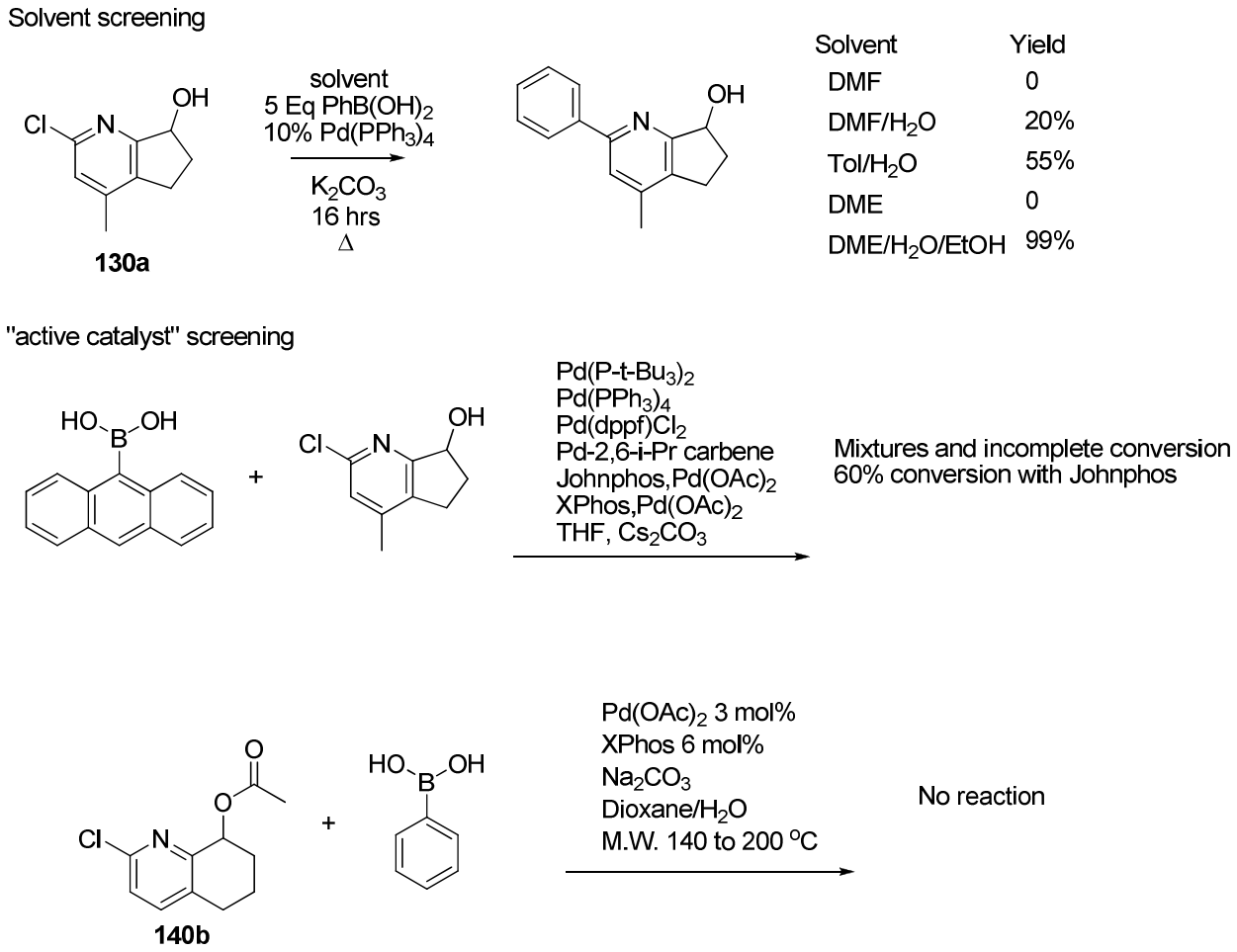

Scheme 24

Realizing the hydroxyl group created a chelating structure with the adjacent pyridine ring that could be responsible for slow to nonexistent catalyst turnover we decided to investigate two possible strategies to circumvent this problem, one incorporating the Suzuki coupling before the hydroxylation (Scheme 25) and a second route via a silyl protected hydroxyl group (Scheme 26).

The Nolan NHC catalyst **144** proved to be extremely effective for the coupling of hindered, insoluble boronic acids with aryl chlorides. Use of microwave tubes as reactors allowed a slight increase in temperature which helped to dissolve highly insoluble coupling

reagents and a static inert atmosphere which prolonged catalyst lifetime. A slight excess of boronic acid was used to ensure complete conversion of the 2-chloropyridine.

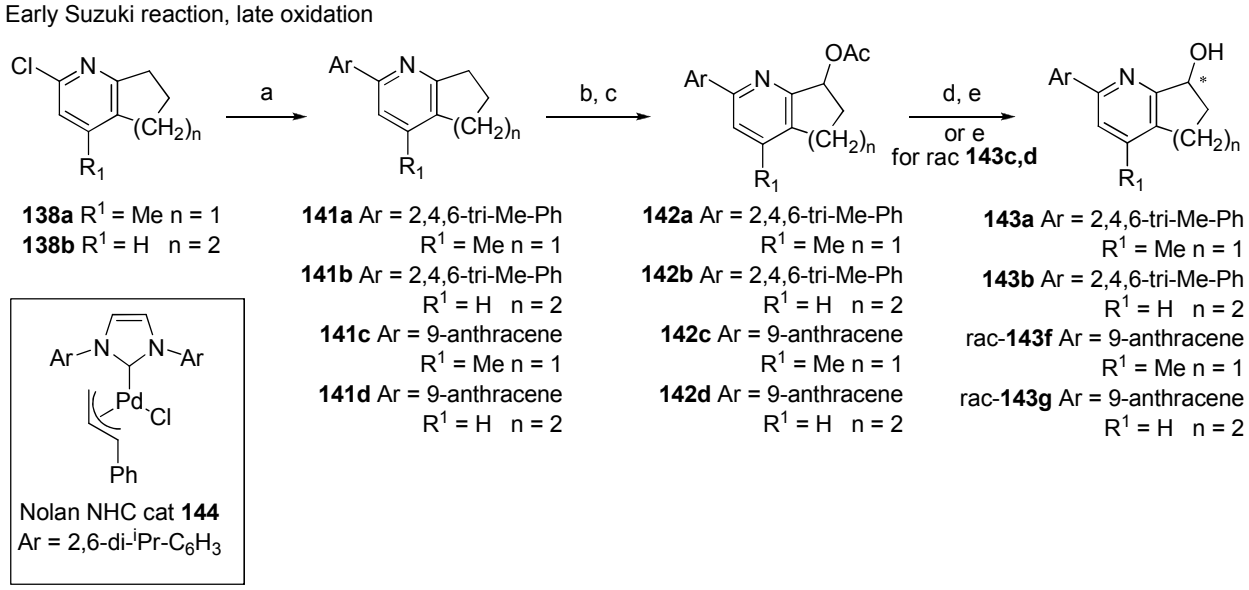

Scheme 25 Conditions : catalyst **144** (1-2 mol%), $ArB(OH)_2$ (1.2 eq), IPA, 4M NaOH (3 eq), 105-115 ˚C, **141a** 86%, **141b** 87%, **141c** 97%, **141d** 90%, b) MCPBA (2-3 eq), c) acetic anhydride, 107 ˚C, yield for b,c **142a** 50%, **142b** 66%, **142c** 39%, **142d** 50%, d) chiral HPLC, e) 4M NaOH, THF, 65 ˚C.

Oxidation with MCPBA gave exothermic reactions with the 2-mesityl-pyridines **142a,b** in greater than 90% yield while anthracene derivatives **142c,d** required mild heating to 42 ˚C to reach completion. Boekelheide rearrangement required higher temperatures for all of the sterically hindered 2-arylpyridines and lower yields were obtained, especially for the easily oxidized anthracene derivatives. Pyridyl esters **142a-c** were amendable to enantiomeric separation by chiral preparative HPLC but **142c,d** were far less soluble in the mobile phases used for this technique. Derivative **142c** was marginally soluble, requiring nearly triple the amount of solvent than the mesityl analogues and thus limiting the amount of material that could be separated in a reasonable amount of time. Pyridyl ester **142d** was to insoluble to be of practical use in this technique. The bulky 2-arylpyridines required strong base and heat to hydrolyze the acetyl group and all attempts to use less harsh conditions failed to produce any product.

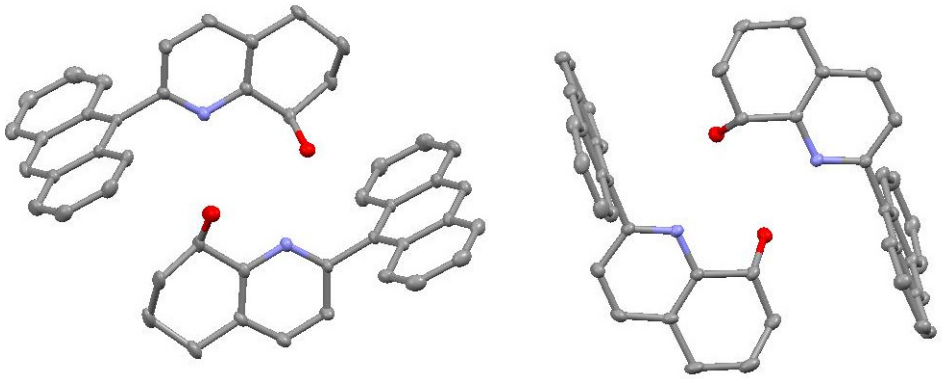

Figure 15. Ortep of *R*-**143g**, hydrogen atoms are omitted for clarity.

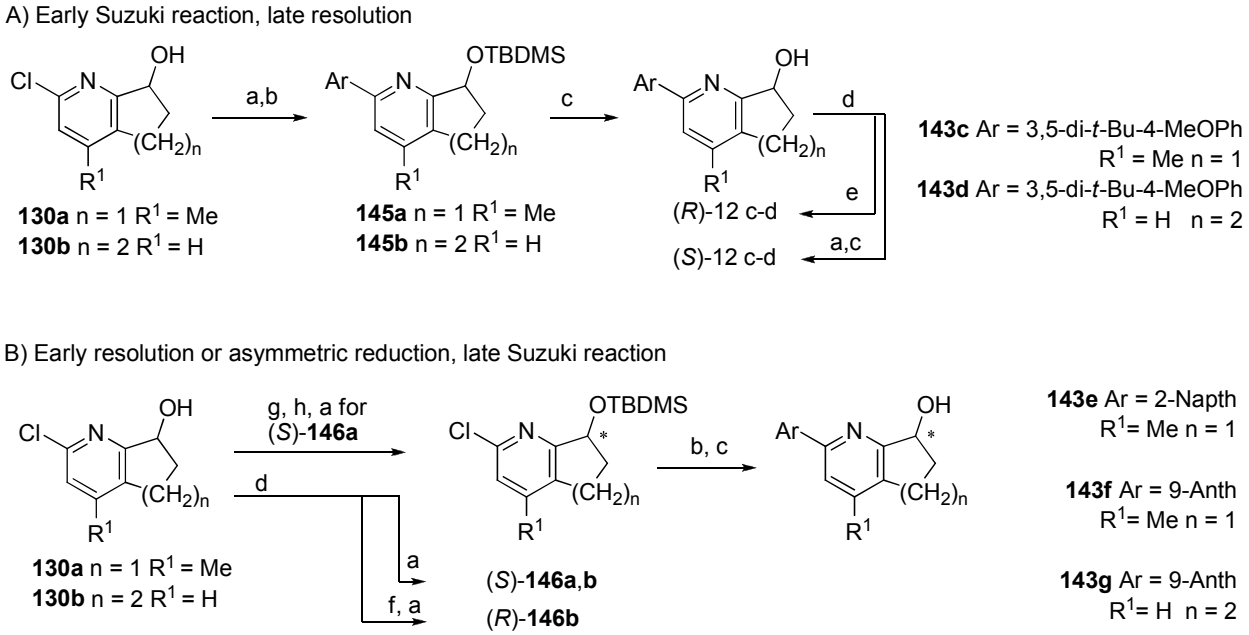

Scheme 26 Conditions: a) TBDMSCl (2.5 eq), imidazole (3 eq), DMF, overnight, 86-98%, b) catalyst **144** 4 mol%, $ArB(OR)_2$ (1.5-2eq), NaOH (3 eq), 50 ˚C, 16 h, 86%, c) TBAF -3H_2O (3 eq), THF, 50˚C, 79-84%, d) Novozyme 435, DIPE, vinyl acetate, e) NaOH, THF, 65 ˚C, f) K_2CO_3, MeOH, 90-95%, g) Swern, 95%, h) (-)DIPCl (1.5 eq), THF, -50 ˚C, 2 days, ethanolamine (1.5 eq), 51% yield 99% ee.

All attempts to resolve the racemic alcohols of the 2-mesityl derivatives **143a,b** and the 2-anthracyl analogues **143g,f** with CALB failed to produce any detectable amounts of product. Likewise, kinetic resolution of the esters **142a-d** with CALB also failed to produce any product. We attribute the loss of reactivity in both the forward and reverse reactions to a locked perpendicular ring system that blocks the approach of the alcohol to the reactive site in the

enzyme. X-ray crystal structures of the *R*-alcohol **143g** indicated a very sequestered hydroxyl group buried in a six-membered ring formed from hydrogen bonding with a second pyridyl alcohol to form a dimer and a second interaction between two anthracene groups bound together by edge face C-H-π interactions that completed an encumbered tetramer (Figure 15).

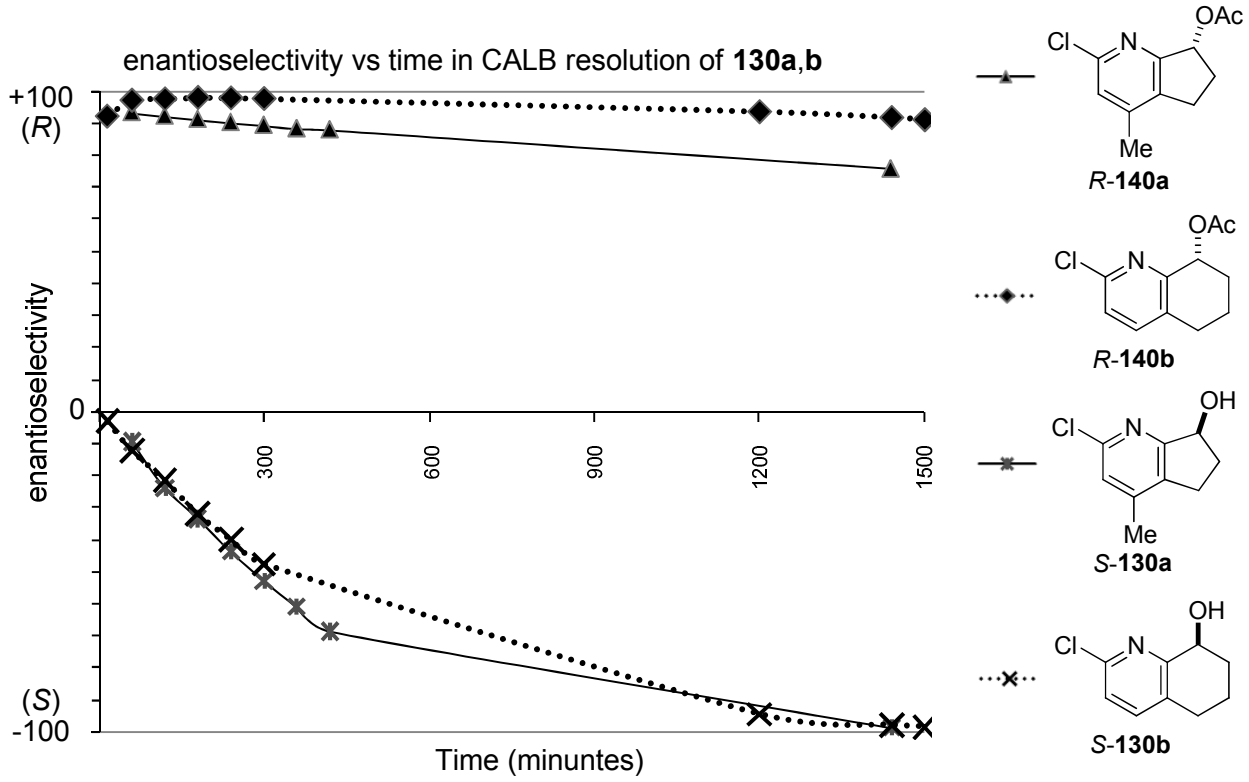

Figure 16. Plot of enantioselectivity of kinetic resolution of **130a,b** vs time.

Fortunately we were able to resolve the chlorides **130a,b** with some success. In small test resolutions we followed the enantioselectivity with time to gain a better understanding of the reaction parameters and optimal time (Figure 16). We found that the racemic tetrahydroquinoline **130b** gave excellent enantioselectivity in production of the *R*-acetate **140b** with a shallow sloped linear behavior; the *S*-alcohol **130b** was produced in 99% ee within 28 hours albeit with a small loss of enantioselectivity of the *R*-acetate. The *R*-acetate **140b** could be easily recrystallized from cold pentane with 56% return of the product in 99% ee. The 5-membered bicyclic racemic **130a** proved to be much more difficult to resolve with a lower ee in the initial acyl ester **140a** formed and a far more dramatic loss of ee with the *R*-acetate **140a** over time. However, the *S*-alcohol of **130a** could be obtained with 99% ee with a small loss of yield.

In contrast to the 2,6-disubstituted-2'-arylpyridylalcohols the bulky 3,5-di-*tert*-butyl-4-methoxyphenyl derivatives **143c,d** were easily resolved with CALB in high enantiomeric excess.[31] This result clearly indicates that bulk is not an issue but accessibility of the enzyme to the hydroxyl group on the substrate.

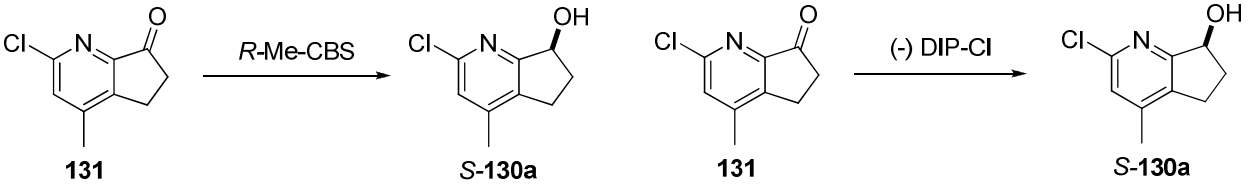

131 → ***S*-130a**

THF-Borane 10-20 mol% cat	rt	88% ee 90% y
THF-Borane 10-20 mol% cat	0 °C	78% ee 65% y
Catechol Borane/ DCM 10-20 mol% cat	-20 °C	90.8% ee 90% y
Catechol Borane/ DCM 10-20 mol% cat	-78 °C	90.6% ee 90% y

131 → ***S*-130a**

THF, slow liquid add 1.3 eq	-78 °C to rt	95% ee
THF, slow liquid add 1.3 eq	-40 °C	96% ee 65% y
THF, solid add 1.5 eq	-50 °C	99.2% ee 50% y

Scheme 27

Dissatisfied with the resolution of **130a** we attempted a number of asymmetric reductions of the parent ketone with a commercial oxazaborolidine catalyst and found similar results to those of Liu[26] and Xie[32] who reported enantioselectivities up to 93% ee (Scheme 27). While reproduction of the results of Liu were not fruitful modification of the reducing reagent to catecolborane, replacing the THF with DCM as solvent, and cooling the reaction to -20 ˚C an ee of 90% could be achieved. We were somewhat more successful using (-)-DIPCl in a stoichiometric reduction which generated the desired *S*-alcohol **130a** in 99% ee and 51% yield. The reduction was extremely sensitive to temperature and addition technique with addition of the solid DIPCl to a -50 ˚C solution in THF and stirring for two days at that temperature providing the optimal yield and selectivity.

All of the pyridyl alcohols and acetates traveled at very similar R_f values on silica gel thus making purification highly problematic. The solution to address this problem in a reproducible manner was the formation of a stable silyl ether with the isolated reaction mixture followed by a simple column. The non-polar silyl ethers washed easily of the silica gel with

non-polar mixtures of DCM and hexane while the more polar acetates were retained and could be eluted with a higher polarity solvent.

Subsequent Suzuki couplings of **146a,b** with 1.5 to 2 equivalents of boronic acid at a 50 ˚C resulted in greater than 90% yield of the desired 2-arylpyridines. Catalyst **144** was quite effective, coupling a handful of very difficult boronic acids at moderate temperatures with **146a,b** (Scheme 28)**.**

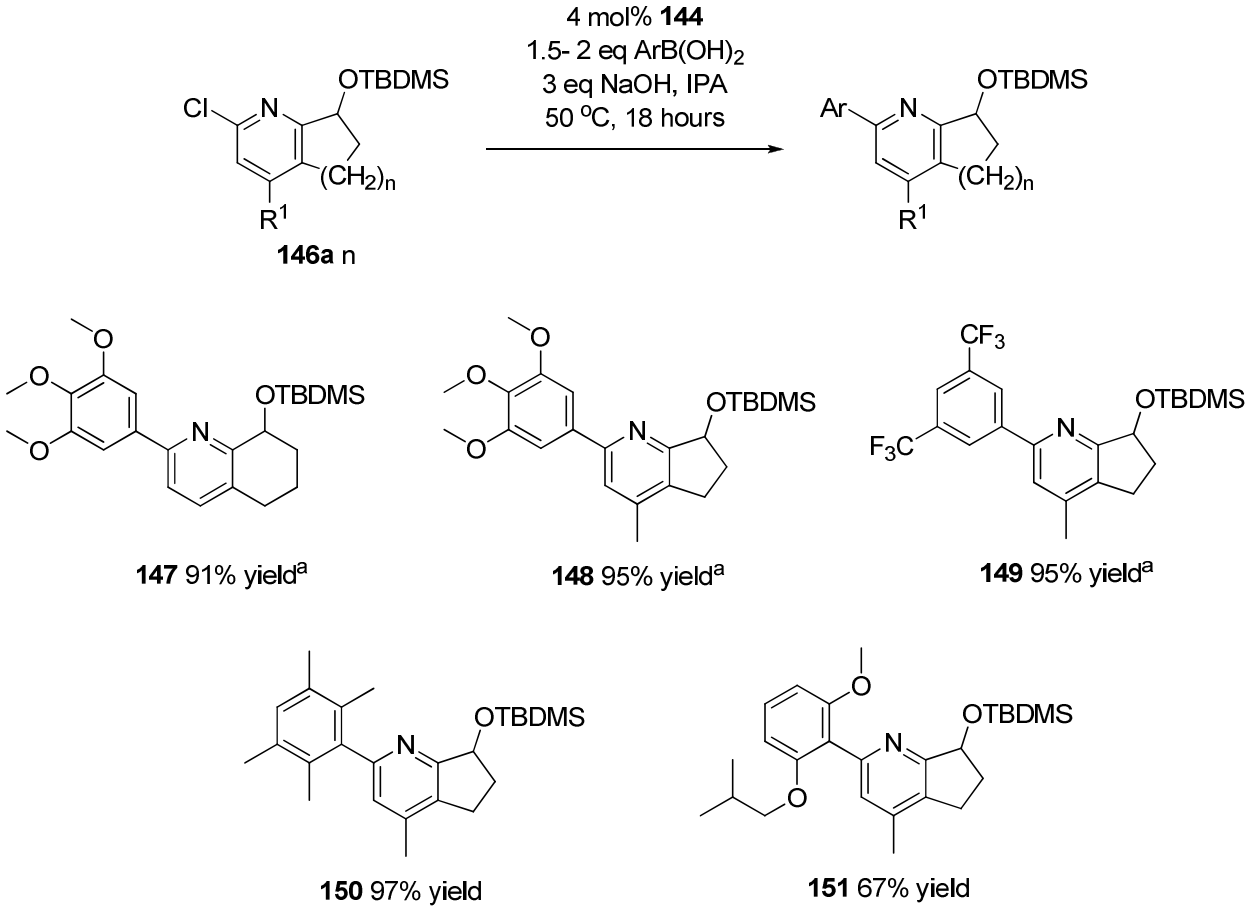

Scheme 28 a) Reference [31].

Nearly all of the products in Scheme 28 were achieved in sgreater than 90% yield with the exception of the very difficult **151** which was obtained in a useful 67% yield, products **147-149** were produced in near perfect yield by Müller[31] using this methodology. The silyl protecting group also had the added benefit of reducing the polarity of the desired compound and facilitating purification by column chromatography. The resulting silyl ethers were sluggish in the deprotection step with TBAF, likely due to the limited approach of the fluorine to the silicon atom but gentle heating furnished the desired alcohols in high yield.

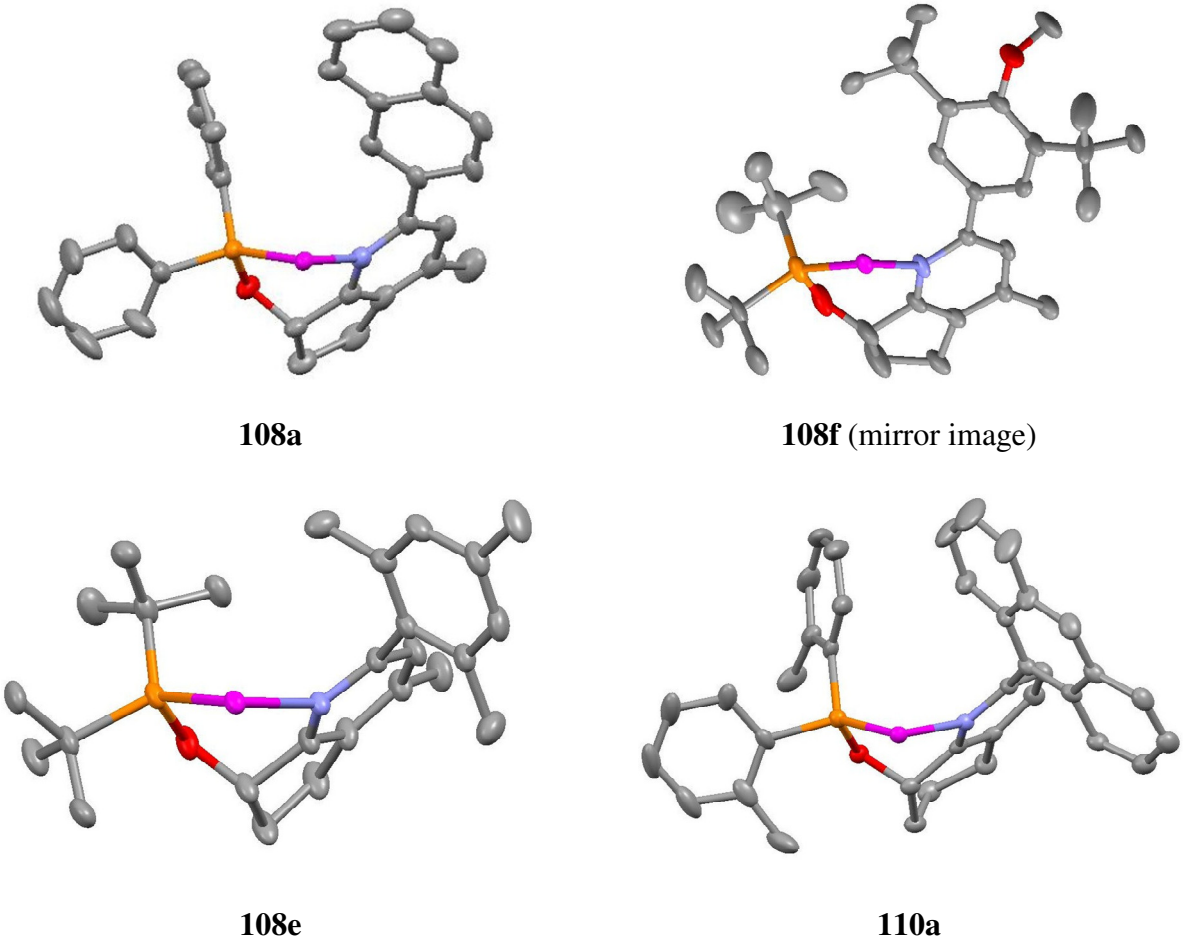

Figure 17. Ortep drawings of **108a**, **108f**[31] (mirror image), **108e**, and **110a** with COD ligand and counterion omitted for clarity.

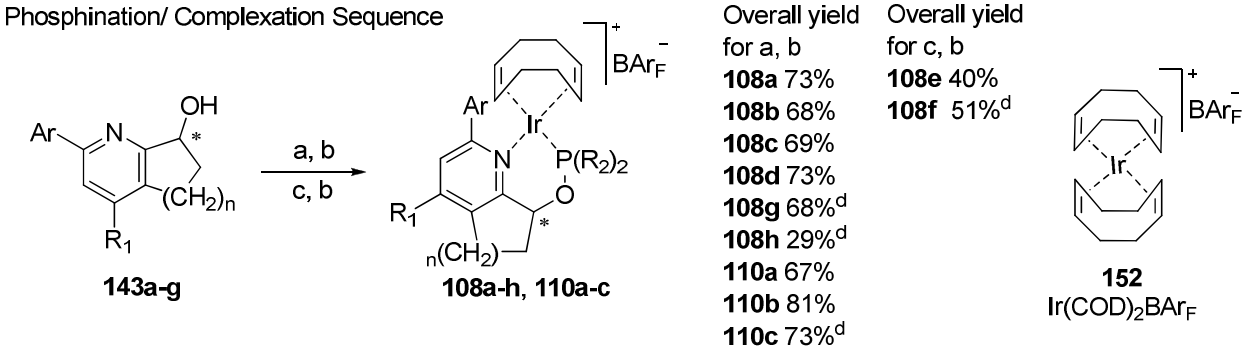

Scheme 29 Conditions: a) DMAP (1 eq), Ar_2PCl (1 eq), THF, 24h, b) complex **152** 1eq, c) KH 1.5 eq, DMF, $ClP(tert\text{-}Bu)_2$, 2 days, d) reference [31].

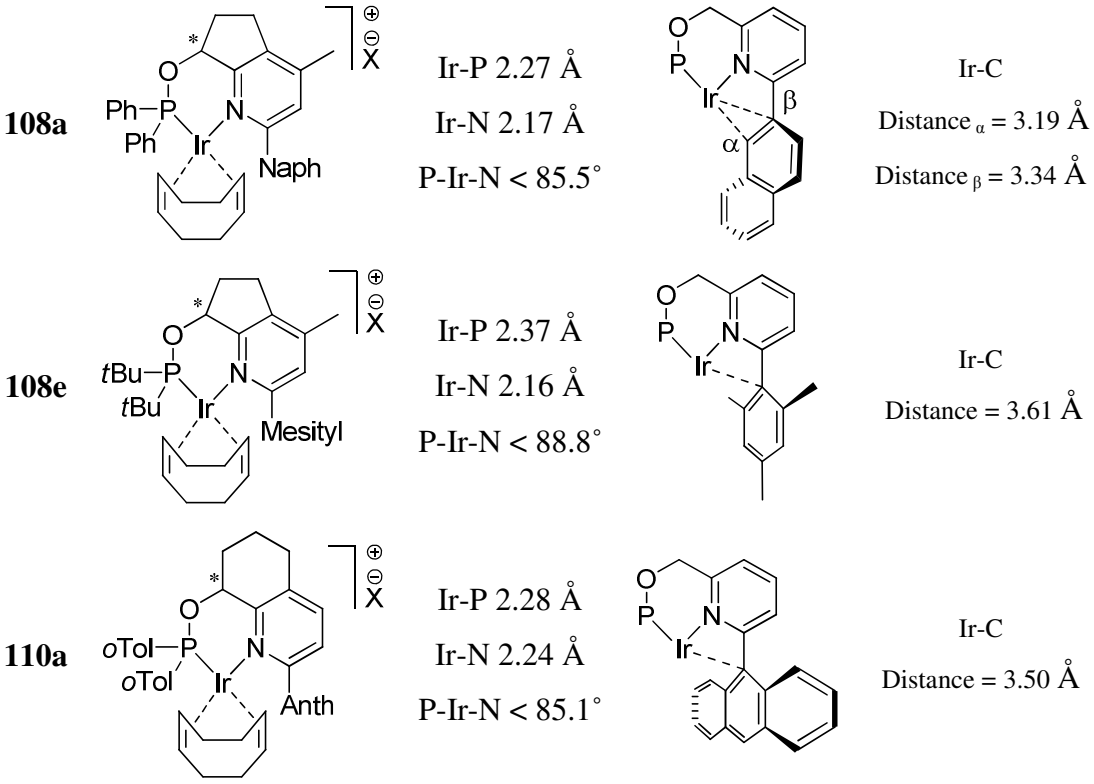

Figure 18. Bond lengths, distances, and angles for 3rd generation chiral Crabtree complexes, X = BAr_F anion, Naph = β-naphthyl, Anth = 9-anthracyl, mesityl = 2,4,6-tri-methylbenzene.

A reaction sequence of the chiral alcohol with diarylphophine chlorides and DMAP as an activating base followed by a simple filtration through silica gel into a solution of $Ir(COD)_2BAr_F$ or $[Ir(COD)Cl]_2$ and $NaBAr_F$ generated the desired complexes in reasonable yields for most of the catalysts (Scheme 29).

Formation of *tert*-butyl derived phosphinites was more challenging, the reactions required concentrated conditions and potassium hydride as base in DMF with extended reaction times. Concentration of the reaction mixture was a critical parameter with the reaction proceeding within reasonable time at higher concentration and slowing down to impractical levels (ca 7-10 days) under more dilute conditions.

X-ray quality crystals of complexes **108a, 108e, 108f,**[31] and **110a** were grown from mixtures of DCM and pentane. The solid state structures indicate a very congested environment about the metal center for all of the catalysts with both the *ortho* and *meta* substituents of the pendant biaryl moiety coming in close contact with substituents on the phosphorus atom (Figure 17).

A list of relevant bond angles, distances, and bond lengths indicates catalyst **108a** has the shortest distance between the coordinating nitrogen and phosphorus atom and a more acute bite angle (Figure 18). This complex also has the shortest contact distance to the pyridyl 2-aryl ring moiety coming within 3.19 Å of the α position and 3.34 Å of the ipso-β position of the naphthyl ring indicating close approach of the metal to the ligand. X-ray crystallography study of catalyst **110a** revealed a phosphorus iridium bond of 2.28 Å, a nitrogen iridium bond distance of 2.24 Å, and an acute value of 85.1˚ for the P, Ir, N bite angle. The distance of the iridium metal atom to the ipso-9-anthracyl carbon was 3.50 Å, similar to the phosphine thiazole based N,P iridium complexes reported by Hedberg et al.[33] Mesityl derivative **108e** had regular length bonds of 2.16 Å for the Ir-N bond and 2.37 Å for the Ir-P bond. The P, Ir, N bite angle for **108e** of 88.8˚ falls in to slightly more acute than the 90˚ angle for a perfect square planar complex.

2.5 Conclusion

A practical route to laboratory scale preparations of 2nd generation chiral pyridyl phosphinite catalysts has been developed. Key features of the synthesis are the optimized, chromatography free synthesis of the majority of intermediates and enzymatic resolution of the racemic alcohols in greater than 99% ee for both enantiomers. Phosphine replacement of the phosphinite group of these ligands leads to unstable complexes which undergo *ortho* metalation of a pendant aromatic ring to yield complexes which are catalytically inactive in asymmetric hydrogenation.

A flexible synthesis to a 3rd generation of chiral pyridyl phosphinite catalyst has been developed to allow late stage diversification of substituents which control selectivity and activity of the resulting catalysts. The late phase variable step and crucial transformation of the synthesis involves the Suzuki cross coupling of pyridyl chlorides with electron rich and sterically hindered boronic acids in high yield.

2.6 References

[1] Brown, J. M. *Hydrogenation of Functionalized Carbon-Carbon bonds*; Springer: Berlin, 1999; Vol. 1.

[2] Johnson, N. B.; Lennon, I. C.; Moran, P. H.; Ramsden, J. A. *Acc. Chem. Res.* **2007**, *40*, 1291.

[3] Noyori, R. *Angew. Chem. Int. Ed.* **2002**, *41*, 2008.

[4] Erre, G.; Enthaler, S.; Junge, K.; Gladiali, S.; Beller, M. *Coord. Chem. Rev.* **2008**, *252*, 471.

[5] Minnaard, A. J.; Feringa, B. L.; Lefort, L.; de Vries, J. G. *Acc. Chem. Res.* **2007**, *40*, 1267.

[6] Tang, W.; Zhang, X. *Chem. Rev.* **2003**, *103*, 3029.

[7] Zhang, W.; Chi, Y.; Zhang, X. *Acc. Chem. Res.* **2007**, *40*, 1278.

[8] Pfaltz, A.; Drury, W. J., III *Proc. Natl. Acad. Sci.* **2004**, *101*, 5723.

[9] Drury, W. J., III; Zimmermann, N.; Keenan, M.; Hayashi, M.; Kaiser, S.; Goddard, R.; Pfaltz, A. *Angewandte Angew. Chem. Int. Ed.* **2004**, *43*, 70.

[10] Bell, S.; Wustenberg, B.; Kaiser, S.; Menges, F.; Netscher, T.; Pfaltz, A. *Science* **2006**, *311*, 642.

[11] Wang, A.; Wüstenberg, B.; Pfaltz, A. *Angew. Chem. Int. Ed.* **2008**, *47*, 2298.

[12] Kaiser, S.; Smidt, S., P.; Pfaltz, A. *Angew. Chem. Int. Ed.* **2006**, *45*, 5194.

[13] Baeza, A.; Pfaltz, A. *Chem. Eur. J.* **2010**, in press.

[14] Yoshinari, T.; Ohmori, K.; Schrems, M. G.; Pfaltz, A.; Suzuki, K. *Angew. Chem. Int. Ed.* **2010**, *49*, 881.

[15] Bianco, G. G.; Ferraz, H. M. C.; Costa, A. M.; Costa-Lotufo, L. c. V.; Pessoa, C. u.; de Moraes, M. O.; Schrems, M. G.; Pfaltz, A.; Silva, L. F. *J. Org. Chem.***2009**, *74*, 2561.

[16] Schrems, M. G.; Pfaltz, A. *Chem. Commun.* **2009**, 6210.

[17] Uenishi, J.; Hamada, M. *Synthesis* **2002**, 625.

[18] Uenishi, J. i.; Hiraoka, T.; Hata, S.; Nishiwaki, K.; Yonemitsu, O.; Nakamura, K.; Tsukube, H. *J. Org. Chem.* **1998**, *63*, 2481.

[19] Maywald, M.; Pfaltz, A. *Synthesis* **2009**, 3654.

[20] Kaiser, S.; Basel, U., Ed. Basel, 2005.

[21] Verendel, J. J.; Andersson, P. G. *Dalton Trans.* **2007**, 5603.

[22] Crabtree, R. H.; Lavin, M. *Chem. Commun* **1985**, 794.

[23] Sprouse, S.; King, K. A.; Spellane, P. J.; Watts, R. J. *J. Am. Chem. Soc.* **1984**, *106*, 6647.

[24] Unpublished results, Andreas Schumacher, Andreas Pfaltz, University of Basel, 2009

[25] Albrecht, M. *Chem. Rev.* **2009**, *110*, 576.

[26] Liu, Q.-B.; Yu, C.-B.; Zhou, Y.-G. *Tetrahedron Lett.* **2006**, *47*, 4733.

[27] Lyle, M. P. A.; Draper, N. D.; Wilson, P. D. *Org. Biomol. Chem.* **2006**, *4*, 877.

[28] Lyle, M. P. A.; Narine, A. A.; Wilson, P. D. *J. Org. Chem.* **2004**, *69*, 5060.

[29] Lyle, M. P. A.; Wilson, P. D. *Org. Lett.* **2004**, *6*, 855.

[30] Meyers, A. I.; Garcia-Munoz, G. *J. Org. Chem.* **1964**, *29*, 1435.

[31] Master Thesis, Marc-André Müller, University of Basel, 2010.

[32] Xie, Y.; Huang, H.; Mo, W.; Fan, X.; Shen, Z.; Shen, Z.; Sun, N.; Hu, B.; Hu, X. *Tetrahedron: Asymmetry* **2009**, *20*, 1425.

[33] Hedberg, C.; Kallstrom, K.; Brandt, P.; Hansen, L. K.; Andersson, P. G. *J. Am. Chem. Soc.* **2006**, *128*, 2995.

Chapter 3

Asymmetric Hydrogenation of Trisubstituted Alkenes with 3rd Generation Chiral Pyridyl Iridium N,P Complexes

"*Dans les champs de l'observation le hasard ne favorise que les esprits préparés.*"

"In the fields of observation chance favors only the prepared mind." –Louis Pasteur

3.1 Introduction

Synthesis of a series of asymmetric catalysts with incremental changes to overall structure allows for the probing of structure selectivity relationships (SSR). Previous work from the 1st and 2nd generation chiral Crabtree's catalyst has allowed for the identification of SSR for the asymmetric hydrogenation of a number of trisubstituted alkenes and serves as an excellent starting point for extension of the high selectivity of these catalysts to substrates that have proven difficult to surmount.

Table 21. Comparison of phosphorus substituents and pyridine substituent on ee.

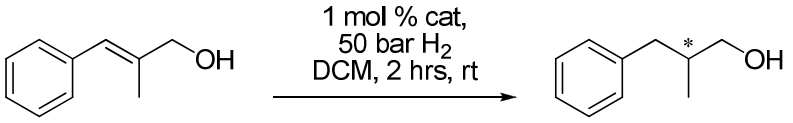

25e **25j**

cat #	structure	ee% (er)	$\Delta\Delta G^{\ddagger}_{RS}$
153a	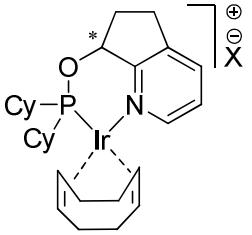	55% (77.5/ 22.5)	-0.72 kcal·mol^{-1} -3.1 kJ·mol^{-1}
153b	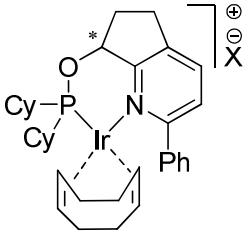	90% (95/ 5)	-1.7 kcal·mol^{-1} -7.3 kJ·mol^{-1}
153c	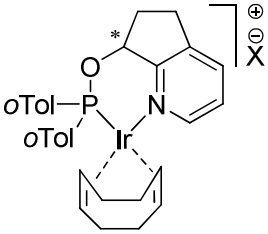	91% (95.5/ 4.5)	-1.8 kcal·mol^{-1} -7.6 kJ·mol^{-1}
107a	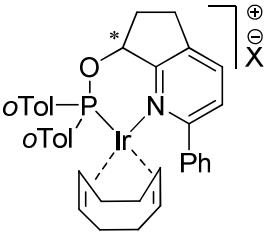	97% (98.5/ 1.5)	-2.5 kcal·mol^{-1} -10.4 kJ·mol^{-1}

X = BAr_F anion, values are taken from reference [1].

Earlier work in the asymmetric hydrogenation of trisubstituted alkenes with the 2nd generation of catalysts indicated a strong enantioselectivity dependence on the nature of the substituents on the phosphorus atom and the group in the 2-position of the pyridine ring (Table 21).

Kaiser's data[1] indicated an increase in steric interaction about the iridium center by replacing hydrogen atom substituted **153a** with the phenyl derivative **153b** increased the ee% by 35% ee or 1 kcal·mol^{-1} difference in terms of activation energy. A similar trend and nearly identical ee% change was observed when replacing the di(cyclohexyl)phosphinite analogue **153a** with the di-(*ortho*-tolyl)phosphinite complex **153c**. The highly selective **107a** combines the individual optimization results into a single catalyst for an increase of 42% ee or 1.8 kcal·mol^{-1} $\Delta\Delta G^{\ddagger}_{RS}$ improvement from the starting complex **153a**. While the inherent SSR is clear in this example this trend does not necessarily apply to other P,N catalysts and substrates. However, good performance of a highly active and selective catalyst in a single class of substrates is common.

While enantiopurity has most often been reported as ee% contributions of structural changes to overall SSR of related catalysts are best evaluated in terms of the differences to the activation barriers of the individual enantiomers. Energy differences of the enantio determining transition states were calculated with the relationship: $\Delta\Delta G^{\ddagger}_{RS} = -RTln$ ($k_{enant\ maj}$/ $k_{enant\ min}$), for convenience the fraction of the minor enantiomer can be calculated from the ee with the equation: $minor_{enant}$ = (100-|ee|)/2. Another useful quantity for describing relative rates is the enantiomeric quotient (e.q. or *q* in this chapter) which is defined as the enantiomeric ratio with a denominator equal to 1.

3.2 Substrates out of reach of the 2nd and 3rd generation chiral pyridyl phosphinite catalysts

While 2nd and 3rd generation chiral pyridyl phosphinite catalysts are remarkably selective for trisubstituted alkenes these catalysts have consistently given inferior results with the substrate classes of imines (section 1.7), 1,1'-disubstituted alkenes (section 1.4), and tetrasubstituted alkenes (section 1.5). Table 22 indicates very poor to no selectivity for the reduction of imines and 1,1'-disubstituted alkenes. Catalysts **108b** and **108c** were especially unreactive towards imine **86a** at 50 bar of H_2. Catalyst **108a**, while showing some conversion, failed to produce

any detectable ee. These catalysts were somewhat more reactive towards the easily reduced 1,1'-disubstituted alkene **61b** but failed to produce useful levels of enantioselectivity.

Table 22. Difficult substrates for 3rd generation chiral pyridyl phosphinite catalysts.

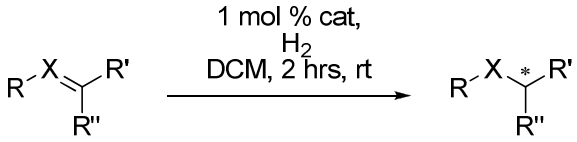

#	Substrate	ee% (conv)		
86a[a]	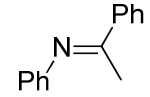	0 (45)	no conv	no conv
61b[b]	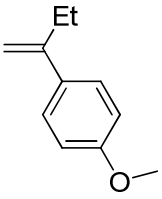	59 (100)	6 (100)	10 (100)
Catalyst	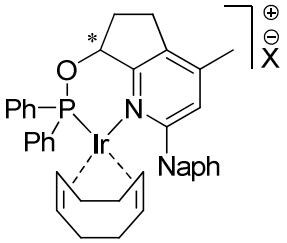	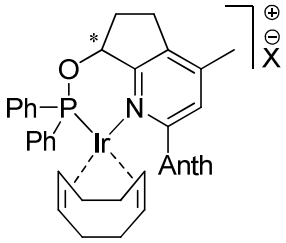	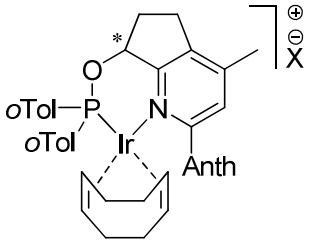	
#		**108a**	**108b**	**108c**

X = BAr_F anion, , Naph = β-naphthyl, Anth = 9-anthracyl, a) reactions were conducted at 50 bar H_2, b) reactions were conducted at 1 bar H_2.

3.3 Asymmetric hydrogenation of substrates with weak coordinating functional groups catalyzed by 3rd generation chiral pyridyl phosphinite catalysts, initial SSR

Iridium based catalysts are the only homogeneous catalysts capable of the asymmetric hydrogenation of alkenes without adjacent coordinating functional groups with useful levels of activity and ee (section 1.1). Noncoordinating substrates **25a-c** are the most investigated substrates in this specific class and serve as useful reference points in an iridium catalysts activity/ selectivity profile. However, given the large number of catalysts that can now reduce these substrates in perfect selectivity and yield, the limited use of such substrates in other synthesis, and the possibility of better performance with substrate classes with greater synthetic utility makes weaker performance with these alkenes less important.

Chiral pyridyl phosphinite catalyst *R*-**107a** of the 2nd generation is capable of reducing substrate **25a** in greater than 99% ee and yield giving the *R* configured product for the *E* configured alkene. The results of the 3rd generation catalysts **108a-c**, **108f-h**,[2] and **110c** are given in Table 23.

Table 23. Asymmetric hydrogenation results for 3rd generation catalysts with substrate **25a**.

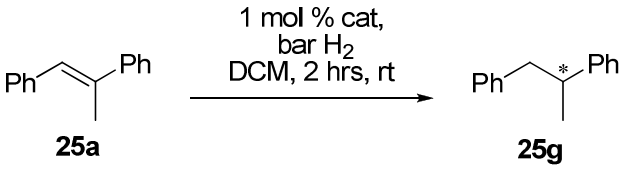

25a **25g**

#	structure[a]	ee% $\Delta\Delta G^{\ddagger}_{RS}$	#	structure[a]	ee% $\Delta\Delta G^{\ddagger}_{RS}$
***S*-108a**	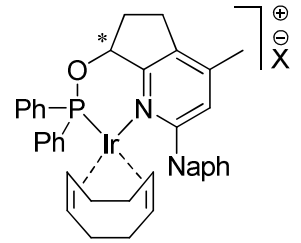	98 (*S*) -2.7 $\frac{kcal}{mol}$	***S*-108g**[b]	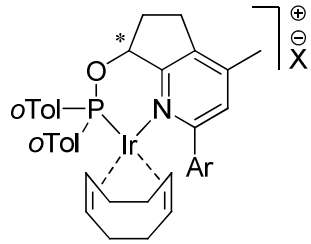	99.2 (*S*) -3.3 $\frac{kcal}{mol}$
***S*-108b**	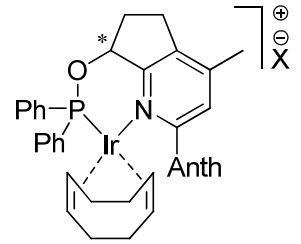	95 (*S*) -2.2 $\frac{kcal}{mol}$	***S*-108h**[b]	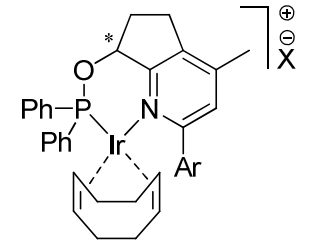	99 (*S*) -3.1 $\frac{kcal}{mol}$
***S*-108c**	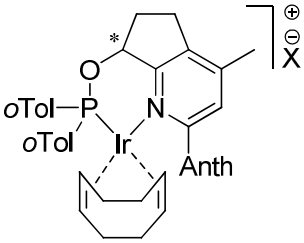	93 (*S*) -2.0 $\frac{kcal}{mol}$	***S*-110c**[b,d]	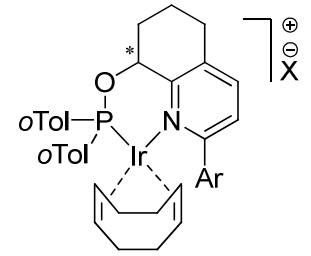	99 (*S*) -3.1 $\frac{kcal}{mol}$
***R*-108f**[b]	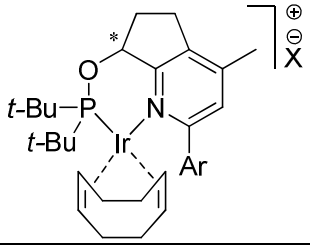	94 (*R*) -2.1 $\frac{kcal}{mol}$	***R*-107a**[c]	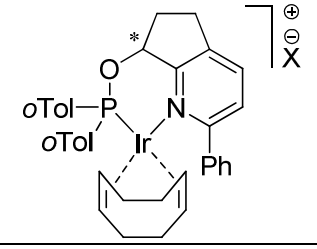	≥ 99 (*R*) ≥ -3.1 $\frac{kcal}{mol}$

a) X = BAr_F anion, Ar = 3,5-di-*tert*-Bu-4-MeOPh, Naph = β-naphthyl, Anth = 9-anthracyl, reactions were conducted at 50 bar H_2 and all conversions were quantitative unless otherwise noted, b) reference [2], c) reference [1], d) 73% conversion.

Considering catalyst **107a** as an optimized point of reference it can be seen that a finite amount of steric interaction is tolerated about the iridium metal center with substrate **25a**. The interaction of phosphorus substituents and the 2-arylpyridine groups was apparent. Use of sterically more demanding aryl groups in the pyridine *ortho* position limits the tolerance/ requirements for the size of the phosphinite substituents. From X-ray crystallography studies of related 2,6-disubstituted complexes the perpendicularly locked biaryl anthracene derivatives **108b,c** retain the shortest contact distances to the phosphinite substituents and also give the lowest enantioselectivities. Increasing the size from β-naphthyl analogue **108a** to the 9-anthracyl derivative **108b** incurs a loss of 0.5 kcal·mol^{-1} in differentiation energy. This steric interaction trend also holds true for the 3,5-di-*tert*-butyl-4-methoxyphenyl derivatives **108f,g**. While the greater degree of rotational freedom and space seems to accommodate the bulky substrate **25a** direct comparison of **108f** with the bis(*ortho*-tolyl) analogue **108g** marks the tolerance limit with a significant loss in activation energy difference of 1.2 kcal·mol^{-1} and a drop in enantiomeric ratio (er) from (99.6:0.4) to (97:3). Also note worthy is the increase in conversion of 73% for the 6-membered ring analogue **110c**, increasing 3 fold from the 22% conversion of the closely related 2nd generation analogue **109** with a simple phenyl group in the 2-pyridyl position, both catalysts gave the same high enantioselectivity of 99% ee.

Substrate **25b** has been noted as being somewhat more difficult to hydrogenate with higher enantioselectivity in the past, however several highly selective catalysts are known at present time. Catalysts **108a-c** demonstrate interesting SSR in this substrate that is quite different from the larger α-methylstilbene **25a** (Table 24).

Apparently with the smaller and less sterically demanding *E* configured alkene **25b** as substrate bulkier substituents about the iridium N,P catalyst are favored for high enantioselectivity. Table 24 illustrates the advantage in using energy calculations or enantiomeric ratio over the enantioselectivity in determining contributions of change in structure to the overall selectivity of the series of catalysts. Making observations solely on ee can be very misleading when evaluating the contributions from increasing the phosphorus substituent size from the diphenylphosphinite analogue **108b** which gives 98.5% ee, or an er of (99.25:0.75) i.e. an enantiomeric quotient (*q*) of 132, with the di-(*ortho*-tolyl)phosphinite derivative **108c** which gives 99.1% ee, or an er of (99.55:0.45) and a quotient of 221. While enantiomeric quotient and

er are more informative about SSR and the relative rate of catalysis, energy calculations are a more sublime description and directly reflect events in the transitions state.

Table 24. Asymmetric hydrogenation of **25b**.

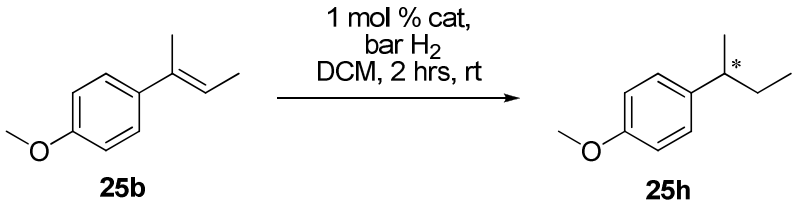

#	structure	ee (er) $\Delta\Delta G^{\ddagger}_{RS}$	#	structure	ee (er) $\Delta\Delta G^{\ddagger}_{RS}$
***S*-108a**	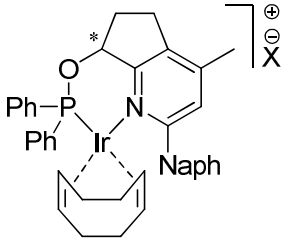	96 (*S*) $\left(\frac{98}{2}\right)$ -2.3 $\frac{kcal}{mol}$	***S*-108c**	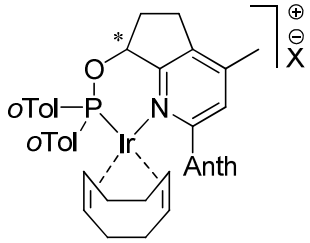	99.1 (*S*) $\left(\frac{99.55}{0.45}\right)$ -3.2 $\frac{kcal}{mol}$
***S*-108b**	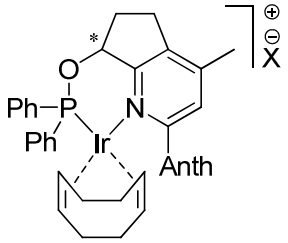	98.5 (*S*) $\left(\frac{99.25}{0.75}\right)$ -2.7 $\frac{kcal}{mol}$	***R*-107a**[a]	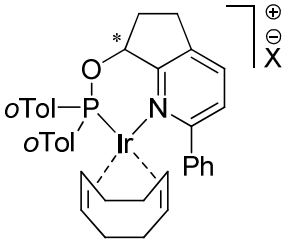	> 99 (*R*) > $\left(\frac{99.5}{0.5}\right)$ > -3.1 $\frac{kcal}{mol}$

X = BAr_F anion, Naph = β-naphthyl, Anth = 9-anthracyl, all reactions were conducted at 50 bar H_2 and all conversions were quantitative unless otherwise noted, a) reference [1].

While phenyl groups can be considered as weakly coordinating functional groups many transition metals are well known to form stable complexes with them. Furthermore, many catalysts which perform well in the asymmetric reduction of alkenes conjugated to aromatic systems fail to produce useful levels of enantioselectivity when those aromatic systems are removed (section 1.3.2). Substrates **34a** with *E* and *Z* configurations were evaluated with a small series of catalysts to gain further understanding of how the changes made in the 3rd generation chiral pyridyl phosphinite catalyst series affect the SSR of trisubstituted alkene reduction when the substrates phenyl group is removed from the site of reduction (Table 25).

Table 25. Asymmetric hydrogenation results for *E*- and *Z*- **34a**.

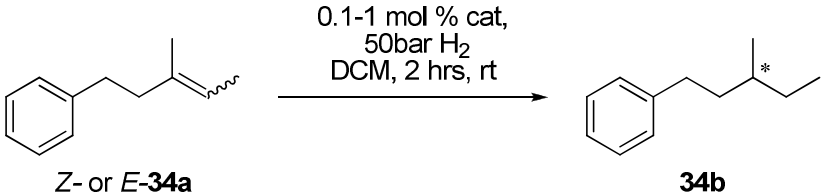

#	substrate *Z*-**34a** structure[a]	ee% (*q*) $\Delta\Delta G^{\ddagger}_{RS}$	#	substrate *E*-**34a** structure[a]	ee% (*q*) $\Delta\Delta G^{\ddagger}_{RS}$
S-**108a**	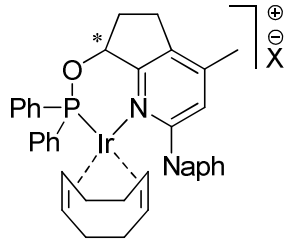	94.9 (*R*) (38.2) -2.2 $\frac{kcal}{mol}$	*S*-**108a**	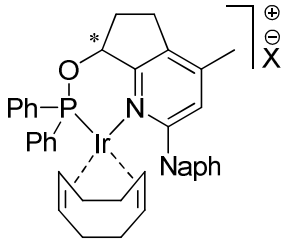	92.4 (*S*) (25.3) -1.9 $\frac{kcal}{mol}$
S-**108b**	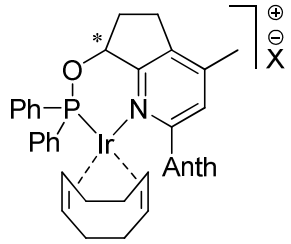	98.9 (*R*) (181) -3.1 $\frac{kcal}{mol}$	*S*-**108b**	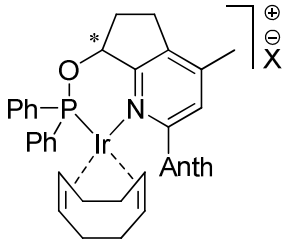	95.6 (*S*) (44.5) -2.2 $\frac{kcal}{mol}$
S-**108c**	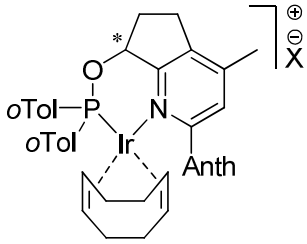	99.1 (*R*) (221) -3.2 $\frac{kcal}{mol}$	*S*-**108c**	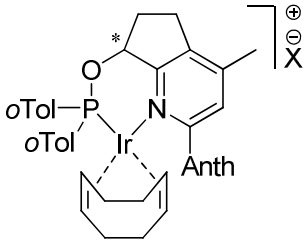	96.5 (*S*) (56.1) -2.4 $\frac{kcal}{mol}$
R-**107a**[b]	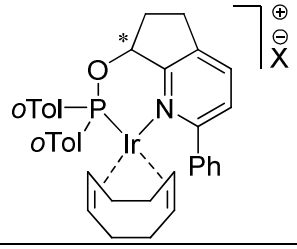	98 (*S*) (99) -2.7 $\frac{kcal}{mol}$	*R*-**107a**[b]	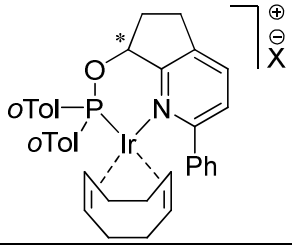	94 (*R*) (32.3) -2.1 $\frac{kcal}{mol}$

a) X = BAr_F anion, Naph = β-naphthyl, Anth = 9-anthracyl, all conversions were quantitative unless otherwise noted, b) reference [1]. The enantiomeric quotient, *q*, is the enantiomeric ratio with a denominator of 1.

Difficulty in reduction of *E* configured alkenes relative to the *Z* isomers with alkyl derived alkenes such as **34a** and **37a** has remained a consistent challenge for the chiral pyridyl phosphinite catalysts. However, catalyst **108c** exhibits a nearly two fold increase in enantiomeric ratio and a decrease of 0.3 kcal in terms of activation energy compared to catalyst

R-**107a** with *E*-**34a**. Comparing the reactivity of substrate *E*-**34a** with *Z*-**34a** we observe a 4-fold increase in er for catalysts **108b,c**, a 3 fold increase for catalyst **107a**, and a 1.5 fold increase for **108a**. This trend closely matches the degree of steric crowding adjacent to the metal center, indicating that increasing steric interaction between the catalyst and substrate increases the selectivity for the more reactive *Z* isomer of this substrate. Thus "tuning" the substrate configuration as well as the catalyst can lead to dramatic increase in terms of enantiomeric ratio and activation energy. For this substrate the least sterically demanding catalyst **108a** with the more difficult isomer *E*-**34a** gave (96.2: 3.8) er while the most sterically demanding catalyst **108c** with the better substrate *Z*-**34a** gave an er of (99.55: 0.45), a 10 fold increase in enantioselectivity.

Table 26. Asymmetric reduction of *E,E*-farnesol.

37a **37b**

#	structure[a]	3*S* 7*R*	3*R* 7*R*	3*R* 7*S*	3*S* 7*S*	ee%	(*q*)
S-**108c**	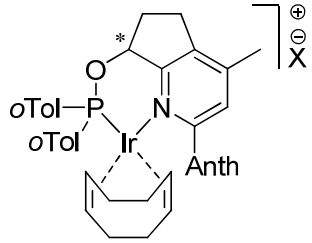	3.86	95.66	0.43	0.05	99.9	(1910)
R-**110a**	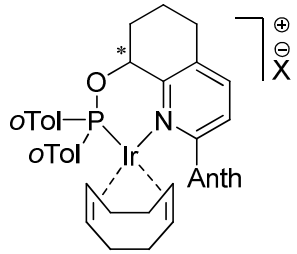	1.02	1.51	4.42	93.05	-96.8	(61.6)

a) X = BAr_F anion, Anth = 9-anthracyl, all conversions were quantitative unless otherwise noted.

Increasing the degree of steric interaction also increases the enantioselectivity for the *E* isomer of **34a**. The sterically hindered anthracene derivative **108c** gives a 70% greater enantiomeric ratio than the phenyl analogue **107a.** This trend holds true in the enantioselective hydrogenation of *E,E*-farnesol[3] (Table 26).

Using the data from reference [3] a 99.3% ee is obtained with catalyst **109** at 1 mol% catalyst loading which translates to an enantiomeric quotient value of 285. In a direct comparison of the effect of increased bulk catalyst **110a** gives a lower ee of 97%, this precipitous loss of selectivity is not entirely surprising with a very sterically demanding catalyst. However, using the more open catalyst **108c** the enantioselectivity increases to a near perfect 99.9% ee with an enantiomeric quotient of 1910 a 6.7 fold increase over catalyst **109** and a 31 fold increase over catalyst **110a**, indicating exceptional selectivity.

3.4 Asymmetric reduction of dihydronaphthaleness

Dihydronaphthalene substrate **25d** has proven difficult for most catalysts. The first reaction to achieve 99% ee was obtained with catalysts **110a,b** (Table 27). The sterically more demanding catalysts gave the best enantioselectivities in general. Catalyst **108a** (not listed in table) gave abysmal levels of enantioselectivity. Catalyst **110a** stood out as the best performer, giving an enantiomeric quotient of 284 while **110b** gave the second highest *q* value of 221.

Given the success of these catalysts with **25d** a more difficult substrate in the form of the isopropyl dihydronaphthalene **154a** was attempted (Table 28). Competing side reactions produced the tetrasubstituted alkene **154c** and the oxidation product naphthalene **154d** in small but measurable quantities. This substrate demonstrates a slightly different trend in enantioselectivity in relation to the catalyst backbone ring size in comparison to studies on *E,E*-farnesol with the more selective catalysts formed from the 6-membered ring series. Catalyst **108c** gives an er of (95.3: 4.7) while **110a** gives an er of (98:2), this equates to 0.5 kcal·mol^{-1} energy difference. Increasing the pressure, concentration, and catalyst loading of **110a** had a beneficial effect on the enantioselectivity and product distribution which gave an excellent enantiomeric ratio of (99:1) and 96% conversion.

In order to test the limits of what was possible with catalyst **110a** substrate **157a** was synthesized from the α-tetralone **155** (Scheme 30). The tertiary alcohol **156** was synthesized by addition of *tert*-butyl lithium to the ketone. The benzylic cation formed by elimination of water from **156** was so favorable that alkene **157a** was present in roughly equal portions to the alcohol when using ammonium chloride as a quenching acid. The reaction was driven to completion by stirring the mixture over dry 4Å molecular sieves in DCM.

Table 27. Asymmetric hydrogenation results for **25d** with 3rd generation catalysts.

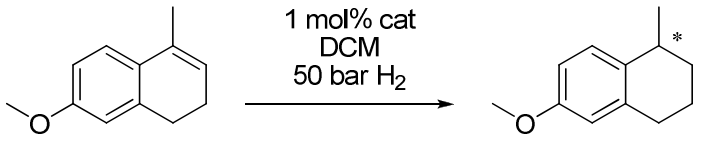

#	structure[a]	ee% $\Delta\Delta G^{\ddagger}_{RS}$	#	structure[a]	ee% $\Delta\Delta G^{\ddagger}_{RS}$
***S*-108b**	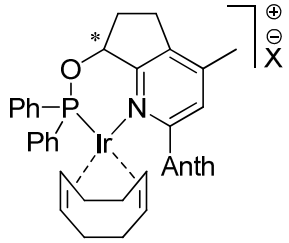	95 (*R*) -2.2 $\frac{kcal}{mol}$	***S*-108g**[b]	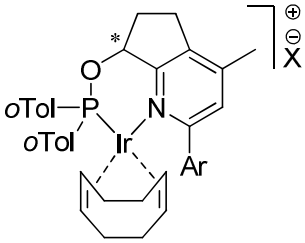	98 (*R*) -2.7 $\frac{kcal}{mol}$
***S*-108c**	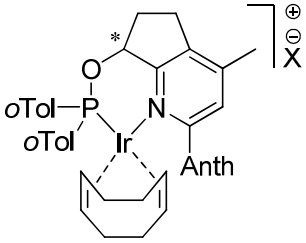	97 (*R*) -2.5 $\frac{kcal}{mol}$	***S*-108h**[b]	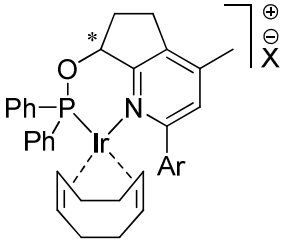	98 (*R*) -2.7 $\frac{kcal}{mol}$
***S*-108d**	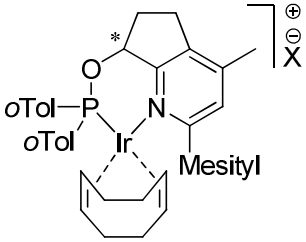	99.0 (*R*) -3.1 $\frac{kcal}{mol}$	***R*-110a**	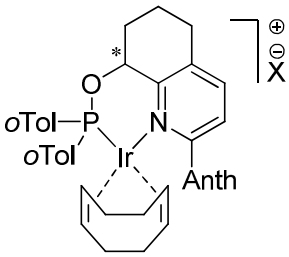	99.3 (*S*) -3.3 $\frac{kcal}{mol}$
***S*-108e**	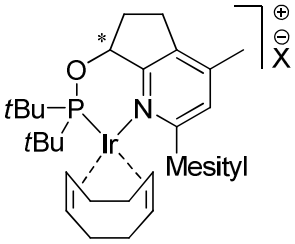	97 (*R*) -2.5 $\frac{kcal}{mol}$	***S*-110b**	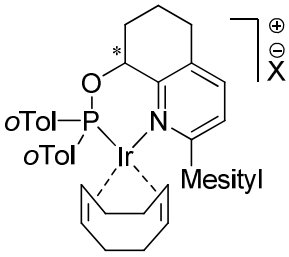	99.1 (*R*) -3.2 $\frac{kcal}{mol}$
***R*-108f**[b]	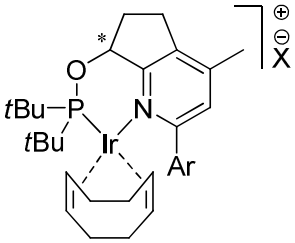	94 (*S*) -2.1 $\frac{kcal}{mol}$	***S*-110c**[b]	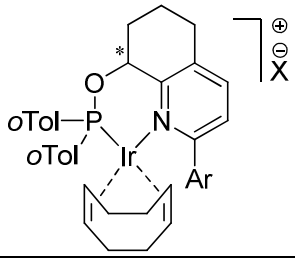	98 (*R*) -2.7 $\frac{kcal}{mol}$

a) X = BAr_F anion, Anth = 9-anthracyl, mesityl = 2,4,6-tri-methylbenzene, Ar = 3,5-di-*tert*-Bu-4-MeOPh, b) reference [2].

Table 28. Asymmetric hydrogenation results for **154a** with 3rd generation catalysts.

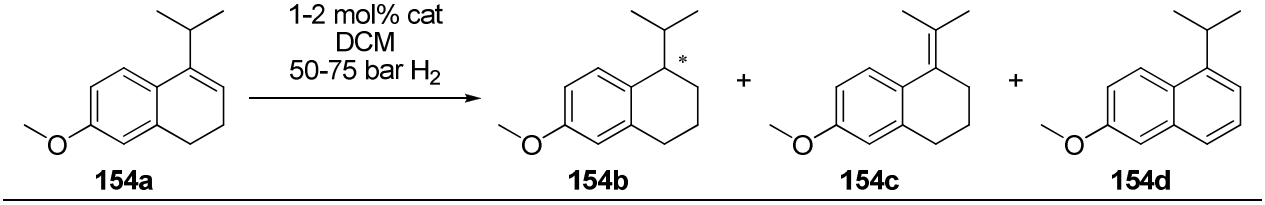

# mol%	structure[a]	ee% $\Delta\Delta G^{\ddagger}_{RS}$	% **154b**	% **154c**	% **154d**
***S*-108c** 1 mol%	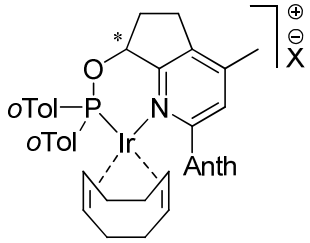	90.6 (*R*) -1.8 $\frac{kcal}{mol}$	96	-	4
***S*-108f**[b] 1 mol%	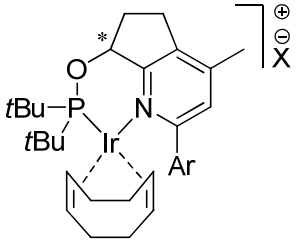	95 (*R*) -2.2 $\frac{kcal}{mol}$	98	-	2
***R*-110a** 1 mol%	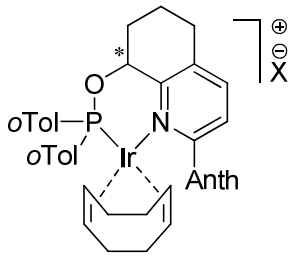	96 (*S*) -2.3 $\frac{kcal}{mol}$	80	1.8	2
***R*-110a**[c] 2 mol%	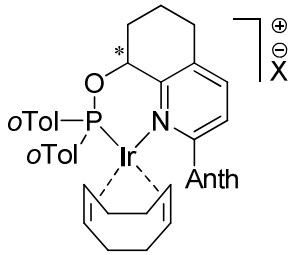	98 (*S*) -2.7 $\frac{kcal}{mol}$	96	1.8	0.8

a) X = BAr_F anion, Anth = 9-anthracyl, Ar = 3,5-di-*tert*-Bu-4-MeOPh, ee and conversion for all products was determined by GC, b) reference [2], c) reaction was run at 2 mol% catalyst loading, 0.25M substrate concentration and 75 bars of H_2 for 3 hours.

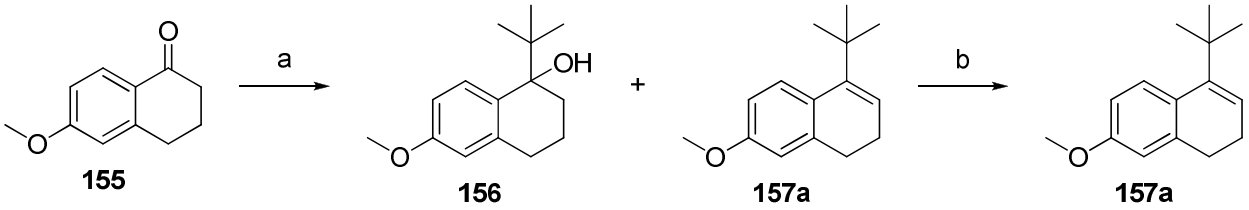

Scheme 30 Conditions: $ZnCl_2$ (0.12 eq), *tert*-butylLi (1.1 eq), 24 hr, NH_4Cl, b) 4Å mol sieve, 11% yield total yield.

Table 29. Asymmetric reduction of **157a** with catalyst **110a**.

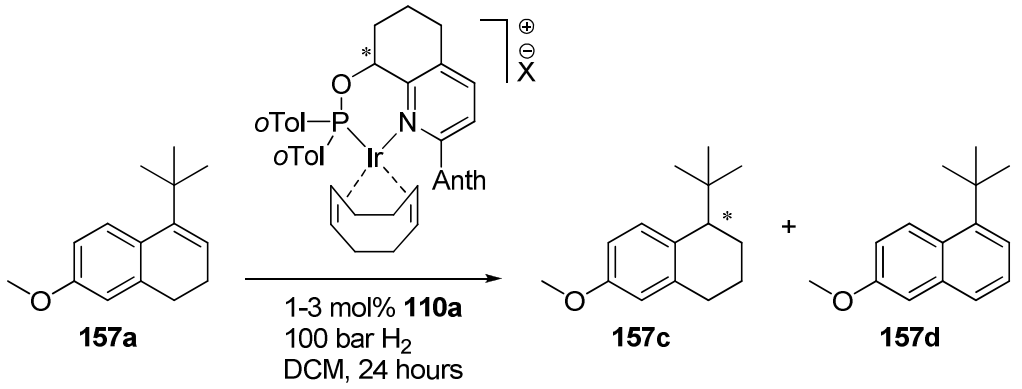

mol% **110a**	ee%	conv% **157c**	conv% **157c**	er	$\Delta\Delta G^{\ddagger}_{RS}$
1[a]	86	59	4	$\left(\frac{93}{7}\right)$	-1.5 $\frac{kcal}{mol}$
2[a]	96	79	21	$\left(\frac{98}{2}\right)$	-2.3 $\frac{kcal}{mol}$
2[b]	97	87	13	$\left(\frac{98.5}{1.5}\right)$	-2.5 $\frac{kcal}{mol}$
3[b]	91	99	trace	$\left(\frac{95.5}{4.5}\right)$	-1.8 $\frac{kcal}{mol}$

X = BAr_F anion, Anth = 9-anthracyl a) reaction was run at 0.2M substrate concentration, b) reaction was run at 1.0M substrate concentration.

Reduction of **157a** proved slow with very high pressures and long reaction times required to reach full conversion. Even at 100 bar H_2 pressure oxidation to the naphthalene was a troubling side reaction. Increasing the concentration and catalyst loading helped to control this greatly but at the price of enantioselectivity when using 3 mol% catalyst loading. Optimal conditions could increase the apparent activation energy difference by a 1 kcal·mol^{-1}, a significant improvement.

Table 30. Summary for the reduction of dihydronaphthalenes with catalyst **110a**.

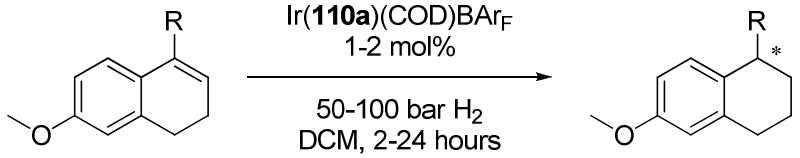

substrate	mol%	pressure	R	ee	$\Delta\Delta G^{\ddagger}_{RS}$	*q*	% prod	% s.prod
25d	1	50 bar	Me	99.3	3.3	284	100	-
154a	2	75 bar	*i*-Pr	98	2.7	99	96	2.4
157a	2	100 bar	*t*-Bu	97	2.5	63.8	87	13

As can be seen from Table 30, while the apparent enantioselectivity is very high for catalyst **110a** asymmetric hydrogenation becomes more difficult as steric hindrance is increased on the substrate. The methyl analogue **25d** is hydrogenated with a 2.9 fold selectivity increase over the isopropyl analogue **154a** and a 4.5 fold increase relative to the *tert*-butyl derivative **157a** in terms of enantiomeric ratio. The product distribution also reflects the difficulty in hydrogenation and the sterically demanding substrates give more byproducts as would be expected.

3.5 Asymmetric hydrogenation of allyilic alcohols and conjugate reduction of α,β-unsaturated esters

Asymmetric reduction of alkenes with adjacent coordinating functional groups is a vastly important topic and it has received voluminous amounts of attention in the literature (see section 1.1, 1.3.5, 1.3.7, and 1.6). Substrates **25e** and **25f,** derived from cinnamic acids, have been featured in many asymmetric hydrogenation screens and are general reference points. Although many catalysts give ee's in to the high nineties with these substrates, few catalysts cross the 99% ee threshold. Additionally, substrate **25e** has been observed to undergo rearrangement to aldehydes in some investigations (see section 1.3.6). These types of substrates have the added disadvantage of having inhibitory behavior towards iridium hydrogenation catalysts. In spite of these detriments, many examples of excellent activity and selectivity in iridium catalyzed hydrogenation of the more coordinating alkenes equals or surpasses that of the rhodium and ruthenium systems.

Table 31. Hydrogenation results for catalyst *E*-α-methylcinnamylalcohol, substrate **25e**.

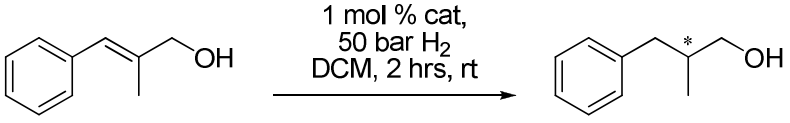

25e **25j**

#	structure[a]	ee% (conv) $\Delta\Delta G^{\ddagger}_{RS}$	#	structure[a]	ee% (conv) $\Delta\Delta G^{\ddagger}_{RS}$
***S*-108a**	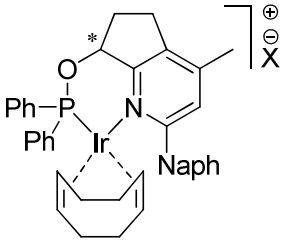	95 (*R*) (full) -2.2 $\frac{kcal}{mol}$	***R*-108f**[c]	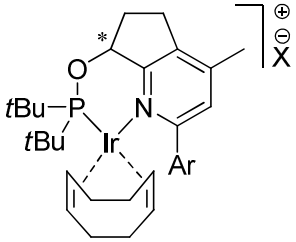	12 (*S*) (62%) -.05 $\frac{kcal}{mol}$
***S*-108b**	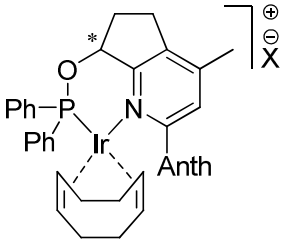	80 (*R*) (full) -1.3 $\frac{kcal}{mol}$	***S*-108g**[c]	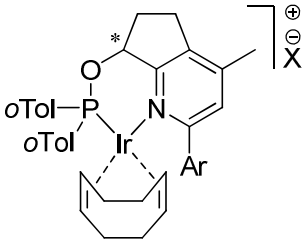	93 (*R*) (full) -2.0 $\frac{kcal}{mol}$
***S*-108c**	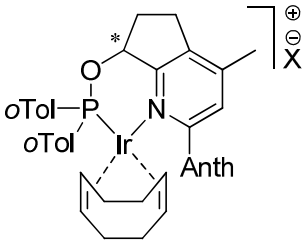	29 (*R*) (25%) -0.4 $\frac{kcal}{mol}$	***S*-108h**[c]	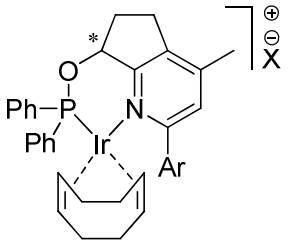	92 (*R*) (70%) -1.9 $\frac{kcal}{mol}$
***S*-108d**	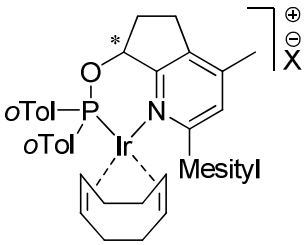	88 (*R*) (full)[b] -1.6 $\frac{kcal}{mol}$	***R*-110a**	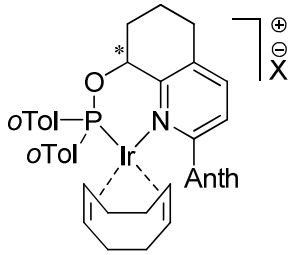	84 (*S*) (full) -1.4 $\frac{kcal}{mol}$
***S*-108e**	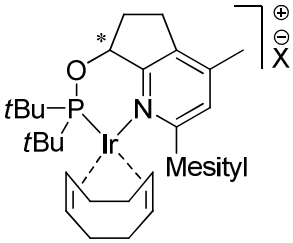	72 (*R*) (full) -1.1 $\frac{kcal}{mol}$	***S*-110b**	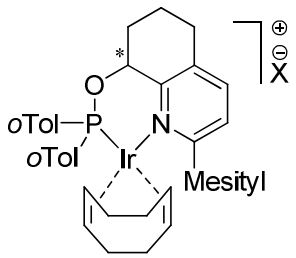	57 (*R*) (34%) -0.8 $\frac{kcal}{mol}$

a) X = BAr_F anion, Naph = β-naphthyl, Anth = 9-anthracyl, mesityl = 2,4,6-tri-methylbenzene, Ar = 3,5-di-*tert*-Bu-4-MeOPh, b) over 80% converted to 2-methyl-3-phenyl-propanal, c) reference [2]. All reactions were conducted at 50 bar of H_2 for 16 hours.

Allylic alcohol **25e** was reduced with a similar SSR trend to substrate **25a** but proved to be more sensitive to the precise steric environment of the catalyst (Table 31). We attribute the loss of activity with the larger ligands to catalyst inhibition by the more strongly coordinating primary hydroxyl group competing for a limited amount of space with the alkene leading to a less reactive system. The best performing catalyst was **108a** which also had the least sterically demanding groups, coming very close to the ee% of **107a,**[4] but in terms of enantiomeric ratio **108a** gave a *q* value of 39 while **107a** was 1.7 fold higher with an enantiomeric quotient of 66. The di(*tert*-butyl)phosphinite catalyst **108f** gave very poor results with 12% ee and 62% conversion in comparison with the closely related di(*o*-tolyl)phosphinite catalyst **108g** which gave 93% ee and full conversion. A similar trend can be seen when changing from the bulky *ortho*-tolyl substituted **108c**, which gives abysmal enantioselectivity of 29%, a 25% yield, and an enantiomeric ratio of (64.5: 35.5), to the less demanding diphenylphosphino derivative **108b** which gives 80% ee, 99% yield, and an er of (90:10).

Steric parameters seem to have far greater consequences for this class of substrate, namely 2-methyl-3-phenyl-propanal, which is produced in trace quantities with catalyst **107a,** became the predominant product with the highly congested **108d**. This finding is consistent with the work of Mazet (section 1.3.6) who has optimized this 1,3 hydride shift into a viable asymmetric process by maximizing steric interactions with the allylic alcohol in a highly restricted pocket about the iridium metal center. Clearly the addition of very sterically demanding aromatic substituents about the metal center creates a more sensitive system and changes that are typically well tolerated with other substrates can have drastic effects under these circumstances.

Having established the 3rd generation chiral pyridyl phosphinite catalysts as effective in the reduction of challenging substrates we turned our attention to the conjugate reduction of ester **158a**. The mesityl derived catalysts **108d** and **108e** reduced the α,β-unsaturated ester in 94% ee and greater than 99% conversion (Table 32). Both *S* configured catalysts gave the desired *R*-**158b** with identical enantiomeric quotient of 32 and -2.0 kcal·mol^{-1} in terms of activation energy.

Table 32. Asymmetric hydrogenation summary results of α,β-unsaturated esters **158a** and **159a**.

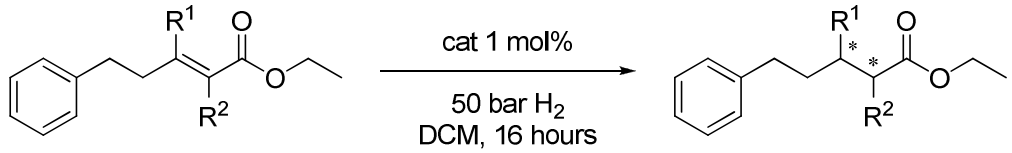

158a R^1 = Me R^2 = H
159a R^1 = H R^2 = Me

158b R^1 = Me R^2 = H
159b R^1 = H R^2 = Me

substrate	R^1	R^2	catalyst	ee%	*q*	$\Delta\Delta G^{\ddagger}_{RS}$
158a	Me	H	*S*-**108d**	94 (*R*)	32	-2.0 $\frac{kcal}{mol}$
158a			*S*-**108e**	94 (*R*)	32	-2.0 $\frac{kcal}{mol}$
159a	H	Me	*S*-**108e**	96 (-)	49	-2.3 $\frac{kcal}{mol}$

All reactions were conducted at 50 bar of H_2 for 16 hours and all hydrogenations reached full conversion.

The reduction of α-substituted esters has been a long standing challenge with iridium N,P catalyzed hydrogenations. Andersson has proposed a rationale for this with a computational model which indicates a steric and electronic mismatch effect for α-methyl cinnamic acid methyl ester with an iridium N,P hydride complex (section 1.2.3).

We attempted the reduction of **159a** and we were surprised to find higher enantioselectivity then with the β-methyl analogue **158a**. Catalyst *S*-**108a** reduced the α-methyl-α,β-unsaturated ester with 96% ee to (-) **159b** with an enantiomeric quotient of 49, a 1.5 fold increase over the β-methyl analogue and an added 0.3 kcal·mol^{-1} in terms of activation energy.

A thorough analysis on a series of esters easily prepared from commercially available α-methylcinnamic acid was quite revealing (Tables 33-35). Hydrogenations of cinnamic esters **160a-c** were quite slow and high pressure with longer reaction times were required to reach full conversion. Catalyst **108e** was clearly the standout with 97% ee for **161a, 161b** and 99.8% ee for **161c**. The size effect of the ester alkyl group appears to be considerable and very sensitive to the catalyst substrate interaction. Most impressively, a 15 fold increase in enantiomeric ratio is observed between the asymmetric hydrogenation of the ethyl and isopropyl cinnamic esters with **108e** as catalyst. Larger ester groups also increased the enantioselectivity for other catalysts by a significant measure. It also appears that the substituents on the phosphorus atom play a crucial role.

Table 33. Asymmetric hydrogenation results for substrate **160a**.

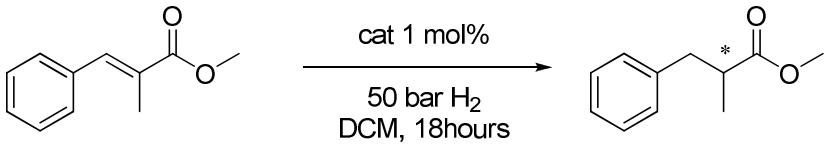

160a **161a**

#	structure[a]	ee% (*q*) $\Delta\Delta G^{\ddagger}_{RS}$	#	structure[a]	ee% (*q*) $\Delta\Delta G^{\ddagger}_{RS}$
***S*-108a**	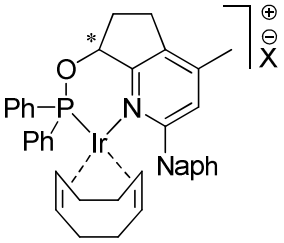	7 (*R*)[c] (1.2) -80 $\frac{cal}{mol}$	***R*-108f**[b]	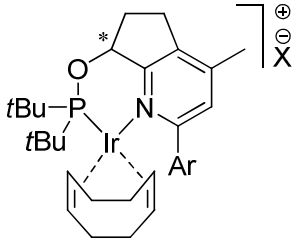	76 (*S*) (7.3) 1.2 $\frac{kcal}{mol}$
***S*-108b**	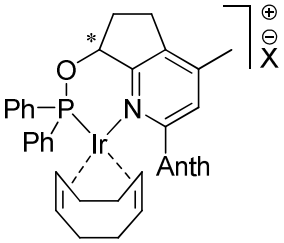	83 (*R*) (10.8) -1.4 $\frac{kcal}{mol}$	***S*-108g**[b]	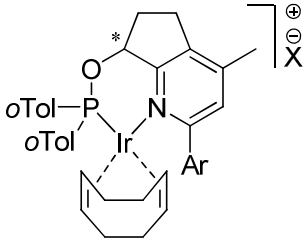	29 (*R*) (1.8) -0.35 $\frac{kcal}{mol}$
***S*-108c**	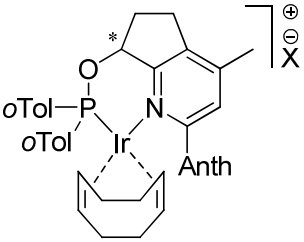	87 (*R*) (14.4) -1.6 $\frac{kcal}{mol}$	***R*-110a**	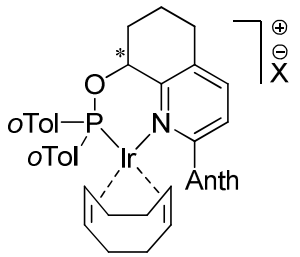	89 (*S*) (17.2) -1.7 $\frac{kcal}{mol}$
***S*-108d**	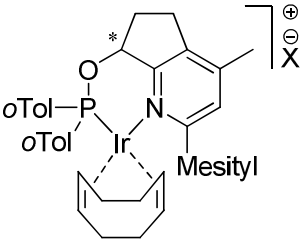	82 (*R*)[d] (10.1) -1.4 $\frac{kcal}{mol}$	***S*-110b**	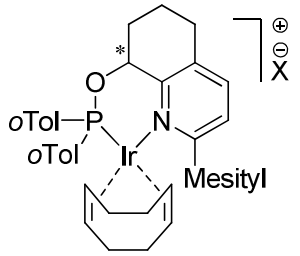	86 (*R*) (13.3) -1.5 $\frac{kcal}{mol}$
***S*-108e**	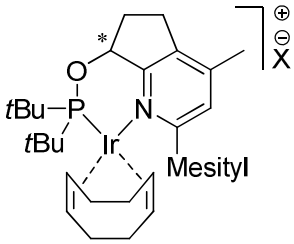	97 (*R*) (65.6) -2.5 $\frac{kcal}{mol}$	***S*-110c**[b]	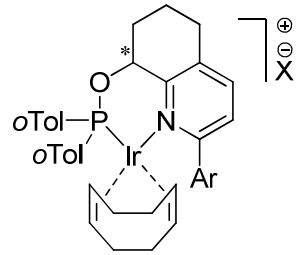	15 (*R*) (1.4) -0.18 $\frac{kcal}{mol}$

a) X = BAr_F anion, Naph = β-naphthyl, Anth = 9-anthracyl, mesityl = 2,4,6-tri-methylbenzene, Ar = 3,5-di-*tert*-Bu-4-MeOPh, b) reference [2], c) 8% conversion, d) 77% conversion.

Table 34. Asymmetric hydrogenation results for substrate **160b**.

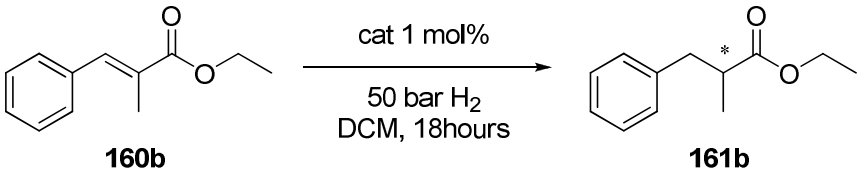

160b **161b**

#	structure[a]	ee% (*q*) $\Delta\Delta G^{\ddagger}_{RS}$	#	structure[a]	ee% (*q*) $\Delta\Delta G^{\ddagger}_{RS}$
***S*-108a**	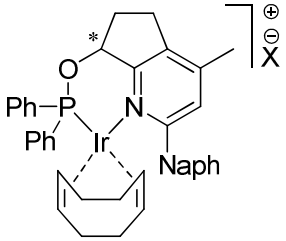	3 (*R*)[c] (1.06) $-35\frac{cal}{mol}$	***R*-108f**[b]	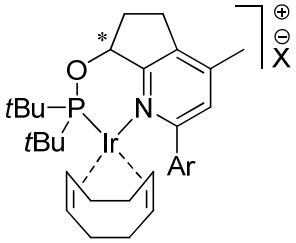	95 (*S*) (39) $2.2\ \frac{kcal}{mol}$
***S*-108b**	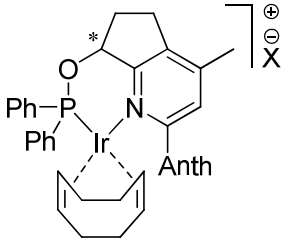	80 (*R*)[d] (9) $-1.3\ \frac{kcal}{mol}$	***S*-108g**[b]	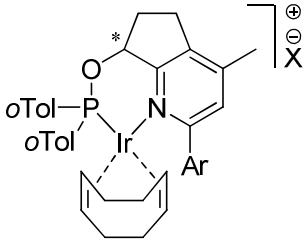	8 (*R*) (1.17) $-94\ \frac{cal}{mol}$
***S*-108c**	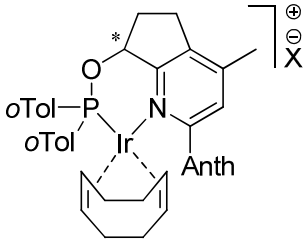	83 (*R*) (10.8) $-1.4\ \frac{kcal}{mol}$	***R*-110a**	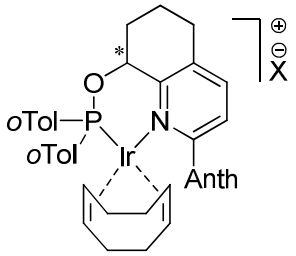	92 (*S*) (24) $-1.9\ \frac{kcal}{mol}$
***S*-108d**	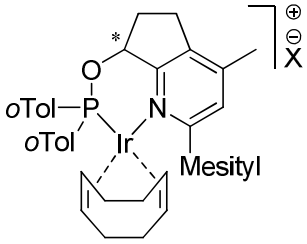	80 (*R*)[e] (9) $-1.3\ \frac{kcal}{mol}$	***S*-110b**	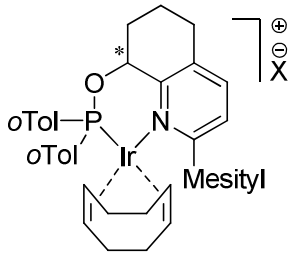	81 (*R*) (9.5) $-1.3\ \frac{kcal}{mol}$
***S*-108e**	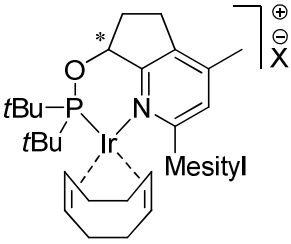	97 (*R*) (65.6) $-2.5\ \frac{kcal}{mol}$	***S*-110c**[b]	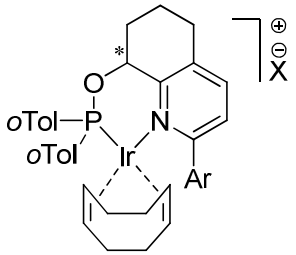	6 (*R*) (1.13) $-71\ \frac{cal}{mol}$

a) X = BAr_F anion, Naph = β-naphthyl, Anth = 9-anthracyl, mesityl = 2,4,6-tri-methylbenzene, Ar = 3,5-di-*tert*-Bu-4-MeOPh, b) reference [2], c) 97% conversion, d) 17% conversion, e) 88% conversion.

Table 35. Asymmetric hydrogenation results for substrate **160c**.

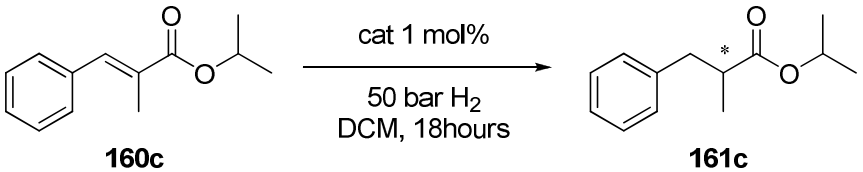

160c **161c**

#	structure[a]	ee% (*q*) $\Delta\Delta G^{\ddagger}_{RS}$	#	structure[a]	ee% (*q*) $\Delta\Delta G^{\ddagger}_{RS}$
***S*-108a**	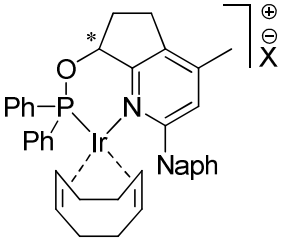	20 (*R*)[c] (1.5) -0.24 $\frac{kcal}{mol}$	***R*-108f**[b]	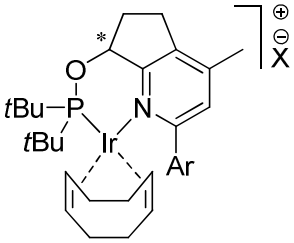	93 (*S*) (27.6) -2.0 $\frac{kcal}{mol}$
***S*-108b**	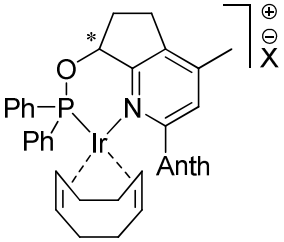	91 (*R*)[d] (21.2) -1.8 $\frac{kcal}{mol}$	***S*-108g**[b]	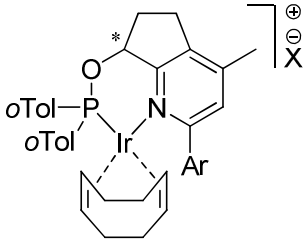	46 (*R*) (2.7) -0.6 $\frac{kcal}{mol}$
***S*-108c**	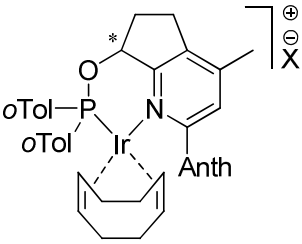	93 (*R*) (27.6) -2.0 $\frac{kcal}{mol}$	***R*-110a**	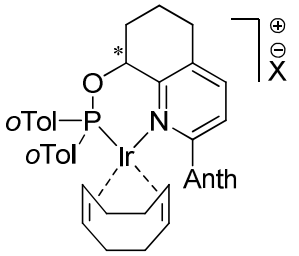	97 (*S*) (65.6) -2.5 $\frac{kcal}{mol}$
***S*-108d**	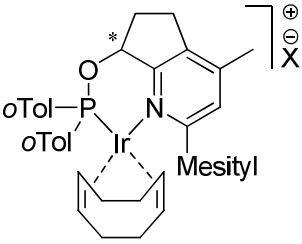	92 (*R*)[e] (24) -1.9 $\frac{kcal}{mol}$	***S*-110b**	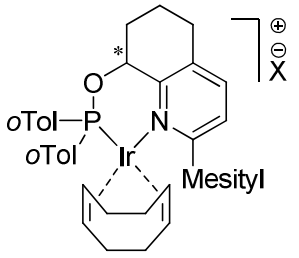	91 (*R*)[f] (21.2) -1.8 $\frac{kcal}{mol}$
***S*-108e**	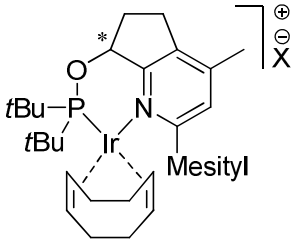	99.8 (*R*) (999) -4.1 $\frac{kcal}{mol}$	***S*-110c**[b]	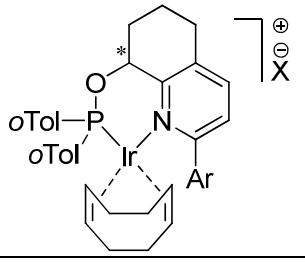	0[g] (0) -1.5 $\frac{kcal}{mol}$

a) X = BAr_F anion, Naph = β-naphthyl, Anth = 9-anthracyl, mesityl = 2,4,6-tri-methylbenzene, Ar = 3,5-di-*tert*-Bu-4-MeOPh, b) reference [2] c) 18% conv, d) 81% conv, e) 69% conv, f) 70% conv, g) 58% conv.

In a similar comparison the di-(*ortho*-tolyl)phosphinite analogue catalyst **108d** gives good enantioselectivity with substrate **108c** in 92%ee and an enantiomeric quotient of 24. However, the closely related di-(*tert*-butyl)phosphinite derivative **108e** gives a much higher enantiomeric quotient of 999, a forty fold increase in selectivity. This difference in selectivity between closely related catalysts high lights how small changes to the catalyst can lead to drastic changes in selectivity and activity.

The results from reduction of **160a-c** stand in sharp contrast to those obtained with the allylic alcohol **25e** which has a closely related geometry to the α-methyl cinnamic esters. Both systems contain a methyl group α to the coordinating oxygen function, *E* geometry about the C=C bond and a conjugated phenyl group but demonstrate opposite trends of SSR with the range of tested catalysts. Structure selectivity relationship studies with allylic alcohol **25e** identified the best performance with a sterically more accessible catalyst whereas the α-methyl-cinnamic esters **160a-c** functions better with large substituents surrounding both the metal center and the ester group. However, both classes of substrates give the same configuration of product from the same catalyst enantiomer. Burgess has also seen large differences in selectivity between allylic alcohols and methyl ester analogues in diastereoselective reductions, but in contrast to our system the alcohol directed the reduction to the opposite enantioface compared to the ester (see section 1.3.4). These results suggest a change in binding modes between these two classes of substrates which implicates a change in the structural requirements for high enantioselectivity.

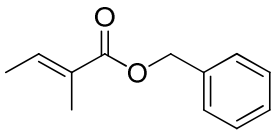

162

80% ee, 100% conversion, -1.3 $\frac{kcal}{mol}$

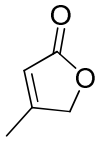

163

No conversion

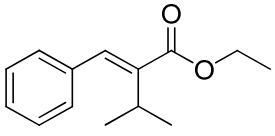

164

88% ee, 100% conversion, -1.6 $\frac{kcal}{mol}$

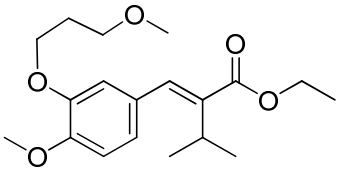

165

23% ee, 35% conversion, -0.3 $\frac{kcal}{mol}$

Figure 18. Asymmetric hydrogenation results of difficult substrates with catalyst **108e**, all hydrogenations were carried out at 50 bar H_2 pressure for 16 hours.

Several challenging α,β-unsaturated esters were hydrogenated with catalyst **108e** with lesser degrees of success (Figure 18). Substrate **163** has proven to be a very difficult substrate for several catalytic systems and in the case of **108e**, completely failed in hydrogenation. Substrate **165**, an important intermediate for the synthesis of the drug Aliskiren, was reduced with abysmal selectivity and conversion, likely due to the chelating polyether inhibiting the catalyst. Further evidence for this is the successful reduction of the closely related ester **164** which gives a reasonable selectivity of 88% ee and full conversion.

3.6 Conclusion

The evaluation of the 3rd generation of chiral pyridyl phosphinite catalysts in the asymmetric reduction of trisubstituted alkenes has provided additional insight to the factors governing structure selectivity relationships for a number of substrates. This chapter marks the highest enantioselectivities recorded to date for the asymmetric hydrogenation of dihydronaphthalenes, *E,E*-farnesol, and α substituted α,β-unsaturated esters.

3.7 References

[1] Doctoral thesis, Kaiser, S.; University of Basel, 2005.

[2] Master Thesis, Müller, M. A.; University of Basel, 2010

[3] Wang, A.; Wüstenberg, B.; Pfaltz, A. *Angew. Chem. Int. Ed.* **2008**, *47*, 2298.

[4] Kaiser, S.; Smidt, S., P.; Pfaltz, A. *Angew. Chem. Int. Ed.* **2006**, *45*, 5194.

Chapter 4

Synthesis and Asymmetric Hydrogenation of Vinyl Fluorides

4.1 Introduction

Organic fluorides are a fast growing class of organic halides due in large part to the pharmaceutical industries increased interest. Until recently strategies that incorporate fluorine into a chiral structure were rare. The vast majority of catalytic methods rely on carbonyl activation chemistry to incorporate fluorine from an electrophilic source typified by reagents such as N-fluorobenzenesulfonimide (NFSI).[1,2] One of the earliest successful strategies involved reduction of 2-fluoro-2-alkenoic acids with a ruthenium BINAP system with high enantioselectivities and yields (Scheme 31).[3] It is interesting to note that both *E* and *Z* fluoroalkenoic acids gave rise to the same enantiomer where as alkenoic acids with a methyl substituent in the 2 position give opposite configurations under similar conditions.

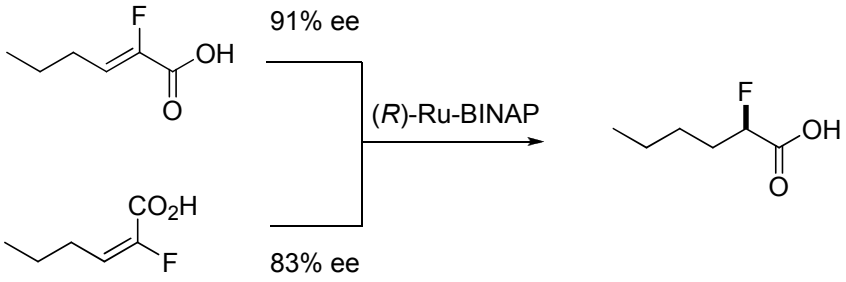

Scheme 31.

Andersson has recently reported the asymmetric hydrogenation of a limited range of fluoro-cinnamic esters and alcohols (section 1.3.3). Although high enantioselectivity could be obtained no examples of fluoroalkenes without adjacent coordinating groups was reported.

Synthesis of stereopure vinyl fluorides is an active research area with much interest vested by both the pharmaceutical and optoelectronic fields. The labs of Burton[4-35] and Haufe[36-46] have provided the largest share of the research in this area.

4.2 Synthesis of vinyl fluorides

Stereospecific synthesis of vinyl fluoride **168** was achieved by a Suzuki[12,47,48] route utilizing a modified procedure to produce α,α'-bromo-fluoro-styrenes[49] in *E/Z* mixtures and subsequent palladium coupling to synthesize fluorostilbene product. Subsequent chromatography and recrystallization provides the desired substrate in moderate yields (50%) and excellent

stereopurity (>99.9%). Fluorostyrene **171** was generated from the corresponding styrene via a Br-F addition followed by elimination to the vinyl fluoride (Scheme 32).

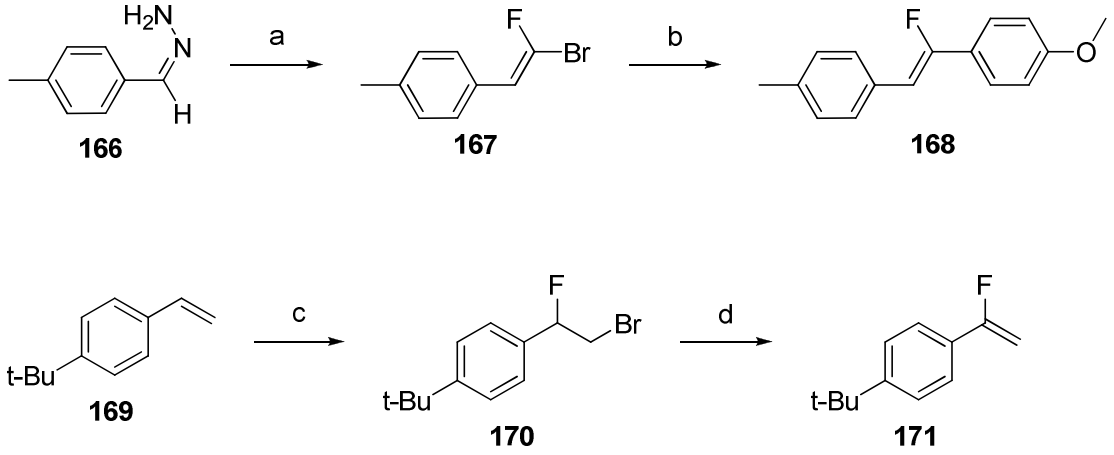

Scheme 32 Conditions: a) CuCl (10 mol%), NH_4OH, CBr_3F (1 eq), *E/Z*:3/1, 34% yield, b) $Pd_2(dba)_3$ (1 mol%), $P(t\text{-}Bu)_3HBF_4$ (4 mol%), $ArB(OH)_2$ (1.2 eq), room temp, 99% *Z*, 50 - 80% yield, c) $(TEA)_3$-HF (4 eq), NBS (1.2 eq), 30% yield, d) KOH (2.5 eq), DMSO, 78% yield.

4.3 Attempted asymmetric reduction of fluoroalkenes

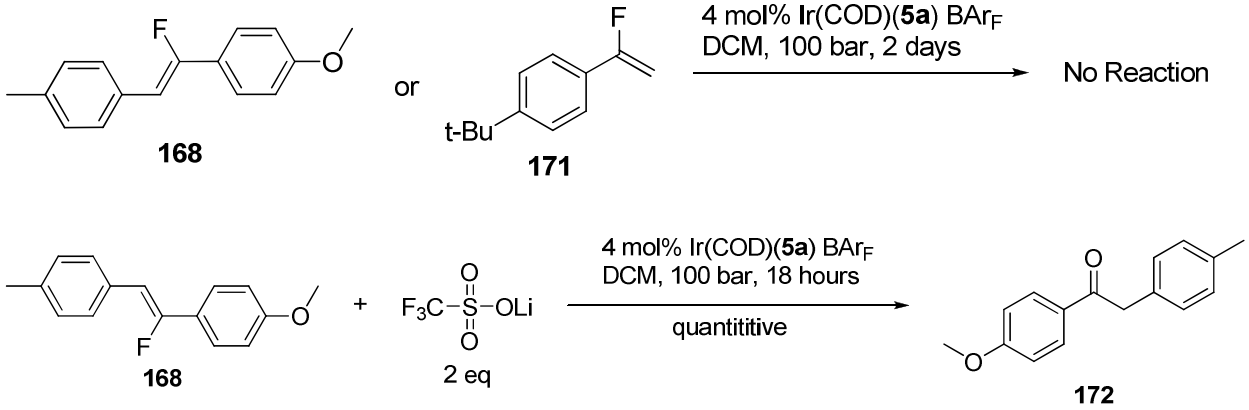

Scheme 33

Fluoroalkenes **168** and **171** were highly unreactive towards hydrogenation in spite of high catalyst loadings (4 mol%), very high pressures, and extended reaction times (Scheme 33). Despite all efforts, these substrates remained completely intact. Addition of a hard lewis acid however produced a new reaction product. Fluoroalkene **168** underwent a metathesis with the lithium triflate to produce a triflate enol ether which rapidly decomposed with moisture and acid

to the corresponding ketone **172**. Conversion to the ketone was quantitative when using 2 equivalents of lithium triflate.

4.4 Conclusion

Reduction of vinyl fluorides without adjacent coordinating groups is not feasible with the current state of the art. Studies with coordinating vinyl fluorides by other labs have indicated a difficult reduction at best and the products are easily obtained in higher yield by other methods which do not require expensive late transition metal based catalysts. However, a new substitution reaction of a fluoride with a triflate anion has been discovered.

4.5 References

[1] Cahard, D.; Xu, X.; Couve-Bonnaire, S.; Pannecoucke, X. *Chem. Soc. Rev.* **2010**, *39*, 558-568.

[2] Ma, J.-A.; Cahard, D. *Chem. Rev.* **2008**, *108*, PR1-PR43.

[3] Saburi, M.; Shao, L.; Sakurai, T.; Uchida, Y. *Tetrahedron Lett.* **1992**, *33*, 7877.

[4] Wang, Y.; Burton, D. J. *Org. Lett.* **2006**, *8*, 1109.

[5] Wang, Y.; Lu, L.; Burton, D. J. *J. Org. Chem.* **2005**, *70*, 10743.

[6] Xu, J.; Burton, D. J. *J. Org. Chem.***2005**, *70*, 4346.

[7] Burton, D. J.; Jairaj, V. *J. Fluorine Chem.* **2005**, *126*, 797.

[8] Xu, J.; Burton, D. J. *J. Fluorine Chem.* **2004**, *125*, 725.

[9] Burton, D. J.; Jairaj, V. *J. Fluorine Chem.* **2004**, *125*, 673.

[10] Lim, C.; Burton, D. J.; Wesolowski, C. A. *J. Fluorine Chem.* **2003**, *119*, 21.

[11] Xu, J.; Burton, D. J. *Tetrahedron Lett.* **2002**, *43*, 4565.

[12] Xu, J.; Burton, D. J. *Tetrahedron Lett.* **2002**, *43*, 2877.

[13] Liu, Q.; Burton, D. J. *Org. Lett.* **2002**, *4*, 1483.

[14] Xu, J.; Burton, D. J. *Org. Lett.* **2002**, *4*, 831.

[15] Liu, Q.; Burton, D. J. *Tetrahedron Lett.* **2000**, *41*, 8045.

[16] Guneratne, R. D.; Burton, D. J. *J. Fluorine Chem.* **1999**, *98*, 11.

[17] Wesolowski, C. A.; Burton, D. J. *Tetrahedron Lett.* **1999**, *40*, 2243.

[18] Blumenthal, E. J.; Burton, D. J. *Isr. J. Chem.* **1999**, *39*, 109.

[19] Davis, C. R.; Burton, D. J. *J. Org. Chem.* **1997**, *62*, 9217.

[20] Lu, L.; Burton, D. J. *Tetrahedron Lett.* **1997**, *38*, 7673.

[21] Xue, L.; Lu, L.; Pedersen, S. D.; Liu, Q.; Narske, R. M.; Burton, D. J. *J. Org. Chem.* **1997**, *62*, 1064.

[22] Davis, C. R.; Burton, D. J. *Tetrahedron Lett.* **1996**, *37*, 7237.

[23] Xue, L.; Lu, L.; Pedersen, S.; Liu, Q.; Narske, R.; Burton, D. J. *Tetrahedron Lett.* **1996**, *37*, 1921.

[24] MacNeil, K. J.; Burton, D. J. *J. Org. Chem.* **1995**, *60*, 4085.

[25] Burton, D. J. *ACS Symp. Series* **1994**, *555*, 297.

[26] Burton, D. J. *Molecular Structure and Energetics* **1988**, *8*, 149.

[27] Heinze, P. L.; Burton, D. J. *J. Org. Chem.* **1988**, *53*, 2714.

[28] Hansen, S. W.; Spawn, T. D.; Burton, D. J. *J. Fluorine Chem.* **1987**, *35*, 415.

[29] Burton, D. J.; Hansen, S. W. *J. Fluorine Chem.* **1986**, *31*, 461.

[30] Heinze, P. L.; Burton, D. J. *J. Fluorine Chem.* **1986**, *31*, 115.

[31] Burton, D. J.; Hansen, S. W. *J. Am. Chem. Soc.* **1986**, *108*, 4229.

[32] Cox, D. G.; Gurusamy, N.; Burton, D. J. *J. Am. Chem. Soc.* **1985**, *107*, 2811.

[33] Burton, D. J.; Cox, D. G. *J. Am. Chem. Soc.* **1983**, *105*, 650.

[34] Burton, D. J.; Hahnfeld, J. L. *J. Org. Chem.* **1977**, *42*, 828.

[35] Wheaton, G. A.; Burton, D. J. *J. Fluorine Chem.* **1976**, *8*, 97.

[36] Kirk, K. L.; Yoshida, S.; Haufe, G.; Meyer, O. G. J.; Rosen, T. C.; Application: WO 2005007614.

[37] Rosen, T. C.; Yoshida, S.; Froehlich, R.; Kirk, K. L.; Haufe, G. *J. Med. Chem.* **2004**, *47*, 5860.

[38] Haufe, G.; Rosen, T. C.; Meyer, O. G. J.; Frohlich, R.; Rissanen, K. *J. Fluorine Chem.* **2002**, *114*, 189.

[39] Rosen, T. C.; Haufe, G. *Tetrahedron Asymm.* **2002**, *13*, 1397.

[40] Haufe, G.; Meyer, O. G. J.; Muck-Lichtenfeld, C. *Coll. Czech. C.C.* **2002**, *67*, 1493.

[41] Ernet, T.; Maulitz, A. H.; Wurthwein, E.-U.; Haufe, G. *Perkin Trans. 1* **2001**, 1929.

[42] Oldendorf, J.; Haufe, G. *J. pr. Ch.* **2000**, *342*, 52.

[43] Meyer, O. G. J.; Frohlich, R.; Haufe, G. *Synthesis* **2000**, 1479.

[44] Bogachev, A. A.; Kobrina, L. S.; Meyer, O. G. J.; Haufe, G. *J. Fluorine Chem.* **1999**, *97*, 135.

[45] Ernet, T.; Haufe, G. *Tetrahedron Lett.* **1996**, *37*, 7251.

[46] Saluzzo, C.; Alvernhe, G.; Anker, D.; Haufe, G. *Tetrahedron Lett.* **1990**, *31*, 2127.

[47] Eddarir, S.; Rolando, C. *J. Fluorine Chem.* **2004**, *125*, 377.

[48] Chen, C.; Wilcoxen, K.; Strack, N.; McCarthy, J. R. *Tetrahedron Lett.* **1999**, *40*, 827.

[49] Nenajdenko, V. G.; Korotchenko, V. N.; Shastin, A. V.; Balenkova, E. S.; Brinner, K.; Ellman, J. A. *Org. Syn.* **2005**, *82*, 93.

Chapter 5

Experimental

5.1 General

All air and moisture sensitive reactions were carried out in an inert atmosphere using standard Schlenk techniques or in an inert atmosphere glove box (MBraun Labmaster 130). Absolute solvents were purchased from Fluka or obtained from a Pure-Solv^{TM} drying system.

Column chromatographic purifications were performed on Merck silica gel 60 (particle size 43-60 μm) under 0.1 – 2 bar nitrogen pressure. The eluents were technical grade and purified by distillation prior to use.

All reagents were purchased from Acros, Aldrich, Alpha, Fluka, Strem or Lancaster and used without further purification unless otherwise noted.

5.2 Analytical Methods

NMR-Spectroscopy: NMR spectra were measured either on a Bruker Advance 400 (400 MHz) or a Bruker Advance DRX 500 (500MHz) spectrometer equipped with BBO broadband probe heads. The chemical shift δ value is given in ppm. The chemical shift δ values were corrected to 7.26 ppm (^{1}H NMR) and 77.0 ppm (^{13}C NMR) for $CHCl_3$, 5.32 ppm (^{1}H NMR) and 54.0 ppm (^{13}C NMR) for CH_2Cl_2, 4.78 ppm and 3.35 ppm (^{1}H NMR) and 49.3 ppm (^{13}C NMR) for CH_3OH, 7.16 ppm (^{1}H NMR) and 128.0 ppm (^{13}C NMR) for C_6H_6, 2.50 ppm (^{1}H NMR) and 39.5 ppm (^{13}C NMR) for $(CH_3)_2SO$. The assignment of ^{1}H and ^{13}C signals was partly made by 2D-NMR, namely COSY, HMQC, HMBC and NOSY. ^{13}C were recorded in ^{1}H decoupled mode. Multiplets were assigned with s (singlet), d (doublet), t (triplet), q (quartet), quint (quintet), sext (sextet), m (multiplet). The index br stands for broad.

Mass Spectrometry (MS): Mass spectra were measured by Dr. H. Nadig (Department of Chemistry, University of Basel) on a VG70-250 (electron ionization (EI)) mass spectrometer or a MAR 312 (fast atom bombardment (FAB)) mass spectrometer. FAB was preformed with 3-nitrobenzyl alcohol (NBA) as matrix. ESI MS spectra were measured on a Finnigan MAT LCQ and a on a Varian 1200L triple Quad MS/MS. The signals are given in mass to charge ratio (m/z). The fragment and intensities are given in brackets. All values are rounded to the nearest whole number.

Infrared Spectroscopy (IR): Infrared spectra were measured on a Perkin Elmer 1600 series FTIR spectrometer. Solid samples were measured as KBr discs or as thin films on NaCl plates.

Absorption bands are given in wave numbers $\tilde{\nu}$ (cm^{-1}). The peak intensity is assigned with s (strong), m (medium) and w (weak). The index br stands for broad.

Melting Point (m.p.): Melting points were measured on a Büchi 535 melting point apparatus and are uncorrected.

Optical Rotation ($[\alpha]_D^{20}$): Optical rotations were measured on a Perkin Elmer Polarimeter 341 in a 1 dm cuvette at 20 ˚C. The concentration (c) is given in g/100 mL.

Gas Chromatography (GC): Gas chromatograms were collected on a Carlo Erba HRGC Mega2 Series 800 (HRGS Mega2) instruments. Achiral separations were performed on a Restek Rtx-1701 column (30m x 0.25mm x 0.25µm) and for chiral separations β and γ cyclodexterine columns (30m x 0.25mm x 0.25µm) were used.

High Performance Liquid Chromatography (HPLC): HPLC analyses were measured on Shimadzu systems with SCL-10A system controller, CTO-10AC column oven, LC10-AD pump system, DGU-14a degasser and SPD-M10A Diode Array or UV/VIS detector. Chiracel brand chiral columns from Daicel Chemical Industries were used with models OD-H, OJ-H, AD-H, OB-H or IC in 4.6 x 250 mm size.

Semipreparative High Performance Liquid Chromatography (HPLC): Seperations by semipreparative HPLC were performed on a Shimadzu system with SIL 10Advp autosampler, CTO 10 Asvp column oven, LC 10 Atvp pump system, FCV 10 Alvp degasser and SPD M10 avp diode array detector. Chiralcel brand columns from Diacel Chemical Industries were used with models OD and AD in size 2 x 25 cm.

Thin Layer Chromatography (TLC): TLC plates were obtained from Whatman (Partisil, 250 µm x 20 cm x 20 cm, florescent model K6F) and the glass was scored and plates broken into 20 x 100 mm size with a glass cutter. TLC were visualized with UV light (254 nm, 366 nm) or with basic permanganate solution or ceric ammonium molybdate solution.

Gas Chromatography with Mass Spectrum detection (GC/MS): HP6890 gas chromatograph with a HP5970A detector equipped with a Machery and Nagel Optima5 5% polyphenylmethylsiloxane column, 25 m x 0.2 mm id and 35 µM film thickness, flow set to 20 psi of hydrogen carrier gas, a 20/1 split ratio. The oven was programmed for a starting

temperature of 100 ˚C, a 2 minute holding time at that temperature, a 10 ˚C/minute ramp with a final temperature of 270 ˚C and a holding time of 10 minutes at that temperature.

Elemental Analysis (EA): Elemental analyses were measured at the Department of Chemistry University of Basel Microanalytical Laboratory by Mr. W. Kirsch on a Leco CHN-900 analyser.

5.3 Buildup of 1,5 dicarbonyl building blocks and intermediates

Intermediate **111:** 3-(Dimethylamino)-1-phenylpropan-1-one

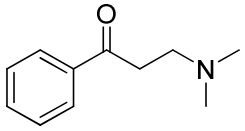

Dimethylamine hydrochloride (52.7 g, 0.65 mol) and paraformaldehyde (19.89 g, 0.22 mol) were weighed into a round bottom flask equipped with a heavy magnetic stir bar. Ethanol (100 mL, absolute) and 1 mL of concentrated hydrochloric acid were added to the dry reagents with mixing. Acetophenone (60 g, 58.5 mL, 0.5 mol) was added to the solution and the reaction was heated to reflux for 3 hours. The hot solution was poured into 450 mLs of acetone and allowed to cool for 2 hours. The resulting crystals were vacuum filtered, washed with acetone and dried on high vacuum for several hours. The free base was liberated by addition of saturated potassium carbonate to an ice cold solution of the hydrochloride salt with strong stirring and an additional 200 grams of ice to assist cooling. The solution was adjusted to 9.5 by checking with pH indicator strips. The cold mixture was extracted with diethyl ether (3 x 150 mL), the fractions were combined and washed with ice cold brine (200 mLs), dried over magnesium sulfate, filtered and concentrated on a rotovap without heating in a room temperature water bath to yield a viscous clear oil (35.4 g, 0.2 mol, 91% yield). A ^{1}H NMR was quickly taken to ensure reasonable quality and the Mannich base was used immediately in the formation of the 1,5 diketone.

Chemical Formula: $C_{11}H_{15}NO$ Molecular Weight: 177.2

^{1}H NMR (400 MHz, $CDCl_3$) δ 7.97 (d, *J* = 7.4 Hz, 2 H), , 7.57 (t, *J* = 7.4 Hz, 1 H), 7.47 (t, *J* = 7.7 Hz, 2 H), 3.26 (t, *J* = 7.3 Hz, 2 H), 2.88 (t, *J* = 7.3 Hz, 2 H), 2.38 (s, 6 H).

Intermediate **112a:** 2-Phenyloctahydrocyclopenta[b]pyran-2,7a-diol

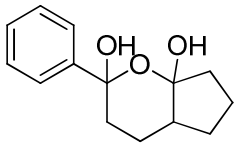

Freshly prepared 3-(dimethylamino)-1-phenylpropan-1-one (**111**), (35.4 g, 0.2 mol) was combined with cyclopentanone (95 g, 100 mL, 1.13 mol) in a round bottom flask and the resulting solution was heated to 145 ˚C for 3 hours. The remaining cyclopentanone was removed by vacuum distillation to result in a viscous yellow oil which was further purified by kugelrohr distillation to yield the crystalline hydrate when left in contact with air overnight (45 g, 0.192 mol, 96%).

Chemical Formula: $C_{14}H_{18}O_3$ Molecular Weight: 234.3

^{1}H NMR (400 MHz, $CDCl_3$) δ 7.96 (d, *J* = 7.3 Hz, 2H), 7.54 (t, *J* = 7.4 Hz, 1H), 7.45 (t, *J* = 7.6 Hz, 2H), 3.18 – 3.03 (m, 2H), 2.35 – 1.96 (m, 6H), 1.85 – 1.73 (m, 2H), 1.56 (ddd, *J* = 16.7, 10.7, 6.6 Hz, 1H).

^{13}C NMR (101 MHz, $CDCl_3$) δ 221.0, 199.8, 136.8, 133.0, 128.5, 128.0, 48.2, 38.1, 36.1, 29.9, 24.2, 20.6.
MS (e.i. 70 eV): m/z (%) 216.1 (15), 133.1 (9), 120.1 (60), 105.0 (100), 77.0 (32).

Intermediate **112b:** 2-Phenyloctahydro-2H-chromene-2,8-diol

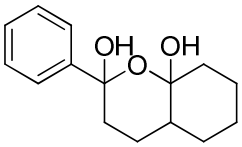

Prepared in an analogous manner to **112a**, yield 98%.

Chemical Formula: $C_{15}H_{20}O_3$ Molecular Weight: 248.3

^{1}H NMR (400 MHz, $CDCl_3$) δ 7.98 (d, *J* = 7.7 Hz, 2H), 7.55 (t, *J* = 7.4 Hz, 1H), 7.45 (t, *J* = 7.6 Hz, 2H), 3.15 – 3.08 (m, 1H), 2.97 (ddd, *J* = 16.9, 8.2, 6.7 Hz, 1H), 2.48 – 2.37 (m, 2H), 2.35 –

2.26 (m, 1H), 2.19 – 2.02 (m, 3H), 1.91 – 1.84 (m, 1H), 1.75 – 1.61 (m, 4H), 1.46 (qd, *J* = 12.1, 3.7 Hz, 1H).

^{13}C NMR (101 MHz, $CDCl_3$) δ 213.2, 200.2, 136.8, 132.9, 128.5, 128.0, 49.9, 42.2, 36.3, 34.5, 28.1, 25.0, 24.4.

MS (e.i. 70 eV): m/z (%) 230.1 (24), 133.1 (14), 120.1 (82), 111.1 (11.1),105.0 (100), 77.0 (41).

Intermediate **120:** 3-(2-Oxocyclohexyl)propanenitrile[1-3]

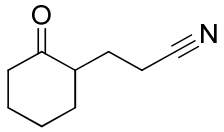

Cyclohexanone (120g, 128 mLs, 1.19 mol), acrylonitrile (64.8g, 80.0 mL, 1.22 mol), cyclohexylamine (4.3 g , 5.0 mL, 43.4 mmol) and acetic acid (525 mg, 0.5 mL, 8.7 mmol) were mixed together in a round bottom flask and heated to 120 ˚C for 3 hours. The resulting liquid is fractionally distilled under vacuum (0.6 mbar, 110 ˚C) to result in a clear oil (154 g, 1.02 mol, 86% yield).

Chemical Formula: $C_9H_{13}NO$ Molecular Weight: 151.2

^{1}H NMR (400 MHz, DMSO) δ 2.42 (ddd, *J* = 19.6, 12.5, 6.7 Hz, 3H), 2.20 (dd, *J* = 13.3, 4.3 Hz, 1H), 2.07 (dtd, *J* = 12.0, 6.0, 3.3 Hz, 1H), 1.99 (ddd, *J* = 9.4, 6.0, 3.0 Hz, 1H), 1.91 (dt, *J* = 21.2, 7.3 Hz, 1H), 1.82 – 1.72 (m, 1H), 1.72 – 1.48 (m, 2H), 1.42 (td, *J* = 13.6, 7.5 Hz, 1H), 1.28 (qd, *J* = 12.5, 3.8 Hz,1H).

MS (e.i. 70 eV): m/z (%) 151.1

5.4 Synthesis of fused ring substituted 2-pyridones

Intermediate **137a:** 4-Methyl-6,7-dihydro-1H-cyclopenta[b]pyridin-2(5H)-one[4-6]

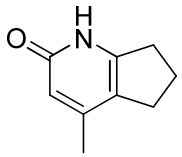

Ethyl acetoacetate (**136**), (116 g, 107 mL, 1 mol), cyclopentanone (84 g, 88.5 mL, 1 mol) and ammonium acetate (77.8 g, 1 mol) were combined together in a 1000 mL flask and heated to 135 ˚C for 18 hours with a reflux condensor and water cooling. The reflux condensor was replaced with a large simple distillation head and a long cooling condensor with a vacuum adapter and 250 mL receiving flask attached at the distilate end. The reaction mixture was partially concentrated by vacuum distilling off the remaining cyclopentanone and acetic acid (ca 90 mL) to yield a very dark, high viscosity solution. The product precipitates as an orange solid overnight, collected by vacuum filtration and the filter cake is washed with 50 mLs of diethyl ether and 50 mls of water. Recrystalized from ethanol or ethyl acetate (100mL) or water (roughly 700 mLs) to yield 29 grams of a white crystaline solid.

Chemical Formula: $C_9H_{11}NO$ Molecular Weight: 149.2

MP: 240 ˚C.

^{1}H NMR (400 MHz, $CDCl_3$) δ 6.91 (s, 1H), 2.99 (t, *J* = 7.8 Hz, 2H), 2.82 (t, *J* = 7.5 Hz, 2H), 2.23 (s, 3H), 2.18 – 2.06 (m, 2H).

^{13}C NMR (101 MHz, $CDCl_3$) δ 160.2, 150.9, 148.4, 120.5, 115.0, 31.0, 28.3, 22.3, 19.7. MS (e.i. 70 eV): m/z (%) 216.1 (15), 133.1 (9), 120.1 (60), 105.0 (100), 77.0 (32).

IR ($\tilde{\nu}$): 3271s, 2916w, 16341, 1535m, 1435m, 1219w, 1173m, 1111w, 957m cm^{-1}.

Intermediate **137b:** 5,6,7,8-Tetrahydroquinolin-2(1H)-one[1, 3]

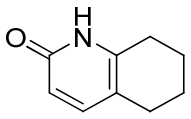

The commercially available 2-pyridone was prepared according to Meyers *et. Al.* with the following procedure and notes: 3-(2-Oxocyclohexyl)propanenitrile (**120**), (30 g, 20.8 mmol) is added to ice cold 98% sulfuric acid (200 mL) under argon with overhead stirring via a dropping funnel over a period of 45 minutes with internal temperature monitoring. On completion of the addition the orange reaction mixture is allowed to warm to room temperature, bubbling of sulfur dioxide is apparent as the reaction proceeds. If addition is carried out to quickly a large exotherm is observed and little or no product will be obtained. On warming the reaction mildly exotherms to 29 ˚C and bubbles become more prevalent. The reaction is stirred for an additional 45 minutes (ca 3 hours total time) and the reaction was carefully poured over a mixture of 1kg of crushed ice and 430 mLs of 32% ammonium hydroxide chilled in a large ice bath with vigorous stirring and cooling. The resulting aqueous solution (pH 9) is extracted with chloroform (9 x 150 mLs), the layers are combined and concentrated at the rotovap to yield 19 grams of crude product which is recrystallized from 1L of hot water which was concentrated to 600 mLs by normal distillation. The resulting long white needles are filtered off by vacuum filtration and dried by pulling air over the filtrate for 2 hours to result in 14 grams of semi-pure product which is further purified by sublimation (0.1 mbar, 100 ˚C, water cooling) to result in 13 grams of pure product as a white powder.

Chemical Formula: $C_9H_{11}NO$ Molecular Weight: 149.2

MP: 204 ˚C.

^{1}H NMR (400 MHz, DMSO) δ 13.24 (s, 1H), 7.16 (d, *J* = 9.1 Hz, 1H), 6.35 (d, *J* = 9.1 Hz, 1H), 2.67 (t, *J* = 5.9 Hz, 2H), 2.45 (t, *J* = 5.8 Hz, 2H), 1.80 – 1.68 (m, 4H).

^{13}C NMR (101 MHz, $CDCl_3$) δ 162.2, 142.9, 142.5, 117.0, 111.7, 26.1, 25.4, 22.17, 21.2.

Elemental Analysis: for $C_9H_{11}NO$ calculated C, 72.46; H, 7.43; N, 9.39 found C, 72.41; H, 7.36; N, 9.39.

5.4 Chlorination of 2-pyridones

General procedure: Solid 2-pyridone (15.7 g, 0.105 mol) and phenylphosphoryl dichloride (55.7 g, 40 mL, 0.285 mol) were added to a 100 mL round bottom flask equipped with a strong egg shaped stir bar, a reflux condenser and an inert gas bubbler, a Teflon sleeve was placed between the reflux condenser and flask to prevent the joints from fusing together. The resulting slurry was heated to 135 ˚C under an argon atmosphere during which time the solids dissolved. The resulting orange solution was stirred for 16 hours at this temperature. A 2 L flask was charged with 500 grams of ice, 60 grams of potassium carbonate, 200 mLs of water, 200 mLs of chloroform and a large and powerful stir bar for mixing viscous slurries. The flask was set in a large ice water bath and the still warm (ca 80 ˚C) highly viscous black reaction mixture was poured gently into the ice/ base quench mixture with a high rate of mixing. It is important to note that the cold reaction mixture forms a black tar which is extremely difficult to work with and ground glass joints fuse together if the entire joint is not protected by a Teflon sleeve. Precautions should be taken as a very exothermic release of gas ensues with the addition of strong acid to potassium carbonate, strong mixing and cooling assist this greatly. The remains of the reaction are washed into the stirring quench mixture with chloroform and the pH is adjusted to 8.5 with the careful addition of portions of potassium carbonate and frequent checking with pH indicator strips. Highly alkaline media will result in pyridone formation and moderate pH of 8.5-9.2 should be maintained. The mixture is poured into a large separatory funnel and the layers are separated. The aqueous layer is back extracted with chloroform (2 x 200 mLs), the layers are combined and dried over magnesium sulfate. The filtered organics were concentrated at a rotovap and the resulting black mixture was purified by Kugelrohr distillation (0.06 mbar, 120-150 ˚C, dry ice cooling) to result in a white solid which slowly darkens on contact with air and light and melts at very moderate temperatures. Note: the products are very pungent, volatile and some people develop a headache and nausea when exposed to the vapors.

Intermediate **138a:** 2-Chloro-4-methyl-6,7-dihydro-5H-cyclopenta[b]pyridine[6-8]

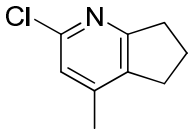

Produced by the general method to yield 15.3 grams of colorless waxy solid which slowly darkens in contact with air and light, 87% yield.

$C_9H_{10}ClN$ Molecular Weight: 167.6

^1H NMR (400 MHz, $CDCl_3$) δ 6.91 (s, 1H), 2.99 (t, *J* = 7.8 Hz, 2H), 2.82 (t, *J* = 7.5 Hz, 2H), 2.23 (s, 3H), 2.19 – 2.05 (m, 2H).

^{13}C NMR (101 MHz, $CDCl_3$) δ 160.2, 150.9, 148.4, 120.5, 115.0, 31.0, 28.3, 22.3, 19.7. MS (e.i. 70 eV): m/z (%) 216.1 (15), 133.1 (9), 120.1 (60), 105.0 (100), 77.0 (32).

IR ($\tilde{\nu}$): 3271s, 2916w, 16341, 1535m, 1435m, 1219w, 1173m, 1111w, 957m cm^{-1}.

MP: 51˚C.

Elemental Analysis: for $C_9H_{10}ClN$ calculated C, 64.48; H, 6.01; N, 8.36 found C, 64.26; H, 6.08; N, 8.23.

Intermediate **138b:** 2-Chloro-5,6,7,8-tetrahydroquinoline

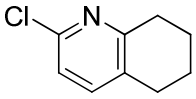

The commercially available compound was prepared using the general procedure outlined above in an identical fashion yielding 14.08 grams, 80.3% as a colorless waxy solid.

Chemical Formula: $C_9H_{10}ClN$ Molecular Weight: 167.6

^1H NMR (400 MHz, $CDCl_3$) δ 7.65 (d, *J* = 8.0 Hz), 7.39 (d, *J* = 8.0 Hz), 3.23 (t, *J* = 6.4 Hz), 3.07 (t, *J* = 6.2 Hz), 2.25 – 2.18 (m), 2.17 – 2.10 (m).

^{13}C NMR (101 MHz, $CDCl_3$) δ 158.2, 147.7, 139.5, 131.0, 121.1, 32.2, 28.0, 22.6, 22.4.

5.5 Synthesis of 2-aryl substituted pyridines

General method A:[9] A 250 mL round bottom flask was charged with 2-Phenyloctahydro-2H-chromene-2,8-diol (**112b**), (16.7 grams, 67.0 mmol), hydroxylamine hydrochloride (9.35 g, 134 mmol) and 50 mLs of absolute ethanol. A water cooled reflux condensor was placed on the flask and the reaction was heated to 110 ˚C with for 5 hours. The reaction was allowed to stand at room temperature overnight and the reaction mixture was concentrated to dryness on a rotovap. The crude solid was worked up by addition of saturated solution of sodium bicarbonate unitl basic pH was reached (ca 8.5), the aqueous layer was extracted with ether (2 x 200 mLs), the organic layers were combined and washed with brine (2 x 100 mLs), dried over magnesium sulfate, filtered and concentrated at the rotovap to yield 14.58 grams of semipure product. This material was taken up in techincal grade acetone (150 mLs), cooled in an ice salt bath and concentrated hydrochloric acid was added dropwise (7 mLs). A white precipitate was immediately visible and persisted with the addition of more acid until the reaction mixture became a very thick slurry. The slurry was stirred for 30 minutes in the cold bath and the precipitate was then isolated by filtration. The filtrate was washed with acetone (2 x 40 mLs) while breaking up the filtrate with a spatula and ensuring efficent washing. The resulting solids were transferred to a large round bottom flask and dried on the rotovap for 1 hour at 70 ˚C and then on high vacuum for several hours to yield 13.7 grams of the hydrochloride 83%. The hydrochloride salt is easily freed by dissolving in dichloromethane and washing with two washes of saturated bicarbonate.

General method B:[10] A 5 mL microwave tube was charged with 2-pyridylchloride (167 mg, 1 mmol), 2-aryl boronic acid or ester (1.15 mmol) and the Nolan palladium NHC carbene catalyst chloro[(1,2,3-n)-3-phenyl-2-propenyl][1,3-bis(2,6-di-i-propylphenyl)-4,5-dihydroimidazol-2-ylidene]palladium(II) (1.9 mg, 2.92 μmol, 0.3 mol%). A stir bar was added and the microwave tube was sealed with a high presure microwave septum. The reaction vessel was purged with argon for 15 minutes by a needle inlet and release needle through the septum. Degassed isopropanol (3 mLs) was added via syringe and the contents were stirred and briefly sonicated until all had dissolved. Degassed aqueous sodium hydroxide (120 mg, 3 mmol) in 250 μL of water was added, the needles were removed and the reaction was heated to 100 ˚C for 48 hours. The vial is then cooled and decapped. The contents were washed into a round bottom flask and the volatiles were removed at a rotovap. The crude solids were taken up in dichloromethane,

washed with saturated sodium bicarbonate (3 x 20 mLs), brine (1 x 20 mLs) and the organics were dried over magnesium sulfate. The volatiles were removed at a rotovap and the solids were taken up in dry hydrochloric acid in ether resulting in the immediate precipitation of a powder which was collected on a glass frit, washed with hexane and the hydrochloride pyridine salt was collected by dissolving in chloroform. The chloroform solution was neutralized with saturated bicarbonate, dried over magnesium sulfate and concentrated to yield the pure 2-arylpyridine.

Intermediate **113a:** 2-Phenyl-6,7-dihydro-5H-cyclopenta[1]pyridine

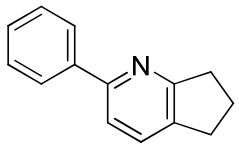

Produced by general method A except using 2-phenyloctahydrocyclopenta[b]pyran-2,7a-diol (**112a**), (35.6 grams, 0.152 mol), hydroxylamine hydrochloride (15.84 grams, 0.228 mol), and twice the described volumes to result in 35 grams of pure pyridine hydrochloride salt 99%.

Chemical Formula: $C_{14}H_{13}N$ Molecular Weight: 195.3

Intermediate **113b:** 2-Phenyl-5,6,7,8-tetrahydroquinoline

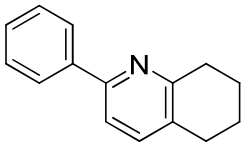

Produced by general method A in exact detail. 83% Yield 13.7 grams (55.7 mmol) of the hydrochloride salt as an off white powder. The following spectral data is for the hydrochloride salt, all data of the free pyridines were in good agreement with the literature.[9]

Chemical Formula: $C_{15}H_{15}N$ Molecular Weight: 209.3

^{1}H NMR (400 MHz, $CDCl_3$) δ 8.11 – 8.05 (m, 1H), 8.02 (d, *J* = 8.2 Hz, 1H), 7.72 (d, *J* = 8.2 Hz, 1H), 7.57 – 7.55 (m, 3H), 3.69 (t, *J* = 6.3 Hz, 2H), 2.93 (t, *J* = 6.2 Hz, 2H), 2.07 (s, 1H), 2.00 – 1.85 (m, 4H).

Intermediate **141c**: 2-(Anthracen-9-yl)-4-methyl-6,7-dihydro-5H-cyclopenta[b]pyridine

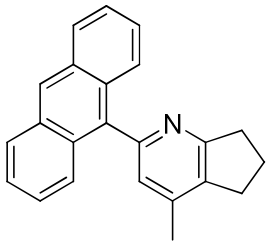

Produced by general method B with the following modifications: 2-Chloro-4-methyl-6,7-dihydro-5H-cyclopenta[b]pyridine (**138a**), (415 mg, 2.49 mmol) was weighed into a 20 mL microwave tube with 2-(anthracen-9-yl)-4,4,5,5-tetramethyl-1,3,2-dioxaborolane (anthracene-9-pinacolboronic ester, 870 mg, 2.86 mmol), the Nolan NHC catalyst (**144**), (16 mg, 24.9 μmol, 1 mol%) and a stir bar. A stir bar was added and the microwave tube was sealed with a high presure microwave septum. The reaction vessel was purged with argon for 15 minutes by a needle inlet and release needle through the septum. Degassed isopropanol (12 mLs) was added via syringe and the contents were stirred and briefly sonicated until all had dissolved. Degassed aqueous sodium hydroxide (4M, 1.87 mL, 7.46 mmol) was added, the needles were removed and the reaction was heated to 105 ˚C for 48 hours. The vial is then cooled and decapped. The contents were washed into a round bottom flask and the volatiles were removed at a rotovap. The crude solids were taken up in dichloromethane, washed with saturated sodium bicarbonate (3 x 60 mLs), brine (1 x 60 mLs) and the organics were dried over magnesium sulfate. The volatiles were removed at a rotovap and the solids were taken up in dry hydrochloric acid in ethanol resulting in a yellow solution which was concentrated to dryness. Ether was added to the solids with sonication and scratching with a spatula. The resulting yellow powder was collected on a glass frit, washed with hexane, small portions of ether, and the hydrochloride pyridine salt was collected by dissolving in chloroform. The chloroform solution was neutralized with saturated bicarbonate, dried over magnesium sulfate and concentrated to yield the pure 2-arylpyridine as a bright yellow solid (748 mg, 2.42 mmol, 97%).

Chemical Formula: $C_{23}H_{19}N$ Molecular Weight: 309.4

^{1}H NMR (500 MHz, $CDCl_3$) δ 8.50 (s, 1H), 8.03 (d, *J* = 8.5 Hz, 2H), 7.65 (d, *J* = 8.8 Hz, 2H), 7.46 – 7.42 (m, 2H), 7.37 – 7.33 (m, 2H), 7.10 (s, 1H), 3.17 (t, *J* = 7.7 Hz, 2H), 3.05 (t, *J* = 7.5 Hz, 2H), 2.37 (s, 3H), 2.26 (p, *J* = 7.7 Hz, 2H).

^{13}C NMR (126 MHz, $CDCl_3$) δ 165.39, 155.84, 143.02, 135.88, 134.82, 131.47, 130.31, 128.38, 127.08, 126.50, 125.54, 125.12, 125.01, 34.60, 29.27, 22.60, 19.02.

MS (e.i. 70 eV): m/z (%) 310.4 (12), 309.4 (59), 308.4 (100), 293.3 (2), 292.3 (5), 291.3 (6), 290.2 (2), 140.7 (3), 140.4 (3).

Intermediate **141a**: 2-Mesityl-4-methyl-6,7-dihydro-5H-cyclopenta[b]pyridine

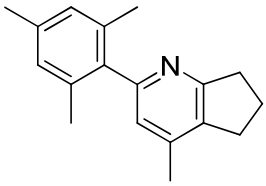

Synthesized by general method B with the following modifications to the amounts used and purification: 2-pyridylchloride (**138a**), (850 mg, 5.09 mmol), 2,4,6-mesitylboronic acid (959 mg, 5.85 mmol), Nolan NHC catalyst (**144**) (64 mg, 9.98 μmol, 2 mol%), 12 mLs of isopropanol, and 4M NaOH (3.8 mLs, 15.3 mmol) were used. Heated to 115˚C to overcome the insolubility of resulting boric eight complex, precipitate becomes loose and reaction mixture becomes less cloudy at higher temperature. Dry hydrochloric acid in ethanol (3 mLs of acetyl chloride in 30 mLs of absolute ethanol) was added to the crude solid after aqueous workup and removed at the rotovap followed by toluene (20 mLs) with subsequent removal by rotovap of the solvent to aid in crystallization. Isolation was identical to general method in all other regards yielding 1.1 grams (86%) of free pyridine after basic workup as an oil. Product can be purified by chromatography (3.5 X 15 cm silica gel, dry load), 30% ethyl acetate in hexane, R_f of product = 0.5.

Chemical Formula: $C_{18}H_{21}N$ Molecular Weight: 251.4

^{1}H NMR (400 MHz, $CDCl_3$) δ 6.89 (s, 2H), 6.77 (s, 2H), 3.05 (t, *J* = 7.8 Hz, 2H), 2.92 (t, *J* = 7.5 Hz, 2H), 2.29 (s, 3H), 2.27 (s, 3H), 2.16 (dt, *J* = 11.0, 7.7 Hz, 2H), 2.01 (s, 6H).

^{13}C NMR (101 MHz, $CDCl_3$) δ 164.8, 157.8, 142.8, 138.2, 136.8, 135.8, 133.7, 128.1, 122.8, 34.4, 29.1, 22.4, 21.0, 20.2, 18.9.

MS (e.i. 70 eV): m/z (%) 252.3 (6), 251.2 (37), 250.0 (100), 237.2 (1.3), 236.2 (8), 235.2 (7), 234.2 (5).

IR (neat ,$\tilde{\nu}$): 2930, 2858, 1612, 1590, 1563, 1460, 1393, 1258, 1181, 1116, 957, 849 cm^{-1}.

Elemental Analysis: for $C_{18}H_{21}N$ calculated C, 86.01; H, 8.42; N, 5.57 found C, 85.59; H, 8.52; N, 5.74.

Intermediate **141d**: 2-(Anthracen-9-yl)-5,6,7,8-tetrahydroquinoline[11]

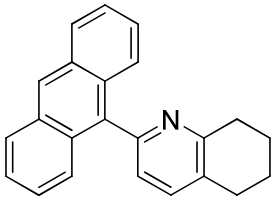

Prepared by general procedure B. Yield of 283 mg (90%) of bright yellow solid after basic workup.

Chemical Formula: $C_{23}H_{19}N$ Molecular Weight: 309.4

^{1}H NMR (400 MHz, $CDCl_3$) δ 8.51 (s, 1H), 8.03 (d, *J* = 8.5 Hz, 2H), 7.64 (dd, *J* = 8.8, 0.9 Hz, 2H), 7.57 (d, *J* = 7.7 Hz, 1H), 7.46 – 7.42 (m, 2H), 7.36 (ddd, *J* = 8.6, 6.5, 1.3 Hz, 2H), 7.24 (d, *J* = 7.7 Hz, 2H), 3.06 (t, *J* = 6.3 Hz, 2H), 2.95 (t, *J* = 6.2 Hz, 2H), 2.05 – 1.91 (m, 4H).

^{13}C NMR (101 MHz, $CDCl_3$) δ 155.4, 150.5, 144.9, 136.8, 131.4, 131.2, 131.0, 129.4, 127.9, 127.6, 125.91, 124.7, 124.6, 28.4, 28.1, 21.7, 21.4.

MS (e.i. 70 eV): m/z (%) 310.4 (12), 309.4 (59), 308.4 (100), 280.3 (18), 279.3 (5), 278.3 (8), 290.2 (2), 140.0 (7), 139.3 (5).

Intermediate **141b** 2-Mesityl-5,6,7,8-tetrahydroquinoline

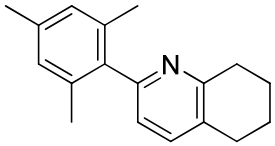

Synthesized by general method B with the following modifications to the amounts used and purification: 2-pyridylchloride (**138b**), (954 mg, 5.70 mmol), 2,4,6-mesitylboronic acid (1.11 mg, 5.85 mmol), Nolan NHC catalyst (74 mg, 11.4 μmol, 2 mol%), 12 mLs of isopropanol, and 4M NaOH (3.8 mLs, 15.26 mmol) were used. Heated to 115 ˚C to overcome the insolubility of resulting boric eight complex, precipitate becomes loose and reaction mixture becomes less cloudy at higher temperature. Dry hydrochloric acid in ethanol (3 mLs of acetyl chloride in 30 mLs of absolute ethanol) was added to the crude solid after aqueous workup and removed at the rotovap followed by toluene (20 mLs) with subsequent removal by rotovap of the solvent to aid in crystallization. Isolation was identical to general method in all other regards yielding 1.25 grams (87%) of free pyridine after basic workup as an oil. Product can be purified by chromatography (3.5 X 15 cm silica gel, dry load), 30% ethyl acetate in hexane.

Chemical Formula: $C_{18}H_{21}N$ Molecular Weight: 251.4

^{1}H NMR (400 MHz, $CDCl_3$) δ 7.39 (d, *J* = 7.7 Hz, 1H), 6.93 (d, *J* = 7.8 Hz, 1H), 6.91 – 6.88 (s, 2H), 2.95 (t, *J* = 6.4 Hz, 2H), 2.81 (t, *J* = 6.3 Hz, 2H), 2.29 (s, 3H), 2.02 (s, 6H), 1.97 – 1.90 (m, 2H), 1.89 – 1.82 (m, 2H).

^{13}C NMR (101 MHz, $CDCl_3$) δ 156.9, 156.8, 137.9, 137.0, 136.9, 135.8, 129.7, 128.2, 121.7, 32.5, 28.6, 23.2, 22.8, 21.0, 20.2.

MS (e.i. 70 eV): m/z (%) 252.3 (6), 251.2 (41), 250.0 (100), 236.2 (1.7), 235.2 (7), 234.2 (5), 223.2 (2.7), 222.2 (9), 221.3 (2).

IR (neat ,$\tilde{\nu}$): 2924, 2850, 1614, 1591, 1561, 1458, 1393, 1252, 1181, 1111, 957, 842 cm^{-1}.

Elemental Analysis: for $C_{18}H_{21}N$ calculated C, 86.01; H, 8.42; N, 5.57 found C, 86.13; H, 8.42; N, 5.52.

5.6 Oxidation of ortho substituted pyridines to pyridine-*N*-oxides

General method A: Ortho functionalized pyridine (53.9 mmol) was dissolved in acetic acid (75 mLs) and 32% hydrogen peroxide was added to this mixture which was then heated to 100˚C for 18 hours. The volatiles were removed at the rotovap and the resulting slurry was dissolved in DCM (300 mLs) and partitioned with 5% sodium bicarbonate (2 x 150 mLs),water (2 x 150 mLs), and brine (2 x 100 mL). The organic layer was dried over magnesium sulfate, filtered and concentrated to dryness to yield essentially pure product (53.6 mmol) which could be further purified by taking up in a minimal amount of toluene (ca 60 mLs) and leaving in the freezer overnight (47.3 mmol).

General method B: Ortho functionalized pyridine (1.62 mmol) was dissolved in 10 mLs of DCM and commercially quality 77% MCPBA was added (500 mg, 2.89 mmol). The flask was equipped with a reflux condenser and the reaction was heated to 42˚C while monitoring the disappearance of starting material by TLC (2-4% TEA in DCM). Reaction is complete within 4 to 6 hours and quenched immediately to prevent over oxidation. The reaction was quenched with a workup by extraction with saturated bicarbonate diluted in water (1:3 v/v, 3 x 50 mL), water (2 x 50 mL) and brine (2 x 50 mL). The organic layer was dried over sodium sulfate, filtered and concentrated at the rotovap for essentially pure product in a yield range of 70-96%.

Intermediate **139a**: 2-Chloro-4-methyl-6,7-dihydro-5H-cyclopenta[b]pyridine-N-oxide[5, 8]

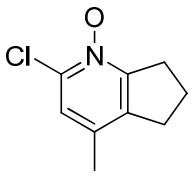

Produced in an identical manner to general method A. Yield 9.30 grams (50.6 mmol) of white crystalline material from 53.9 mmol of starting material (94% isolated yield).

Chemical Formula: $C_9H_{10}ClNO$ Molecular Weight: 183.6

MP: 172 ˚C.

^{1}H NMR (400 MHz, $CDCl_3$) δ 7.11 (s, 1H), 3.19 (t, *J* = 7.6 Hz, 2H), 2.92 (t, *J* = 7.6 Hz, 2H), 2.23 (s, 3H), 2.19 – 2.05 (m, 2H).

^{13}C NMR (101 MHz, $CDCl_3$) δ 163.4, 153.4, 133.8, 133.7, 125.3, 30.7, 30.4, 22.0, 18.0. MS (e.i. 70 eV): m/z (%) 183 (83), 166 (100), 151 (18), 131 (52), 77 (18).

IR ($\tilde{\nu}$): 3032w, 1805w, 1659w, 1512w, 1458m, 1381m, 1227s, 1173s, 1072m, 910s cm^{-1}.

Intermediate **139b**: 2-Chloro-5,6,7,8-tetrahydroquinoline -N-oxide[1, 7, 8, 11, 12]

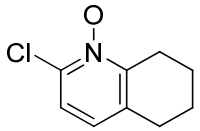

Produced in an identical manner to general method A. Yield 9.2 grams (50.3 mmol) of white crystalline material from 53.9 mmol of starting material (93% isolated yield).

Chemical Formula: $C_9H_{10}ClNO$ Molecular Weight: 183.6

^{1}H NMR (400 MHz, $CDCl_3$) δ 7.23 (d, *J* = 8.3 Hz, 2H), 6.92 (d, *J* = 8.3 Hz, 2H), 2.95 (t, *J* = 6.6 Hz, 2H), 2.74 (t, *J* = 6.0 Hz, 2H), 1.92 – 1.84 (m, 2H), 1.78 – 1.70 (m, 2H).

^{13}C NMR (101 MHz, $CDCl_3$) δ 150.5, 139.1, 134.2, 125.8, 122.9, 28.3, 25.5, 21.7, 21.4.

Intermediate **114b**: 2-Phenyl-5,6,7,8-tetrahydroquinoline-N-oxide[9]

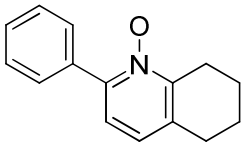

Produced by method A except using 20.4 grams (97.6 mmol) of starting pyridine 2-phenyl-5,6,7,8-tetrahydroquinoline, 150 mL of acetic acid and 13.3 mLs of 32% hydrogen peroxide resulting in 19.9 grams (88.8 mmol), 91% yield.

Chemical Formula: $C_{15}H_{15}NO$ Molecular Weight: 225.3

^{1}H NMR (400 MHz, $CDCl_3$) δ 7.79 – 7.75 (m, 2H), 7.48 – 7.38 (m, 3H), 7.22 (d, *J* = 8.1 Hz, 1H), 7.08 (d, *J* = 8.1 Hz, 1H), 3.01 (t, *J* = 6.5 Hz, 2H), 2.81 (t, *J* = 6.1 Hz, 2H), 1.97 – 1.89 (m, 2H), 1.80 (dtd, *J* = 9.2, 6.2, 2.8 Hz, 2H).

^{13}C NMR (101 MHz, $CDCl_3$) δ 149.5, 146.9, 135.0, 133.4, 129.4, 129.0, 128.1, 126. 123.4, 28.7, 25.2, 22.1, 21.6.

Intermediate **141a**-*N*-oxide: 2-Mesityl-4-methyl-6,7-dihydro-5H-cyclopenta[b]pyridine-*N*-oxide

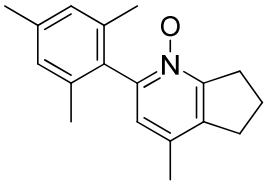

Produced by general method B except running the reaction at room temperature on 1 gram (4.00 mmol) of 2-arylpyridine **141a**, addition of 1.5 grams (6.00 mmol) MCPBA is quite exothermic. An additional 250 mg (1.41 mmol) of oxidant is added 2 hours into reaction to drive the reaction to completion, total time 5 hours. Aqueous workup was identical to that outlined in general method B, yielding 950 mg (3.55 mmol, 89%) as a viscous clear wax which crystallized on standing for a few hours.

Chemical Formula: $C_{18}H_{21}NO$ Molecular Weight: 267.4

^{1}H NMR (400 MHz, $CDCl_3$) δ 6.92 (s, 2H), 6.83 (s, 1H), 3.24 (t, *J* = 7.7 Hz, 2H), 2.97 (t, *J* = 7.6 Hz, 2H), 2.31 (s, 3H), 2.25 (s, 3H), 2.26 – 2.17 (m, 2H), 2.05 (s, 6H).

^{13}C NMR (101 MHz, $CDCl_3$) δ 152.5, 147.4, 139.2, 138.3, 136.8, 132.5, 130.2, 128.2, 126.7, 30.5, 30.3, 21.9, 21.1, 19.8, 18.1.

Intermediate **141c**-*N*-oxide: 2-(Anthracen-9-yl)-4-methyl-6,7-dihydro-5H-cyclopenta[b]pyridine-*N*-oxide

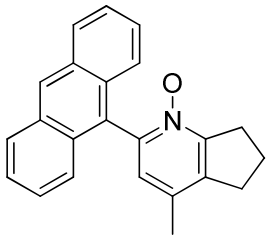

Produced by general method B on 700 mg (2.26 mmol) of 2-arylpyridine **141c** with 557 mg (2.26 mmol) of MCPBA and heating to 42 ˚C. An additional 125 mg (0.71 mmol) of MCPBA was added 3 hours into the reaction to drive the reaction to completion. Workup was identical to that on general method B to yield 521 mg (1.6 mmol, 71% yield) as a yellow solid.

Chemical Formula: $C_{23}H_{19}NO$ Molecular Weight: 325.4

^{1}H NMR (500 MHz, $CDCl_3$) δ 8.57 (s, 1H), 8.04 (t, *J* = 9.7 Hz, 2H), 7.55 (d, *J* = 8.6 Hz, 2H), 7.47 – 7.43 (m, 2H), 7.42 – 7.39 (m, 2H), 7.09 (s, 1H), 3.34 (t, *J* = 7.6 Hz, 2H), 3.11 (t, *J* = 7.6 Hz, 2H), 2.33 (s, 3H), 2.36 – 2.27 (m, 2H).

^{13}C NMR (126 MHz, $CDCl_3$) δ 153.4, 145.9, 140.7, 133.0, 131.8, 130.8, 129.1, 129.0, 127.9, 126.8, 125.8, 125.6, 31.1, 30.8, 22.5, 18.5.

Intermediate **141d**-*N*-oxide: 2-(Anthracen-9-yl)-5,6,7,8-tetrahydroquinoline-*N*-oxide[11]

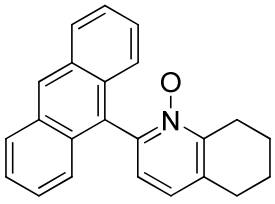

Produced by general method B except using 501 mg (1.62 mmol) of 2-arylpyridine **141d** and 397 mg (1.619 mmol) of MCPBA to yield 506 mg (1.55 mmol, 96%) as a colorless solid.

Chemical Formula: $C_{23}H_{19}NO$ Molecular Weight: 325.4

^{1}H NMR (500 MHz, $CDCl_3$) δ 8.57 (s, 1H), 8.05 (d, *J* = 8.4 Hz, 2H), 7.51 (d, *J* = 8.6 Hz, 2H), 7.47 – 7.43 (m, 2H), 7.41 – 7.38 (m, 2H), 7.25 (d, *J* = 6.8 Hz, 1H), 7.20 (d, *J* = 7.9 Hz, 1H), 3.07

(t, *J* = 6.4 Hz, 2H), 2.95 (t, *J* = 6.1 Hz, 2H), 2.00 (dt, *J* = 12.1, 6.2 Hz, 2H), 1.90 (dt, *J* = 11.3, 5.9 Hz, 2H).

^{13}C NMR (126 MHz, $CDCl_3$) δ 155.3, 150.2, 145.5, 136.2, 131.8, 130.5, 129.1, 128.9, 128.3, 126.9, 126.3, 125.8, 125.6, 29.2, 25.4, 22.5, 22.2.

Intermediate **141b**-*N*-oxide: 2-Mesityl-5,6,7,8-tetrahydroquinoline-*N*-oxide

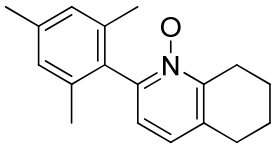

Produced by general method B except using 800 mg (3.18 mmol) of 2-arylpyridine **141b** and 1.17 g (4.78 mmol calculated for 70% b/w). A significant exotherm occurred on addition of the oxidant so the reaction was stirred at room temperature. Stirred for 5 hours and worked up as in general method B to yield 810 mg (3.03 mmol, 95%) as a clear solid.

Chemical Formula: $C_{18}H_{21}NO$ Molecular Weight: 267.4

^{1}H NMR (400 MHz, $CDCl_3$) δ 7.04 – 6.97 (m, 2H), 6.93 (s, 2H), 2.99 (t, *J* = 6.5 Hz, 2H), 2.82 (t, *J* = 6.1 Hz, 2H), 2.31 (s, 3H), 2.04 (s, 6H), 1.98 – 1.86 (m, 2H), 1.86 – 1.76 (m, 2H).

^{13}C NMR (101 MHz, $CDCl_3$) δ 149.2, 147.0, 138.3, 136.6, 134.7, 130.7, 128.2, 125.1, 123.9, 28.7, 24.9, 22.1, 21.7, 21.1, 19.7.

5.7 Boekelheide rearrangement of pyridines of *N*-oxides

General method: Pyridine-*N*-oxide (37.3 mmol) was added to a round bottom flask with 60 mLs of acetic anhydride. The reaction was stirred for 1 hour at room temperature and then a reflux condenser was placed on the reaction vessel followed by heating to 80 ˚C for 5 hours. The reaction was cooled and the condenser was exchanged for a vacuum distillation head. The volatiles were vacuum distilled off and the resulting viscous oil was taken up in 100 mLs of DCM and washed with saturated sodium bicarbonate (3 x 100 mLs), brine (100 mLs), dried over magnesium sulfate, filtered and concentrated to dryness at a rotovap. The crude product can be purified by chromatography (3.5 X 15 cm silica gel, dry load) or carried through to ester hydrolysis.

Intermediate **140a**: 2-Chloro-4-methyl-6,7-dihydro-5H-cyclopenta[b]pyridin-7-yl acetate[5-8]

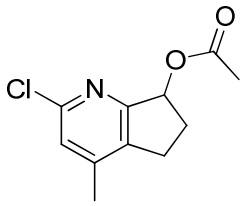

Produced in exact detail with the general method resulting in 6.85 grams (30.4 mmol, 81%) of a colorless solid in good accordance with the literature.

Chemical Formula: $C_{11}H_{12}ClNO_2$ Molecular Weight: 225.7

^{1}H NMR (400 MHz, $CDCl_3$) δ 7.09 (s, 1H), 6.03 (dd, *J* = 4.3, 4.3 Hz, 1H), 3.04-2.91 (m, 1H), 2.78 (ddd, *J* = 16.3, 8.8, 5.0 Hz, 1H), 2.66 (dddd, *J* = 14.2, 8.8, 7.5, 5.3 Hz, 1H), 2.29 (s, 3H), 2.11 (s, 3H), 2.11-2.05 (m, 1H).

^{13}C NMR (101 MHz, $CDCl_3$) δ 175.8, 165.5, 149.1, 145.9, 135.1, 121.8, 61.5, 34.0, 28.6, 22.4, 18.8.
MS (e.i. 70 eV): m/z (%) 182 (100), 165 (60), 154 (10), 130 (12), 43 (16).

IR ($\tilde{\nu}$): 2955w, 2854w, 1736s, 1589m, 1435m, 1366m, 1304w, 1227s, 1103m, 1042s, 934m, 887m, 864w, 733w, 687w, 633w cm^{-1}.

Intermediate **140b**: 2-Chloro-5,6,7,8-tetrahydroquinolin-8-yl acetate[1, 11, 13, 14]

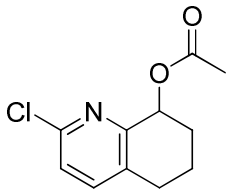

Produced with the general method except using 9.0 grams (49.2 mmol) of **139b**. Resulting in 8.5 grams (37.7 mmol, 77%) of a colorless solid in good accordance with the literature.

Chemical Formula: $C_{11}H_{12}ClNO_2$ Molecular Weight: 225.7

^{1}H NMR (400 MHz, $CDCl_3$) δ 7.41 (d, *J* = 8.1 Hz, 1H), 7.19 (d, *J* = 8.1 Hz, 1H), 5.85 (t, *J* = 4.4 Hz, 1H), 2.83 (dt, *J* = 17.0, 5.0 Hz, 2H), 2.76 – 2.65 (m, 1H), 2.21 – 2.12 (m, 1H), 2.10 (s, 3H), 2.04 – 1.95 (m, 1H), 1.95 – 1.88 (m, 1H), 1.88 – 1.78 (m, 1H).

^{13}C NMR (101 MHz, $CDCl_3$) δ 170.6, 154.1, 149.2, 140.3, 132.9, 124.3, 70.8, 29.0, 28.1, 21.8, 18.5.

Intermediate **142c**: 2-(Anthracen-9-yl)-4-methyl-6,7-dihydro-5H-cyclopenta[b]pyridin-7-yl acetate

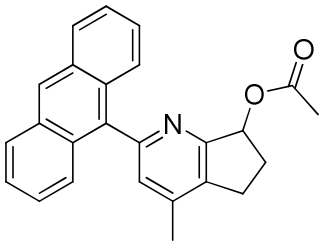

Produced by the general method except 500mg (1.54 mmol) of the pyridine-*N*-oxide was dissolved in 10 mLs of acetic anhydride and heated to 107 ˚C for 20 hours. Workup is identical to the general procedure accept the product was additionally purified by chromatography (2 X 15 cm silica gel, dry load) with 30% ethyl acetate/ hexane as an eluent to yield 400 mg (1.09 mmol, 71%) of pure product.

HPLC conditions: ADH column, 1% isopropanol in heptanes with a flow rate of 0.5 mLs/min and a temperature of 25 ˚C. Elution times T_r = 22 and T_s = 32 minutes. Semiprep conditions AD column, 0.5% isopropanol in hexanes with a flow rate of 6.0 mLs/min and a temperature of 25 ˚C T_R = 58 min and T_s = 82 min.

Chemical Formula: $C_{25}H_{21}NO_2$ Molecular Weight: 367.4

^{1}H NMR (400 MHz, $CDCl_3$) δ 8.52 (s, 1H), 8.52 (s, 1H), 8.03 (dd, *J* = 8.4, 5.2 Hz, 2H), 7.67 – 7.64 (m, 1H), 7.57 (dd, *J* = 8.8, 0.8 Hz, 1H), 7.48 – 7.42 (m, 2H), 7.40 – 7.32 (m, 2H), 7.27 (s, 1H), 6.17 (dd, *J* = 7.4, 3.7 Hz, 1H), 5.30 (d, *J* = 2.2 Hz, 2H), 3.19 (ddd, *J* = 14.6, 9.0, 6.0 Hz, 1H), 3.00 (ddd, *J* = 16.5, 9.0, 4.5 Hz, 1H), 2.79 (dddd, *J* = 13.4, 9.0, 7.4, 5.9 Hz, 1H), 2.42 (s, 3H), 2.27 – 2.18 (m, 1H), 2.06 – 2.06 (m, 1H).

MS (e.i. 70 eV): m/z (%) 368.2 (3), 367.2 (15), 308.2 (37), 307.2 (95), 306.1 (100), 305.1 (7), 304.1 (5), 293.12 (2.5), 292.12 (11), 291.1 (13), 154.1 (2), 153.6 (7), 153.1 (4), 152.6 (2), 146.6 (3), 146.1 (10), 145.6 (7).

Elemental Analysis: for $C_{25}H_{21}NO_2$ calculated C, 81.72; H, 5.76; N, 3.81 found C, 81.34; H, 5.93; N, 3.53.

Intermediate **142d**: 2-(Anthracen-9-yl)-5,6,7,8-tetrahydroquinolin-8-yl acetate

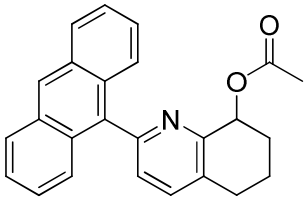

Produced by a modified Boekelheide rearrangement with trifluoroacetic anhydride. The pyridine-*N*-oxide (506 mg, 1.55 mmol) was added to a young tube and (816 mg, 540µL, 3.88 mmol) of trifluoroacetic anhydride was added at 0 ˚C. The reaction was allowed to warm to room temp and followed by TLC (9:1:0.2 DCM: ether: TEA) $R_{f\ noxide}$= 0.5, $R_{f\ product}$= 0.7. No reaction was observed for several hours so the sealed young tube was heated to 50˚C overnight. Some starting material remained so the reaction was cooled, an additional 5 mLs of trifluoroacetic anhydride and 5 mLs DCM, sealed and heated for 16 hours. When all the starting material had been consumed the volatiles were removed by vacuum and a liquid nitrogen cooled trap to collect the very caustic and reactive trifluoroacetic acid and anhydride. The resulting crude material appeared to have both the hydrolyzed and esterified alcohols present so the entire mixture was stirred in 20 mLs absolute methanol and potassium carbonate for 4 hours. After filtration and concentration the desired alcohol was purified by chromatography (2 X 15 cm silica gel, dry load) with a gradient eluent of ethyl acetate hexane starting from 100% hexane and working to 50% ethyl acetate. Yield of 310 mg of alcohol (61%).

The parent alcohol (48 mg, 0.147 mmol) was acylated with DMAP (36 mg, 0.295 mmol) and acetic anhydride (30 mg, 0.295 mmol) in DCM. Worked up the reaction by extraction with saturated sodium bicarbonate (3 x 5 mLs), brine (2 x 5 mL) and dried by passing through a pipette column of sodium sulfate, concentrated to dryness to yield essentially pure product (41 mg, 75%).

HPLC conditions: The product was analyzed on the OD-H, 10% isopropanol in heptanes with a flow rate of 0.5 mLs/min and a temperature of 25 ˚C. Elution times T_1= 22 and T_2= 32 minutes. The ester proved to insoluble for purification by preparative HPLC, 40 mg completely crystallizes out of 2 mLs of isopropanol.

Chemical Formula: $C_{25}H_{21}NO_2$ Molecular Weight: 367.4

^{1}H NMR (500 MHz, $CDCl_3$) δ 8.52 (s, 1H), 8.04 (d, *J* = 8.4 Hz, 2H), 7.73 – 7.63 (m, 3H), 7.45 (t, *J* = 7.4 Hz, 2H), 7.38 (t, *J* = 6.6 Hz, 3H), 6.01 (s, 1H), 2.37 (d, *J* = 11.5 Hz, 1H), 2.22 (s, 1H), 2.17 (t, *J* = 12.8 Hz, 1H), 2.07 (d, *J* = 14.4 Hz, 1H), 2.05 (s, 3H), 1.96 (d, *J* = 6.2 Hz, 1H).

^{13}C NMR (126 MHz, $CDCl_3$) δ 170.2, 166.3, 155.9, 153.4, 137.3, 134.8, 132.2, 131.5, 131.4, 130.2, 130.0, 128.4, 128.3, 127.5, 126.4, 126.3, 126.0, 125.7, 125.5, 125.0, 71.6, 28.8, 28.32, 21.4, 18.2.

Intermediate **142b**: 2-Mesityl-5,6,7,8-tetrahydroquinolin-8-yl acetate

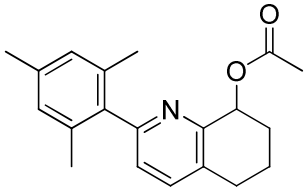

Produced by the general method except 800mg (3.00 mmol) of the pyridine-N-oxide was dissolved in 10 mLs of acetic anhydride and heated to 107˚C for 20 hours. Workup is identical to the general procedure accept the product was additionally purified by chromatography (3.5 X 15 cm silica gel, dry load) with a gradient of ether and DCM starting from 0% ether and working to 5% changing the concentration by 2.5% for every two column lengths. Product R_f = 0.65 in 2% ether in DCM and streaks badly. Yield after column is 750 mg (2.42 mmol, 81%).

HPLC conditions: OD column, 5% isopropanol in heptanes with a flow rate of 1.0 mLs/min and a temperature of 25 ˚C. Elution times 5.7 and 6.5 minutes. Semiprep conditions OD column, 0.5% isopropanol in hexanes with a flow rate of 6.0 mLs/min and a temperature of 25 ˚C T_S = 30.8 min and T_R = 39.2 min.

Chemical Formula: $C_{20}H_{23}NO_2$ Molecular Weight: 309.4

^{1}H NMR (400 MHz, $CDCl_3$) δ 7.50 (d, *J* = 7.9 Hz, 1H), 7.09 (d, *J* = 7.9 Hz, 1H), 6.92 (s, 2H), 5.91 (t, *J* = 4.1 Hz, 1H), 2.91 (dt, *J* = 16.7, 4.6 Hz, 1H), 2.85 – 2.76 (m, 1H), 2.30 (s, 3H), 2.26 (dd, *J* = 6.4, 3.5 Hz, 1H), 2.11 – 2.06 (m, 1H), 2.04 (s, 9H), 2.01 – 1.91 (m, 1H), 1.91 – 1.82 (m, 1H).

^{13}C NMR (101 MHz, $CDCl_3$) δ 170.2, 157.7, 152.8, 137.4, 137.2, 135.9, 131.2, 128.4, 124.3, 71.5, 28.8, 28.2, 21.4, 21.0, 20.2, 18.2.

Intermediate **142a**: 2-Mesityl-4-methyl-6,7-dihydro-5H-cyclopenta[b]pyridin-7-yl acetate

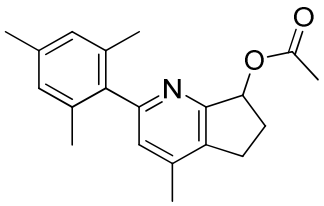

Produced by the general method except 1.00g (3.74 mmol) of the pyridine-N-oxide was dissolved in 10 mLs of acetic anhydride and heated to 107˚C for 20 hours. Workup is identical to the general procedure accept the product was additionally purified by chromatography on silica gel with a gradient of ether and DCM starting from 0% ether and working to 5% changing the concentration by 2.5% for every two column lengths. Product R_f= 0.7 in 2% ether in DCM and streaks badly. Yield after column (3.5 X 15 cm silica gel, dry load) is 650 mg (2.10 mmol, 56%).

HPLC conditions: ADH column, 1% isopropanol in heptanes with a flow rate of 0.75 mLs/min and a temperature of 25 ˚C. Elution times 11.7 and 23.7 minutes. Semiprep conditions AD column, 1% isopropanol in hexanes with a flow rate of 6.0 mLs/min and a temperature of 25 ˚C min T_S = 20.3 min and T_R = 39.0.

Chemical Formula: $C_{20}H_{23}NO_2$ Molecular Weight: 309.4

^{1}H NMR (500 MHz, $CDCl_3$) δ 6.96 (s, 1H), 6.90 (s, 2H), 6.08 (dd, *J* = 7.4, 3.7 Hz, 1H), 3.12 – 3.00 (m, 1H), 2.88 (tt, *J* = 9.0, 5.5 Hz, 1H), 2.76 – 2.63 (m, 1H), 2.33 (s, 3H), 2.30 (s, 3H), 2.24 – 2.09 (m, 1H), 2.07 (s, 3H), 2.02 (s, 6H).

^{13}C NMR (126 MHz, $CDCl_3$) δ 171.0, 159.6, 159.5, 144.1, 137.6, 137.3, 135.8, 135.1, 128.3, 125.3, 78.1, 30.4, 26.5, 21.4, 21.1, 20.3, 18.8.

5.8 2-Chloropyridylalcohols: Racemates and enantioselective methods for preparation of single enantiomers and the necessary intermediates.

5.8.1 Racemic 2-chloropyridylalcohols

General method: The parent 2-chloropyridylalcohol acetate ester was deprotected by placing 27.0 mmol of the starting material into an oven dried round bottom flask with 215 mmol of finely divided potassium carbonate and 100 mLs of absolute methanol. The reaction was sealed with a septum and stirred at a high rate of mixing. The reaction was monitored with TLC. When the starting material was completely consumed the reaction was diluted with dichloromethane (200 mLs) and passed through a pad of celite. The filter was washed with DCM (2 x 50 mL) and the resulting solution was extracted with water (300 mL) and the aqueous layer was back extracted with DCM (4 x 50 mL), the organic layer was dried over magnesium sulfate, filtered and concentrated at a rotovap to yield the crude product which was then purified by chromatography.

Intermediate **130a**: 2-Chloro-4-methyl-6,7-dihydro-5H-cyclopenta[b]pyridin-7-ol[7, 8]

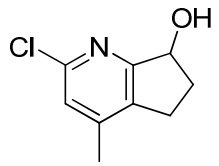

Produced in identical fashion to the general example and in good agreement with the literature to yield 4.36 grams (23.8 mmol, 88%) from 6.10 grams of starting material. Purified by chromatography (5.5 X 17 cm silica gel, dry load), R_f= 0.4 for product in 1:1 ethyl acetate/ hexane.

Chemical Formula: $C_9H_{10}ClNO$ Molecular Weight: 183.6

MP: 108 ˚C.

^{1}H NMR (400 MHz, $CDCl_3$) δ 7.03 (s, 1H), 5.17 (dd, *J* = 7.4, 5.8 Hz, 1H), 2.94 (ddd, *J* = 16.3, 9.0, 4.1 Hz, 1H), 2.75 – 2.66 (m, 1H), 2.55 (dddd, *J* = 13.4, 8.5, 7.6, 4.1 Hz, 1H), 2.27 (s, 3H), 2.05 (dddd, *J* = 13.6, 9.1, 6.6, 5.8 Hz, 1H).

^{13}C NMR (101 MHz, $CDCl_3$) δ 164.6, 149.9, 147.3, 134.7, 123.5, 74.2, 32.2, 25.5, 18.5. MS (e.i. 70 eV): m/z (%) 182 (20), 155 (100), 127 (29), 91 (15), 77.0 (7).

IR ($\tilde{\nu}$): 3420s, 2970w, 1589m, 1535m, 1435m, 1373m, 1188s, 1096s, 1065m, 1018m, 957m, 887w, 856s cm^{-1}.

Elemental Analysis: for $C_9H_{10}ClNO$ calculated C, 58.86; H, 5.49; N, 7.63; found C, 58.84; H, 5.42; N, 7.51

Intermediate **130b**: 2-Chloro-5,6,7,8-tetrahydroquinolin-8-ol[1, 11, 12]

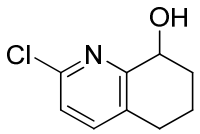

Produced by the general method except using 1.2 grams (5.37 mmol) of acetate, 1.2 grams (8.69 mmol) of potassium carbonate and 20% of the volumes for extraction as described. Yield after chromatography (3.5 X 15 cm silica gel, dry load) 970 mg (5.30 mmol, 97%), in good agreement with the literature.

Chemical Formula: $C_9H_{10}ClNO$ Molecular Weight: 183.6

^{1}H NMR (400 MHz, $CDCl_3$) δ 7.37 (d, *J* = 8.1 Hz, 1H), 7.13 (d, *J* = 8.1 Hz, 1H), 4.68 (t, *J* = 6.6 Hz, 1H), 3.63 (d, *J* = 1.1 Hz, 1H), 2.84 – 2.67 (m, 2H), 2.27 – 2.18 (m, 1H), 1.90– 1.72 (m, 2H).

5.8.2 Swern oxidation of 2-pyridyl alcohols to provide ketones

Intermediate **131**: 2-Chloro-4-methyl-5H-cyclopenta[b]pyridin-7(6H)-one

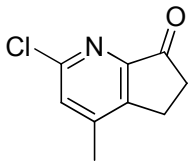

A 500 mL Schlenk flask is dried under vacuum with a heat gun and allowed to cool to room temperature under an active vacuum. The flask is placed under an inert atmosphere and charged with 150 mL of dry chloroform (amylenes as inhibitor). Oxalyl chloride (1.37 mL, 16.3 mmol) was added and the solution was cooled to -78 ˚C. DMSO (3.9 mL, 54.9 mmol) was added and the reaction was stirred 10 minutes. The parent alcohol (2.50 g, 13.6 mmol) dissolved in dry

chloroform (120 mL) was added and the resulting mixture was stirred at -78 ˚C for 15 minutes. Triethylamine (9.56 mL, 68.8 mmol) was added and the reaction was allowed to come to room temperature. The reaction mixture was quenched with saturated sodium bicarbonate with slow pipette addition at first followed by pouring into sodium bicarbonate solution (200 mL), followed by extraction with brine (3 x 100 mL), drying of the organic layer over magnesium sulfate, filtration and concentration to yield a crude dark product. The crude material was purified by chromatography (3.5 X 15 cm silica gel, dry load) with MTBE/ hexane 50:50 to yield 2.34 g (12.9 mmol, 95%) as a white solid.

Chemical Formula: C_9H_8ClNO Molecular Weight: 181.6

MP: 166 ˚C.

^{1}H NMR (400 MHz, $CDCl_3$) δ 7.29 (s, 1H), 3.01 (dd, *J* = 6.6, 4.7 Hz, 2H), 2.77 – 2.72 (m, 2H), 2.39 (s, 3H).

^{13}C NMR (101 MHz, $CDCl_3$) δ 203.6, 153.5, 153.0, 149.2, 148.5, 128.4, 34.8, 21.8, 17.6. MS (e.i. 70 eV): m/z (%) 181 (100), 153 (42), 139 (34), 118 (27), 91 (18), 77 (12), 51 (8).

IR ($\tilde{\nu}$): 3062w, 2988w, 1713s, 1582m, 1435m, 1389w, 1281m, 1258w, 1204m, 1111s, 914w, 872s, 733m, 648m cm^{-1}.

5.8.3 Asymmetric reduction of 2-chloro-4-methyl-5H-cyclopenta[b]pyridin-7(6H)-one with *R*-methyl-CBS and catecholborane or (-)B-Chlorodiisopinocamphylborane

Intermediate *S*-**130a**: (*S*)-2-chloro-4-methyl-6,7-dihydro-5H-cyclopenta[b]pyridin-7-ol

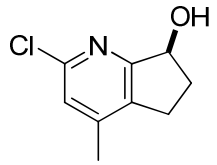

CBS reduction: Ketone (88 mg, 0.485 mmol) and *R*-methyl-CBS (10 mol%) are added together in a 50 mL Schlenk flask in the glove box with a stir bar. The flask is equipped with a rubber septum and brought outside the glove box. Absolute DCM (20 mL) was added and the reaction was cooled to -20 ˚C in an isopropanol bath cooled with a digital refrigerated circulator. Catecholborane (116 mg, 0.967 mmol) was diluted in 2 mLs of absolute DCM and added

dropwise over 15 minutes. The reaction was stirred for 48 hours at that temperature. The reaction was quenched with 4M lithium hydroxide (2 mL) and the reaction was removed from the cold bath and stirred for 30 minutes at that temperature. Water was added (10 mL), the layers were separated and the organic layer was passed through a short filtration column of silica (pipette column, 2 cc), the silica was washed with ethyl acetate and the organics were combined and concentrated to yield essentially pure product in 90.8% ee (*S* selective), which matched the racemic product its spectra.

HPLC: Separated on a chiral ADH column with a mobile phase of 10% isopropanol in heptanes with a flow rate of 0.5 mLs/minute and 25 ˚C, T_S = 13.2 minutes, T_R = 14.8 minutes.

(-)B-Chlorodiisopinocamphylborane reduction: Optimized conditions: Ketone **131** (0.5 grams, 2.76 mmol) was added to a Schlenk flask in the glove box with absolute THF (20 mL). The flask was brought outside the box and cooled in a circulated bath at -50 ˚C for thirty minutes. (-)DIP-Cl (1.3 g, 4.06 mmol) was added as a solid under argon at that temperature, the flask was sealed and stirred at that temperature for two days. Diethanolamine (426 mg, 391µL, 4.06 mmol) was added cold and the reaction was allowed to stir for 1 hour while the diethylolaminoboranate is precipitated. The solution is filtered on a Schlenk frit under argon and the filtrate washed with 5 mLs of THF. The solution is worked up with 4 mLs of 4M lithium hydroxide, transferred to a separatory funnel and DCM is added (200mL). The solution is extracted with water (2 x 200 mL), followed by brine (100 mL). The organic layer was dried over magnesium sulfate, filtered and concentrated to yield the crude product. The product was purified by chromatography (2 X 15 cm silica gel, dry load) with a gradient of ethyl acetate/ hexanes starting from pure hexanes and ending with 30% ethyl acetate. Yield of 256 mg (1.39 mmol, 50.6%). Product ee of 99.1% using HPLC conditions above.

$[\alpha]_D^{20}$ = -25 at a concentration of 0.12.

5.8.4 Asymmetric kinetic resolution of pyridyl alcohols with *Candida Antarctica Lipase B*

General procedure A: A 25 mL Schlenk flask equipped with a micro stir bar and rubber septum was dried under vacuum with a heat gun. The flask was placed under argon and the pressure was turned off to prevent the unwanted aerosol of the dry reagents. Racemic pyridyl alcohol (50 mg, 0.272 mmol) and *Candida Antarctica Lipase B* immobilized on resin, Novozyme® 435 (5 mg),

were added quickly in succesion and the flask was placed under vacuum and then backfilled with argon for three cycles. Dry, degased diisopropyl ether (10 mL, inhibited with BHT) was transferred to the flask by syringe under argon. The flask was placed into a 67 ˚C oil bath and 1 mL of vinyl acetate was added. The reaction was stirred at this temperature and aliquots of 100 μL were taken at regular intervals with a syringe. The aliquot was passed through a micronfilter into an HPLC vial, the volatiles were dried under a stream of nitrogen and 1 mL of HPLC grade isopropanol was added and the aliquot analyzed by chiral HPLC. The reaction was removed from the heat after the enantioselectivity had reached 99% for either the alcohol or ester and cooled in an ice bath. The contents were removed with a needle and syringe and filtered through a large micronfilter. The volatiles were removed at the rotovap and tert-butyldimethylsilyl chloride (106 mg, 0.680 mmol) and imidazole (55.5 mg, 0.816 mmol) were added to the flask with a stir bar and septum. The contents were purged with an inert atmosphere through needles in the septum and dry DMF (1 mL) was added. The reaction was stirred overnight and worked up by the addition of 3 mLs of ethyl acetate, extracted with water (4 x 4 mL), saturated ammonium chloride (2 x 2 mL), dried over magnesium sulfate, filtered and concentrated to dryness. A small column with a three solvent gradient was used to purify the sample by chromatography (1 X 10 cm silica gel, dry load) the products starting with 25% DCM in hexane and working to 100% DCM in steps of 25% every two column lengths followed by 10% ethyl acetate/ DCM to move the ester. Reaction is selective for the *R* acetate and *S* alcohol.[15, 16]

General procedure B: A 500 mL 4 neck reactor equipped with an overhead stirrer, condenser, inert gas inlet and bubbler was flame dried under a purge of argon. Racemic pyridyl alcohol (830 mg, 4.52 mmol) and *Candida Antarctica Lipase B* immobilized on resin, Novozyme® 435 (130 mg), were added under gentle argon purge in succesion and the flask was sealed with a ruber septum. Dry, degased diisopropyl ether (120 mL, inhibited with BHT) was transferred to the reactor by a double ended cannula pressure transfer under argon. The flask was placed into a 67 ˚C oil bath and 20 mL of vinyl acetate was added. The reaction was stirred at 900 rpm at this temperature and aliquots were taken and treated the same as in the general procedure A in the text above. The reaction was removed from the heat after the enantioselectivity had reached 99% for either the alcohol or ester and allowed to cool for ease of manipulation, filtered, the filter was washed with ethyl acetate (20mL), and the resin was recovered. The volatiles were removed at the rotovap and tert-butyldimethylsilyl chloride (1.75 g, 11.4 mmol) and imidazole

(930 mg, 13.7mmol) were added to the flask with a stir bar and septum. The contents were purged with an inert atmosphere through needles in the septum and dry DMF (20 mL) was added. The reaction was stirred overnight and was worked up by the addition of 50mLs of ethyl acetate, extracted with water (4 x 100 mL), saturated ammonium chloride (2 x 50 mL), dried over magnesium sulfate, filtered and concentrated to dryness. Purified by column chromatography (3.5 X 15 cm silica gel, dry load), TBDMS ether elutes very rapidly in 50% DCM/ hexane, acetyl ester was eluted with 30% ethylacetate hexane. The TBDMS protecting group could be removed by heating the protected ether with 3 equivalents of TBAF trihydrate in dry THF with heating to 50 ˚C for 5 hours followed by aqueous workup. The acetate protecting group could be removed by using the same conditions for the racemate.

Intermediate **145a**: (*S*)-7-(tert-butyldimethylsilyloxy)-2-chloro-4-methyl-6,7-dihydro-5H-cyclopenta[b]pyridine

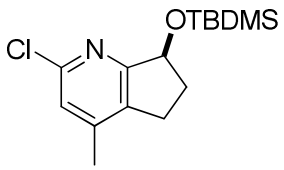

Produced by general method A, yield 31.5 mg (0.106 mmol, 40%). 99.3% Enantioselectivity measured from the parent alcohol.

HPLC: Separated the parent alcohol on a chiral ADH column with a mobile phase of 5% isopropanol in heptanes with a flow rate of 0.5 mLs/minute and 40 ˚C, $T_{(R)\text{-acetate}}$ = 12.69 minutes, $T_{(S)\text{-acetate}}$= 13.68 minutes, $T_{(S)\text{-alcohol}}$= 17.2 minutes, $T_{(R)\text{- alcohol}}$ = 19.49 minutes.

Chemical Formula: $C_{15}H_{24}ClNOSi$ Molecular Weight: 297.9

^{1}H NMR (500 MHz, $CDCl_3$) δ 6.82 (s, 1H), 4.96 (t, *J* = 5.3 Hz, 1H), 2.78 (dt, *J* = 14.7, 10.8 Hz, 1H), 2.55 – 2.43 (m, 1H), 2.32 – 2.20 (m, 1H), 2.08 (s, 3H), 1.86 (dq, *J* = 8.7, 4.7 Hz, 1H), 0.77 (s, 9H), 0.05 (s, 3H), -0.00 (s, 3H).

^{13}C NMR (126 MHz, $CDCl_3$) δ 150.6, 146.8, 135.0, 123.7, 76.2, 34.1, 26.3, 26.0, 18.8, -3.8, -4.3.

MS (FAB NBA): m/z (%): 298.1 (52), 282.1 (17), 240.1 (100), 166.0 (61), 73.0 (32).

Elemental Analysis: for $C_{15}H_{24}ClNOSi$ calculated C, 60.48; H, 8.12; N, 4.70 found C, 60.62; H, 8.39; N, 4.59.

Intermediate **145b**: (*S*)-8-(tert-butyldimethylsilyloxy)-2-chloro-5,6,7,8-tetrahydroquinoline

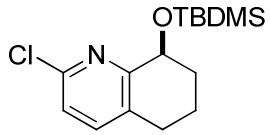

Synthesized with general procedure B in identical detail. Yield of the protected silyl ether 563 mg (1.90 mmol, 41.7% yield) 99% enantioselectivity based on HPLC analysis of parent alcohol.

HPLC: Separated on a chiral ADH column with a mobile phase of 5% isopropanol in heptanes with a flow rate of 0.5 mLs/minute and 40 ˚C, $T_{(R)\text{-acetate}}$ = 12.05 minutes, $T_{(S)\text{-acetate}}$=13.82 minutes, $T_{(S)\text{-alcohol}}$= 15.8 minutes, $T_{(R)\text{- alcohol}}$ = 17.23 minutes.Chemical Formula: $C_{15}H_{24}ClNOSi$ Molecular Weight: 297.9

^{1}H NMR (400 MHz, $CDCl_3$) δ 7.32 (d, *J* = 8.1 Hz, 1H), 7.10 (d, *J* = 8.1 Hz, 1H), 4.74 (t, *J* = 4.5 Hz, 1H), 2.78 (dt, *J* = 17.0, 5.3 Hz, 1H), 2.72 – 2.57 (m, 1H), 2.13 – 1.94 (m, 2H), 1.94 – 1.81 (m, 1H), 1.73 (tdd, *J* = 8.3, 6.0, 2.9 Hz, 1H), 0.91 – 0.87 (m, 9H), 0.21 (d, *J* = 3.1 Hz, 3H), 0.10 (d, *J* = 3.1 Hz, 3H).

^{13}C NMR (126 MHz, $CDCl_3$) δ 158.5, 148.6, 140.0, 131.4, 123.2, 69.8, 32.5, 28.3, 26.3, 26.1, 18.7, -3.7, -4.6.

MS (FAB NBA): m/z (%): 298.1 (35), 282.1 (17), 240.1 (100), 166.0 (34), 73.0 (26).

Intermediate *R*-**130b**: (*R*)-2-chloro-5,6,7,8-tetrahydroquinolin-8-ol

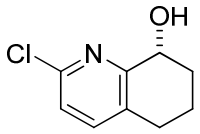

Synthesized by general method B from hydrolysis of the ester after chromatography (2 X 15 cm silica gel, dry load) and enantio enrichment by recrystallization of the parent ester (432 mg, 1.92 mmol, 97% ee) from 7 mLs of hot hexane cooled to -20 ˚C overnight. Enriched ester was hydrolyzed under identical conditions to the racemate, resulting in 300 mg (1.64 mmol, 36% yield) in 99% enantioselectivity.

$[\alpha]_D^{20}$ = -88 at a concentration of 0.71.

Intermediate *S*-**130b**: (S)-2-chloro-5,6,7,8-tetrahydroquinolin-8-ol

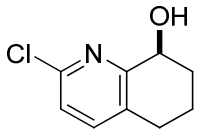

Produced by general method A except the silyl ether formation was omitted and the resulting alcohol was purified by chromatography (1 X 7 cm silica gel, dry load), 20% ethyl acetate in hexane to yield 18 mg (98.4 μmol, 36% yield) in 99% ee.

$[\alpha]_D^{20}$ = +90.5 at a concentration of 0.54.

5.9 Synthesis of 2-diarylphophorylmethyl-2-phenyl-cycloalkylpyridines and attempted complexation with Iridium.

5.9.1 Formation of methanol intermediates from addition of lithium metalated pyridines and carbonyl reagents.

Intermediate **125**: (2-Phenyl-5,6,7,8-tetrahydroquinolin-8-yl)methanol

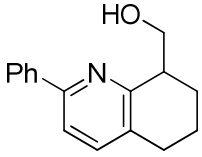

2-Phenyl-5,6,7,8-tetrahydroquinoline (**113b**), (3.3 g, 15.7 mmol) was added to a flame dried Schlenk flask under argon and absolute THF (50 mL) was introduced via syringe. The flask was cooled to -78 ˚C and *n*-butyl lithium (10.8 mL, 17.36 mmol) 1.6 M in hexane was added dropwise over 15 minutes. The reaction was stirred for 1 hour at this temperature and paraformaldehyde (707 mg, 23.6 mmol) was added under argon. The reaction was allowed to warm to room temperature over three hours, during which time most of the solid paraformaldehyde dissolved into the reaction mixture. The reaction was quenched with saturated ammonium chloride (100 mL) and stirred overnight in the slightly acidic solution to assist in breaking up formaldehyde oligamers. The mixture was poured into a large separatory funnel and ethyl acetate (200 mL) and water (500 mL) were added. The organic layer was washed with water (2 x 500 mL), brine (2 x 100 mL), dried over magnesium sulfate, filtered and concentrated to dryness. The crude material was purified by chromatography (3.5 X 15 cm silica gel, dry load) using a gradient of ethyl acetate hexane from 0 to 50% to elute the pure product in 61% yield as an off white solid (2.28 g, 9.60 mmol).

Chemical Formula: $C_{16}H_{17}NO$ Molecular Weight: 239.3

^{1}H NMR (400 MHz, $CDCl_3$) δ 7.90 – 7.86 (m, 2H), 7.55 – 7.43 (m, 4H), 7.43 – 7.37 (m, 1H), 6.26 (s, 1H), 4.08 – 3.54 (m, 2H), 3.11 (dq, *J* = 15.0, 4.9 Hz, 1H), 2.94 – 2.68 (m, 2H), 2.13 – 1.89 (m, 2H), 1.91 – 1.66 (m, 1H), 1.59 – 1.33 (m, 1H).

Diphenyl(2-phenyl-6,7-dihydro-5H-cyclopenta[b]pyridin-7-yl)methanol

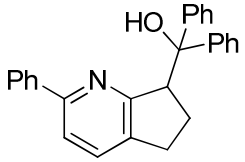

2-Phenyl-6,7-dihydro-5H-cyclopenta[1]pyridine (990 mg, 5.07 mmol) was added to a flame dried Schlenk flask under argon and absolute THF (20 mL) was introduced via syringe. The flask was cooled to -78 ˚C and N-butyl lithium (3.17 mL, 5.07 mmol) 1.6 M in hexane was added dropwise over 15 minutes. The reaction was stirred for 1 hour at this temperature and benzophenone (922 mg, 5.07 mmol) was added under argon. The reaction was allowed to warm to room temperature over three hours, during which time most of the solid paraformaldehyde

dissolved into the reaction mixture. The reaction was quenched with saturated ammonium chloride (30 mL) and stirred 10 minutes in the slightly acidic solution. The mixture was poured into a separatory funnel and ethyl acetate (100 mL) and water (200 mL) were added. The organic layer was washed with water (2 x 100 mL), brine (2 x 50 mL), dried over magnesium sulfate, filtered and concentrated to dryness. The crude material was purified by by chromatography (3.5 X 15 cm silica gel, dry load) using ethyl acetate/ hexane of 5% to elute the pure product in 80% yield as an off white solid (1.53 g, 4.05 mmol).

Chemical Formula: $C_{27}H_{23}NO$ Molecular Weight: 377.5

^{1}H NMR (400 MHz, $CDCl_3$) δ 7.95 (d, *J* = 7.1 Hz, 2H), 7.55 (dd, *J* = 15.1, 7.7 Hz, 3H), 7.50 – 7.36 (m, 6H), 7.32 (t, *J* = 7.2 Hz, 1H), 7.16 – 7.00 (m, 6H), 4.32 (t, *J* = 7.6 Hz, 1H), 2.96 – 2.64 (m, 1H), 2.48 – 2.32 (m, 2H), 2.32 – 2.20 (m, 1H).

5.9.2 Chloromethylpyridine

Intermediate **126**: 8-(Chloromethyl)-2-phenyl-5,6,7,8-tetrahydroquinoline

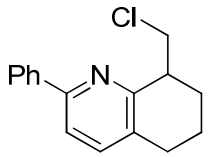

(2-Phenyl-5,6,7,8-tetrahydroquinolin-8-yl)methanol (**125**), (2.28 g, 9.54 mmol) was taken in 10 mL of DCM and 20 mL of thionyl chloride was added. The resulting solution was heated to reflux under an argon atmosphere for 2 hours. The reaction volatiles were removed by high vacuum with a liquid nitrogen trap attached with a short piece of chemically inert vacuum hose to catch the caustic by products and excess reagent. The resulting yellow oil was taken up in 100 mL of DCM and washed in a separatory funnel with saturated bicarbonate (2 x 50 mL), brine (2 x 50 mL), dried over magnesium sulfate, filtered and concentrated at the rotovap to yield the pure chloride in 95% yield (2.34 g, 9.08 mmol). The product slowly reacts with itself at room temperature and should be used immediately.

Chemical Formula: $C_{16}H_{16}ClN$ Molecular Weight: 257.8

^{1}H NMR (400 MHz, $CDCl_3$) δ 8.00 (dt, *J* = 3.2, 1.8 Hz, 2H), 7.52 (d, *J* = 8.0 Hz, 1H), 7.49 – 7.42 (m, 3H), 7.42 – 7.35 (m, 1H), 4.34 (dd, *J* = 10.5, 3.4 Hz, 1H), 4.02 (dd, *J* = 10.5, 8.7 Hz,

1H), 3.41 – 3.22 (m, 1H), 2.92 – 2.70 (m, 2H), 2.30 – 2.09 (m, 1H), 2.09 – 1.87 (m, 2H), 1.87 – 1.68 (m, 1H).

^{13}C NMR (101 MHz, $CDCl_3$) δ 156.2, 154.4, 139.8, 138.0, 131.9, 129.0, 127.1, 118.6, 49.4, 43.6, 29.3, 26.8, 20.9.

5.9.3 Formation of phosphine oxides

Intermediate **127**: 8-((Diphenylphosphoryl)methyl)-2-phenyl-5,6,7,8-tetrahydroquinoline

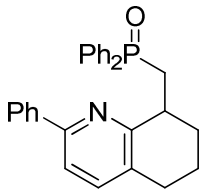

8-(Chloromethyl)-2-phenyl-5,6,7,8-tetrahydroquinoline (**126**), (500 mg, 1.94 mmol) was added to a dry Schlenk flask and placed under an inert atmosphere of argon. Absolute THF (10 mL) was added and the flask was cooled to 0 ˚C at which time commercially available potassium diphenylphosphide (1.95 mL, 1.95 mmol) was added via syringe and the reaction was allowed to warm up to room temperature overnight. The reaction was quenched with water (10 mL) and hydrogen peroxide (32%, 15 mL). The oxidation was allowed to stir for 4 hours with good mixing and the contents of the flask were transferred to a separatory funnel with 20 mLs of ethyl acetate. The organic layer was washed with water (2 x 50 mL), bicarbonate (1 x 25 mL), brine (2 x 50 mL), dried over magnesium sulfate, filtered and concentrated at the rotovap to yield the crude phosphine oxide which was purified by chromatography (2 X 15 cm silica gel, dry load) with a gradient elution of ethyl acetate/ hexane from 0 to 100% ethyl acetate, taking steps in polarity of 25%. Yield of 558 mg (1.32 mmol, 68%).

Chemical Formula: $C_{28}H_{26}NOP$ Molecular Weight: 423.5

^{1}H NMR (400 MHz, $CDCl_3$) δ 8.19 – 8.07 (m, 2H), 8.07 – 7.97 (m, 2H), 7.82 – 7.70 (m, 2H), 7.57 – 7.46 (m, 6H), 7.42 (dtd, *J* = 8.3, 7.3, 1.8 Hz, 5H), 3.69 (ddd, *J* = 15.4, 8.1, 1.7 Hz, 1H), 3.53 – 3.26 (m, 1H), 2.94 – 2.62 (m, 2H), 2.40 (ddd, *J* = 24.5, 15.9, 10.3 Hz, 2H), 2.08 – 1.94 (m, 1H), 1.94 – 1.82 (m, 1H), 1.80 – 1.67 (m, 1H).

^{31}P NMR (162 MHz, $CDCl_3$) δ 30.44 (d, *J* = 9.5 Hz).

Intermediate **127b**: 8-((Dio-tolylphosphoryl)methyl)-2-phenyl-5,6,7,8-tetrahydroquinoline

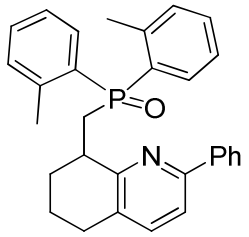

Under inert atmosphere conditions di-o-tolylphophine chloride (540 mg, 2.17 mmol) was added in absolute THF to pieces of sodium metal (99.9 mg, 4.34 mmol) in a young tube inside the glovebox. The reaction was capped, brought outside the box and heated to 70 ˚C for 5 hours. On heating the initial color was yellow with large amounts of sodium chloride precipitating. The solution darkened to a red color as the anion was formed. After most of the sodium had been consumed the reaction was cooled to room temperature and the solution was filtered into a Schlenk flask containing 8-(chloromethyl)-2-phenyl-5,6,7,8-tetrahydroquinoline (559 mg, 2.17 mmol) in absolute THF (10 mL). The reaction was allowed to stir for 5 hours. The reaction was quenched with water (10 mL) and hydrogen peroxide (32%, 15 mL). The oxidation was allowed to stir for 4 hours with good mixing and the contents of the flask were transferred to a separatory funnel with 20 mLs of ethyl acetate. The organic layer was washed with water (2 x 50 mL), bicarbonate (1 x 25 mL), brine (2 x 50 mL), dried over magnesium sulfate, filtered and concentrated at the rotovap to yield the crude phosphine oxide which was purified by chromatography (2 X 15 cm silica gel, dry load) with a gradient elution of ethyl acetate/ hexane from 0 to 100% ethyl acetate, taking steps in polarity of 25%. Yield of 637 mg (1.41 mmol, 65%). The product can be purified by semipreprative HPLC.

HPLC: Separated on a chiral ADH column with a mobile phase of 10% isopropanol in heptanes with a flow rate of 0.5 mLs/minute and 25˚C, T_1= 26.0 minutes, T_2 = 61.7 minutes. Semiprep conditions: chiral AD column with 10% isopropanol in heptanes with a flow rate of 6 mLs/minute and 25˚C, T_1= 51.0 minutes, T_2 = 121.4 minutes.

Chemical Formula: $C_{30}H_{30}NOP$ Molecular Weight: 451.5

^{1}H NMR (400 MHz, $CDCl_3$) δ 8.51 (dd, *J* = 12.1, 7.7 Hz, 1H), 8.09 – 7.97 (m, 2H), 7.80 – 7.67 (m, 1H), 7.51 (d, *J* = 7.9 Hz, 1H), 7.49 – 7.38 (m, 5H), 7.38 – 7.30 (m, 2H), 7.23 (dd, *J* = 10.6,

5.2 Hz, 2H), 7.17 (dd, *J* = 7.5, 4.1 Hz, 1H), 3.86 – 3.70 (m, 1H), 3.54 – 3.32 (m, 1H), 2.78 (tq, *J* = 16.8, 5.8 Hz, 2H), 2.48 (dt, *J* = 10.5, 5.5 Hz, 1H), 2.42 (d, *J* = 6.7 Hz, 6H), 2.10 – 1.98 (m, 1H), 1.98 – 1.85 (m, 1H), 1.75 (qdd, *J* = 11.1, 5.6, 2.8 Hz, 1H).

^{13}C NMR (101 MHz, $CDCl_3$) δ 154.4, 142.4 (d, *J* = 8.5 Hz), 141.7 (d, *J* = 8.5 Hz), 140.0, 138.14, 133.56 (d, *J* = 10.0 Hz), 126.0 (dd, *J* = 11.7, 7.3 Hz), 36.8, 34.8, 34.0, 30.6, 29.3, 25.7, 21.7 (dd, *J* = 14.4, 4.0 Hz), 21.0.

^{31}P NMR (162 MHz, $CDCl_3$) δ 32.57.

5.9.4 Phosphine oxide reduction and complexation

Intermediate **128**: 8-((diphenylphosphino)methyl)-2-phenyl-5,6,7,8-tetrahydroquinoline

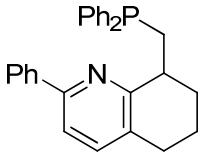

8-((Diphenylphosphoryl)methyl)-2-phenyl-5,6,7,8-tetrahydroquinoline (**127**), (65 mg, 0.153 mmol) was added to a young tube and phenylsilane (600 μL, 526.2 mg, 4.86 mmol) was added under argon and the contents were heated to 120 ˚C for 20 hours. The volatiles were removed by vacuum at 100 ˚C for several hours. The flask was allowed to come to room temperature and brought inside the box. Degassed silica gel (4 grams) was added with 20 mLs of absolute toluene and the slurry was stirred for 3 hours, the silica gel was filtered off and then washed with 5 mLs of absolute THF. The volatiles were then removed by vacuum outside the box and the resulting viscous glaze was brought back inside the box for manipulation into an NMR tube. The ^{1}H NMR and ^{31}P were taken in dry degassed $CDCl_3$ the phosphine was used immediately for complexation.

Chemical Formula: $C_{28}H_{26}NP$ Molecular Weight: 407.5

^{1}H NMR (400 MHz, $CDCl_3$) δ 7.96 (d, *J* = 7.4 Hz, 2H), 7.71 – 7.63 (m, 2H), 7.43 (dd, *J* = 6.7, 5.3 Hz, 2H), 7.41 – 7.11 (m, 11H), 3.16 (ddd, *J* = 13.9, 4.8, 3.1 Hz, 1H), 3.04 – 2.87 (m, 1H), 2.78 – 2.58 (m, 2H), 2.18 – 2.00 (m, 2H), 1.83 (ddt, *J* = 15.6, 8.6, 5.6 Hz, 2H), 1.71 – 1.53 (m, 1H).

^{31}P NMR (162 MHz, $CDCl_3$) δ -22.53.

Complex **123a**: Iridium(I) [(1,2,5,6-η)-1,5-cyclooctadiene][8-((diphenylphosphino-κ*P*)methyl)-2-phenyl-5,6,7,8-tetrahydroquinoline-κ*N*]-, hexafluorophosphate(-)

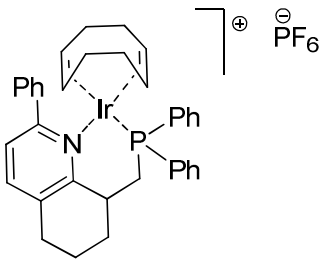

8-((Diphenylphosphino)methyl)-2-phenyl-5,6,7,8-tetrahydroquinoline (**128**), (50 mg, 0.123 mmol) was added to a Schlenk flask and dissolved in absolute DCM (4 mL). Chloro-1,5-cyclooctadiene iridium(I) dimer (41.2 mg, 61.4 μmol) was added under argon and the reaction was allowed to stir for 3 hours. Ammonium hexafluorophosphate was added (24 mg, 0.147 mmol) and the reaction stirred for 2 hours. The resulting slurry was filtered and the reaction concentrated to dryness at the rotovap, the resulting impure material was dried onto 500 mg of silica gel and chromatographed on a small column, ether to remove unreacted phosphine and then DCM to elute the product, yield 17.8 mg (20.9 μmol, 17%) as an orange solid. Recrystallized from 200 μL of DCM and 2 mL of pentane, suitable for Xray diffraction.
Chemical Formula: $C_{36}H_{38}F_6IrNP_2$ Molecular Weight: 852.8

^{1}H NMR (400 MHz, $CDCl_3$) δ 7.78 (d, *J* = 8.0 Hz, 1H), 7.73 (t, *J* = 7.4 Hz, 1H), 7.61 – 7.58 (m, 3H), 7.53 (d, *J* = 7.5 Hz, 3H), 7.48 (dd, *J* = 14.9, 4.6 Hz, 7H), 7.42 – 7.31 (m, 5H), 4.51 (t, *J* = 6.7 Hz, 1H), 4.33 (dd, *J* = 15.9, 9.5 Hz, 1H), 4.17 (t, *J* = 7.0 Hz, 1H), 3.18 – 3.08 (m, 1H), 2.95 (s, 2H), 2.52 (ddd, *J* = 14.8, 10.7, 5.9 Hz, 4H), 2.32 (ddd, *J* = 16.6, 13.4, 8.1 Hz, 2H), 1.99 (d, *J* = 6.3 Hz, 2H), 1.82 – 1.70 (m, 4H), 1.42 – 1.34 (m, 1H).

^{13}C NMR (101 MHz, $CDCl_3$) δ 160.2 (d, *J* = 54.7 Hz), 141.7, 139.2, 135.6, 133.3 (d, *J* = 11.2 Hz), 132.0 (d, *J* = 14.3 Hz), 131.2, 131.0 (d, *J* = 9.4 Hz), 130.25, 130.0 (d, *J* = 9.7 Hz), 129.60 (d, *J* = 10.1 Hz), 125.1, 124.5, 88.4 (d, *J* = 5.3 Hz), 68.7 (d, *J* = 84.9 Hz), 41.1 (d, *J* = 5.6 Hz), 36.3 (d, *J* = 4.9 Hz), 35.8, 32.16 (d, *J* = 14.0 Hz), 30.1, 29.8, 29.7, 29.5, 28.6, 23.9, 20.3.

^{19}F NMR (376 MHz, $CDCl_3$) δ -73.67, -75.57.

^{31}P NMR (162 MHz, $CDCl_3$) δ -0.11, -130.60 – -162.11 (m).

MS (MALDI): 708.2 (100%), 706.2 (57%), 709.2 (39%), 707.2 (23%), 710.2 (7.4%).

Complex **123b**: Attempted synthesis of Iridium(I) [(1,2,5,6-η)-1,5-cyclooctadiene][8-((diphenylphosphino-κP)methyl)-2-phenyl-5,6,7,8-tetrahydroquinoline-κN]-tetrakis[3,5-bis(trifluoromethyl)phenyl]borate(-)

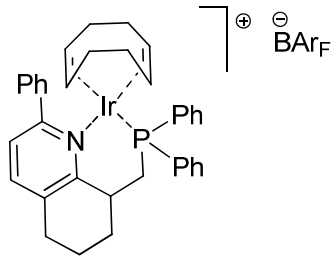

All manipulations for the next two steps were carried out in the glove box. 8-((Diphenylphosphino)methyl)-2-phenyl-5,6,7,8-tetrahydroquinoline (**123b**), (32 mg, 0.123 mmol) was added to a NMR tube with absolute deuterated DCM (0.5 mL). Chloro-1,5-cyclooctadiene iridium(I) dimer (26.4 mg, 39.3 μmol) was added and the tube was capped with a tight rubber 5 mm septum which was then fixed in place with copious amounts of parafilm. The resulting red solution was shaken thoroughly and allowed to react for 3 hours, after which time a proton and phosphorous NMR were obtained. A very peculiar proton spectrum indicated very broad peaks from which little structural information could be obtained. The phosphorous NMR indicated a 10 to 1 ratio of the expected resonance with a new resonance at 0 ppm.

^{1}H NMR (400 MHz, CD_2Cl_2) δ 8.07 – 7.98 (m, 1H), 7.91 (ddd, *J* = 9.9, 6.5, 3.2 Hz, 1H), 7.75 – 7.70 (m, 1H), 7.68 – 7.59 (m, 1H), 7.48 (d, *J* = 8.0 Hz, 1H), 7.39 (t, *J* = 7.5 Hz, 2H), 7.34 – 7.26 (m, 4H), 5.53 (ddd, *J* = 7.2, 5.2, 1.9 Hz, 1H), 5.22 (d, *J* = 1.0 Hz, 1H), 4.96 (s, 1H), 4.22 – 4.06 (m, 1H), 3.84 (t, *J* = 13.3 Hz, 1H), 3.51 (d, *J* = 12.3 Hz, 1H), 2.74 (dt, *J* = 10.8, 7.6 Hz, 1H), 2.62 (ddd, *J* = 14.7, 10.7, 5.8 Hz, 1H), 2.48 (d, *J* = 34.7 Hz, 1H), 2.40 – 2.30 (m, 1H), 2.25 – 1.99 (m, 3H), 1.82 (dd, *J* = 12.9, 6.5 Hz, 1H), 1.75 – 1.48 (m, 2H), 1.45 (d, *J* = 9.3 Hz, 1H), 1.41 (s, 3H), 1.25 (dd, *J* = 9.9, 5.6 Hz, 1H), 1.18 (s, 1H), 0.99 (s, 1H), 0.88 – 0.78 (m, 1H).

^{31}P NMR (162 MHz, CD_2Cl_2) δ 11.48, -0.34.

The NMR tube was then brought back inside the box, the parafilm was cut from the tube with a sharp scissors and the contents were poured into a vial with sodium tetrakis[3,5-bis(trifluoromethyl)phenyl]borate dissolved in 0.6 mLs of deuterated DCM. The resulting solution was filtered through a micronfilter into a NMR tube. The tube was capped and sealed with parafilm and a proton and phosphorous NMR were obtained. The phosphorous NMR indicated that the new peak at 0 ppm was the sole species. Attempts at chromatography (pipette column 2 cc silica gel) resulted in loss of almost all mass, resulting in 2 mg of orange material which did not match any of the crude intermediate spectra.

^{1}H NMR (400 MHz, CD_2Cl_2) δ 7.72 (s, 1H), 7.56 (dd, *J* = 24.3, 11.8 Hz, 1H), 7.44 (s, 1H), 7.29 (d, *J* = 7.9 Hz, 1H), 4.51 (s, 1H), 4.29 (s, 1H), 4.08 (s, 1H), 3.22 (s, 1H), 3.16 – 3.09 (m, 1H), 2.82 (d, *J* = 5.7 Hz, 1H), 2.69 (t, *J* = 13.5 Hz, 1H), 2.59 – 2.52 (m, 1H), 2.41 (dd, *J* = 19.6, 7.3 Hz, 1H), 2.29 – 2.15 (m, 1H), 2.03 – 1.83 (m, 1H), 1.81 – 1.68 (m, 1H), 1.61 (s, 1H), 1.50 (s, 1H), 1.40 – 1.23 (m, 1H), 1.19 (s, 1H), 1.09 (d, *J* = 8.8 Hz, 1H), 0.86 (s, 1H).

^{31}P NMR (162 MHz, CD_2Cl_2) δ -0.34.

5.10 Suzuki reaction of hindered boronic acids and esters with 2-chloropyridine-O-terbutyldimethylsilyl ether derivatives

General procedure A: 2-Chloropyridine-O-TBDMS ether (100 mg, 0.336 mmol), boronic acid (0.672 mmol), and Nolan NHC catalyst (8.6 mg, 13.7 μmol, 4 mol%) were added to a 5 mL microwave tube with a stir bar, the tube was sealed with a microwave septum and the contents were thoroughly purged with 2 bars of argon through a needle inlet/outlet for 15 minutes. Sodium tert-butoxide (0.29 M, 2.5 mL, 0.725 mmol) was added under purge. The purge needles were removed and the contents of the flask were pulverized with a sonicator for 15 minutes. The reaction was stirred at 50 ˚C for 24 hours. The reaction was worked up by extraction with DCM (25 mL) and water (2 x 25 mL), followed by brine (1 x 25 mL). The organic layer was dried over magnesium sulfate, filtered and concentrated at the rotovap to provide crude product which was purified by column chromatography (1 X 10 cm silica gel, dry load) with a hexane/ DCM gradient starting from pure hexane and working in 20% change in solvent every 2 column lengths. Product typically elutes in the 40-60% range of DCM while the byproduct from protonation of the boronic acid reagent comes earlier.

General procedure B: 2-Chloropyridine-O-TBDMS ether (100 mg, 0.336 mmol), boronic acid (1.08 mmol), and Nolan NHC catalyst (8.6 mg, 13.7 μmol, 4 mol%) were added to a 20 mL microwave tube with a stir bar, the tube was sealed with a microwave septum and the contents were thoroughly purged with 2 bars of argon through a needle inlet/outlet for 15 minutes. Isopropanol was degassed by bubbling argon through the solvent in a septumed flask with needles and with stirring for 20 minutes, 10.0 mL was added to the microwave tube by syringe and the contents were sonicated with stirring for 20 minutes. Thoroughly degassed (as for the isopropanol) aqueous sodium hydroxide (4.0 M, 500 μL, 2.0 mmol) was added under purge. The purge needles were removed and the contents of the flask were pulverized with a sonicator for 5 minutes. The reaction was stirred at 50 ˚C for 24 hours. The reaction was worked up by extraction with DCM (50 mL) and water (2 x 50 mL), followed by brine (1 x 50 mL). The organic layer was dried over magnesium sulfate, filtered and concentrated at the rotovap to provide crude product which was purified by column chromatography (1 X 10 cm silica gel, dry load) with a hexane/ ethyl acetate gradient starting from pure hexane and working in 15% change in solvent every 2 column lengths until 75% ethyl acetate is reached.

General procedure C: 2-Chloropyridine-O-TBDMS ether (315 mg, 1.06 mmol), boronic acid (2.12 mmol), and Nolan NHC catalyst (27 mg, 42.4 μmol, 4 mol%) were added to a 20 mL microwave tube with a stir bar, the tube was sealed with a microwave septum and the contents were thoroughly purged with 2 bars of argon through a needle inlet/outlet for 15 minutes. Isopropanol was degassed by bubbling argon through the solvent in a septumed flask with needles and with stirring for 20 minutes, 14.0 mL was added to the microwave tube by syringe and the contents were sonicated with stirring for 20 minutes. Thoroughly degassed (as for the isopropanol) aqueous sodium hydroxide (4.0 M, 795 μL, 3.18 mmol) was added under purge. The purge needles were removed and the contents of the flask were pulverized with a sonicator for 5 minutes. The reaction was stirred at 50 ˚C for 24 hours. The reaction was worked up by extraction with DCM (100 mL) and water (2 x 100 mL), followed by brine (1 x 100 mL). The organic layer was dried over magnesium sulfate, filtered and concentrated at the rotovap to provide crude product which was purified by column chromatography (2 X 16 cm silica gel, dry load) with a hexane/ DCM gradient starting from pure hexane and working in 20% change in solvent every 2 column lengths until pure DCM is reached.

Intermediate **143i-**OTBDMS: 7-(Tert-butyldimethylsilyloxy)-2-(2-fluorophenyl)-4-methyl-6,7-dihydro-5H-cyclopenta[b]pyridine

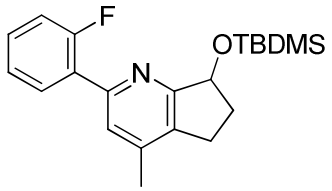

Synthesized by general procedure A. Yield 110mg (0.309 mmol, 92%).

Chemical Formula: $C_{21}H_{28}FNOSi$ Molecular Weight: 357.5

^{1}H NMR (400 MHz, $CDCl_3$) δ 8.11 (td, *J* = 7.9, 1.9 Hz, 1H), 7.51 (d, *J* = 2.1 Hz, 1H), 7.33 (dddd, *J* = 8.1, 7.0, 4.9, 1.9 Hz, 1H), 7.26 – 7.21 (td, *J* = 7.9, 1.9 Hz, 1H), 7.12 (ddd, *J* = 11.6, 8.1, 1.2 Hz, 1H), 5.24 (dd, *J* = 7.1, 4.9 Hz, 1H), 3.01 (ddd, *J* = 16.2, 8.7, 5.0 Hz, 1H), 2.80 – 2.68 (m, 1H), 2.45 (dddd, *J* = 13.4, 8.5, 7.1, 5.0 Hz, 1H), 2.31 (s, 3H), 2.12 – 2.00 (m, 1H), 0.99 – 0.96 (m, 9H), 0.28 – 0.24 (m, 3H), 0.20 – 0.18 (m, 3H).

^{13}C NMR (101 MHz, $CDCl_3$) δ 164.5, 162.2, 159.7, 152.4, 144.0, 134.8, 131.6 (d, *J* = 3.1 Hz), 130.1 (d, *J* = 8.5 Hz), 129.5, 128.6, 128.3 (d, *J* = 11.5 Hz), 124.8, 124.7, 116.4 (d, *J* = 23.5 Hz), 76.8, 34.2, 26.4, 26.3, 19.2, 19.00, -3.8, -4.2.
^{19}F NMR (376 MHz, $CDCl_3$) δ -117.91.

MS (FAB NBA): m/z (%): 359.1 (20), 358.1 (100), 357.1 (9), 301.1 (24), 300.1 (96), 299.0 (6.4), 227.1 (21), 226.1 (93), 225.0 (11).

Intermediate ***rac*-143e**-OTBDMS: 7-(Tert-butyldimethylsilyloxy)-4-methyl-2-(naphthalen-2-yl)-6,7-dihydro-5H-cyclopenta[b]pyridine

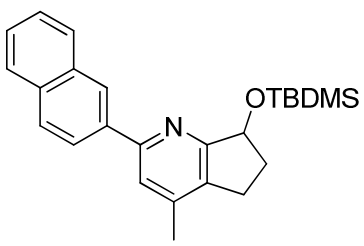

Synthesized by general method A. Yield 127 mg (0.326 mmol, 97%) as an oil.

Chemical Formula: $C_{25}H_{31}NOSi$ Molecular Weight: 389.6

^{1}H NMR (500 MHz, $CDCl_3$) δ 8.54 (s, 1H), 8.24 (dd, *J* = 8.6, 1.7 Hz, 1H), 7.92 (d, *J* = 8.3 Hz, 2H), 7.89 – 7.82 (m, 1H), 7.58 (s, 1H), 7.54 – 7.43 (m, 2H), 5.28 (dd, *J* = 7.1, 5.3 Hz, 1H), 3.02 (ddd, *J* = 16.0, 8.7, 4.7 Hz, 1H), 2.82 – 2.67 (m, 1H), 2.59 – 2.42 (m, 1H), 2.35 (s, 3H), 2.14 – 1.97 (m, 1H), 1.02 (s, 9H), 0.30 (s, 3H), 0.25 (s, 3H).

^{13}C NMR (126 MHz, $CDCl_3$) δ 164.6, 156.5, 144.3, 137.6, 134.6, 133.9, 133.8, 129.0, 128.5, 128.0, 126.5, 126.4, 126.3, 125.2, 120.8, 76.8, 34.3, 26.4, 26.2, 19.2, 19.1, -3.89, -4.1.

Intermediate *rac*-**143f**-OTBDMS: 2-(Anthracen-9-yl)-7-(tert-butyldimethylsilyloxy)-4-methyl-6,7-dihydro-5H-cyclopenta[b]pyridine

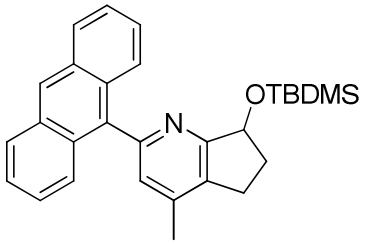

Produced by general method A. Yield 125 mg (2.85 mmol, 85%) as a high viscosity oil.

Chemical Formula: $C_{29}H_{33}NOSi$ Molecular Weight: 439.7

^{1}H NMR (500 MHz, $CDCl_3$) δ 8.51 (s, 1H), 8.02 (t, *J* = 9.6 Hz, 2H), 7.80 (d, *J* = 8.8 Hz, 1H), 7.70 (d, *J* = 8.8 Hz, 1H), 7.49 – 7.40 (m, 2H), 7.38 – 7.30 (m, 2H), 7.16 (d, *J* = 8.0 Hz, 1H), 5.28 (dd, *J* = 6.6, 3.0 Hz, 1H), 3.27 – 3.12 (m, 1H), 2.94 – 2.82 (m, 1H), 2.48 (ddt, *J* = 13.5, 8.6, 6.7 Hz, 1H), 2.37 (s, 3H), 2.24 – 2.13 (m, 1H), 0.90 (d, *J* = 5.7 Hz, 9H), 0.14 (s, 3H), 0.08 (d, *J* = 5.9 Hz, 3H).

^{13}C NMR (126 MHz, $CDCl_3$) δ 165.0, 156.9, 143.9, 136.3, 134.9, 131.9, 131.8, 130.7, 130.5, 128.8, 128.5, 127.6, 127.5, 127.3, 126.9, 125.7, 125.7, 125.5, 125.3, 76.9, 34.1, 26.8, 26.3, 22.7, 19.1, 18.8, 14.5, -3.8, -4.2.

IR (neat ,$\tilde{\nu}$): 2927, 2854, 1669, 1591, 1459, 1360, 1316, 1254, 1084, 1027, 1113, 881 cm^{-1}.

Intermediate ***S*-143e**-OTBDMS: (*S*)-7-(tert-butyldimethylsilyloxy)-4-methyl-2-(naphthalen-2-yl)-6,7-dihydro-5H-cyclopenta[b]pyridine

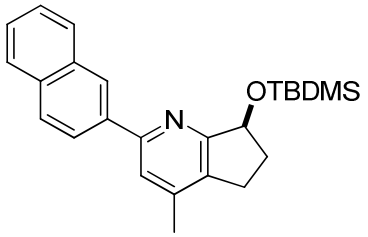

Synthesized by general method A with enantiopure 2-chloropyridine. All spectral properties matched those of the racemate. Yield 122 mg (0.313 mmol, 93%).

Intermediate ***S*-143f**-OTBDMS: (*S*)-2-(anthracen-9-yl)-7-(tert-butyldimethylsilyloxy)-4-methyl-6,7-dihydro-5H-cyclopenta[b]pyridine

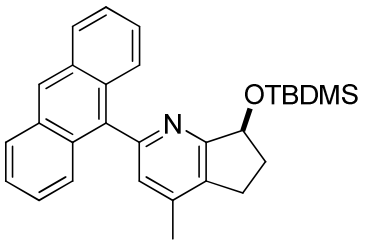

Synthesized by general method A with enantiopure S-2-chloropyridine. All spectral properties matched those of the racemate. Yield 139 mg (0.316 mmol, 94%) as an oil.

Intermediate ***rac*-150**-OTBDMS: 7-(tert-butyldimethylsilyloxy)-4-methyl-2-(2,3,5,6-tetramethylphenyl)-6,7-dihydro-5H-cyclopenta[b]pyridine

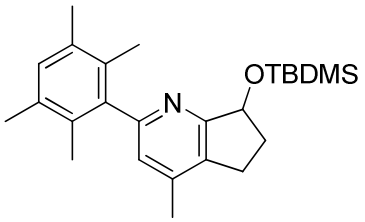

Synthesized by general method B with racemic 2-chloropyridine. Purified material readily crystallizes out of 1 mL of hexane. Yield 129 mg (0.326 mmol, 97%).

Chemical Formula: $C_{25}H_{37}NOSi$ Molecular Weight: 395.7

^{1}H NMR (500 MHz, $CDCl_3$) δ 6.99 (s, 1H), 6.62 (s, 1H), 5.22 – 5.09 (m, 1H), 4.69 (s, 1H), 3.03 – 2.87 (m, 1H), 2.74 – 2.57 (m, 1H), 2.41 (qd, *J* = 12.9, 5.9 Hz, 1H), 2.24 (d, *J* = 3.4 Hz, 9H), 2.15 (s, 6H), 2.09 – 1.99 (m, 1H), 0.95 (s, 9H), 0.23 (s, 3H), 0.18 (s, 3H).

^{13}C NMR (126 MHz, $CDCl_3$) δ 164.7, 152.1, 150.6, 146.8, 134.8, 134.6, 123.9, 123.7, 119.4, 76.2, 34.1, 26.3, 26.0, 24.9, 20.2, 18.8, 18.8, 12.0, -3.8, -4.3.

MS (FAB NBA): m/z (%): 397.1 (3), 396.2 (5), 395.1 (3).

Intermediate *rac*-**151**-OTBDMS: 7-(Tert-butyldimethylsilyloxy)-2-(2-isobutoxy-6-methoxyphenyl)-4-methyl-6,7-dihydro-5H-cyclopenta[b]pyridine

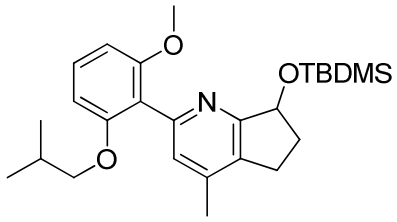

Synthesized by general method B with racemic 2-chloropyridine. Product is a clear high viscosity oil. Yield 100 mg (0.227 mmol, 67%).

Chemical Formula: $C_{26}H_{39}NO_3Si$ Molecular Weight: 441.7

^{1}H NMR (500 MHz, $CDCl_3$) δ 7.35 (t, *J* = 8.3 Hz, 1H), 7.10 (s, 1H), 6.71 (dd, *J* = 12.5, 8.4 Hz, 2H), 5.31 (dd, *J* = 6.3, 2.9 Hz, 1H), 3.82 (s, 3H), 3.75 (p, *J* = 8.9 Hz, 2H), 3.23 – 3.08 (m, 1H), 2.84 (ddd, *J* = 15.8, 8.5, 3.7 Hz, 1H), 2.45 (tt, *J* = 13.8, 6.9 Hz, 1H), 2.37 (s, 3H), 2.23 – 2.13 (m, 1H), 2.06 – 1.90 (m, 1H), 1.01 (s, 9H), 0.92 (dd, *J* = 15.6, 9.4 Hz, 6H), 0.29 (s, 3H), 0.17 (s, 3H).

^{13}C NMR (126 MHz, $CDCl_3$) δ 163.8, 158.8, 158.1, 153.2, 142.6, 134.1, 129.3, 126.5, 120.8, 105.8, 104.6, 77.0, 75.4, 56.3, 34.3, 28.5, 26.6, 26.3, 19.5, 19.4, 18.9, 18.7, -3.8, -4.2.

MS (FAB NBA): m/z (%): 442.1 (2), 441.1 (5), 386.1 (7), 385.1 (26), 384.1 (100).

Intermediate ***S*-143g-**OTBDMS: (S)-2-(anthracen-9-yl)-8-(tert-butyldimethylsilyloxy)-5,6,7,8-tetrahydroquinoline

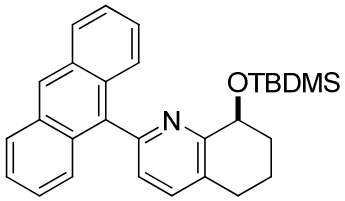

Synthesized by general method C with 550 mg (1.85 mmol) enantiopure (*S*)-8-(tert-butyldimethylsilyloxy)-2-chloro-5,6,7,8-tetrahydroquinoline. Product is a clear high viscosity oil. Yield 760 mg (1.73 mmol, 93%).

Chemical Formula: $C_{29}H_{33}NOSi$ Molecular Weight: 439.7

^{1}H NMR (500 MHz, $CDCl_3$) δ 8.52 (s, 1H), 8.04 (dd, *J* = 8.4, 2.9 Hz, 2H), 7.74 (d, *J* = 8.8 Hz, 1H), 7.66 (d, *J* = 8.8 Hz, 1H), 7.59 (d, *J* = 7.7 Hz, 1H), 7.45 (dd, *J* = 14.7, 7.2 Hz, 2H), 7.34 (dd, *J* = 13.9, 6.0 Hz, 2H), 7.30 (d, *J* = 7.7 Hz, 1H), 4.92 (s, 1H), 3.01 (dt, *J* = 16.8, 4.6 Hz, 1H), 2.94 – 2.80 (m, 1H), 2.25 (dd, *J* = 22.8, 18.1 Hz, 1H), 2.19 – 2.08 (m, 1H), 2.02 (dd, *J* = 24.7, 12.0 Hz, 1H), 1.86 (dd, *J* = 9.4, 3.5 Hz, 1H), 0.87 (s, 9H), 0.08 (d, *J* = 6.9 Hz, 3H), -0.06 (s, 3H).

^{13}C NMR (101 MHz, $CDCl_3$) δ 158.07, 155.46, 137.39, 136.15, 131.84, 131.77, 131.14, 130.59, 130.45, 128.80, 128.49, 127.55, 127.50, 126.79, 125.99, 125.76, 125.49, 125.31, 70.39, 32.72, 28.76, 26.28, 18.63, 17.88, -3.71, -4.45.

MS (FAB NBA+KCl): m/z (%): 442.1 (10), 441.1 (34), 440.1 (83), 439.1 (8), 384.1 (11), 383.1 (33), 382.1 (100).

IR (neat ,$\tilde{\nu}$): 2928, 2854, 1671, 1593, 1458, 1354, 1311, 1251, 1085, 1027, 881, 835, 776, 753 735 cm^{-1}

Elemental Analysis: calculated: C, 79.22; H, 7.57; N, 3.19 found: C, 79.09; H, 7.61; N, 3.01

Intermediate ***R*-143g-**OTBDMS: (*R*)-2-(anthracen-9-yl)-8-(tert-butyldimethylsilyloxy)-5,6,7,8-tetrahydroquinoline

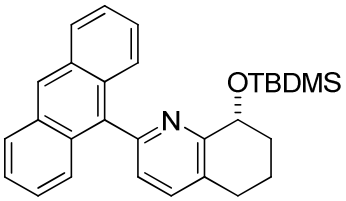

Synthesized by general method C with enantiopure (*R*)-8-(tert-butyldimethylsilyloxy)-2-chloro-5,6,7,8-tetrahydroquinoline. Product is a clear high viscosity oil. Yield 440 mg (1.00 mmol, 94%). Product matched the opposite enantiomer in perfect agreement in spectra and properties.

Chemical Formula: $C_{29}H_{33}NOSi$ Molecular Weight: 439.7

5.11 Sterically encumbered 2-arylpyridyl alcohols, racemates and enantiomers

General method A, cleavage of tert-butyldimethylsilyl ethers: The 2-arylpyridyl silyl ether (0.200 mmol) was taken up in 5 mL of dry THF and solid tetrabutylammonium fluoride trihydrate (195 mg, 0.600 mmol) was added and the reaction was heated to 50 ˚C for 4 hours. The reaction was monitored by TLC, if the conversion was incomplete and additional amount of TBAF was added and the heating continued (100 mg, 0.307 mmol). The heating was stopped when full conversion was achieved by pouring the reaction after cooling to room temperature into an appropriately sized separatory funnel, addition and washing of the flask into the funnel with 25 mLs of ethyl acetate and extraction with water (3 x 30 mL). The organic layer was washed with brine (2 x 25 mL), dried over). The organic layer was dried over magnesium sulfate, filtered and concentrated at the rotovap to provide the pure product.

General method B: The parent acetate ester (0.565 mmol) was deprotected by placing of the starting material into an oven dried round bottom flask with 10 mL of THF with 1 mL of 4M sodium hydroxide. The reaction was heated to 65 ˚C at a high rate of mixing and the reaction was monitored with TLC. When the starting material was completely consumed the reaction was diluted with ethyl acetate (20 mLs) and transferred to a separatory funnel. The organic layer was washed with water (2 x 20 mL) and the aqueous layer was back extracted with ethyl acetate (5 mL). The organic layer was washed with brine (2 x 20 mL), dried over magnesium sulfate,

filtered and concentrated at a rotovap to yield the product. If further purification was necessary the product was chromatographed (1 X 10 cm silica gel, dry load) with ethyl acetate/ hexane 1:4.

Intermediate *S*-**143a**: (*S*)-2-mesityl-4-methyl-6,7-dihydro-5H-cyclopenta[b]pyridin-7-ol

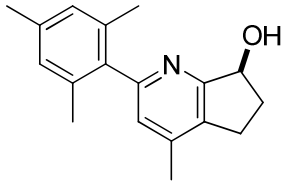

Synthesize by general method B from 165 mg of the S ester to yield 135 mg (0.505 mmol, 89%) of product after chromatography (1 X 10 cm silica gel, dry load) with 20% ethyl acetate to remove trace impurities.

Chemical Formula: $C_{18}H_{21}NO$ Molecular Weight: 267.4

^{1}H NMR (500 MHz, $CDCl_3$) δ 6.91 (s, 2H), 6.88 (s, 1H), 5.38 – 4.97 (m, 1H), 3.77 (s, 1H), 2.96 (ddd, *J* = 16.1, 9.1, 3.9 Hz, 1H), 2.86 – 2.66 (m, 1H), 2.61 – 2.42 (m, 1H), 2.31 (d, *J* = 5.9 Hz, 6H), 2.12 – 1.78 (m, 7H).

^{13}C NMR (126 MHz, $CDCl_3$) δ 164.4, 158.9, 144.5, 137.9, 137.6, 136.2, 133.7, 128.5, 124.9, 75.3, 32.5, 26.2, 21.4, 20.6, 19.0.

MS (e.i. 70 eV): m/z (%) 268.2 (7), 267.2 (37), 266.2 (48), 250.2 (5), 249.2 (22), 248.2 (100), 235.2 (2), 234.2 (11), 233.1 (10), 232.1 (6).

Elemental Analysis: for $C_{18}H_{21}NO$ calculated C, 80.86; H, 7.92; N, 5.24; found C, 79.20; H, 7.70; N, 4.55.

Intermediate *rac*-**143b**: 2-Mesityl-5,6,7,8-tetrahydroquinolin-8-ol

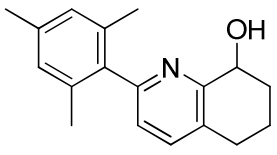

Synthesized by taking the racemic ester (100 mg, 0.323 mmol) in 20 mL of dry methanol and adding 1 gram of very finely divided potassium carbonate to a stirred mixture. Extractive workup

with 50 mL of DCM and 50 mL of water, separated and the organic layer was dried over magnesium sulfate, filtered and concentrated resulting in 85 mg (0.323 mmol) of product.

Chemical Formula: $C_{18}H_{21}NO$ Molecular Weight: 267.4

^{1}H NMR (400 MHz, $CDCl_3$) δ 7.48 (d, *J* = 7.8 Hz, 1H), 7.06 (d, *J* = 7.8 Hz, 1H), 6.96 (s, 2H), 4.72 (dd, *J* = 14.1, 8.5 Hz, 1H), 4.13 (s, 1H), 2.98 – 2.77 (m, 2H), 2.45 – 2.24 (m, 4H), 2.03 (d, *J* = 15.4 Hz, 7H), 1.94 – 1.76 (m, 2H).

Intermediate *rac*-**143h**: 4-Methyl-2-(piperidin-1-yl)-6,7-dihydro-5H-cyclopenta[b]pyridin-7-ol

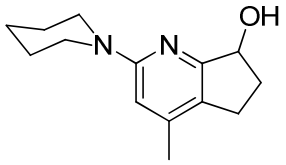

Synthesized from the racemic 2-chloro-4-methyl-6,7-dihydro-5H-cyclopenta[b]pyridin-7-ol (**130a**), (134 mg, 0.732 mmol) placed in a microwave tube with potassium carbonate (500 mg, 3.62 mmol) and piperdine (500 mg, 5.88 mmol) and DMF was added (10 mL). The tube was capped and microwaved at 200 ˚C for 20 minutes. The reaction was worked up by transferring the contents to a separatory funnel with 50 mL of ethyl acetate and extracting with water (3 x 100 mL), brine (50 mL), drying over magnesium sulfate, filtration, and concentration of the crude product onto silica gel for column chromatography. Chromatographed (1 X 10 cm silica gel, dry load) with 20% ethyl acetate hexane to yield 88 mg (0.379 mmol, 52%) of pure product.

The enantiomers were separated on the AD column with a flow of 6 mL/min and polarity of 20% isopropanol in hexane at room temp, T_s = 22 min and T_r = 50 min.

Chemical Formula: $C_{14}H_{20}N_2O$ Molecular Weight: 232.3

^{1}H NMR (500 MHz, $CDCl_3$) δ 6.37 (s, 1H), 5.02 (t, *J* = 6.7 Hz, 1H), 3.47 (d, *J* = 5.4 Hz, 4H), 2.81 (ddd, *J* = 15.2, 9.0, 3.4 Hz, 1H), 2.67 – 2.56 (m, 1H), 2.56 – 2.43 (m, 1H), 2.18 (d, *J* = 8.0 Hz, 3H), 1.93 (ddt, *J* = 13.1, 9.0, 6.7 Hz, 1H), 1.62 (s, 6H).

^{13}C NMR (126 MHz, $CDCl_3$) δ 162.0, 161.2, 145.6, 124.4, 107.6, 75.7, 47.4, 33.0, 25.9, 25.6, 25.1, 19.5.

Intermediate *S*-**143b**: (*S*)-2-mesityl-5,6,7,8-tetrahydroquinolin-8-ol

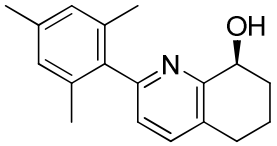

Synthesized by general method B from 158 mg (0.511 mmol) ester. Yield 129 mg (0.482 mmol, 94%).

Chemical Formula: $C_{18}H_{21}NO$ Molecular Weight: 267.4

^{1}H NMR (500 MHz, $CDCl_3$) δ 7.47 (d, *J* = 7.8 Hz, 1H), 7.06 (d, *J* = 7.8 Hz, 1H), 6.95 (s, 2H), 4.72 (t, *J* = 6.9 Hz, 1H), 4.08 (s, 1H), 3.00 – 2.76 (m, 2H), 2.34 (d, *J* = 10.0 Hz, 4H), 2.05 (d, *J* = 13.4 Hz, 7H), 1.98 – 1.75 (m, 2H).

^{13}C NMR (126 MHz, $CDCl_3$) δ 158.1, 157.1, 138.0, 137.9, 137.5, 136.3, 129.5, 128.8, 123.8, 69.4, 30.9, 28.5, 21.5, 20.7, 20.1.

MS (e.i. 70 eV): m/z (%) 268.2 (8), 267.2 (38), 266.2 (39), 250.2 (8), 249.2 (28), 248.2 (100), 235.2 (2), 234.2 (10), 233.1 (6), 232.1 (6).

$[\alpha]_D^{20}$ = +57.4 at a concentration of 0.51.

Elemental Analysis: for $C_{18}H_{21}NO$ calculated C, 80.86; H, 7.92; N, 5.24; found C, 80.75; H, 7.93; N, 5.00.

Intermediate *S*-**143f**: (*S*)-2-(Anthracen-9-yl)-4-methyl-6,7-dihydro-5H-cyclopenta[b]pyridin-7-ol

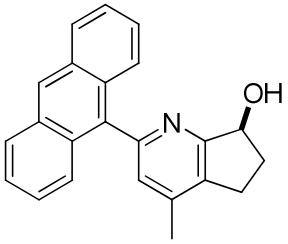

Synthesized by method B from 94 mg (0.214 mmol) of TBDMS ether. Yield after chromatography using 5% ether in DCM is 55 mg (0.169 mmol, 79%).

Chemical Formula: $C_{23}H_{19}NO$ Molecular Weight: 325.4

^{1}H NMR (500 MHz, $CDCl_3$) δ 8.52 (s, 1H), 8.04 (dd, *J* = 8.5, 3.0 Hz, 2H), 7.66 – 7.52 (m, 2H), 7.50 – 7.40 (m, 2H), 7.38 – 7.33 (m, 1H), 7.33 – 7.29 (m, 1H), 7.18 (s, 1H), 5.24 (t, *J* = 6.3 Hz, 1H), 4.04 – 3.53 (m, 1H), 3.10 – 2.92 (m, 1H), 2.87 – 2.71 (m, 1H), 2.46 (dd, *J* = 19.2, 14.7 Hz, 1H), 2.36 (s, 3H), 2.04 – 1.88 (m, 1H).

^{13}C NMR (126 MHz, $CDCl_3$) δ 164.9, 156.9, 144.7, 135.4, 134.7, 131.7, 130.6, 130.5, 128.8, 128.7, 127.7, 127.1, 126.6, 126.5, 126.0, 125.4, 125.3, 75.3, 32.4, 26.3, 19.0.

Intermediate ***S*-143e**: (*S*)-4-methyl-2-(naphthalen-2-yl)-6,7-dihydro-5H-cyclopenta[b]pyridin-7-ol

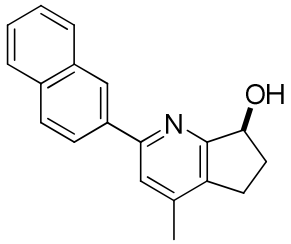

Synthesized by general method A except using 40 mg (0.103 mmol) of starting silyl ether and producing 25.1 mg of alcohol (91.2 μmol, 89%).

Chemical Formula: $C_{19}H_{17}NO$ Molecular Weight: 275.3

^{1}H NMR (400 MHz, $CDCl_3$) δ 8.44 (s, 1H), 8.11 (dd, *J* = 8.6, 1.8 Hz, 1H), 7.96 – 7.89 (m, 2H), 7.86 (dd, *J* = 5.2, 4.2 Hz, 1H), 7.55 (s, 1H), 7.53 – 7.46 (m, 2H), 5.29 (dd, *J* = 7.2, 6.1 Hz, 1H), 3.27 (s, 1H), 3.00 (ddd, *J* = 16.2, 9.0, 3.9 Hz, 1H), 2.89 – 2.68 (m, 1H), 2.68 – 2.48 (m, 1H), 2.35 (s, 3H), 2.20 – 1.98 (m, 1H).

Intermediate ***S*-143g**: (*S*)-2-(anthracen-9-yl)-5,6,7,8-tetrahydroquinolin-8-ol

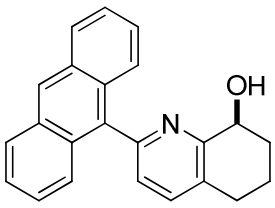

Synthesized by general method A except using 700 mg (1.59 mmol) of the silyl ether, 2 g (6.36 mmol) of tetrabutyl ammonium fluoride trihydrate in 50 mL of absolute THF and stirring for 18 hours under argon followed by heating to 60 ˚C for 2 hours to remove the last traces of starting material. A trace of the *R* enantiomer was present in the HPLC so the product was purified by fractional recrystallization from toluene (500 mg in 20 mL). Scalemic product crystallizes while enantiopure remains in solution. Yield of enantiopure 350 mg (1.07 mmol, 68%). X-ray quality crystals were grown from 300 mg in 12 mls of boiling isopropanol followed by cooling to -20˚C overnight for quantitative return of material.

HPLC conditions: ODH column, 30% isopropanol in heptanes with a flow rate of 0.5 mLs/min and a temperature of 25 ˚C. Elution times T_S = 9 minutes and T_R = 18minutes.

Chemical Formula: $C_{23}H_{19}NO$ Molecular Weight: 325.4

^{1}H NMR (400 MHz, $CDCl_3$) δ 8.55 (s, 1H), 8.06 (d, *J* = 8.4 Hz, 2H), 7.64 (t, *J* = 8.4 Hz, 2H), 7.59 (d, *J* = 8.8 Hz, 1H), 7.48 (dd, *J* = 17.6, 10.5 Hz, 2H), 7.42 – 7.31 (m, 3H), 4.84 (t, *J* = 7.0 Hz, 1H), 3.98 (s, 1H), 3.23 – 2.82 (m, 2H), 2.56 – 2.28 (m, 1H), 2.29 – 2.06 (m, 1H), 2.06 – 1.85 (m, 2H).

^{13}C NMR (101 MHz, $CDCl_3$) δ 158.6, 155.5, 137.6, 135.2, 131.8, 130.6, 130.5, 130.4, 128.9, 128.8, 127.9, 126.6, 126.4, 126.3, 126.2, 126.0, 125.6, 125.5, 69.4, 31.0, 28.7, 20.0.

MS (e.i. 70 eV): m/z (%) 327.1 (3), 326.1 (23), 325.1 (100), 324.1 (73), 309.1 (3), 308.1 (19), 307.1 (68), 306.1 (82), 305.1 (5), 304.1 (10), 297.1 (2), 296.1 (7), 294.1 (5),.

$[\alpha]_D^{20}$ = +4.0 at a concentration of 1.10.

Intermediate ***R*-143g**: (*R*)-2-(anthracen-9-yl)-5,6,7,8-tetrahydroquinolin-8-ol

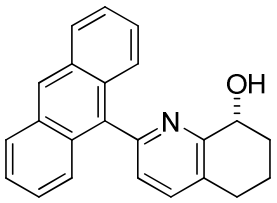

Synthesized by general method A except using 420 mg (0.957 mmol) of the silyl ether, 3 g (9.5 mmol) of tetrabutyl ammonium fluoride trihydrate in 50 mL of absolute THF and heating to 60 ˚C for 6 hours. Fractional recrystallization from 12 mL of toluene to precipitate the scalemic product yields the enantiopure product in the remaining solvent, 268 mg (0.824 mmol, 86%). The product matched the opposite enantiomer in its spectral and physical properties.

HPLC conditions: ODH column, 30% isopropanol in heptanes with a flow rate of 0.5 mLs/min and a temperature of 25 ˚C Elution times T_s = 9 minutes and T_r = 18.

Chemical Formula: $C_{23}H_{19}NO$ Molecular Weight: 325.4

5.12 Phosphonite formation and iridium complexation

General method: Pyridyl alcohol (87.9 μmol) and DMAP (10.7 mg, 87.9 μmol) were added to a 4 mL vial with a small stir bar. The vial was loosely capped and brought inside the box. Absolute THF (500 μL) was added to the vial and the contents were stirred into solution. Chlorodiphenylphosphine (19.4 mg, 87.9 μmol) was weighed into a separate vial and (500 μL) was added. The solution was transferred to the stirring mixture of DMAP and pyridyl alcohol with a syringe and the contents of the vial and syringe were washed into the reaction mixture with THF (3 x 250 μL). An immediate white precipitate was formed on addition of the chlorophosphine and the reaction was stirred for 30 minutes. The slurry was filtered through a small pipette plug of silica and the silica washed with an additional THF (2 x 1 mL) into a young tube with a stir bar. The tube was sealed, brought outside the box and the volatiles were removed on a Schlenk line. Absolute DCM (5 mL) was added to the tube under argon followed by solid iridium(I), bis[(1,2,5,6-η)-1,5-cyclooctadiene]-, tetrakis[3,5-bis(trifluoromethyl)phenyl]borate) (112.7 mg, 88.6 μmol). The tube is sealed and resulting solution is stirred for 2.5 hours at 45 ˚C. The reaction is then cooled and the contents are rotary evaporated onto silica, loaded onto a column (1 X 10 cm silica gel, dry load) prepared with hexane and chromatographed with the appropriate combination of ether/hexane and then DCM. The resulting red solids are recrystallized from DCM/ hexane to obtain solid X-ray quality crystals.

Complex *S*-**108a**: Iridium(I) [(1,2,5,6-η)-1,5-cyclooctadiene][(*S*)-7-(diphenylphosphinooxy-κ*P*)-4-methyl-2-(naphthalen-2-yl)-6,7-dihydro-5H-cyclopenta[b]pyridine-κ*N*]-tetrakis[3,5-bis(trifluoromethyl)phenyl]borate(-)

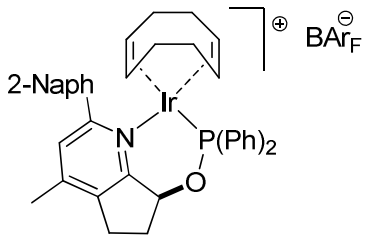

Synthesized by the general method to yield 107 mg (65.9 μmol, 73%). Chromatographed (1 X 10 cm silica gel, dry load) with 30% ether in hexane to remove byproducts, 50% DCM hexane and final elution with pure DCM.

Chemical Formula: $C_{71}H_{50}BF_{24}IrNOP$ Molecular Weight: 1623.1

MP: 198-200 ˚C

^{1}H NMR (500 MHz, $CDCl_3$) δ 8.21 (s, 1H), 7.95 – 7.82 (m, 3H), 7.71 – 7.62 (m, 11H), 7.62 – 7.54 (m, 2H), 7.51 – 7.44 (m, 3H), 7.42 (s, 4H), 7.41 – 7.32 (m, 6H), 6.40 – 6.22 (m, 1H), 4.48 (s, 1H), 4.22 (s, 1H), 3.01 (dddd, J = 17.3, 14.1, 9.2, 2.4 Hz, 2H), 2.86 (ddt, J = 24.3, 16.0, 8.1 Hz, 2H), 2.69 – 2.58 (m, 1H), 2.57 – 2.45 (m, 1H), 2.29 (s, 3H), 2.08 – 1.94 (m, 1H), 1.83 (dd, J = 15.3, 7.8 Hz, 2H), 1.71 (dt, J = 13.7, 9.2 Hz, 1H), 1.60 – 1.48 (m, 1H), 1.22 – 1.12 (m, 1H), 1.06 – 0.93 (m, 1H), 0.53 (dt, J = 13.3, 9.2 Hz, 1H).

^{13}C NMR (126 MHz, $CDCl_3$) δ 162.1 (dd, J_{BC} = 99.6, 49.9 Hz), 161.0, 160.2 (d, J_{PC} = 3.6 Hz), 150.1, 138.3, 136.5, 136.1, 135.6, 135.2, 134.6, 133.4, 132.6, 132.2, 131.7, 130.7 (d, J_{PC} = 14.1 Hz), 130.1, 129.7 (d, J_{PC} = 11.0 Hz), 129.4 (d, J = 10.9 Hz), 129.2, 128.9, 128.7 (dd, J_{FC} = 18.5, 12.6 Hz), 128.2, 126.0, 125.8, 124.7, 123.9, 121.7, 117.9, 99.4 (d, J_{PC} = 9.5 Hz), 90.4 (d, J_{PC} = 14.9 Hz), 85.7, 69.5, 63.8, 36.3, 34.4, 30.1 (d, J_{CP} = 10.2 Hz), 28.7, 26.7, 24.5, 19.2.

^{31}P NMR (162 MHz, $CDCl_3$) δ 146.2. ^{19}F NMR (376 MHz, $CDCl_3$) δ -63.5.

MS (FAB, NBA): 763.3 (2), 762.3 (10), 761.3 (41.5%), 760.2 (100), 759.2 (31), 758.2 (62), 654.1 (3), 653.1 (6), 652.1 (7), 651.1 (18), 650.1 (22), 648.1 (15).

IR ($\tilde{\nu}$): 2955w, 1611, 1481, 1456, 1437, 1354, 1277, 1125, 1043, 1016, 999, 965, 927, 886, 854, 838, 743, 712, 682, 669 cm^{-1}.

$[\alpha]_D^{20}$ = +20.4 at a concentration of 0.71.

Elemental Analysis: for $C_{71}H_{50}BF_{24}IrNOP$ calculated C, 52.54; H, 3.10; N, 0.86; found C, 52.46; H, 3.07; N, 0.72.

Complex ***S*-108i**: Iridium(I) [(1,2,5,6-η)-1,5-cyclooctadiene][(*S*)-7-(diphenylphosphinooxy-κ*P*)-4-methyl-2-(piperidin-1-yl)-6,7-dihydro-5H-cyclopenta[b]pyridine-κ*N*]-tetrakis[3,5-bis(trifluoromethyl)phenyl]borate(-)

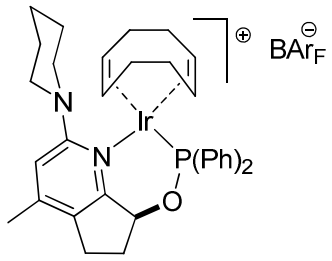

Synthesized by the general method except using 13 mg (56 μmol) of pyridyl alcohol, 6.8 mg (56 μmol) of DMAP, 12.3 (56 μmol) of chlorodiphenylphosphine and 71.2 mg (56 μmol) of iridium(I)$(COD)_2BAr_F$ to yield 40 mg (25.3 μmol, 45%).

Chemical Formula: $C_{66}H_{53}BF_{24}IrN_2OP$ Molecular Weight: 1580.1

MP: 168-171 ˚C

^{1}H NMR (500 MHz, $CDCl_3$) δ 7.64 (s, 8H), 7.54 – 7.46 (m, 2H), 7.44 (s, 4H), 7.40 – 7.28 (m, 6H), 7.21 (ddd, *J* = 9.6, 6.6, 2.9 Hz, 2H), 6.49 (s, 1H), 6.34 (dd, *J* = 12.5, 7.1 Hz, 1H), 5.53 – 5.41 (m, 1H), 4.73 (dd, *J* = 7.4, 3.6 Hz, 1H), 3.75 (s, 1H), 3.47 (s, 2H), 3.21 – 3.08 (m, 2H), 2.93 – 2.85 (m, 1H), 2.81 (dd, *J* = 16.0, 9.9 Hz, 1H), 2.69 (dt, *J* = 16.2, 8.3 Hz, 1H), 2.64 – 2.57 (m, 1H), 2.53 (ddd, *J* = 20.9, 10.2, 5.3 Hz, 1H), 2.44 – 2.27 (m, 2H), 2.13 (s, 3H), 2.07 (dt, *J* = 10.9, 5.6 Hz, 2H), 2.01 (dt, *J* = 13.4, 9.0 Hz, 1H), 1.84 – 1.72 (m, 1H), 1.64 – 1.52 (m, 3H), 1.49 (s, 2H), 1.41 – 1.29 (m, 3H).

^{13}C NMR (126 MHz, $CDCl_3$) δ 164.7, 162.1 (dd, J_{BC} = 99.7, 49.8 Hz), 158.0 (d, J_{PC} = 12 Hz), 135.2, 132.4, 132.1, 131.8 – 131.7 (d, J_{PC} = 9 Hz), 131.3, 131.0 (d, J_{PC} = 14.1 Hz), 129.9, 129.6

(d, J_{PC} = 11.0 Hz), 129.4 (d, J_{PC} = 2.9 Hz), 129.3 (d, J_{PC} = 2.2 Hz), 129.17 (dd, J_{PC} = 21, 10 Hz), 128.9 (dd, J_{PC} = 22.5, 11.5 Hz), 128.2, 126.0, 123.9, 121.7, 117.8, 114.6, 103.8 (d, J = 11.3 Hz), 96.4 (d, J = 12.6 Hz), 87.2, 64.8, 59.1, 37.4, 33.3, 30.7 (d, J = 10.9 Hz), 29.1, 25.6, 25.1, 23.9, 19.5.

^{31}P NMR (162 MHz, $CDCl_3$) δ 147.2. ^{19}F NMR (376 MHz, $CDCl_3$) δ -62.7.

MS (FAB, NBA): 719.3 (9), 718.3 (40), 717.3 (100), 716.3 (31), 715.3 (69), 611.2 (2), 610.2 (4), 609.2 (11), 608.2 (21), 607.2 (49), 606.2 (23), 605.2 (45), 604.2 (15).

$[\alpha]_D^{20}$ = +54.0 at a concentration of 0.50.

Elemental Analysis: for $C_{66}H_{53}BF_{24}IrN_2OP$ calculated C, 50.17; H, 3.38; N, 1.77; found C, 50.06; H, 3.32; N, 1.51.

Complex ***S*-108b**: Iridium(I) [(1,2,5,6-η)-1,5-cyclooctadiene][(S)-2-(anthracen-9-yl)-7-(diphenylphosphinooxy κP)-4-methyl-6,7-dihydro-5H-cyclopenta[b]pyridine-κN]-tetrakis[3,5-bis(trifluoromethyl)phenyl]borate(-)

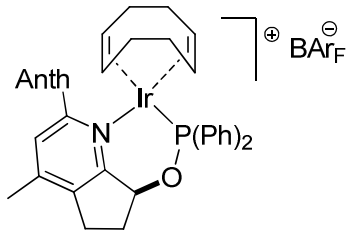

Synthesized by the general method except using 23.6 mg (72.6 μmol) of pyridyl alcohol, 8.8 mg (72.6 μmol) of DMAP, 16 mg (72.6 μmol) of chlorodiphenylphosphine and 71.2 mg (72.6 μmol) of iridium(I)$(COD)_2BAr_F$ to yield 89 mg (49.0 μmol, 68%).

Chemical Formula: $C_{75}H_{52}BF_{24}IrNOP$ Molecular Weight: 1673.2

MP: 98-101 ˚C

^{1}H NMR (400 MHz, $CDCl_3$) δ 8.71 (s, 1H), 8.11 (dd, J = 8.2, 5.1 Hz, 2H), 7.72 (s, 8H), 7.61 (qd, J = 6.7, 4.0 Hz, 4H), 7.55 (td, J = 6.0, 2.4 Hz, 2H), 7.50 (dd, J = 9.6, 3.9 Hz, 7H), 7.49 – 7.41 (m, 5H), 7.40 – 7.33 (m, 4H), 6.73 (d, J = 8.7 Hz, 1H), 6.30 – 6.19 (m, 2H), 5.13 (s, 1H), 3.75 (s, 1H), 3.35 – 3.20 (m, 1H), 3.04 (ddd, J = 17.2, 9.5, 4.4 Hz, 1H), 2.99 – 2.88 (m, 1H), 2.89 – 2.74

(m, 1H), 2.70 – 2.55 (m, 1H), 2.47 (s, 3H), 2.27 – 2.09 (m, 1H), 2.05 (t, J = 7.4 Hz, 1H), 1.63 (dd, J = 14.5, 9.0 Hz, 2H), 1.46 – 1.40 (m, 2H), 1.01 (dd, J = 15.7, 9.9 Hz, 2H), 0.66 – 0.47 (m, 2H), 0.21 – 0.05 (m, 1H).

^{13}C NMR (101 MHz, $CDCl_3$) δ 163.5 – 160.7 (dd, J_{BC} = 99.6, 49.9 Hz), 159.0, 150.1, 139.4, 135.2, 134.0, 133.5 (d, J_{PC} = 6.5 Hz), 132.9, 132.4 (d, J_{PC} = 14.7 Hz), 132.1, 131.2 (d, J_{PC} = 5.1 Hz), 131.1, 130.94 (d, J_{PC} = 11.4 Hz), 130.6 (d, J_{PC} = 13.2 Hz), 130.4 (d, J_{PC} = 5.6 Hz), 129.7 (d, J_{PC} = 10.7 Hz), 129.5, 129.3 (d, J_{PC} = 2.5 Hz), 129.2, 129.1, 129.0 (m$_{BC}$), 128.9 – 128.8 (m$_{FC}$), 128.6, 127.7, 126.4 (d$_{PC}$, J = 17.5 Hz), 124.8, 123.7 (d, J = 12.8 Hz), 120.9, 117.9, 95.1 (d, J_{PC} = 7.8 Hz), 87.5 (d, J_{PC} = 18.7 Hz), 84.63 (s, 1H), 69.4, 68.1 , 36.3, 35.8, 29.8 (d, J_{PC} = 10.0 Hz), 27.8, 27.5, 24.6, 19.2.

^{31}P NMR (162 MHz, $CDCl_3$) δ 149.2. ^{19}F NMR (376 MHz, $CDCl_3$) δ -63.1.

MS (FAB, NBA): m/z: 813.3 (2), 812.3 (12), 811.3 (48), 810.2 (100), 808.2 (65), 809.2 (37), 704.2 (6), 703.2 (10), 702.2 (15), 701.2 (11), 700.2 (11).

IR ($\tilde{\nu}$): 2887w, 1737w, 1608, 1485, 1463, 1438, 1352s, 1272s, 1157, 1112s, 1093, 999w, 958, 885, 838, 738, 711, 696, 680, 669, 642, 619 cm^{-1}.

$[\alpha]_D^{20}$ = +39.4 at a concentration of 0.60.

Elemental Analysis: for $C_{75}H_{52}BF_{24}IrNOP$ calculated C, 53.84; H, 3.13; N, 0.84; found C, 53.78; H, 3.17; N, 0.77.

Complex ***S*-108c**: Iridium(I) [(1,2,5,6-η)-1,5-cyclooctadiene][((*S*)-2-(anthracen-9-yl)-7-(di-tolylphosphinooxy-κ*P*)-4-methyl-6,7-dihydro-5H-cyclopenta[b]pyridine-κ*N*]-tetrakis[3,5-bis(trifluoromethyl)phenyl]borate(-)

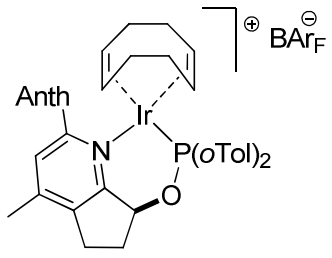

Synthesized by the general method except using 24.2 mg (74.5 μmol) of pyridyl alcohol, 9.1 mg (74.5 μmol) of DMAP, 18.5 mg (74.5 μmol) of chlorodiphenylphosphine and 94 mg (74.5 μmol) of iridium(I)$(COD)_2BAr_F$ to yield 87 mg (51.1 μmol, 69%).

Chemical Formula: $C_{77}H_{56}BF_{24}IrNOP$ Molecular Weight: 1701.2

MP: 103-105 ˚C

^{1}H NMR (500 MHz, CDCl3) δ 8.64 (s, 1H), 8.10 (d, *J* = 8.5 Hz, 1H), 8.00 (d, *J* = 8.5 Hz, 1H), 7.69 (s, 8H), 7.55 (s, 1H), 7.45 (d, *J* = 12.4 Hz, 5H), 7.43 – 7.37 (m, 2H), 7.33 – 7.28 (m, 2H), 7.21 (dd, *J* = 21.2, 13.3 Hz, 3H), 7.10 (dd, *J* = 24.6, 16.6 Hz, 1H), 6.93 (s, 2H), 6.20 (m2H), 5.02 (s, 1H), 3.13 (d, *J* = 7.5 Hz, 1H), 2.98 (dd, *J* = 16.2, 8.5 Hz, 2H), 2.82 – 2.48 (m, 4H), 2.38 – 2.24 (m, 4H), 2.24 – 1.90 (m, 6H), 1.85 (dd, *J* = 15.8, 8.0 Hz, 1H), 1.78 – 1.39 (m, 3H), 1.29 – 1.08 (m, 2H), 0.84 (ddd, *J* = 31.4, 25.0, 19.3 Hz, 2H), 0.51 (d, *J* = 9.9 Hz, 1H).

^{13}C NMR (126 MHz, $CDCl_3$) δ 162.1 (dd, J_{BC} = 99.7, 49.8 Hz), 159.9, 150.4, 141.4 (d, J_{PC} = 30.5 Hz), 139.6, 135.2, 133.3, 132.5, 131.3, 131.0, 130.8, 130.3, 129.7-129.6 (m), 129.5, 129.3, 129.2 (dd, J_{PC} = 21, 10 Hz), 128.9 (dd, J_{PC} = 22.5, 11.5 Hz), 128.1 (d, J_{FC} = 21.6 Hz), 126.4 (d, J_{PC} = 6.9 Hz), 126.1, 124.7, 123.9, 121.7, 117.9 (t, J_{PC} = 14.6 Hz), 85.0, 36.4 – 36.1 (m), 33.6, 29.8 (d, J_{PC} = 10.2 Hz), 27.6, 25.4, 23.1(d, J_{PC}= 10.5 Hz), 19.1.

^{31}P NMR (162 MHz, $CDCl_3$) δ 149.2. ^{19}F NMR (376 MHz, $CDCl_3$) δ -63.1.

MS (FAB, NBA): m/z: 841.3 (3), 840.3 (13), 839.3 (50), 838.3 (100.0), 837.3 (34), 836.3 (66), 733.2 (2.4), 732.2 (6), 731.2 (16), 730.2 (40), 729.2 (39), 728.2 (53), 727.2 (31), 726.2 (43), 725.2 (15).

IR ($\tilde{\nu}$): 2882w, 1737w, 1608, 1463, 1354s, 1273s, 1157, 1112s, 1037, 960, 885, 839, 738, 712, 669, 622 cm^{-1}.

$[\alpha]_D^{20}$ = +44.0 at a concentration of 0.92.

Elemental Analysis: for $C_{77}H_{56}BF_{24}IrNOP$ calculated C, 54.36; H, 3.32; N, 0.82; found C, 53.98; H, 3.35; N, 0.67.

Complex *S*-**110b**: Iridium(I) [(1,2,5,6-η)-1,5-cyclooctadiene][(*S*)-8-(dio-tolylphosphinooxy-κ*P*)-2-mesityl-5,6,7,8-tetrahydroquinoline-κ*N*]-tetrakis[3,5-bis(trifluoromethyl)phenyl]borate(-)

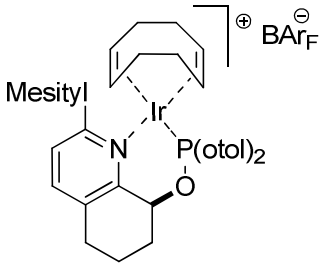

Synthesized by the general method except using 25.8 mg (96.8 μmol) of pyridyl alcohol, 11.8 mg (96.8 μmol) of DMAP, 24 mg (96.8 μmol) of chlorodiphenylphosphine and 122.7 mg (96.8 μmol) of iridium(I)$(COD)_2BAr_F$ to yield 128 mg (77.8 μmol, 81%).

Chemical Formula: $C_{72}H_{58}BF_{24}IrNOP$ Molecular Weight: 1643.2

MP: 203-04 ˚C

^{1}H NMR (500 MHz, CDCl3) δ 7.76 (s, 8H), 7.65 (d, *J* = 7.9 Hz, 1H), 7.56 (s, 4H), 7.40 (dt, *J* = 13.1, 7.3 Hz, 3H), 7.24 (s, 1H), 7.22 – 7.11 (m, 3H), 7.08 (d, *J* = 15.9 Hz, 1H), 6.95 (s, 1H), 6.73 (d, *J* = 52.5 Hz, 1H), 6.42 (d, *J* = 5.0 Hz, 1H), 5.58 (s, 1H), 3.88 (s, 1H), 3.46 (d, *J* = 45.0 Hz, 1H), 3.19 – 2.72 (m, 6H), 2.67 (d, *J* = 12.9 Hz, 1H), 2.53 – 2.23 (m, 7H), 2.23 – 1.86 (m, 9H), 1.81 (s, 4H), 1.27 (dd, *J* = 19.8, 12.6 Hz, 4H).

^{13}C NMR (101 MHz, $CDCl_3$) δ 162.1 (dd, J_{BC} = 102.0, 46.9 Hz), 141.7, 140.9, 137.0, 135.3 (d, J_{PC} = 26.4 Hz, 6H), 132.7, 130.8, 129.6 (d, J_{PC} = 30.7 Hz), 128.9 (t, J_{FC} = 13.4 Hz), 126.7 (d, *J* = 11.1 Hz), 126.3, 123.6, 120.9 – 120.6 (m_{PC}), 117.8, 99.2, 64.9, 37.2 (d, J_{PC} = 27.5 Hz), 34.6, 30.3 (d, J_{PC} = 9.6 Hz), 28.5, 27.9, 25.3, 22.5, 21.4, 21.0, 17.3.

^{31}P NMR (202 MHz, $CDCl_3$) δ 158.2 (broad), 146.4 (broad).

MS (FAB, NBA): m/z: 783.3 (2), 782.3 (10), 781.3 (43), 780.3 (100), 779.3 (29), 778.3 (60), 674.2 (4), 673.2 (10), 672.2 (27), 671.2 (29), 670.2 (52), 669.2 (23), 668.2 (33).

IR ($\tilde{\nu}$): 2929w, 2357, 1737w, 1614, 1460, 1352s, 1271s, 1159, 1117s, 1037, 960, 931, 877, 854, 839, 757, 744, 711, 692, 680, 668, 638, 619 cm^{-1}.

$[\alpha]_D^{20}$ = +37.0 at a concentration of 0.38.

Elemental Analysis: for $C_{72}H_{58}BF_{24}IrNOP$ calculated C, 52.63; H, 3.56; N, 0.85; found C, 52.49; H, 3.66; N, 0.70.

Complex ***S*-108d**: Iridium(I) [(1,2,5,6-η)-1,5-cyclooctadiene][(*S*)-7-(dio-tolylphosphinooxy-κ*P*)-2-mesityl-4-methyl-6,7-dihydro-5H-cyclopenta[b]pyridine-κ*N*]-tetrakis[3,5-bis(trifluoromethyl)phenyl]borate(-)

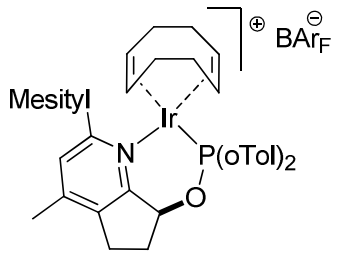

Synthesized by the general method except using 31.0 mg (115.9 μmol) of pyridyl alcohol, 14.1 mg (115.9 μmol) of DMAP, 24 mg (115.9 μmol) of chlorodiphenylphosphine and 147.5 mg (115.9 μmol) of iridium(I)$(COD)_2BAr_F$ to yield 139 mg (84.6 μmol, 73%).

Chemical Formula: $C_{72}H_{58}BF_{24}IrNOP$ Molecular Weight: 1643.2

MP: 162-165 ˚C

^{1}H NMR (500 MHz, $CDCl_3$) δ 7.87 (d, *J* = 79.0 Hz, 1H), 7.64 (s, 8H), 7.44 (s, 4H), 7.27 (dd, *J* = 17.3, 9.4 Hz, 3H), 7.16 (d, *J* = 25.9 Hz, 3H), 6.96 (s, 3H), 6.82 (s, 1H), 6.26 (s, 2H), 5.25 (d, *J* = 28.2 Hz, 1H), 3.47 (s, 1H), 3.20 (d, *J* = 3.1 Hz, 1H), 2.99 (s, 1H), 2.91 – 2.78 (m, 1H), 2.65 (s, 4H), 2.50 – 2.30 (m, 2H), 2.25 (d, *J* = 9.0 Hz, 3H), 2.21 (d, *J* = 18.7 Hz, 4H), 2.07 (t, *J* = 35.5 Hz, 5H), 1.77 (s, 4H), 1.49 (s, 2H), 1.27 (dd, *J* = 14.5, 7.4 Hz, 2H), 1.18 (s, 2H).

^{13}C NMR (126 MHz, $CDCl_3$) δ 162.1 (dd, J_{BC} = 99.5, 49.9 Hz), 141.57 – 141.27 (m), 140.8, 138.7, 135.2, 132.6, 131.7, 129.7 – 128.8 (m_{PC}), 128.8, 128.2, 126.6 – 126.4 (m), 126.0, 123.8 121.7, 117.8, 33.6, 29.7, 28.0 – 27.9 (m_{PC}), 27.2, 26.1, 23.2 (d, J_{PC} = 16 Hz), 21.4, 21.0, 19.0.

^{31}P NMR (202 MHz, $CDCl_3$) δ 163.8, 151.0. ^{11}B NMR (160 MHz, $CDCl_3$) δ -6.58.

MS (FAB, NBA): m/z: 783.3 (2), 782.3 (10), 781.3 (43), 780.3 (100), 779.3 (30), 778.3 (60), 674.2 (3), 673.2 (6), 672.2 (18), 671.2 (24), 670.2 (39), 669.2 (20), 668.2 (30).

IR ($\tilde{\nu}$): 2929w, 2357, 1737w, 1614, 1460, 1352s, 1271s, 1159, 1117s, 1037, 960, 931, 877, 854, 839, 757, 744, 711, 692, 680, 668, 638, 619 cm^{-1}.

$[\alpha]_D^{20}$ = +32.0 at a concentration of 0.34.

Elemental Analysis: for $C_{72}H_{58}BF_{24}IrNOP$ calculated C, 52.63; H, 3.56; N, 0.85; found C, 52.59; H, 3.50; N, 1.08.

Complex ***S*-110a**: Iridium(I) [(1,2,5,6-η)-1,5-cyclooctadiene][((*S*)-2-(anthracen-9-yl)-8-(di-tolylphosphinooxy-κ*P*)-5,6,7,8-tetrahydroquinoline-κ*N*]-tetrakis[3,5-bis(trifluoromethyl)phenyl]borate(-)

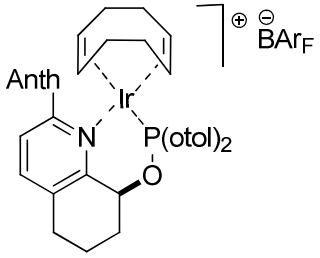

Synthesized by the general method except using 31.0 mg (115.9 μmol) of pyridyl alcohol, 14.1 mg (115.9 μmol) of DMAP, 24 mg (115.9 μmol) of chlorodiphenylphosphine and 147.5 mg (115.9 μmol) of iridium(I)$(COD)_2BAr_F$ to yield 139 mg (84.6 μmol, 73%).

Chemical Formula: $C_{77}H_{56}BF_{24}IrNOP$ Molecular Weight: 1701.2

MP: 231-232 ˚C

^{1}H NMR (400 MHz, $CDCl_3$) δ 8.73 (s, 1H), 8.18 (d, *J* = 8.6 Hz, 1H), 8.09 (d, *J* = 8.5 Hz, 1H), 7.81 – 7.69 (m, 9H), 7.69 – 7.56 (m, 2H), 7.56 – 7.46 (m, 6H), 7.46 – 7.27 (m, 6H), 7.13 – 7.02 (m, 1H), 6.89 (d, *J* = 7.8 Hz, 1H), 6.60 (s, 1H), 6.34 (t, *J* = 11.0 Hz, 1H), 5.26 (d, *J* = 26.9 Hz, 1H), 3.51 (s, 1H), 3.07 (d, *J* = 17.1 Hz, 1H), 2.94 (ddd, *J* = 17.5, 13.5, 7.6 Hz, 1H), 2.78 – 2.52 (m, 4H), 2.39 – 2.17 (m, 3H), 2.13 (d, *J* = 15.5 Hz, 3H), 2.02 (dd, *J* = 24.2, 7.4 Hz, 2H), 1.65 (ddd, *J* = 78.0, 27.9, 9.5 Hz, 4H), 1.24 (dd, *J* = 27.5, 6.3 Hz, 1H), 1.07 – 0.90 (m, 1H), 0.88 – 0.64 (m, 2H), 0.27 (dd, *J* = 11.1, 7.8 Hz, 1H).

^{13}C NMR (126 MHz, $CDCl_3$) δ 162.1 (dd, J_{BC} = 99.5, 49.9 Hz), 159.8, 141.6, 136.4 – 136.2 (m_{BC}), 135.2, 134.4 – 133.6 (m_{PC}), 132.8 (d, J_{PC} = 9.75 Hz), 132.2, 131.4, 131.0, 130.4, 129.7, 129.4, 129.3, 129.1, 129.1 – 129.0 (m_{PC}), 128.9 – 128.7 (m_{PC}), 128.2, 127.9 – 127.8 (m_{FC}), 126.7, 126.5, 126.3, 124.7, 123.6, 120.9, 117.9, 66.5, 36.6, 34.7, 30.9 – 29.6 (d, J_{PC} = 9.75 Hz), 28.7, 27.6, 24.7, 22.7 – 21.9 (d, J_{PC} = 4.6 Hz), 17.4.

^{31}P NMR (162 MHz, $CDCl_3$) δ 149.2. ^{19}F NMR (376 MHz, $CDCl_3$) δ -63.1.

MS (FAB, NBA): m/z: 841.3 (4), 840.3 (13), 839.3 (49), 838.3 (100.0), 837.3 (33), 836.3 (62), 733.2 (3), 732.2 (6), 731.2 (19), 730.2 (42), 729.2 (33), 728.2 (50), 727.2 (22), 726.2 (24), 725.2 (10).

IR (ṽ): 2882w, 2359, 1737w, 1608, 1463, 1352s, 1274s, 1159, 1117s, 1064, 970, 958, 885, 869, 838, 804, 712, 669, 621 cm^{-1}.

$[\alpha]_D^{20}$ = +69.0 at a concentration of 0.28.

Elemental Analysis: for $C_{77}H_{56}BF_{24}IrNOP$ calculated C, 54.36; H, 3.32; N, 0.82; found C, 54.35; H, 3.37; N, 0.71.

Complex ***R*-110a**: Iridium(I) [(1,2,5,6-η)-1,5-cyclooctadiene][((*R*)-2-(anthracen-9-yl)-8-(di-tolylphosphinooxy-κ*P*)-5,6,7,8-tetrahydroquinoline-κ*N*]-tetrakis[3,5-bis(trifluoromethyl)phenyl]borate(-)

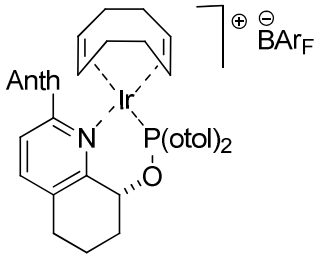

Synthesized by the general method except using 127.0 mg (390.0 μmol) of pyridyl alcohol, 47.5 mg (390.0 μmol) of DMAP, 97 mg (390.0 μmol) of chlorodiphenylphosphine and 595.0 mg (468.0 μmol) of iridium(I)$(COD)_2BAr_F$ to yield 400 mg (235.1 μmol, 60%). The physical properties matched the opposite enantiomer.

Chemical Formula: $C_{77}H_{56}BF_{24}IrNOP$ Molecular Weight: 1701.2

$[\alpha]_D^{20}$ = -71.0 at a concentration of 0.25.

Complex *S*-**108e**: Iridium(I) [(1,2,5,6-η)-1,5-cyclooctadiene][S)-7-(di-tert-butylphosphinooxy-κP)-2-mesityl-4-methyl-6,7-dihydro-5H-cyclopenta[b]pyridine-κN]-tetrakis[3,5-bis(trifluoromethyl)phenyl]borate(-)

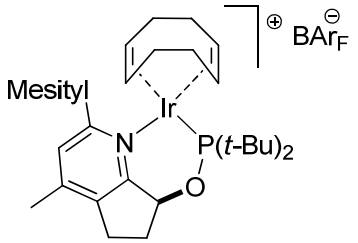

In the glove box the alcohol (50 mg, 189.0 μmol) is added to a dry Young tube with a stir bar. Potassium hydride (11.1 mg, 280.5 μmol) was carefully added to reaction vessel followed by di-*tert*-butylchlorophosphine (34.0 mg, 189.0 μmol) added as a solution in dry DMF (150 μL). The sides of the vessel were rinsed with dry DMF (2 x 150 μL), the reaction vessel was sealed and brought outside the box. The reaction was stirred for 48 hours, at which time a liquid nitrogen cold trap was attached with a short line directly to the reaction vessel. The flask was cooled to 0 ˚C and carefully evacuated to avoid bumping. After the gas bubble had ceased the vessel was placed in a mildly warm water bath to assist removal of DMF, periodically change the bath for more warm water. The flask was left at high vacuum in a warm water bath for 3 hours to result in a red foam. The flask was sealed under vacuum and brought back inside the glove box. Dry THF (500 μL) was added and the liquid was filtered into a vial containing a solution of iridium(I)(COD)$_2$BAr$_F$ (240 mg, 189.0 μmol) in 1 mL of THF with the use of a syringe and micron filter. The reaction vessel was washed and filtered into the vial with additional THF (2 x 500 μL). The resulting dark red solution was stirred for 6 hours and then brought outside the box, stripped onto silica gel and chromatographed (1 X 10 cm silica gel, dry load) with 50/50 hexane/ ether followed by elution of the product with DCM. The resulting dark red material was recrystallized from 1 mL of DCM/ 4 mL of hexane layered carefully and allowed to stand in the refrigerator for 48 hours to yield dark red crystals of X-ray quality. Yield 120 mg (76. 2 μmol, 40%). The mother liquor was concentrated and a second batch of crystals was obtained from DCM/ hexane (25 mg, 15.9 μmol, 8.4%).

Chemical Formula: $C_{66}H_{62}BF_{24}IrNOP$ Molecular Weight: 1575.2

MP: 113-115 ˚C

^{1}H NMR (500 MHz, $CDCl_3$) δ 7.71 (s, 8H), 7.52 (s, 4H), 7.16 (s, 1H), 7.06 (s, 1H), 6.92 (s, 1H), 5.48 (t, *J* = 5.8 Hz, 1H), 5.44 (s, *J* = 16.7, 10.8 Hz, 1H), 5.02 (s, 1H), 4.08 – 3.82 (m, 1H), 3.16 (p, *J* = 7.8 Hz, 1H), 3.06 (dt, *J* = 16.9, 8.3 Hz, 1H), 2.91 (dd, *J* = 17.2, 8.4 Hz, 1H), 2.64 (s, 3H), 2.45 (ddd, *J* = 33.2, 15.0, 8.1 Hz, 2H), 2.36 (d, *J* = 3.3 Hz, 6H), 2.25 – 2.11 (m, 1H), 2.04 (tdd, *J* = 16.3, 10.9, 5.7 Hz, 1H), 1.99 – 1.91 (m, 1H), 1.80 (dd, *J* = 15.5, 7.5 Hz, 1H), 1.74 – 1.62 (m, 4H), 1.45 (d, *J* = 13.4 Hz, 9H), 1.23 – 0.98 (m, 3H), 0.82 (d, *J* = 14.3 Hz, 10H).

^{13}C NMR (126 MHz, $CDCl_3$) δ 162.5 (dd, J_{BC} = 99.5, 49.9 Hz), 160.6, 150.0, 140.2, 138.1, 137.5, 136.0 (d, J_{PC} = 30.9 Hz), 134.8, 132.4, 129.3 (d, J_{PC} = 5.2 Hz), 129.0, 128.8 (m $_{BC}$), 128.5, 127.8, 125.6, 123.4, 121.3, 117.4, 92.7 (d, J_{PC} = 5.7 Hz), 85.8, 80.8 (d, J_{PC} = 18.1 Hz), 71.1, 57.6, 53.4, 40.3 (dd, J_{PC} = 70.1, 19.7 Hz), 37.5 (d, J_{PC} = 3.8 Hz,), 35.3, 31.6, 29.8 – 29.4 (m$_{PC}$), 28.6, 28.0 (d, *J* = 6.3 Hz), 27.7, 27.3, 24.9, 24.3, 22.6, 20.8 (d, *J* = 21.9 Hz), 18.5, 14.10.

^{31}P NMR (162 MHz, $CDCl_3$) δ 139.5.

MS (FAB, NBA): m/z: 714.3 (7), 713.3 (36), 712.3 (100), 711.3 (26), 710.3 (60), 606.2 (5), 605.2 (21), 604.2 (52), 603.2 (17), 602.2 (39).

IR ($\tilde{\nu}$): 2929, 2879w, 2354, 1737w, 1610, 1463, 1456s, 1352, 1271s, 1164, 1122s, 1047, 1037, 962, 885, 838, 808, 715, 667, 636 cm^{-1}.

$[\alpha]_D^{20}$ = -9.0 at a concentration of 0.52.

Elemental Analysis: for $C_{66}H_{62}BF_{24}IrNOP$ calculated C, 50.33; H, 3.97; N, 0.89; found C, 50.01; H, 4.18; N, 0.92.

5.13 Synthesis of Iridium(I) bis[(1,2,5,6-η)-1,5-cyclooctadiene]- tetrakis[3,5-bis(trifluoromethyl)phenyl]borate(-)

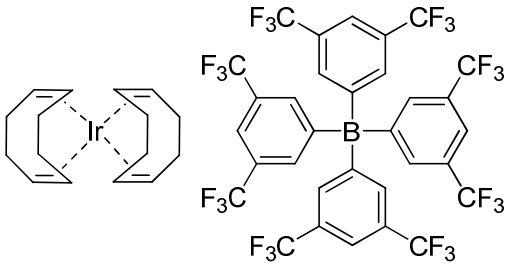

Chloro(1,5-cyclooctadiene)iridium(I) dimer (130.7 mg, 194.6 μmol) was added to a dry 25 mL flask and dissolved by stirring in 8 mL of absolute DCM. Cyclooctadiene (63.1 mg, 71.7 μL, 584 μmol) was added by syringe and the reaction was stirred for 30 minutes at room temperature. Sodium tetrakis[3,5-bis(trifluoromethyl)phenyl]borate (362 mg, 408.6 μmol) was added as a solid and the very dark red solution was stirred for 2 hours at room temperature. The solution was filtered through a 2 gram silica pipette column which was washed with an additional 7 mL of DCM. The solvent was concentrated at a rotovap to dryness. The resulting crude mixture was taken up in 5 mL of DCM, filtered through a micron filter and layered with 5 ml of hexane. Crystallization at -20 ˚C overnight followed by cold vacuum filtration and washing with -20˚C hexane (2 x 25 mL) provided very large dark red high symmetry crystals of X-ray diffraction quality which were dried on a high vacuum for 3 hours to provide 470 mg of pure product (370 μmol, 95%).

Chemical Formula: $C_{48}H_{36}BF_{24}Ir$ Molecular Weight: 1271.8

^{1}H NMR (400 MHz, $CDCl_3$) δ 7.69 (d, J = 2.3 Hz, 2H), 7.54 (s, 1H), 4.99 (s, 2H), 2.49 – 2.33 (m, 2H), 2.33 – 2.16 (m, 2H).

^{13}C NMR (101 MHz, $CDCl_3$) δ 162.0 (dd, J_{BC} = 99.7, 50.0 Hz), 135.2, 129.3 (ddd, J_{BC} = 57.5, 18.7, 15.6 Hz), 124.9 (d, $^{1}J_{FC}$ = 272.7 Hz), 118.2 – 117.7 (m_{BC}), 101.5, 30.7.

^{19}F NMR (376 MHz, $CDCl_3$) δ -63.5.

5.14 Substrates and intermediates

Intermediate **167**: 1-(2-Bromo-2-fluorovinyl)-4-methylbenzene[17]

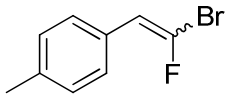

(4-Methylbenzylidene)hydrazine (810 mg, 6.03 mmol) was added to a twenty five mL flask with copper(I) chloride and 10 mL of DMSO. The solution was placed into an ice bath and concentrated ammonia (6 mL, 32%) was added followed by tribromofluoromethane (590 µL, 1.63 g, 6.03 mmol). The reaction was allowed to come to room temperature and stirred overnight. The reaction was poured into a separatory funnel with 100mLs of ether, washed with water (2 x 50 mL), brine (2 x 50 mL), and the separated organic layer was dried over magnesium sulfate, filtered and concentrated. Chromatography (3.5 X 15 cm silica gel) with hexane as an eluent provided 450 mg (2.09 mmol, 34.7%) product in a 1 to 3 ratio of cis to trans bromide as a colorless oil which quickly goes dark on exposure to light, temperature and air. All data matched well with the reported literature.

Chemical Formula: C_9H_8BrF Molecular Weight: 215.1

^{1}H NMR (400 MHz, $CDCl_3$) δ 7.38 (E, d, *J* = 8.1 Hz, 0.6 H), 7.29 (Z, d, *J* = 8.2 Hz, 2H), 7.16 (E/Z, t, *J* = 8.8 Hz, 2.6 H), 6.63 (E, d, *J* = 15.2 Hz, 0.3H), 5.94 (Z, d, *J* = 33.1 Hz, 1H), 2.36 (E, s, 1H), 2.34 (E, s, 3H).

^{19}F NMR (376 MHz, $CDCl_3$) δ -67.61 (d, *J* = 15.3 Hz), -69.98 (d, *J* = 33.1 Hz).

Substrate **168**: (*Z*)-1-(2-fluoro-2-(4-methoxyphenyl)vinyl)-4-methylbenzene

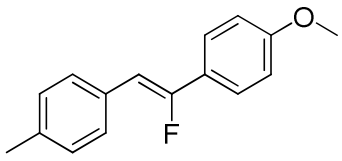

1-(2-Bromo-2-fluorovinyl)-4-methylbenzene (1.2 g, 4.89 mmol), palladium(0)dibenzylideneacetone (22.4 mg, 24.5 µmol, 1 mol%), tri-tert-butylphosphonium tetrafluoroborate (56.7 mg, 195 µmol, 4 mol%), cesium fluoride (2.58 g, 17.2 mmol), and p-

methoxyphenylboronic acid (880 mg, 5.8 mmol) were all placed together in a 25 mL round bottom flask which was sealed with a rubber septum, purged for 10 minutes with argon and dry, degassed DME (15 mL) was added. The reaction was stirred for 3 days after which time the contents were filtered through a pad of celite, concentrated onto silica gel and chromatographed with 20% DCM in hexane. The resulting *E/Z* mixture was recrystallized from hexane to give 550 mg (2.27 mmol, 46%) of the pure *Z* isomer.

Chemical Formula: $C_{16}H_{15}FO$ Molecular Weight: 242.3

^{1}H NMR (400 MHz, $CDCl_3$) δ 7.63 – 7.54 (m, 2H), 7.51 (d, *J* = 8.2 Hz, 2H), 7.18 (t, *J* = 9.6 Hz, 2H), 6.98 – 6.86 (m, 2H), 6.15 (d, *J* = 40.1 Hz, 1H), 3.85 (s, 3H), 2.36 (s, 3H).

^{19}F NMR (376 MHz, $CDCl_3$) δ -115.44 (d, *J* = 40.1 Hz).

Intermediate **170**: 1-(2-Bromo-1-fluoroethyl)-4-*tert*-butylbenzene

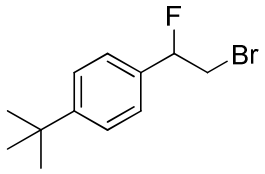

N-bromosuccinamide (2.3 g, 12.9 mmol) was added to 30 mL of DCM followed by hydrofluoric acid triethylamine complex (3/1) (6mL) at 0 ˚C. The reaction was allowed to stir for 20 minutes to form the interhalon and 4-tert-butylstyrene (1.62 g, 10.1 mmol) was added to a flask. The reaction was stirred for 4 hours at room temperature, poured into a separatory funnel and washed with 2 M hydrochloric acid (3 x 50 mL). The organic layer was dried over magnesium sulfate, filtered and concentrated onto silica gel which was quickly chromatographed with 100% hexane and switching to 35% DCM in hexane to remove most of the product quickly. The fractions were concentrated to dryness and used immediately in the next step. Compound is highly unstable, yield of 750 mg (28.7%).

Chemical Formula: $C_{12}H_{16}BrF$ Molecular Weight: 259.2

^{1}H NMR (400 MHz, $CDCl_3$) δ 7.45 – 7.41 (m, 2H), 7.29 (dd, *J* = 8.7, 0.4 Hz, 2H), 5.60 (ddd, *J* = 46.9, 8.2, 3.9 Hz, 1H), 3.78 – 3.50 (m, 2H), 1.33 (d, *J* = 2.0 Hz, 9H).

^{19}F NMR (376 MHz, $CDCl_3$) δ -173.90 (ddd, *J* = 47.0, 27.0, 14.5 Hz).

Substrate **171**: 1-*tert*-butyl-4-(1-fluorovinyl)benzene

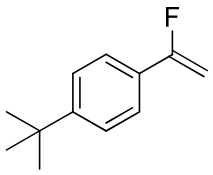

1-(2-Bromo-1-fluoroethyl)-4-*tert*-butylbenzene (750 mg, 2.89 mmol) was added to a 25 mL flask with DMSO (10 mL) and potassium hydroxide (400 mg, 7.14 mmol) was dissolved in 400 µL of water and added dropwise to the reaction. The reaction was then stirred for 6 hours and poured into a separatory funnel with 20 mL of diethyl ether and washed with 50 mL of 0.5 M HCl, water (2 x 50 mL) and brine (2 x 50 mL). The organic layer was dried over magnesium sulfate, filtered and concentrated at the rotovap to yield the crude material which was purified by kugelrohr distillation (5 mTorr, 100 ˚C) to obtain 400 mg (2.25 mmol, 78%) as a clear oil which was used in hydrogenation experiments immediately. The compound decomposes slowly at -20˚C to give a black tar like substance.

Chemical Formula: $C_{12}H_{15}F$ Molecular Weight: 178.2

^{1}H NMR (400 MHz, $CDCl_3$) δ 7.53 – 7.47 (m, 2H), 7.43 – 7.37 (m, 2H), 4.99 (dd, *J* = 50.0, 3.4 Hz, 1H), 4.80 (dd, *J* = 17.9, 3.4 Hz, 1H), 1.34 (d, *J* = 4.0 Hz, 9H).

^{19}F NMR (376 MHz, $CDCl_3$) δ -108.94 (dd, *J* = 50.0, 18.0 Hz).

Intermediate **158**: Ethyl 3-methyl-5-phenylpent-2-enoate[18]

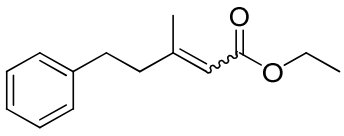

Potassium tert-butoxide (5.35 g, 55.7 mmol) was transferred to a large Young tube which was evacuated and placed under argon. Absolute THF (50 mL) was added to the tube by cannula followed by triethyl phosphonoacetate (10.4 g, 46.44 mmol) was syringed into the reaction vessel at room temperature. A mild exotherm occurred on addition and a homogenous solution was obtained after 30 minutes of stirring at ambient temperature. The reaction mixture was

cooled to -50 ˚C for 30 minutes and 4-phenyl-2-butanone (6.53 g, 44.12 mmol) was added cold and the reaction allowed to warm to room temperature overnight. The reaction was quenched with water (25 mL) and washed with into ethyl acetate (100 mL) into a separatory funnel. Brine was added (50 mL) and the layers shaken and separated. The organic layer was washed with more brine (2 x 100 mL), dried over magnesium sulfate, filtered and concentrated at the rotovap to yield the crude material which was purified by kugelrohr distillation (5 mTorr, 100˚C) to obtain 7.0 g (32.2 mmol, 69%) as a slightly yellow oil.

Chemical Formula: $C_{14}H_{18}O_2$ Molecular Weight: 218.3

^{1}H NMR (400 MHz, $CDCl_3$) δ 7.29 (t, *J* = 7.3 Hz, 2H), 7.19 (dd, *J* = 13.4, 7.1 Hz, 3H), 5.70 (dd, *J* = 10.1, 1.2 Hz, 1H), 4.15 (q, *J* = 7.1 Hz, 2H), 2.85 – 2.73 (m, 2H), 2.54 – 2.38 (m, 2H), 2.21 (dd, *J* = 4.7, 1.1 Hz, 3H), 1.28 (t, *J* = 7.1 Hz, 3H).

Intermediate **158**: (*E*)-3-methyl-5-phenylpent-2-enoic acid[19]

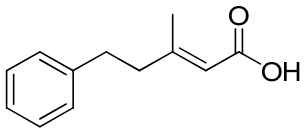

Ethyl 3-methyl-5-phenylpent-2-enoate (5.20 g, 23.8 mmol) was dissolved in 25 mL of methanol and added to a flask containing sodium hydroxide (2.80 g, 70.0 mmol) in 100 mL of water. The resulting slurry was heated to 100 ˚C for 4 hours during which time the slurry became a clear solution. The reaction was cooled to 0 ˚C and the solution was acidified with concentrated hydrochloric acid to a pH of 2, during which time the acid precipitated as a white powder. The resulting slurry was taken up and transferred with 200 mL of diethyl ether to a separatory funnel. The layers were thoroughly shaken, and the organic layer was separated and washed with brine (3 x 100 mL). The organic layer was dried over magnesium sulfate, filtered and concentrated to dryness at a rotovap. The resulting crude acid was taken up in ethyl acetate (ca 4 grams of crude in 50 mL) and cyclohexylamine (3.13 g, 3.6 mL, 31.5 mmol) was added dropwise to the quickly stirring solution, immediate white precipitate was formed, the solution became a thick slurry on complete addition of the cyclohexylamine. An additional 120 mL of ethyl acetate was added to the slurry followed by heating to reflux with strong stirring. On dissolution of the precipitate the solution was allowed to cool to room temperature, and then further cooled to -20 ˚C in an ice salt

bath. The resulting white precipitate was filtered off by vacuum filtration and the filtrate washed with a 50 mL portion of diethyl ether cooled in the ice salt bath. A small portion of the precipitate was partitioned with 2 M HCl and ethyl acetate, the layers separated and the organic layer was dried over magnesium sulfate, concentrated and the small aliquot analyzed by GC to find a 95:5 ratio of cis/trans isomers in favor of the trans. The precipitate was (3 grams) was taken up in 100 mL of ethyl acetate and recrystallized and treated as before to find a ratio of 99 to 1. The resulting 2.4 grams of salt was taken up in DCM (50 mL) and 2 M HCl (100 mL). The slurry was mixed into solution until no precipitate was present, the layers were separated and the organic layer was washed with additional 2 M HCl (2 x 50 mL) and brine (2 x 50 mL), dried over magnesium sulfate, filtered and the solution was concentrated to dryness at a rotovap. The resulting acid (1.6 g) was taken up in hot hexane (6 mL) and allowed to stand overnight at -20˚C. The resulting large clear crystals were quickly isolated by vacuum filtration to yield 1.2 g (6.31 mmol).

Chemical Formula: $C_{12}H_{14}O_2$ Molecular Weight: 190.2

^{1}H NMR (400 MHz, $CDCl_3$) δ 11.76 (s, 1H), 7.31 (dd, *J* = 10.1, 4.5 Hz, 6H), 7.25 – 7.14 (m, 9H), 5.71 (d, *J* = 1.2 Hz, 3H), 2.81 (dd, *J* = 9.3, 6.8 Hz, 6H), 2.59 – 2.38 (m, 6H), 2.22 (d, *J* = 1.2 Hz, 9H).

GC: General conditions, the injector was set to 270 ˚C, oven temperature 100 ˚C held for 3 minutes and a ramp of 7˚C/min to 230˚C for 10 minues, detector was set to 250 ˚C and a pressure of 60 kPa. T_{trans} = 27.1 min T_{cis} = 27.8 min.

Substrate **158a**: (*E*)-ethyl 3-methyl-5-phenylpent-2-enoate[18]

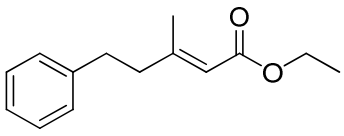

(*E*)-3-methyl-5-phenylpent-2-enoic acid (1.20 g, 6.30 mmol) was refluxed in a mixture of absolute ethanol (50 mL) and 10 grams of magnesium sulfate with a catalytic amount of p-toluene sulfonic acid. The reaction was allowed to reflux under an inert atmosphere for 8 hours after which time the reaction was cooled, filtered, concentrated and the concentrate was dissolved in ether and saturated sodium bicarbonate (50/ 100 mL). The organic layer was

thoroughly shaken with the aqueous mixture, washed with brine (2 x 50 mL), dried over magnesium sulfate, filtered and concentrated at the rotovap. Kugelrohr distillation gave 750 mg (3.44 mmol, 54.6%) of pure product which was indiscernible from the cis trans miture by NMR.

Chemical Formula: $C_{14}H_{18}O_2$ Molecular Weight: 218.3

Substrate **163**: 4-methylfuran-2(5H)-one[21]

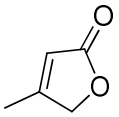

3-Methylbut-2-enoic acid (6.00 g, 60.0 mmol), N-bromosuccinamide (11.8 g, 66.2 mmol) and 1,1'-azobis(1-cyclohexanecarbonitrile) (400 mg, 1.64 mmol, 2.7 mol%) were added to a dry three neck 100 mL flask equipped with a Schlenk line adapter, reflux condenser and Schlenk bubbler. The apparatus was evacuated and back filled with argon 3 times followed by the addition of 60 mL of carbon tetrachloride which had been degassed and transferred via cannula. The reaction was heated under argon for 3 hours during which time a significant amount of succinamide precipitated out of solution. The reaction was allowed to cool, followed by further cooling with an ice bath for 30 minutes to precipitate all the byproducts. The reaction mixture was filtered by vacuum, the filter cake was washed with DCM (2 x 50 mL) and the solvent was poured into a separatory funnel and carefully worked up with the addition of ice cold solution of sodium hydroxide (2.69 grams, 67.3 mmol) in 60 mL of water. The layers were separated setting aside the aqueous layer for further synthesis. The organic layer was washed with water (2 x 50 mL) and the washes were added to the previous extracts. The organic layer was further washes with brine (2 x 50 mL), filtered, dried over magnesium sulfate and partially concentrated without heat at the rotovap. The resulting liquid was purified by distillation yielding 2.1 grams (21.4 mmol, 35.7 %) of pure product matching the commercially available material and literature data. Chemical Formula: $C_5H_6O_2$ Molecular Weight: 98.1

^{1}H NMR (400 MHz, $CDCl_3$) δ 5.94 – 5.69 (m, 1H), 4.71 (dd, *J* = 1.7, 0.8 Hz, 2H), 2.24 – 1.99 (m, 3H).

(*E*)-ethyl 4-chloro-3-methylbut-2-enoate[21]

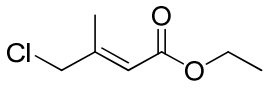

The aqueous layer from the above step was acidified with 2 M HCl (50 mL) and extracted with diethyl ether (4 x 50 mL), the combined organic layers were washed with brine (3 x 25 mL), dried over magnesium sulfate and concentrated at the rotovap. Dry HCl in absolute ethanol was generated by adding absolute ethanol (100 mL) to a purged 200 mL three neck flask containing 20 grams of sodium chloride and a reflux condenser equipped with a Schlenck bubbler. The flask was cooled in an ice bath and acetyl chloride (7 mL) was added dropwise with strong stirring. The apparatus was brought out of the cold bath and the viscous oil from the previous step was taken up in 20 mL of absolute ethanol and added to the strongly acidic solution of ethanol. The mixture was heated to reflux overnight, cooled, filtered, and poured into a large separatory funnel containing 100 mL diethyl ether and 250 mL ice cold water. The organic layer was extracted with additional water (3 x 100 mL), followed by 5% bicarbonate (2 x 100 mL), and brine (2 x 25 mL). The organic layer was dried over magnesium sulfate, filtered and partially concentrated to 20 mL, the organics were transferred to a smaller flask and the remaining volatiles were purified by normal distillation followed by careful vacuum distillation using a water aspirator and an in line liquid nitrogen trap to prevent loss of product. The receiving flask was cooled in a dry ice acetone bath, product distills at 70 to 85˚C at roughly 50 mbar. The product was found to contain a small amount of bromide so the resulting oil was taken up in DCM (10 mL) and 1 gram of tetrabutyl ammonium chloride was added and the reaction was stirred for overnight. The solution was extracted with water (5 x 10 mL), brine (2 x 10 mL), dried over magnesium sulfate, filtered and concentrated without heat, yielding 910 mg (5.60 mmol, 9.3%).

Chemical Formula: $C_7H_{11}ClO_2$ Molecular Weight: 162.6

^{1}H NMR (500 MHz, $CDCl_3$) δ 5.96 (s, 1H), 4.18 (q, *J* = 7.1 Hz, 2H), 4.04 (s, 2H), 2.23 (s, 3H), 1.28 (t, *J* = 7.1 Hz, 3H).

^{13}C NMR (126 MHz, $CDCl_3$) δ 166.4, 152.3, 119.4, 60.5, 50.3, 17.1, 14.6.

GC/MS: Modified temperature program of 80˚C for 3 minutes followed by a ramp of 10˚C/ minute, 270˚C final temperature and holding there for 10 minutes. Retention time of 8.2 minutes for the chloride and 9.3 minutes for the bromide.

MS (EA, 70mV): m/z: 165.2 (1), 164.2 (10), 163.2 (1), 162.2 (34), 136.2 (24), 134.2 (71), 119.2 (42), 117.2 (120), 99.2 (21), 98.2 (71), 97.2 (27), 91.2 (16), 89.2 (48), 53.2 (161).

Elemental Analysis: for $C_7H_{11}ClO_2$ calculated C, 51.70; H, 6.82; found C, 51.64; H, 6.91.

4-Bromonaphthalen-1-ol[22]

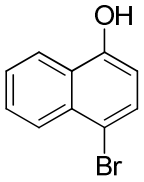

Synthesized by a modified literature procedure, ω-napthol (7.28 g, 50.56 mmol) was dissolved in 200 mL of DCM and was stirred at a high rate of mixing while a solution of NBS (10.8 g, 60.7 mmol) in DCM (500 mL) was added dropwise over 45 minutes. The resulting solution was stirred for 16 hours and the reaction progress checked by TLC (25% DCM/hexane, product R_f = 0.3, start material R_f = 0.9). The reaction was then heated to reflux for 1 hour and stirred for an additional 3 hours while cooling to room temperature, during which time the starting material was completely consumed. The reaction was poured into a separatory funnel with 100mLs of DCM, washed with 2M HCl (3 x 200 mL), brine (2 x 100 mL), and the separated organic layer was dried over magnesium sulfate, filtered and concentrated to dryness to yield a dark oil which crystallized on standing (10.8 g). The crude was taken up and recrystallized in 100 mL of refluxing heptanes, filtered hot, and allowed to cool to room temperature during which time large needles grew out of the mother liquor. The needles were isolate by vacuum filtration and washed with ice cold hexane, transferred to a round bottom flask and dried on the rotovap to yield a first crop of 3.8 grams of pure material. A second crop of crystals was obtained by concentrating the mother liquor to dryness, taking up the remaining material in 60 mLs of refluxing heptanes, filtered hot and the cooling solution provided an additional 3.7 grams of pure material after washing with cold hexane and drying on a rotovap. Total yield of 7.5 grams (33.6 mmol, 66%) with the physical and spectral properties in good agreement with the literature.

Chemical Formula: $C_{10}H_7BrO$ Molecular Weight: 223.1

^{1}H NMR (400 MHz, DMSO) δ 10.51 (s, 1H), 8.25 (dd, *J* = 37.6, 8.0 Hz, 1H), 8.03 (t, *J* = 10.3 Hz, 1H), 7.68 – 7.61 (m, 2H), 7.59 – 7.51 (m, 1H), 6.83 (d, *J* = 8.1 Hz, 1H).

^{13}C NMR (400 MHz, DMSO) δ 153.3, 131.8, 130.1, 127.8, 126.0, 125.9, 125.5, 122.7, 109.8, 108.9.

MS (EA, 70mV) m/z: 224.9 (11), 224.0 (99), 223.0 (12), 222.0 (100), 116.1 (9), 115.0 (96), 114.0 (15).

(4-Bromonaphthalen-1-yloxy)(*tert*-butyl)dimethylsilane

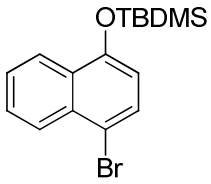

4-Bromonaphthalen-1-ol (3.40 g, 15.3 mmol), *tert*-butyldimethylsilyl chloride (4.56 g, 30.5 mmol) and imidazole (3.15 g, 45.7 mmol) were added to a dry 50 mL flask with a stir bar and rubber septum. The flask was purged with argon for 5 minutes and absolute DMF (20 mL) was added and the mixture was stirred overnight. The reaction was poured into a separatory funnel with 100 mL of ether, extracted with water (3 x 100 mL), brine (2 x 50 mL), the organic layer was separated and dried over magnesium sulfate, filtered, and concentrated to dryness at a rotovap. The resulting crude material was recrystallized from hot heptanes (20mL) and filtered hot. Upon cooling the recrystallization gave glass like cubes on standing at room temperature overnight. Yield 4.6 (13.6 mmol, 89%).

Chemical Formula: $C_{16}H_{21}BrOSi$ Molecular Weight: 337.3

^{1}H NMR (400 MHz, $CDCl_3$) δ 8.19 (dd, *J* = 13.7, 8.4 Hz, 2H), 7.66 – 7.56 (m, 2H), 7.56 – 7.48 (m, 1H), 6.75 (d, *J* = 8.1 Hz, 1H), 1.10 (d, *J* = 2.9 Hz, 9H), 0.47 – 0.11 (m, 6H).

^{13}C NMR (400 MHz, $CDCl_3$) δ 151.6, 132.9, 129.6, 129.2, 127.5, 127.0, 125.9, 123.1, 113.8, 113.1, 25.8, -4.3.

Tert-butyl(4-(3,4-dichlorophenyl)naphthalen-1-yloxy)dimethylsilane

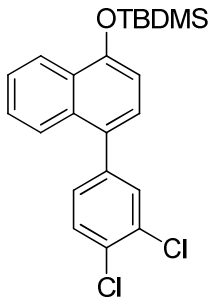

(4-Bromonaphthalen-1-yloxy)(tert-butyl)dimethylsilane (1.01 g, 2.98 mmol), 3,4-dichlorophenylboronic acid (626 mg, 3.28 mmol), and palladium acetate (6.7 mg, 29.8 μmol, 1.0 mol%) were added to a 100 mL Schlenk flask with a stir bar and sealed with a septum. In two separate flasks were placed sodium carbonate (966 mg, 8.94 mmol) dissolved in water (10 mL) and DMF (10 mL), the flasks were sealed with septa and degassed with argon bubbled through needles for 15 minutes. The DMF was transferred to the Schlenk flask and the contents dissolved with stirring over 5 minutes. The degassed aqueous base was then added and the reaction was heated to 50 ˚C for 4 hours, during which time the solution went from palladium black to a grey color as the catalyst was consumed. The flask was then cooled, the contents were transferred to a separatory funnel with 50 mL of ether and the organic layer was washed with water (3 x 50 mL) and brine (2 x 50 mL). The organic layer was separated and dried over magnesium sulfate, filtered and concentrated onto silica gel. The crude material was purified by chromatography (100% hexane, R_f = 0.5 for product, 0.9 for starting material, 3.5 X 20 cm silica gel, dry load). Some starting material was recovered (132 mg, 13%) and 630 mg (1.56 mmol, 52%) of the product was obtained as a white solid.

Chemical Formula: $C_{22}H_{24}Cl_2OSi$ Molecular Weight: 403.4

^{1}H NMR (400 MHz, $CDCl_3$) δ 8.37 – 8.26 (m, 1H), 7.82 – 7.77 (m, 1H), 7.59 (d, *J* = 2.0 Hz, 1H), 7.45 (d, *J* = 8.4 Hz, 1H), 7.50 – 7.44 (m, 2H), 7.32 (dd, *J* = 8.4, 2 Hz, 1H), 7.25 (d, *J* = 7.4 Hz, 1H), 6.92 (d, *J* = 7.8 Hz, 1H), 1.24 – 1.08 (m, 9H), 0.41 – 0.32 (m, 6H).

^{13}C NMR (101 MHz, $CDCl_3$) δ 152.3, 141.4, 132.9, 132.7, 132.4, 131.4, 131.0, 130.5, 130.0, 128.4, 127.5, 127.1, 125.7, 125.6, 123.4, 112.3, 26.3, 18.9, -3.8.

MS (EA, 70mV) m/z: 407.1 (2), 406.1 (9), 405.1 (12), 404.1 (45), 403.1 (18), 402.1 (64), 350.0 (4), 349.0 (16), 348.0 (24), 347.0 (73), 346.0 (37), 314.0 (2), 313.0 (13), 312.0 (13), 311.0 (8), 310.0 (35), 298.0 (2), 297.0 (12), 296.0 (7), 295.0 (31).

Elemental Analysis: for $C_{22}H_{24}Cl_2OSi$ calculated C, 65.50; H, 6.00; found C, 65.58; H, 5.95.

4-(3,4-Dichlorophenyl)naphthalen-1-ol

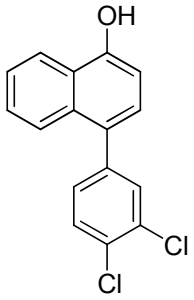

Tert-butyl(4-(3,4-dichlorophenyl)naphthalen-1-yloxy)dimethylsilane (500 mg, 1.24 mmol) was added to a Schlenk flask and the flask was placed under an inert atmosphere of argon, THF (25 mL was added to the flask followed by tetrabutyl ammonium fluoride trihydrate (1.7 g, 4.12 mmol). The reaction was stirred at 50 ˚C for 5 hours during which time the solution goes black from the resulting anion. The reaction is cooled and the THF is removed by vacuum/ cold trap directly from the Schlenk flask. The contents are dissolved in ethyl acetate (25 mL) and washed with 2 M HCl (2 x 25 mL), water (4 x 100 mL), brine (2 x 50 mL), dried over magnesium sulfate, filtered and concentrated at the rotovap. Purified by column chromatography (50% DCM/ hexane, R_f = .42 for product, 2 x 16 cm silica gel, dry load), yielding 321 mg (1.11 mmol, 89%) as a white solid. Chemical Formula: $C_{16}H_{10}Cl_2O$ Molecular Weight: 289.2

^{1}H NMR (400 MHz, DMSO) δ 10.40 (s, 1H), 8.24 (dd, *J* = 6.6, 3.1 Hz, 1H), 7.73 (d, *J* = 8.2 Hz, 1H), 7.70 (t, *J* = 3.3 Hz, 1H), 7.66 (d, *J* = 2.0 Hz, 1H), 7.49 (dd, *J* = 6.5, 3.3 Hz, 2H), 7.42 (dd, *J* = 8.3, 2.0 Hz, 1H), 7.28 (d, *J* = 7.8 Hz, 1H), 6.95 (d, *J* = 7.8 Hz, 1H).

^{13}C NMR (101 MHz, DMSO) δ 153.5, 141.1, 131.5, 131.5, 131.0, 130.4, 130.2, 129.5, 127.8, 127.4, 126.8, 124.7, 124.5, 124.4, 122.4, 107.6.

Substrate **157a**: 4-*tert*-butyl-7-methoxy-1,2-dihydronaphthalene

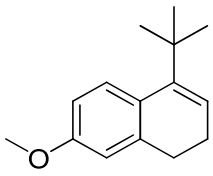

Anhydrous zinc chloride (1 g, 7 mmol) was added to a 250 mL Schlenk flask with absolute THF (100 mL). *Tert*-butyl lithium (1.6 M, 50 mL, 80 mmol) was added at -20 ˚C and the reaction was allowed to stir at that temperature for 1 hour. 6-Methoxy-α-tetralone (12 g, 68.2 mmol) was added to the reaction mixture as a solid. The resulting reaction was stirred overnight at room temperature. The next morning the reaction was cooled to 0 ˚C and a solution of saturated ammonium chloride (40 mL) was carefully added with vigorous stirring by pipette portions over 20 minutes. The solution was allowed to warm to room temperature and stirred for an additional half hour. The contents of the flask were transferred to a separatory funnel with 100 mL of ethyl acetate, washed with additional ammonium chloride (2 x 100 mL), water (3 x 100 mL), brine (2 x 100 mL) and dried over magnesium sulfate. NMR of the crude material indicated that roughly a third of the product had been converted with half of the converted product as the desired alkene. The crude mixture of 6-methoxy-α-tetralone and tert-butylated product was partially purified by column chromatography with 100% hexane. The crude mix of desired alkene, alcohol and a slight trace of tetralone (3 grams) were taken up in 100 mL of DCM and 25 grams of activated 4Å molecular sieves and the reaction was sealed with a rubber septum and stirred overnight. Crude NMR indicated that the remaining alcohol had been converted to the alkene. Column chromatography (5.5 X 22 cm silica gel) with hexane furnished the desired product as 1.6 grams (7.4 mmol, 11%) of viscous oil which crystallized into a white solid on standing at room temperature.

Chemical Formula: $C_{15}H_{20}O$ Molecular Weight: 216.3

^{1}H NMR (400 MHz, $CDCl_3$) δ 7.57 (d, J = 8.1 Hz, 1H), 6.76 – 6.72 (m, 2H), 5.98 (t, J = 4.9 Hz, 1H), 3.82 (s, 3H), 2.65 (t, J = 7.8 Hz, 2H), 2.21 – 2.11 (m, 2H), 1.34 (s, 9H).

^{13}C NMR (101 MHz, $CDCl_3$) δ 157.7, 144.9, 141.0, 128.2, 127.3, 122.1, 114.1, 110.5, 55.5, 35.3, 31.4, 30.3, 23.8.

MS (EA, 70mV) m/z: 217.3 (11), 216.3 (66), 201.3 (34), 186.3 (13), 173.3 (25), 159.3 (113), 144.2 (38), 128.2 (28), 115.2 (40.

Elemental Analysis: for $C_{15}H_{20}O$ calculated C, 83.29; H, 9.32; found C, 83.44; H, 9.50.

(*E*)-2-oxo-2-phenylethyl 2-methylbut-2-enoate

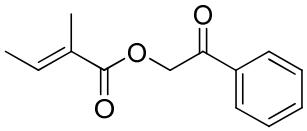

Tiglic acid (1 g, 10.0 mmol) was dissolved in 20 mL of absolute DCM and triethylamine (1.53 mL, 1.11 g, 11 mmol) was added. Alpha-bromoacetophenone (1.83 g, 9.15 mmol) was added and the reaction was allowed to stir for 5 hours. The solution was poured into a separatory funnel with bicarbonate (50 mL), washed with additional bicarbonate (2 x 50 mL), water (2 x 50 mL), 0.5 M HCl (2 x 50 mL), brine (2 x 50 mL) and the organic layer was dried over sodium sulfate, filtered and concentrated to dryness. The product was recrystallized by heating in hexane (10 mL), filtration and cooling to -20 ˚C overnight. Yield of 1.39 grams of a white low melting solid (6.37 mmol, 64%).

Chemical Formula: $C_{13}H_{14}O_3$ Molecular Weight: 218.2.

^{1}H NMR (400 MHz, $CDCl_3$) δ 7.94 (dt, *J* = 8.5, 1.6 Hz, 1H), 7.63 – 7.58 (m, 1H), 7.52 – 7.46 (m, 1H), 7.04 (qq, *J* = 7.1, 1.5 Hz, 1H), 5.40 (s, 1H), 1.91 (p, *J* = 1.4 Hz, 3H), 1.84 (dq, *J* = 7.1, 1.3 Hz, 3H).

5.15 *In Situ* complexation applied to a Phox catalyzed asymmetric hydrogenation

Iridium(I)$(COD)_2BAr_F$ (6.35 mg, 4.99 μmol, 2 mol%) was weighed into a 4 mL vial. (*S*)-2-(2-(dio-tolylphosphino)phenyl)-4-isopropyl-4,5-dihydrooxazole "PHOX" (2.20 mg, 5.49 μmol, 2.2 mol%) and (*E*)-prop-1-ene-1,2-diyldibenzene (48.6 mg, 250 μmol) were weighed out and added to the vial in air. Fresh absolute DCM (500 μL) was added to the vial followed by a rapid color change from dark violet to light orange as the complexation consumes the metal precursor. A stir bar is added and the vial is placed into an autoclave. The reactor is purged with hydrogen for 30 seconds and pressurized to 50 bar of hydrogen. The reaction was stirred for 8 hours and the pressure was carefully released. The solvent was removed by rotary evaporation and the

resulting oil was taken up in ether, filtered through a plug of silica and the solvent was rotary evaporated off to yield 41 mg (209 μmol , 83.6%) of pure reduced alpha-methyl-stilbene in 88.5% ee in *R* configuration.

5.16 Hydrogenation products and general procedures for asymmetric reduction

General procedure A, standard conditions: The individual precatalyst metal complexs were each weighed into reaction vials (1 μmol, 1 mol%). The substrate was weighed into separate vial (400 μmol) and absolute DCM (2000 μL) was added fresh from either a Fluka crown cap bottle or a Grubbs type solvent system. The substrate was dissolved and transferred to the reaction vials (500 μL/ reaction, 100 μmol/ reaction), followed by the addition of a stir bar and the vials were then placed into an autoclave. The autoclave was purged with hydrogen for 30 seconds and then the system was sealed and pressurized to a given pressure between 50 and 100 bar. The reaction was stirred at 900 rpm for a given length of time between 2 and 24 hours. The autoclave was vented and the individual vials were placed on a hot plate adapted with a multivial aluminum heating block set to 50 ˚C. The individual reactions were concentrated with stirring in the block for 1 hour while silica gel pipette columns were prepared. The resulting viscous oil was taken up in 0.5 mL of diethyl ether, passed through the pipette column (1.5 cc silica gel) and collected in a small vial, the column was washed with an additional amount of ether (1.5 mL) and the solution was concentrated on the same heating block. A small portion of the sample was taken in isopropanol and analyzed by chiral HPLC or in hexane and analyzed by GC.

General procedure B: Identical to procedure A except a variable amount of precatalyst was weighed out (2-5 μmol, 2-5 mol%) and the substrate was prepared for 500 mM or (100 μmol substrate)/(200 μL) in absolute DCM.

Product **159b**: (*R*)-ethyl 2-methyl-5-phenylpentanoate

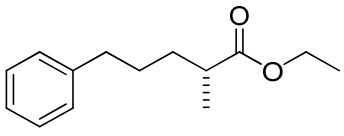

HPLC conditions: Chiral OB-H with a flow rate of 0.8 mL/min and a polarity of 97:3 heptanes to isopropanol at 20 ˚C, T_1 = 9.1 minutes and T_2 = 14.8 minutes. Enantiomers were identified by peak reversal between opposite configured catalysts *S*-**7e** and *R*-**9a**, conversion by GC.

Chemical Formula: $C_{14}H_{20}O_2$ Molecular Weight: 220.3

^{1}H NMR (400 MHz, C_6D_6) δ 7.18 – 7.14 (m, 2H), 7.06 (dd, *J* = 14.7, 7.2 Hz, 3H), 3.95 (q, *J* = 7.1 Hz, 2H), 2.43 (t, *J* = 7.7 Hz, 2H), 2.38 – 2.27 (m, 1H), 1.69 (dddd, *J* = 12.9, 10.6, 7.8, 5.4 Hz, 1H), 1.64 – 1.44 (m, 2H), 1.39 – 1.25 (m, 1H), 1.05 (d, *J* = 7.0 Hz, 3H), 0.95 (t, *J* = 7.1 Hz, 3H).

^{13}C NMR (101 MHz, C_6D_6) δ 175.9, 142.4, 128.7, 128.6, 126.1, 59.9, 39.6, 36.1, 33.7, 29.4, 17.3, 14.3.

^{1}H NMR (500 MHz, $CDCl_3$) δ 7.28 (d, *J* = 7.5 Hz, 1H), 7.26 (m, 1H), 7.18 (t, *J* = 7.9 Hz, 3H), 4.12 (q, *J* = 7.1 Hz, 2H), 2.61 (t, *J* = 7.6 Hz, 2H), 2.50 – 2.38 (m, 1H), 1.71 (dt, *J* = 14.2, 7.4 Hz, 1H), 1.62 (dt, *J* = 15.2, 7.5 Hz, 2H), 1.46 (dt, *J* = 19.7, 6.7 Hz, 1H), 1.24 (t, *J* = 7.1 Hz, 3H), 1.14 (d, *J* = 6.9 Hz, 3H).

^{13}C NMR (126 MHz, $CDCl_3$) δ 177.2, 142.6, 128.8, 128.7, 126.1, 60.5, 39.8, 36.2, 33.8, 29.5, 17.5, 14.7.

MS (EI, 70 eV): m/z: 220.4.

$[\alpha]_D^{20}$ = -16.0 at a concentration of 0.14 and ee = 95.6%.

Product **161b**: (*R*)-ethyl 2-methyl-3-phenylpropanoate

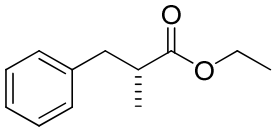

HPLC conditions: Chiral OB-H with a flow rate of 0.8 mL/min and a polarity of 97:3 heptanes to isopropanol at 25 ˚C, T_1 = 10.4 minutes and T_2 = 11.5 minutes.

Chemical Formula: $C_{12}H_{16}O_2$ Molecular Weight: 192.3

^{1}H NMR (500 MHz, $CDCl_3$) δ 7.28 - 7.26 (m, 2H), 7.20 (t, *J* = 7.4 Hz, 1H), 7.17 (d, *J* = 7.4 Hz, 2H), 4.09 (q, *J* = 7.1 Hz, 2H), 3.01 (dt, *J* = 21.8, 10.9 Hz, 1H), 2.78 – 2.60 (m, 2H), 1.19 (t, *J* = 7.1 Hz, 3H), 1.15 (d, *J* = 6.7 Hz, 3H).

^{13}C NMR (126 MHz, $CDCl_3$) δ 176.5, 139.8, 129.4, 128.7, 126.7, 60.7, 41.9, 40.1, 17.2, 14.6.

$[\alpha]_D^{20}$ = -33.0 at a concentration of 0.17 and ee = 97%.

Elemental Analysis: for $C_{12}H_{16}O_2$ calculated C, 74.97; H, 8.39; found C, 74.58; H, 8.46.

Product **161a**: (*R*)-methyl 2-methyl-3-phenylpropanoate

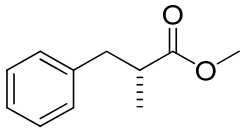

HPLC conditions: Chiral OB-H with a flow rate of 0.8 mL/min and a polarity of 97:3 heptanes to isopropanol at 25 ˚C, T_R = 10.8 minutes and T_S = 11.6 minutes.

Chemical Formula: $C_{11}H_{14}O_2$ Molecular Weight: 178.2

^{1}H NMR (500 MHz, $CDCl_3$) δ 7.29 - 7.26 (m, 2H), 7.20 (t, *J* = 7.2 Hz, 1H), 7.16 (d, *J* = 7.5 Hz, 2H), 3.64 (s, 3H), 3.03 (dd, *J* = 13.3, 6.7 Hz, 1H), 2.78 – 2.70 (m, 1H), 2.66 (dd, *J* = 13.3, 7.8 Hz, 1H), 1.15 (d, *J* = 6.9 Hz, 3H).

^{13}C NMR (126 MHz, $CDCl_3$) δ 177.0, 139.8, 129.4, 128.8, 126.7, 52.0, 41.8, 40.1, 17.1.

$[\alpha]_D^{20}$ = -34.0 at a concentration of 0.16 and ee = 96.6%.

Product **161c**: (*R*)-isopropyl 2-methyl-3-phenylpropanoate

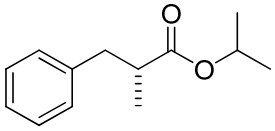

HPLC conditions: Chiral OB-H with a flow rate of 1.0 mL/min and a polarity of 100% heptanes at 20 ˚C, T_R = 7.45 minutes and T_S = 8.15 minutes, substrate T_{sub} = 9.45 minutes.

Chemical Formula: $C_{13}H_{18}O_2$ Molecular Weight: 206.3

^{1}H NMR (500 MHz, $CDCl_3$) δ 7.28 - 7.25 (m, 2H), 7.19 (dd, *J* = 14.3, 7.2 Hz, 3H), 4.96 (hept, *J* = 6.1 Hz, 1H), 2.99 (dd, *J* = 11.9, 5.6 Hz, 1H), 2.77 – 2.58 (m, 2H), 1.19 (d, *J* = 6.2 Hz, 3H), 1.14 (d, *J* = 6.4 Hz, 3H), 1.12 (d, *J* = 6.2 Hz, 3H).

^{13}C NMR (126 MHz, $CDCl_3$) δ 176.1, 139.9, 129.4, 128.7, 126.6, 67.8, 42.0, 40.1, 22.1, 22.1, 17.2.

$[\alpha]_D^{20}$ = -43.0 at a concentration of 0.13 and ee = 99.1%.

Elemental Analysis: for $C_{13}H_{18}O_2$ calculated C, 75.69; H, 8.80; found C, 75.88; H, 8.97.

Product **157b**: (*R*)-1-tert-butyl-6-methoxy-1,2,3,4-tetrahydronaphthalene

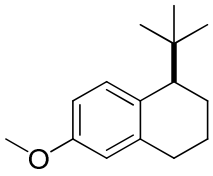

Synthesized by procedure B. HPLC conditions: Chiral OD-H with a flow rate of 1.0 mL/min and a polarity of 100% heptanes at 20˚C, T_1 = 6.3 minutes and T_2 = 8.7 minutes, substrate T_{sub} = 14.7 minutes, aromatic side product T_{ar} =10.7.

Chemical Formula: $C_{15}H_{22}O$ Molecular Weight: 218.3

^{1}H NMR (400 MHz, $CDCl_3$) δ 7.06 (d, *J* = 8.4 Hz, 1H), 6.66 (dd, *J* = 8.4, 2.8 Hz, 1H), 6.62 (d, *J* = 2.7 Hz, 1H), 3.79 (s, 3H), 2.75 – 2.54 (m, 3H), 2.02 – 1.89 (m, 1H), 1.89 – 1.80 (m, 2H), 1.51 – 1.37 (m, 1H), 0.90 (s, 9H).

^{13}C NMR (101 MHz, $CDCl_3$) δ 157.6, 141.9, 132.5, 131.2, 113.6, 110.6, 55.5, 47.1, 36.3, 30.7, 28.9, 25.8, 22.8.

$[\alpha]_D^{20}$ = -24.0 at a concentration of 0.22 and ee = 96.0%.

5.17 References

[1] Mazet, C.; Roseblade, S.; Kohler, V.; Pfaltz, A. *Org. Lett.* **2006**, *8*, 1879-1882.

[2] Castelijns, A. M. C. F.; Dielemans, H. J. A.; (DSM N.V., Neth.). Application: EP EP, **1993**, p 8 pp.

[3] Meyers, A. I.; Garcia-Munoz, G. *J. Org. Chem.* **1964**, *29*, 1435.

[4] Sakurai, A.; Midorikawa, H. *Bull. Chem. Soc. Jap.* **1968**, *41*, 165.

[5] Voss, F. Masterarbeit, Univeristy Of Basel, **2007**.

[6] Liu, Q.-B.; Yu, C.-B.; Zhou, Y.-G. *Tetrahedron Lett.* **2006**, *47*, 4733.

[7] Lyle, M. P. A.; Narine, A. A.; Wilson, P. D. *J. Org. Chem.* **2004**, *69*, 5060.

[8] Lyle, M. P. A.; Wilson, P. D. *Org. Lett.* **2004**, *6*, 855.

[9] Kaiser, S.; Smidt, S. R.; Pfaltz, A. *Angew. Chem. Int. Ed.* **2006**, *45*, 5194.

[10] Navarro, O.; Marion, N.; Mei, J. G.; Nolan, S. P. *Chem. Eur. J.* **2006**, *12*, 5142.

[11] Zimmerman, S. C.; Zeng, Z.; Wu, W.; Reichert, D. E. *J. Am. Chem. Soc.* **1991**, *113*, 183.

[12] Xie, Y.; Huang, H.; Mo, W.; Fan, X.; Shen, Z.; Shen, Z.; Sun, N.; Hu, B.; Hu, X. *Tetrahedron: Asymmetry* **2009**, *20*, 1425.

[13] Zimmerman, S. C.; Zeng, Z. *J. Org. Chem.* **1990**, *55*, 4789.

[14] Roseblade, S. J.; Pfaltz, A. *Synthesis-Stuttgart* **2007**, 3751.

[15] Uenishi, J.; Hamada, M. *Synthesis* **2002**, 625.

[16] Maywald, M.; Pfaltz, A. *Synthesis* **2010** 3654.

[17] Shastin, A. V.; Muzalevsky, V. M.; Balenkova, E. S.; Nenajdenko, V. G. *Mendeleev Comm.* **2006**, 179.

[18] Schonleber, M.; Hilgraf, R.; Pfaltz, A. *Adv. Synth. Cat.* **2008**, *350*, 2033.

[19] von Matt, P.; Pfaltz, A. *Tetrahedron: Asymmetry* **1991**, *2*, 691.

[20] Jeon, H.-S.; Yeo, J. E.; Jeong, Y. C.; Koo, S. *Synthesis* **2004**, *2004*, 2813.

[21] Gu, L.; Wang, B.; Kulkarni, A.; Geders, T. W.; Grindberg, R. V.; Gerwick, L.; Hakansson, K.; Wipf, P.; Smith, J. L.; Gerwick, W. H.; Sherman, D. H. *Nature* **2009**, *459*, 731.

[22] Ganguly, N. C.; De, P.; Dutta, S. *Synthesis* **2005**, 1103.

Chapter 6

Appendix

6.1 Crystallographic Data

The X-ray structures were measured by Mr. Markus Neuburger (Department of Chemistry,University of Basel) on a Nonius KappaCCD diffractometer, solved using direct methods (SIR92[1]) and refined with Crystals[2] by Mr. Markus Neuburger, Dr. Silvia Schaffner and Mr. Marcus Schrems (Department of Chemistry, University of Basel). Hydrogen atoms were added geometrically.

	123a	***R*-143g**
formula	$C_{36}H_{38}F_6IrNP_2$	$C_{23}H_{19}NO$
M_r [gmol^{-1}]	852.86	325.41
shape	plate	block
color	red	colorless
crystal system	triclinic	Triclinic
space group	P -1	P 1
crystal size [mm^3]	0.03_0.12_ 0.18	0.08_0.17_0.26
a [Å]	9.6179(5)	7.6503(2)
b [Å]	11.2735(5)	12.8616(4)
c [Å]	15.4148(8)	18.8654(6)
α [°]	79.979(2)	106.2280(10)
β [°]	80.975(3)	98.815(2)
γ [°]	87.440(2)	101.2650(10)
V [Å^3]	1625.25(14)	1704.86(9)
Z	2	4
F(000)	844.00	688.00
Θ range for data collection [°]	1.835-29.171	1.704-30.526
ρ_{calcd} [gcm^{-3}]	1.743	1.268
absorption coeff. μ [mm^{-1}]	4.268	0.077
measured reflections	25816	36112
independent reflections	7106	10342
used reflections[b]	5952	9563
parameters refined	415	901
R[c]	0.0527	0.0408
R_w[d]	0.0490	0.0472
goodness of fit	1.1406	1.1103

[a] All data were collected using Mo K_α (λ = 0.71073 Å) at 173 K. [b] Observation criterion: $I > 3\sigma(I)$. [c] $R = \Sigma||F_0| - |F_C|| / \Sigma|F_0|$. [d] $R_w = \{\Sigma[w(F_0 - F_C)^2] / \Sigma[w(F_0)^2]\}^{1/2}$.

	***S*-108a**	***S*-108e**	***S*-110a**
formula	$C_{71}H_{50}BF_{24}IrNOP$	$C_{66}H_{62}BF_{24}IrNOP$	$C_{77}H_{56}BF_{24}IrNOP$
M_r [gmol^{-1}]	1623.14	1656.36	1701.25
shape	plate	block	block
color	red	orange	red
crystal system	triclinic	orthorhombic	triclinic
space group	P -1	P 2_1 2_1 2_1	P 1
crystal size [mm^3]		0.11_0.17_0.31	0.10_ 0.13_ 0.19
a [Å]	13.9209(3)	13.5137(6)	12.8218(4)
b [Å]	15.6412(4)	19.4816(9)	14.8360(5)
c [Å]	17.1341(4)	27.1434(11)	18.8757(6)
α [°]	104.9140(10)	90	96.898(2)
β [°]	106.3840(10)	90	99.557(2)
γ [°]	102.4700(10)	90	95.874(2)
V [Å^3]	3286.93(14)	7146.0(5)	3487.6(2)
Z	2	4	2
F(000)	1608	3316.40	1692
Θ range for data collection [°]	0.995-28.788	0.996-30.507	0.995- 32.031
ρ_{calcd} [gcm^{-3}]	1.640	1.539	1.620
absorption coeff. μ [mm^{-1}]	2.169	2.037	2.049
measured reflections	254629	121195	116236
independent reflections	81216	21519	47604
used reflections[b]	31557	18688	40264
parameters refined	955	993	1964
R[c]	0.0358	0.0264	0.0273
R_w[d]	0.0889	0.0285	0.0307
goodness of fit	1.0548	1.1252	0.9675

[a] All data were collected using Mo K_α (λ = 0.71073 Å) at 173 K. [b] Observation criterion: $I > 3\sigma(I)$. [c] $R = \Sigma||F_0| - |F_C|| / \Sigma|F_0|$. [d] $R_w = \{\Sigma[w(F_0 - F_C)^2] / \Sigma[w(F_0)^2]\}^{1/2}$.

6.2 List of abreviations

Å	Angstrom (10^{-10} M)
Ac	acyl
Anth	anthracyl
Ar	Aromatic
BAr_F	Tetrakis[3,5-bis(trifluoromethyl)phenyl]borate
Bn	benzyl
boc	*tert*-butoxycarbonyl
Bu	butyl
Bz	benzoyl
cal	calorie
CALB	*Candida Antarctica* lipase B
calc.	calculated
Cat, cat	catalyst
COD	cyclooctadiene
Conv, conv	conversion
Cy	cyclohexyl
d	doublet
DCM	dichloromethane
DFT	density functional thereom
DIPCl	B-Chlorodiisopinocamphylborane
DIPE	diisopropylether
DMAP	4-dimethylaminopyridine
DME	1,2-dimethoxyethane
DMF	*N,N'*-dimethylformamide
DMSO	dimethylsulfoxide
ee	enantiomeric excess
EI	electron impact
ent, enant	enantiomer
eq	equivalent
er	enantiomeric ratio

ESI	electron spray ionization
Et	ethyl
EtOAc	ethyl acetate
EWG	electron withdrawing group
FAB	fast atom bombardment
GC	gas chromatography
HPLC	high pressure liquid chromatography
hr	hour
i-Bu, ^{i}Bu	isobutyl
IPA	isopropyl alcohol
i-Pr, ^{i}Pr	isopropyl
J	coupling constant
k	rate constant
kcal	kilocalorie
kJ	kilojoule
L	Liter
M	Molar
M	Metal
m	*meta*
m/z	mass charge ratio
Me	methyl
Mesityl	2,4,6-trimethylbenzene
mL	milliliter
mol	mole
MS	mass spectrometry
Naph	naphthyl
n-Bu	*normal*-butyl
NMR	nuclear magnetic resonance
n-Pr	*normal*-probyl
o	*ortho*
Ph	phenyl

q	Enantiomeric quotient, (er with denominator = 1)
q	quartet
quint	quintet
rac	racemic
R_t	retention time
rt	room temperature
sep	septet
t	triplet
TBAF	tetrabutylammonium fluoride
TBME	*tert*-butylmethyl ether
t-Bu, ^{t}Bu, *tert*-Bu	*teriaryt*-butyl
THF	tetrahydrofuran
TLC	thin layer chromatography
TMS	trimethylsilyl
Tol	tolyl, toluene
tosyl	tosylate
Xyl	xylyl
α	alpha position
β	beta positon
δ	part per million
λ	nanometer
μ	micro
π	pi orbital
Σ	sum
σ	sigma orbital

6.3 References

[1] Altomare, A.; Cascarno, G.; Giacovazzo, C.; Guagliardi, A. *J. Appl. Crystallogr*. **1993**, *26*, 343.

[2] Watkin, D.; Cooper, R.; Prout C. K.; *Z. Kristallogr.* **2002**, *217*, 429.

Curriculum Vitae
David Harrison Woodmansee

(email: David.Woodmansee@unibas.ch)

Date Birth: 23 July 1973
Place Birth: San Diego, California
Nationality: United States of America
Marital Status: Married, EU citizen
Address: Kasernenstrasse 32, 4058 Basel, Switzerland

Professional and Acedemic Experience

- 2006-2010 University of Basel department of chemistry Ph.D. work "*Chiral Iridium Pyridyl Phosphinite Catalysts and the Development of Structure Selectivity Relationships in the Asymmetric Hydrogenation of Trisubstituted Alkenes*" under Professor A. Pfaltz
- 2003-2006 Senior research associate, conducted independent research in hit to full lead optimization in several disease indications, particular emphasis driving SAR and PK/ toxicology parameters for brain penetrative molecules, Genomics Institute for the Novartis Research Foundation (GNF), San Diego CA, USA
- 2002 Senior research associate, conducted independent research in hit to lead optimization in tyrosine kinase inhibitors, oncology department Ontogen corporation, Carlsbad CA, USA
- 2000-2002 Research Associate, Polyolefin catalysts preparation and ligand design University of California Santa Barbara (UCSB), Bazan group,
- 1997-2000 San Diego State University (SDSU) Dept. of Chemistry, Walsh Research group, Masters of Organic Chemistry awarded
- 1997 Industrial internship in scale up of HIV antiprotease inhibitor Viracept at Agouron pharmaceuticals (now Pfizer) process development
- 1995-1997 SDSU Dept. of Chemistry, Walsh Research group, B.S. in Chemistry with an emphasis in Biochemistry awarded
- 1995-1997 Walsh group undergraduate research in asymmetric catalysis
- 1994-1995 Hare group undergraduate research in entomology and natural product synthesis, research in evaluating the structure activity profile of pheromones, Dept. of Entomology University of California, Riverside (UCR), USA
- 1992-1995 University of California Riverside Dept. of Biochemistry, undergraduate

Additional Experience

- Research advisor of 3 master students at University of Basel and teaching assistant for introductory and advanced organic chemistry lab for chemists, duties included direction of research projects and instruction of new techniques to inexperienced chemists

- Close collaboration with multidisciplinary teams in preclinical settings with urgent time constraints
- Experience with HTS, parallel synthesis and automated methodology as well as solid and solution phase combinatorial chemistry
- Experienced and educated in the optimization of ADME/Tox parameters in hit to lead and animal models settings

Publications

(1) Woodmansee, D.H.; Müller, M.; Neuburger, M.; Pfaltz, A. *Chem. Sci.* **2010**, 1, 72-78.

(2) Yang, K.; He, X.; Choi, H.-S.; Wang, Z.; Woodmansee, D. H.; Liu, H. *Tetrahedron Lett.* **2008**, *49*, 1725-1728.

(3) Tully, D. C.; Liu, H.; Chatterjee, A. K.; Alper, P. B.; Williams, J. A.; Roberts, M. J.; Mutnick, D.; Woodmansee, D. H.; Hollenbeck, T.; Gordon, P.; Chang, J.; Tuntland, T.; Tumanut, C.; Li, J.; Harris, J. L.; Karanewsky, D. S. *Bioorg. Med. Chem. Lett.* **2006**, *16*, 5107-5111.

(4) Tully, D. C.; Liu, H.; Chatterjee, A. K.; Alper, P. B.; Epple, R.; Williams, J. A.; Roberts, M. J.; Woodmansee, D. H.; Masick, B. T.; Tumanut, C.; Li, J.; Spraggon, G.; Hornsby, M.; Chang, J.; Tuntland, T.; Hollenbeck, T.; Gordon, P.; Harris, J. L.; Karanewsky, D. S. *Bioorg. Med. Chem. Lett.***2006**, *16*, 5112-5117.

(5) Tully, D. C.; Liu, H.; Alper, P. B.; Chatterjee, A. K.; Epple, R.; Roberts, M. J.; Williams, J. A.; Nguyen, K. T.; Woodmansee, D. H.; Tumanut, C.; Li, J.; Spraggon, G.; Chang, J.; Tuntland, T.; Harris, J. L.; Karanewsky, D. S. *Bioorg. Med. Chem. Lett.* **2006**, *16*, 1975-1980.

(6) Fang, X.; Woodmansee, D.; Bu, X.; Bazan, G. *Angew. Chem. Int. Ed.* **2003**, *42*, 4510-4514.

(7) Kim, Y. H.; Kim, T. H.; Lee, B. Y.; Woodmansee, D.; Bu, X.; Bazan, G. C. *Organometallics* **2002**, *21*, 3082-3084.

(8) Woodmansee, D. H.; Bu, X.; Bazan, G. C. *Chem. Comm.***2001**, 619-620.

(9) Pritchett, S.; Woodmansee, D. H.; Gantzel, P.; Walsh, P. J. *J. Am. Chem. Soc.* **1998**, *120*, 6423-6424.

(10) Pritchett, S.; Woodmansee, D. H.; Davis, T. J.; Walsh, P. J. *Tetrahedron Lett.***1998**, *39*, 5941-5942.

(11) Ho, D. E.; Betancort, J. M.; Woodmansee, D. H.; Larter, M. L.; Walsh, P. J. *Tetrahedron Lett.* **1997**, *38*, 3867-3870.

Patents

(1) Liu, H.; Woodmansee, D. H. "Preparation of purine derivatives and compositions as inhibitors of cannabinoid receptor 1 activity," WO 2008134300, **2008**, p 51pp.

(2) Liu, H.; He, X.; Choi, H.-S.; Yang, K.; Woodmansee, D.; Wang, Z.; Ellis, D. A.; Wu, B.; He, Y.; Nguyen, T. N. "Preparation of pyrazolopyrimidinones and analogs, and their compositions as cannabinoid CB1 receptor inhibitors," WO 2006047516, **2006**, p 259 pp.

(3) He, Y.; Woodmansee, D.; Choi, H.-S.; Wang, Z.; Wu, B.; Nguyen, T. “Stereoselective synthesis of chiral arylpyrrolidones,” WO 2006081562, **2006**, p 45pp.

(4) Liu, H.; Tully, D. C.; Chatterjee, A.; Alper, P. B.; Woodmansee, D. H.; Mutnick, D. “Preparation of amino acid derivatives as cathepsin S inhibitors,” WO 2005107464, **2005**, p 61 pp.

(5) Liu, H.; Chatterjee, A.; Tully, D. C.; Alper, P. B.; Bursulaya, B.; Guo, J.; Woodmansee, D.; Mutnick, D.; Karanewsky, D. S.; He, Y. “Inhibitors of cathepsin S and pharmaceutical compositions containing cathepsin S inhibitors,” WO 2005034848, **2005**, p 125 pp.

(6) Liu, H.; Alper, P.; Chatterjee, A.; Tully, D.; Bursulaya, B.; Woodmansee, D.; Epple, R.; Harris, J. L.; Li, J. “Inhibitors of cathepsin S for use in pharmaceuticals,” WO 2004084843, **2004**, p 166 pp.

Books

Woodmansee, D.H.; Pfaltz A. “Iridium Catalyzed Asymmetric Hydrogenation of Olefins with Chiral N,P and C,N Ligands,” in *Iridium in Organic Synthesis*; Andersson, P.G. ed.; Springer, Berlin, **2010** in press.